Beachrock formation around a highly altered estuarine area in a temperate coastline

Ane Iturregui Torre

May 2016

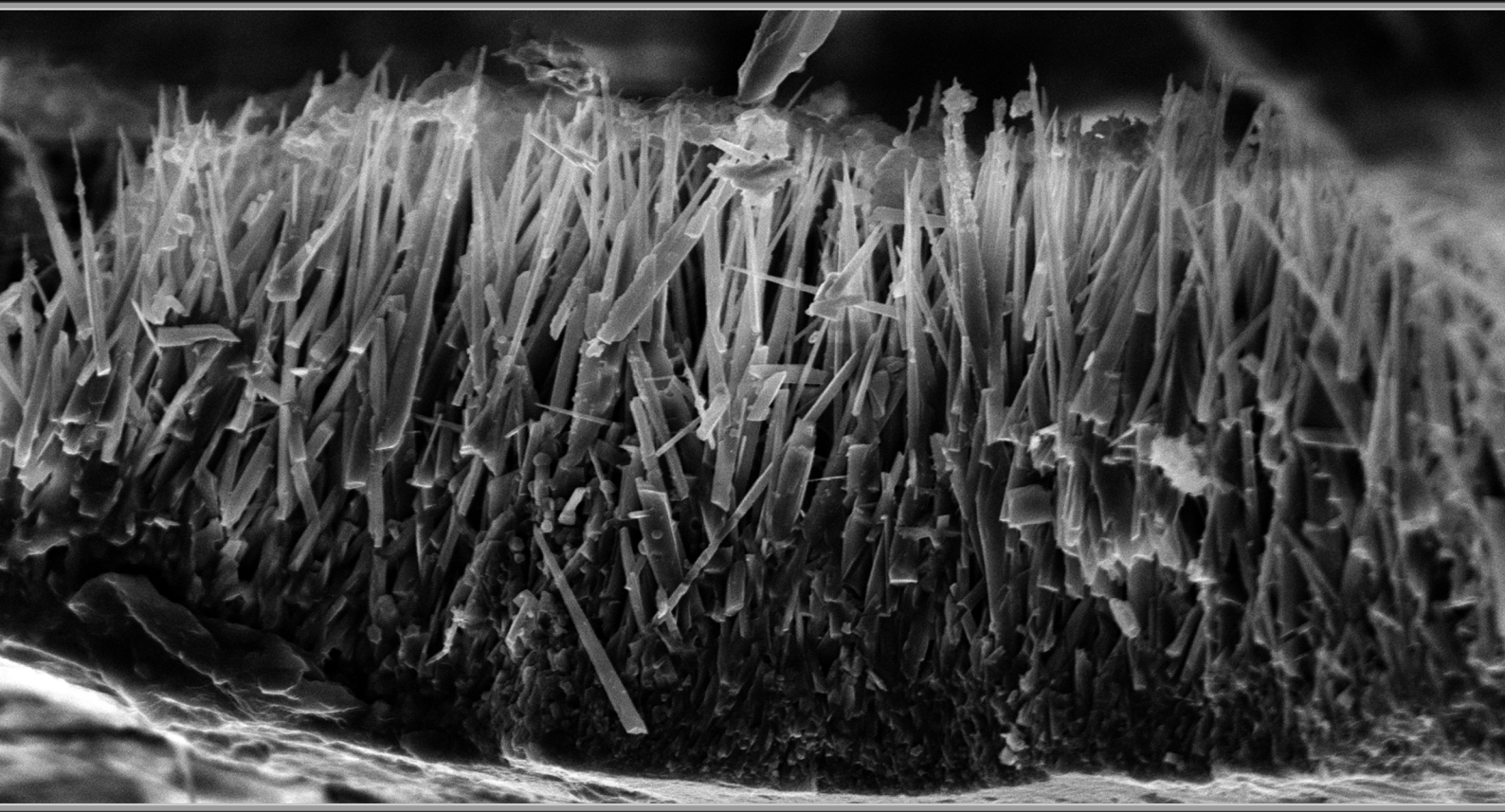

eman ta zabal zazu

Universidad del País Vasco

Euskal Herriko Unibertsitatea

eman ta zabal zazu

Universidad del País Vasco
Euskal Herriko Unibertsitatea

Department of Analytical Chemistry

Beachrock formation around a highly altered estuarine area in a temperate coastline

Report to compete for the International PhD degree

Ane Iturregui Torre

May 2016

Acknowledgments

I would like to sincerely acknowledge the many contributors that helped this thesis to become a reality. I am grateful for the predoctoral fellowship awarded by the Department of Education, Language Policies and Culture of the Basque Government, as well as for the economic aid provided during my predoctoral stay at the University of Kansas. Also, for the financial support received from:

- PRIACE project (Ref. CTM2012-36612) from the Spanish Ministry of Economy and Competitiveness (MINECO) and FEDER funding.

- SUDOE Interreg IV B Programme through the ORQUE SUDOE project (Ref. SOE3/P2/F591/5) funded by the European Regional Development Fund (EU/UE-FEDER/ERDF).

- Research Excellence Consolidated Groups Program funded by the Government of the Basque Country from 2013 to 2018 (Ref. IT-742-13).

Special thanks deserve Dr. Juan Ignacio Baceta and Dr. Xabier Murelaga from the Department of Stratigraphy and Palaeontology of the University of the Basque Country, for the relevant contribution in this research, through their support in the sampling campaigns, their facilities and their knowledge.

I would like to express my sincere gratitude to the Department of Geology of The University of Kansas (KU) (Lawrence, Kansas, USA), especially to Luis A. Gonzalez, for giving me the opportunity to perform a great part of the research in his group and for his valuable support particularly in the interpretation of the isotope data.

My thankfulness goes also to the technical support and knowledge provided by Alfredo Sarmiento in the Singular Coupled Multispectroscopy Laboratory (LASPEA) from the Research General Services of the UPV/EHU (SGIker) (UPV/EHU, MICINN, GV/EJ, ERDF and ESF).

I would like to mention the Bizkaia Provincial Council for providing me helpful tools for the understanding of the field, like through the disposition of orthophotos.

Además, me gustaría mostrar mi gratitud a los constituyentes del grupo de investigación IBeA del Departamento de Química Analítica por permitirme realizar la tesis. Quería dar las gracias especialmente a mis directores, Juan Manuel Madariaga (también por su indispensable labor como tutor) e Irantzu Martínez Arkarazo, por la dedicación y esfuerzo de ambos, y primordialmente por su ayuda en esta última etapa de la tesis. Agradezco también la relevante ayuda proporcionada por Marian Olazabal para la consecución del trabajo.

Se suele decir que *team work makes the dream work* y desde luego, no podía faltar mi más sincero agradecimiento hacia Nikole, que como pionera del grupo en *beachrocks* me ha facilitado las bases para poder llevar a cabo mi trabajo, y desde un punto de vista más personal, por los muchos momentos que hemos pasado aprendiendo juntas, del beachrock, y de la vida. Y por estar ahí, milesker!. También me siento encantada y muy agradecida de haber compartido estos años con Olivia, por toda su ayuda técnica sobre todo con la portada y por todos los ratos que hemos pasado juntas. Desde luego que también estoy encantada y muy agradecida por todo lo vivido con Julene y Leti, sin las cuales mi experiencia durante estos años no hubiese sido la misma. Ha sido un enorme placer encontrarme con Marco y Arri, por todos los ratos buenos que he pasado con ellos, así como con Nagore, por poner además su granito de arena cuando más hace falta. Eskerrik asko también a Iratxe, Maite, Hector, Cristina, Iker y todos los compañeros con los que me he ido cruzando por Zamudio.

Tampoco me olvido de Mireia, Ekhiñe, Oscar y Oihana, con los que empecé esta andadura. De Josean y Azibar por su ayuda técnica y anímica en momentos “críticos” y no tan críticos. De Laura, porque fue un placer trabajar con ella. De Arantza, Julen así como de Ainara, Oier, Itsaso, Olaia, Leire K., Leire M., Haizea, Naiara, Paty, Ibo, Maitane y de todos los compañeros de Leioa que han amenizado mis horas de trabajo allí. Hablando de compañeros de trabajo y amigos, mi experiencia en Kansas no hubiese sido la misma sin las amistades que hice en Lawrence y sin todas las personas que me encontré en el camino, que hicieron de mi estancia una experiencia memorable.

A mis amigos, que, además de aprender y divertirnos juntos, han sido un apoyo muy importante durante la tesis. A mi familia, por estar siempre ahí y por hacerme sentir muy afortunada de tenerles. Creo que Nerea y Jon podrían ser unos prometedores especialistas en arenas cementadas! Particularmente, a mi querida Leire, por sus consejos y por su apoyo a lo largo de los años, junto con Egoitz. Sobre todo a Iker, porque sobran las palabras.

Y ante todo, a aita y ama, por ser las piezas indispensables de este puzzle y porque con sus palabras y su paciencia, han estado siempre ahí allanando el camino.

“If I have seen further it is by standing on the shoulder of giants”

Isaac Newton

Acknowledgments

I would like to sincerely acknowledge the many contributors that helped this thesis to become a reality. I am grateful for the predoctoral fellowship awarded by the Department of Education, Language Policies and Culture of the Basque Government, as well as for the economic aid provided during my predoctoral stay at the University of Kansas. Also, for the financial support received from:

- PRIACE project (Ref. CTM2012-36612) from the Spanish Ministry of Economy and Competitiveness (MINECO) and FEDER funding.

- SUDOE Interreg IV B Programme through the ORQUE SUDOE project (Ref. SOE3/P2/F591/5) funded by the European Regional Development Fund (EU/UE-FEDER/ERDF).

- Research Excellence Consolidated Groups Program funded by the Government of the Basque Country from 2013 to 2018 (Ref. IT-742-13).

Special thanks deserve Dr. Juan Ignacio Baceta and Dr. Xabier Murelaga from the Department of Stratigraphy and Palaeontology of the University of the Basque Country, for the relevant contribution in this research, through their support in the sampling campaigns, their facilities and their knowledge.

I would like to express my sincere gratitude to the Department of Geology of The University of Kansas (KU) (Lawrence, Kansas, USA), especially to Luis A. Gonzalez, for giving me the opportunity to perform a great part of the research in his group and for his valuable support particularly in the interpretation of the isotope data.

My thankfulness goes also to the technical support and knowledge provided by Alfredo Sarmiento in the Singular Coupled Multispectroscopy Laboratory (LASPEA) from the Research General Services of the UPV/EHU (SGIker) (UPV/EHU, MICINN, GV/EJ, ERDF and ESF).

I would like to mention the Bizkaia Provincial Council for providing me helpful tools for the understanding of the field, like through the disposition of orthophotos.

Además, me gustaría mostrar mi gratitud a los constituyentes del grupo de investigación IBeA del Departamento de Química Analítica por permitirme realizar la tesis. Quería dar las gracias especialmente a mis directores, Juan Manuel Madariaga (también por su indispensable labor como tutor) e Irantzu Martínez Arkarazo, por la dedicación y esfuerzo de ambos, y primordialmente por su ayuda en esta última etapa de la tesis. Agradezco también la relevante ayuda proporcionada por Marian Olazabal para la consecución del trabajo.

Se suele decir que *team work makes the dream work* y desde luego, no podía faltar mi más sincero agradecimiento hacia Nikole, que como pionera del grupo en *beachrocks* me ha facilitado las bases para poder llevar a cabo mi trabajo, y desde un punto de vista más personal, por los muchos momentos que hemos pasado aprendiendo juntas, del beachrock, y de la vida. Y por estar ahí, milesker!. También me siento encantada y muy agradecida de haber compartido estos años con Olivia, por toda su ayuda técnica sobre todo con la portada y por todos los ratos que hemos pasado juntas. Desde luego que también estoy encantada y muy agradecida por todo lo vivido con Julene y Leti, sin las cuales mi experiencia durante estos años no hubiese sido la misma. Ha sido un enorme placer encontrarme con Marco y Arri, por todos los ratos buenos que he pasado con ellos, así como con Nagore, por poner además su granito de arena cuando más hace falta. Eskerrik asko también a Iratxe, Maite, Hector, Cristina, Iker y todos los compañeros con los que me he ido cruzando por Zamudio.

Tampoco me olvido de Mireia, Ekhiñe, Oscar y Oihana, con los que empecé esta andadura. De Josean y Azibar por su ayuda técnica y anímica en momentos “críticos” y no tan críticos. De Laura, porque fue un placer trabajar con ella. De Arantza, Julen así como de Ainara, Oier, Itsaso, Olaia, Leire K., Leire M., Haizea, Naiara, Paty, Ibo, Maitane y de todos los compañeros de Leioa que han amenizado mis horas de trabajo allí. Hablando de compañeros de trabajo y amigos, mi experiencia en Kansas no hubiese sido la misma sin las amistades que hice en Lawrence y sin todas las personas que me encontré en el camino, que hicieron de mi estancia una experiencia memorable.

A mis amigos, que, además de aprender y divertirnos juntos, han sido un apoyo muy importante durante la tesis. A mi familia, por estar siempre ahí y por hacerme sentir muy afortunada de tenerles. Creo que Nerea y Jon podrían ser unos prometedores especialistas en arenas cementadas! Particularmente, a mi querida Leire, por sus consejos y por su apoyo a lo largo de los años, junto con Egoitz. Sobre todo a Iker, porque sobran las palabras.

Y ante todo, a aita y ama, por ser las piezas indispensables de este puzzle y porque con sus palabras y su paciencia, han estado siempre ahí allanando el camino.

“If I have seen further it is by standing on the shoulder of giants”

Isaac Newton

Contents

Abstract

Beachrocks are friable to well-cemented sedimentary coastal structures typically formed in the intertidal zone due to the precipitation of carbonate compounds (principally) that act as cements, packing together the wide array of sediments that might be present in the beach. These structures have been commonly registered in tropical and subtropical zones, in contrast to the temperate latitude where the beachrocks object of study are located. More exactly, this thesis is focused on beachrock outcrops from Arrigunaga and La Salvaje beach, which are situated in the vicinity of the Nerbioi-Ibaizabal estuary (Bilbao, North of Spain), an area highly altered by the industrialization and urbanization process occurred more than a century ago.

In this context, a first approach to the compositional characteristics were obtained, thanks to an examination of different grain sizes in beachrock samples of the Arrigunaga beach. This way, regarding the cements, it was first estimated that calcium carbonate cements could exist within the beachrock formations. In reference to the framework grains, an anthropogenic input of metals was suggested on account of the greater metal content measured in coarser grain sizes. In view of those results, anthropogenic materials, represented by diverse slag trapped within the beachrock outcrops, were examined more in detail through Raman spectroscopy. Considering the composition of the analysed slag (containing for instance, hematite, cristobalite, tephroite, rhodonite or labradorite), they might derive from the industrial activities developed nearby, denoting the recent formation of the beachrock. In addition, thanks to Raman spectroscopy, with a remarkable contribution of *in situ* analyses, possible hydration and decaying intermediate products were identified (like gypsum or thaumasite), suggesting the kind of reactions that might occur within these deposits, leading to believe that they are daily dynamic systems exposed to weathering processes that can cause transformations in the slag.

Furthermore, quantitative elemental analyses were performed over beachrock samples from Arrigunaga and La Salvaje beach, by means of ICP-MS, aided by chemometric analyses, to examine and assess the contamination that they might retain. The elemental distribution was found to be different along both beaches, probably due to their different locations, characteristics, and the diverse impact factors that they have been exposed to. In Arrigunaga beach, although the regeneration process occurred in the late 90s will be taken into account, the major elements (Ca, Al, Mg, Fe, Mn and K) seem to be accumulated in the northern area, while other metals are more widespread along the beach. In La Salvaje beach, in contrast, the concentration of many elements (such as, Sn, Hg, Tl, Zn, Ti, Mo, Ba, Mn), decreases from the southwestern area towards the mid part of the beach, with the exception of a significantly higher concentration of Fe, which comes in agreement with the blackening of the loose sand, probably because of the accumulation of iron rich particles derived from industrial wastes. In any case, the contamination

assessment suggested that the beachrock outcrops examined in both settings evidenced a moderate to high contamination degree.

Regarding the cements, an investigation based on staining methods, microscopic techniques (polarization microscopy, fluorescence microscopy and electron microscopy, including SEM-EDX and BSE), together with XRD and Raman spectroscopy, diverse phases were identified: (1) a micritic coating primarily composed of HMC, containing on average 10.7-14.3% mol $MgCO_3$; (2) an isopachous acicular rim, which is the predominant carbonate cement and it is formed with aragonite crystals; (3) infiltrated micritic particles that can be found over the aragonite crystals or occluding the pore space, only in certain areas of Arrigunaga beach; (4) ferruginous cements composed of various iron oxides and oxyhydroxides (like hematite, limonite, lepidrocrocite, goethite and magnetite) as well as, other sporadic composites like Fe and Mn carbonates.

According to these characteristics and evidenced also by stable isotope analyses ($\delta^{13}C$ and $\delta^{18}O$) of the carbonate cements, in Arrigunaga, the beachrock outcrops would be formed under mixed shallow marine-meteoric conditions, while in La Salvaje beach the diagenetic environment seems to be mainly shallow marine. Furthermore, the stable isotope analyses also allowed to confirm that part of the cements are related with marine fluids that might have been influenced by the oxidation of organic matter. On the whole, the diverse characteristics of the cements suggest that they were exposed to changing diagenetic environments, where the cementation was likely to be induced by a combination of biological and chemical factors that lead to the conditions required for the precipitation of the carbonate cements.

Resumen

Las arenas cementadas, también conocidas como “beachrock”, son estructuras sedimentarias costeras que se forman en la zona intermareal debido a la precipitación de carbonatos (principalmente) que actúan como cementos, agregando los diversos granos que puede haber presentes en la playa, convirtiendo la arena suelta en arena consolidada. Estas estructuras son típicas en regiones tropicales y subtropicales, y en cambio, menos frecuentes en las zonas templadas, como es el caso del área de estudio. Concretamente, el presente trabajo se centra en la investigación de las arenas cementadas de playa de Arrigunaga y de La Salvaje, las cuales se sitúan en los alrededores del estuario Nerbioi-Ibaizabal (Bilbao, Norte de España), un área drásticamente alterada debido al proceso de industrialización y urbanización que tuvo lugar hace más de un siglo.

En este contexto, en primer lugar se obtuvieron unas nociones sobre las características composicionales de los afloramientos de arena cementada, mediante el análisis químico sobre materiales clasificados en función de distintos tamaños de partícula. En base a ello, se pudo estimar que los cementos están compuestos de carbonato de calcio y además, se evidenció la presencia de aportes externos de origen antropogénico. En vista de esos resultados, los materiales antropogénicos, representados por las diversas escorias atrapadas en los afloramientos de arena cementada, se analizaron por espectroscopia Raman. Considerando la composición de las escorias (conteniendo por ejemplo, hematita, cristobalita, tefroita, rodonita y labradorita), podrían proceder de las actividades industriales desarrolladas en el entorno y denotan la reciente formación del fenómeno. Es más, gracias a la espectroscopia Raman, especialmente a los análisis *in situ*, se han identificado posibles productos de alteración, lo cual induce a plantear las posibles reacciones que pueden estar ocurriendo en estos depósitos y considerarlos como sistemas dinámicos que están expuestos a los efectos de la intemperie.

En un siguiente paso, se realizaron análisis cuantitativos de muestras de *beachrock* tanto de la playa de Arrigunaga como de La Salvaje, mediante ICP-MS junto con análisis quimiométricos, para examinar y evaluar la contaminación que posiblemente está retenida en ellas. La distribución elemental difiere a lo largo de cada una de las playas, posiblemente debido a su distinta localización, sus características y los diversos factores de impacto a las que han estado expuestos. En la playa de Arrigunaga, teniendo en cuenta la regeneración a la que se sometió a finales de los años 90, se vio que los elementos mayoritarios (Ca, Al, Mg, Fe, Mn y K) se acumulan al norte, mientras que el resto de los metales están más distribuidos a lo largo de la playa. En la playa de La Salvaje en cambio, la concentración de varios elementos (como Sn, Hg, Tl, Zn, Ti, Mo, Ba, Mn) disminuye desde el suroeste de la playa hacia la zona media, a excepción del hierro, que presenta una concentración significativamente más alta coincidiendo con el ennegrecimiento de la arena suelta debido probablemente a la acumulación de partículas de

hierro derivadas de restos industriales. De todas formas, los afloramientos de arena cementada analizados en ambos emplazamientos muestran un grado de contaminación que podría clasificarse de moderado a alto.

En lo que a los cementos que compactan las arenas se refiere, un estudio basado en técnicas de tinción, técnicas microscópicas (microscopía de luz polarizada, microscopía de fluorescencia y microscopía electrónica, incluyendo SEM-EDS y BSE), complementado por XRD y espectroscopia Raman, ha permitido identificar diversas fases: (1) una cubierta micrítica compuesta principalmente por HMC (contiene, como promedio, 10.7-14.3% mol $MgCO_3$); (2) un revestimiento isopaco acicular, compuesto principalmente de aragonito, que es el cemento predominante; (3) partículas infiltradas que pueden encontrarse tanto sobre los cristales de aragonito, como ocupando el espacio de poro, solamente en áreas concretas de la playa de Arrigunaga; (4) cementos ferruginosos compuestos de varios óxidos e oxihidróxidos de hierro (como por ejemplo, hematita, limonita, lepidocrocita, goetita y magnetita) así como otros compuestos más esporádicos como carbonatos de Fe y Mn.

Además, los análisis de isotopos estables ($\delta^{13}C$ y $\delta^{18}O$) realizados sobre los cementos de carbonato, han permitido suponer que los afloramientos de Arrigunaga se han formado en un ambiente meteórico-marino poco profundo, mientras que los de La Salvaje parecen haberse formado principalmente en un entorno marino poco profundo. Igualmente, el análisis de isotopos estables también ha permitido confirmar que parte de los cementos pueden estar relacionados con fluidos marinos que han estado influenciados por ejemplo por la oxidación de material orgánica. En términos generales, las diversas características de los cementos sugieren que han estado expuestos a ambientes diagenéticos variables, donde la cementación fue posiblemente inducida por una combinación de factores biológicos y químicos que dieron paso a las condiciones requeridas para la precipitación de los cementos.

Laburpena

Harea zementatuak, "beachrock" moduan ere ezagunak, kostaldeko egitura sedimentarioak dira. Marearteko zonaldean eratzen dira, zementu gisa jarduten duten karbonatoen hauspeatzearen ondorioz (gehien bat), hondartzan egon daitezkeen sedimentu aleek bat egiten dutenean, hau da, harea soltea harea kontsolidatu bilakatzen da. Egitura hauek eskualde tropikal eta subtropikaletan dira ohikoak, baina ez horrenbeste ikerlan honen aztergai den eremua bezalako eskualde epeletan. Zehazki, lan honetan Arrigunaga eta La Salvaje hondartzak aztertu dira, Nerbioi-Ibaizabal itsasadarraren inguruan kokatuta daudenak (Bilbo, Espainiako iparraldea). Eremu hau erabat eraldatutako estuarioa da, orain dela mende bat baino gehiago gertatutako industrializazio eta urbanizazio prozesua arrazoi.

Testuinguru honetan, harea zementatuen ezaugarri orokorrak partikula tamaina ezberdinetan sailkatutako laginen gaineko analisi kimikoaren bidez determinatu ditugu. Horrela, zementua kaltzio karbonatoz osatuta egon daitekeela behatu, eta gainera, jatorri antropogenikoa izan zezaketen partikulen presentzia agerian jarri dugu. Emaitza horiek ikusita, harea zementatuetan harrapaturiko fundizio labeetako zepak aztertu ditugu Raman espektroskopia bidez. Analisi horien emaitzen arabera (adibidez, hematita, kristobalita, tefroita, rodonita edo labradorita bezalako konposatuak), esan dezakegu zabor horien jatorria inguruneko jarduera industrialak direla, eta hortaz, ikuspegi geologikotik, harea hauen zementazioa gertatu berri den fenomenoa izan daitekeela. Bestalde, Raman espektroskopiari esker, batez ere, *in situ* analisiei esker, *beachrock* hauek inguruneko baldintzen eraginpean dauden sistema dinamikoak izan daitezkeela frogatu dugu, zepen transformazio produktuak identifikatu eta horien formazioa azalduko luketen erreakzioak proposatu baititugu.

Hurrengo urrats batean, Arrigunagako eta La Salvajeko hondartzetan dauden harea zementatuen metalen azterketa kuantitatiboa egin dugu. Zehazki, ICP-MS eta analisi kimiometrikoak burutuz, egitura horietan harrapatuta egon daitekeen kutsaduraren ikuskapena eta balorazioa egin dugu. Gunearen arabera, elementuen distribuzioa desberdina dela antzeman da hondartza bietan, seguruenik, bakoitzaren kokapena, ezaugarriak eta jasandako ingurumen aldaketak ezberdinak direlako. Arrigunaga hondartzan, 90.hamarkadaren amaieran egindako egokitzapen prozesua kontuan izan beharra dago eta egun elementu nagusiak (Ca, Al, Mg, Fe, Mn eta K) iparraldean metatzen dira gehien bat, beste metalak hondartzan luzetara sakabanatuta daudelarik. La Salvaje hondartzan aipatzekoa da, ordea, hainbat elementuren kontzentrazioa (esaterako, Sn, Hg, Tl, Zn, Ti, Mo, Ba edo Mn) hondartzako hego-mendebaldetik erdialderantz murriztuz doala; salbuespena burdinaren kasua izango litzateke. Izan ere, burdinaren kontzentrazioa altuagoa baita La Salvajeko hondartzaren erdialdean dagoen harea zementatuan, non harea soltearen kolorea nabarmenki beltzagoa den, beharbada jatorri industrialaren eta gehien bat burdinez osotuta dauden hondakin industrialen ondorioz. Orokorrean, esan daiteke

hondartza bietan aztertutako egiturek analizatutako elementuei dagokienean duten kutsadura maila moderatu eta altu bitartekoa dela.

Zementuei dagokienez, tindatze metodoak, teknika mikroskopikoak (argi polarizatuaren mikroskopia, fluoreszentzia mikroskopia eta mikroskopio elektronikoa) erabiliz, baita Raman espektroskopiaz eta X izpien difrakzioaz baliatuz, hainbat fase identifikatu ditugu: (1) gehien bat HMCz osotutako geruza mikritikoa (10.7-14.3% mol $MgCO_3$ dituena bataz beste); (2) estaldura azikularra, gehien bat aragonitoz osotuta dagoena eta nagusi den zementu fasea dena; (3) infiltratutako partikulak, aragonitozko kristalen gainean edo ale arteko poroak betez egon daitezkeenak eta Arrigunagako gune konkretu batzuetako laginetan baino aurkitu ez ditugunak,; (4) burdinez osatutako zementuak, gehienbat burdin oxido eta oxihidroxidoz osatuak (esaterako, hematita, limonita, lepidokrozita, goetita eta magnetita), baina noizbehinka Fe eta Mn karbonatoak ere izan ditzaketenak.

Horrez gain, isotopo egonkorren analisien ($\delta^{13}C$ eta $\delta^{18}O$) arabera Arrigunagako harea zementatuak azaleko meteoriko-itsasaldeko ingurunean eratu zirela, eta La Salvajekoak ostera, itsasaldekoan gehien bat. Era berean, isotopo egonkorren analisiak zementuak sortu direneko itsas urak nolabait adibidez materia organikoaren oxidazioaz eraginda egon ahal direla baieztatu du. Oro har, zementuen ezaugarriek, harea zementatuak ingurune diagenetiko aldakorren eraginpean daudela adierazten dute, non zementuen hauspeaketarako, eta ondorioz, zementazioa gertatzeko, beharrezkoak diren baldintzen artean faktore biologiko zein kimikoak aurkitzen ditugun.

“Una madrugada, en el instante más bajo de una bajamar, abandonaron el Océano y pisaron la playa de Arrigunaga cuarenta y ocho bichitos verdes. Carbono, Hidrógeno, Nitrógeno y Oxígeno se miraron, orgullosos de su obra. Aunque, de pronto, les sobresaltó una visión de lo que sería el futuro. Y se estremecieron.”

Ramiro Pinilla
(*Andanzas de Txiki Baskardo*, 1980)

Chapter 1

Introduction

Beachrocks enclose a coastal phenomenon that could lead to the formation of cemented structures which can be rather diverse and complex in source. Furthermore, in this case it might be necessary to bear in mind the historical background of the area in an attempt to recognize the peculiarities of the beachrock formations under study. Therefore, to enlighten the reader on this subject, the information gathered along these pages accounts for the fundamentals of beachrock phenomenon, and describes the context of the Nerbioi-Ibaizabal estuary, to set the basis to understand the uncommon beachrock formations object of study.

3.1 Beachrock

1.1.1 Definition and nature

Beachrocks are defined as friable to well-cemented sedimentary coastal structures typically formed in the intertidal zone (Figure 1.1.) due to the precipitation of carbonates (principally) that act as cements, packing together the wide array of sediments that might be present in the beach.

Beachrock formations can be vastly diverse in grain size, composition and mineralogy, however, the morphology is considered as characteristically uniform, forming lithified subhorizontal layers, in the form of beds or slabs, that tend to dip seaward[1] (Figure 1.2). In this sense, seaward is where the oldest bands are commonly found, and they are seldom outcropping in the surf and swash zones (also known as *foreshore*) (Figure 1.1)[2,3].

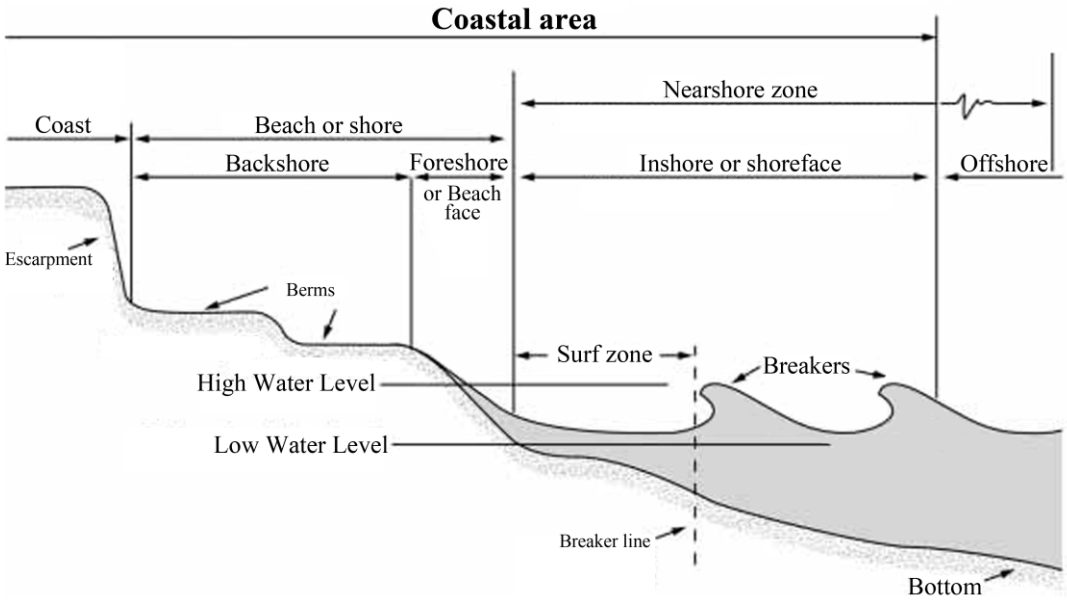

Figure 1.1. Diagram showing a typical beach profile. Beachrocks usually form in the intertidal zone (the area between tide marks) and outcrop in the surf and swash zones (or *foreshore*). Source: Dean and Dalrymple (2002)[4].

[1] Taborosi D., Mylroie J.E., Hirakawa K., and Mylroie J.R., **2006**. *A new morphology of beachrock: stalactitic deposits of lithified beach sand.* In: Gamble D. and Davis L. (Eds.), Proceedings of the 12th Symposium on the Geology of the Bahamas and other Carbonate Regions, pp. 228-232.
[2] Strasser, A., Davaud, E., Jedoui, Y., **1989**. *Carbonate cements in Holocene beachrock: example from Bahiret et Biban, southeastern Tunisia*. Sedimentary Geology 62, 89-100.
[3] Vousdoukas M.I., Velegrakis A.F., Karambas T.V., **2009**. *Morphology and sedimentology of a microtidal beach eith beachrocks: Vatera, Lesbos, NE Mediterranean*. Continental Shelf Research 29, 1937-1947.
[4] Dean R.G., Dalrymple R.A., **2002**. *Coastal processes with engineering applications*. Cambridge University Press, Cambridge, 471 pp.

Beachrocks are generally formed by multiple units that account for diverse episodes of cementation and exposure[5]. Thus, they can be commonly found forming a set of allied but dissimilar deposits[6] (Figure 1.2). Indeed, sometimes beachrocks can be present along the whole length of the beach, but they can also be discontinuous throughout the coast, as they might emerge as patches limited by loose sediments or by their complete ending[6,7]. Probably, the formation and preservation of a beachrock unit on a certain area of the beach is indirectly proportional to an increase in the wave energy and frequency of beach erosion along the shore[5].

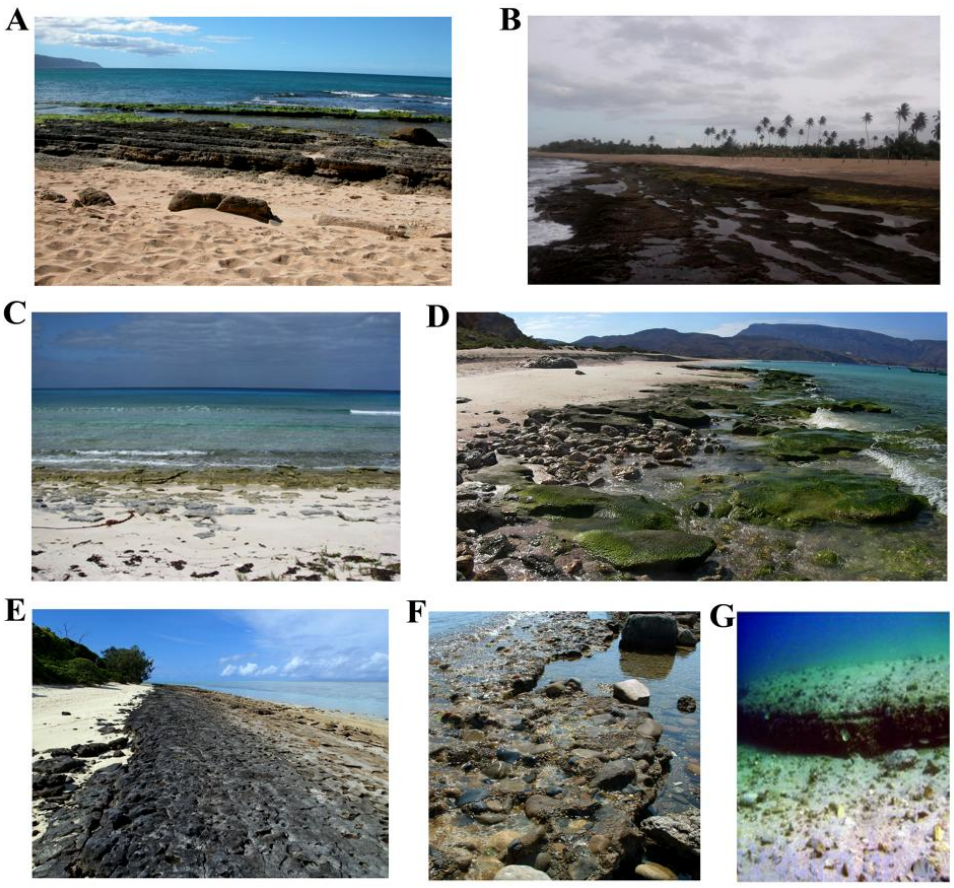

Figure 1.2. A) Stratified layers of beachrocks dipping seaward, in Oahu, Hawaii. B) Exposed beachrock formations from Hatillo, Puerto Rico. C) Beachrock from San Salvador, Bahamas. D) Beachrock slabs from Socrota, Yemen. E) Beachrock from Heron Island, with a blackish coloration due to a thin crust of cyanobacteria and lichen covering the surface. F) Diverse clasts cemented in a beachrock from Messina, Italy. G) Underwater beachrock platform from the Peloponnese, in Greece.

[5] Turner R.J., **2005**. *Beachrock*. In: Schwartz M.L. (Ed.), Encyclopaedia of Coastal Science. Kluwer Academic Publishers, The Netherlands, pp. 183-186.
[6] Taborosi D., Mylroie J.E., Hirakawa K., and Mylroie J.R., **2006**. *A new morphology of beachrock: stalactitic deposits of lithified beach sand.* In: Gamble D. and Davis L. (Eds.), Proceedings of the 12th Symposium on the Geology of the Bahamas and other Carbonate Regions, pp. 228-232.
[7] Vousdoukas M.I., Velegrakis A.F., Karambas T.V., **2009**. *Morphology and sedimentology of a microtidal beach eith beachrocks: Vatera, Lesbos, NE Mediterranean*. Continental Shelf Research 29, 1937-1947.

According to the literature, the thickness of these sedimentary structures can vary from a few centimeters to as much as five meters, but generally, they are around two meters thick. The level of cementation can differ depending on diverse factors, such as composition, porosity or permeability, but it is believed that the precipitation of cements occurs more rapidly in the top of a beachrock unit[8].

1.1.2 Occurrence and distribution

Numerous studies have been carried out in reference to this phenomenon since the early 19th century, when authors like Sir Francis Beauford (1817)[9], Chamisso (1821)[10], Moresby (1835)[11], Darwin (1841)[12], Dana (1849)[13] or Gardiner (1898)[14], firstly recognized the presence of beachrock formations.

Afterwards, during the early 20th century, various authors outlined the first knowledge around the characteristics of these structures, pointing that it is a process common in tropical and subtropical coasts[15-17]. More contemporary studies indicate that beachrock can also occur in temperate[18] and cold latitudes[19]. However, warm climates with calcium carbonate-rich pore waters are generally considered as fundamental requisites for beachrock formation[20].

A thorough review performed by Vousdoukas et al. (2007)[21], representatively describes the distribution of beachrock formations. According to their analysis, the Mediterranean and Caribbean Seas, the tropical and subtropical Atlantic coasts, together

[8] Turner R.J., **2005**. *Beachrock*. In: Schwartz M.L. (Ed.), Encyclopaedia of Coastal Science. Kluwer Academic Publishers, The Netherlands, pp. 183-186.
[9] Goudie A., **1969**. *A note on Mediterranean beachrock: its history*. Atoll Research Bulletin 126, 11-14.
[10] Chamisso A.V., **1821**. *Bemerkungen und Ansichten von dem Naturforscher der Expedition*. In: Kotzebue, O. V., Entdeckungs-Reise in die Sud-See und nach der Berings-Strasse zur Erforschung einer nordostlichen Durchfahrt. vol. 3, Hofmann, Weimear, 240 pp.
[11] Moresby R., **1835**. *Extracts from commander Moresby's report on the northern atolls of the Malvides*. Journal of the Royal Geographical Society 5, 398-404.
[12] Darwin C., **1841**. *On a remarkable bar of sandstone off Pernambuco on the coast of Brazil*. The London, Edinburgh and Dublin Philosophical Magazine 19, pp. 257-260.
[13] Dana, J. D., **1875**. *Corals and coral islands*. London, Sampson Low, Marstonk Low and Searle, 338 pp.
[14] Gardiner J.S., **1898**. *The coral reefs of Funafuti, Rotuma and Fiji together with some notes on the structure and formation of coral reefs*. Cambridge Philosophical Society Proceedings, 9, 417-503.
[15] Vaughan T. W. **1914**. *Building of the Marquesas and Tortugas atolls and a sketch of the geologic history of the Florida reef tract*. Carnegie Institution of Washington Publication 182, Papers of the Department of Marine Biology 5, 55-67.
[16] Ginsburg R.N., **1953**. *Beach rock in South Florida*. Journal of Sedimentary Petrology 23, 85-92.
[17] Russell R.J., **1959**. *Caribbean beach rock observation*. Zeitschrift Fur Geomorpholigie 3, 227-236.
[18] Zenkovitch V.P., **1967**. *Processes of Coastal development*. Oliver and Boyd, London, 738 pp.
[19] Kneale D. and Viles H.A., **2000**. *Beach cement: incipient $CaCO_3$-cemented beachrock development in the upper intertidal zone, North Uist, Scotland*. Sedimentary Geology 132, 165-170.
[20] Gischler E., Lomando A.J., **2007**. Beachrock and Intertidal Precipitates. In: Nash D.J., McLaren S.J. (Eds.), Geochemical Sediments and Landscapes. Wiley-Blackwell, UK, pp. 365-390.
[21] Vousdoukas M.I., Velegrakis A.F., Plomaritis T.A., **2007**. *Beachrock occurrence, characteristics, formation mechanisms and impacts*. Earth-Science Reviews 85, 23-46.

with the atolls of the Pacific and Indian Oceans could be considered as the "hot spots" of beachrock occurrence (Figure 1.3). The majority of the studies reported in the literature, focus Australia (49), Greece (38) and then Brazil (36), as the areas with most reported beachrock occurrences. In addition, Israel, Seychelles and Puerto Rico comprise the greatest beachrock occurrences per coastline length.

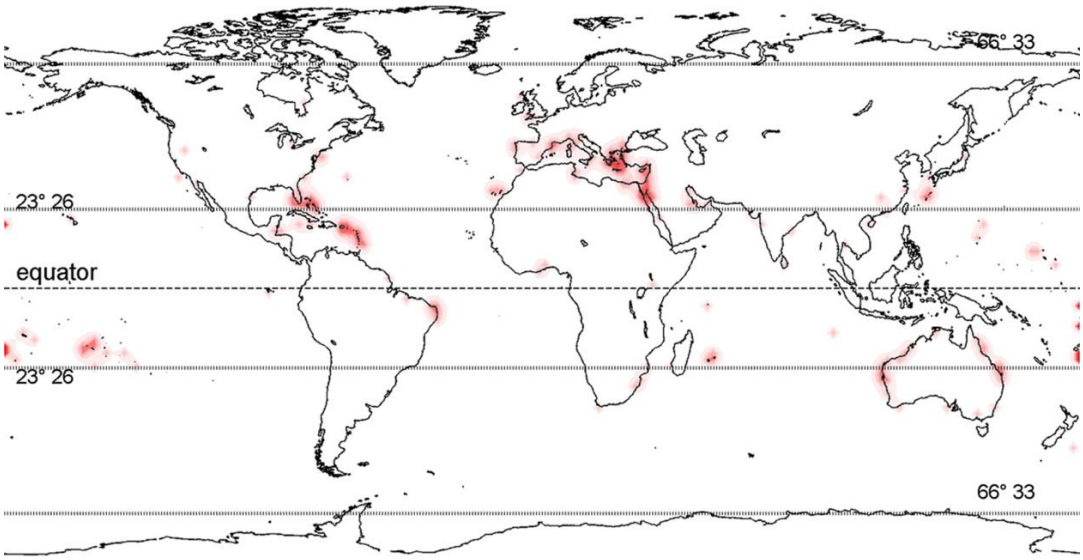

Figure 1.3. Prevailing geographical distribution of documented beachrock formations (the more intense the reddish shade, the greater is the occurrence). Source: Vousdoukas (2007)[22].

On the whole, diverse beachrock occurrences are described in *tropical or subtropical zones with humid climate* (for instance, in the Pacific Ocean[23], the Caribbean area[24], the Atlantic coast of Africa[25] and Brazil[26], in the Indian Ocean[27] and Australia[28]); in *tropical or subtropical zones with arid or semiarid climate* (like the Persian Gulf[29] and

[22] Vousdoukas M.I., Velegrakis A.F., Plomaritis T.A., **2007**. *Beachrock occurrence, characteristics, formation mechanisms and impacts*. Earth-Science Reviews 85, 23-46.
[23] Prager E.J., **1991**. *Anatomy of a Galapagos beachrock*. Sea Frontiers 37, 36-39.
[24] Gischler E., Lomando A.J., **1997**. *Holocene cemented beach deposits in Belize*. Sedimentary Geology 110, 277-297.
[25] Amieux P., Bernier P., Dalongeville R., Medwecki V., **1989**. *Cathodoluminescence of carbonate-cemented Holocene beachrock from the Togo coastline (West Africa): an approach to early diagenesis*. Sedimentary Geology 65, 261-272.
[26] Amaral R.F., Bezerra F.H.R., **2006**. *Mapping beachrock fracturing and erosion using small format aerial photography in northeastern Brazil*. Journal of Coastal Research 39, 270-274.
[27] Ramkumar M., Pattabhi Ramayya M., Gandhi M.S., **2000**. *Beachrock exposures at wave cut terraces of Modern Godavari delta: their genesis, diagenesis and indications on coastal submergence and sea-level rise*. Indian Journal of Geo-Marine Sciences 29, 219-223.
[28] Scoffin T.P., Stoddart D.R., **1983**. *Beachrock and intertidal sediments.* In: Goudie A.S., Pye K. (Eds.), Chemical Sediments and Geomorphology. Academic Press, London, pp. 401-425.
[29] Kendall C.G.S.C., Sadd J.L., Alsharhan A., **1994**. *Holocene marine cement coatings on beach-rocks of the Abu Dhabi coastline (UAE): analogs for cement fabrics in ancient limestones*. Carbonates and Evaporites 9, 119-131.

the Red Sea[30]); in *mediterranean climate zones* (principally around the Mediterranean Sea[31]) as well as in *temperate climates* (mainly around the Atlantic Ocean[32], but also close to the Black Sea[33] and the Indian Ocean[34]). Beachrock occurrences from Polar Regions have not been reported yet[35].

Vousdoukas et al. (2007)[36], mentioned 91 beachrock locations in all these areas, and it is remarkable that only 8 of them are located in a temperate climate. Updating that list, some new cases can be found for instance in the United Kingdom[37], French West Indies[38], Spain[39], Turkey[40] or Taiwan[41]. But, in any case, studies of beachrock occurrences located in a temperate zone are still a minority in the available literature.

Taking into consideration the above mentioned information it can be said that, regarding the occurrence, beachrock formations are common in tropical and subtropical areas (0-40º latitude), but they have seldom been documented in cold-temperate zones (40-66º latitude). As mentioned by some authors[35-36], the minor presence of temperate beachrocks in the literature leads to believe that colder latitudes do not encourage the formation of beachrocks. Thus, the investigation of beachrock formations located in temperate settings might be necessary as it would provide with further valuable information to comprehend the precipitation of carbonates in the marine realm, allowing the understanding of uncommon beachrock formations.

[30] Friedman G.M., Gavish E., **1971**. *Mediterranean and Red Sea (Gulf of Aqaba) beachrocks*. In: Bricker O.P. (Ed.), Carbonate Cements. The Johns Hopkins Press, Baltimore, M.D., pp. 13-16.
[31] Bernier P., Dalongeville R., **1996**. *Mediterranean coastal changes recorded in beach-rock cementation*. Zeitschrift für Geomorphologie 102, 185-198.
[32] Rey D., Rubio B., Bernabeu A.M., Vilas F., **2004**. *Formation, exposure, and evolution of a high-latitude beachrock in the intertidal zone of the Corrubedo complex (Ria de Arousa, Galicia, NW Spain)*. Sedimentary Geology 169, 93-105.
[33] Georgiev V.M., **1989**. *Recent beach rock formation in the Alepou Bay, Bulgarian Black Sea coast*. Comptes rendus de l'Academie bulgare des Sciences 42, 73-76.
[34] Siesser, W.G., **1974**. *Relict and recent beachrock from Southern Africa*. Geological Society of America Bulletin 85, 1849-1854.
[35] Gischler E., Lomando A.J., **2007**. *Beachrock and Intertidal Precipitates*. In: Nash D.J., McLaren S.J. (Eds.), Geochemical Sediments and Landscapes. Wiley-Blackwell, UK, pp. 365-390.
[36] Vousdoukas M.I., Velegrakis A.F., Plomaritis T.A., **2007**. *Beachrock occurrence, characteristics, formation mechanisms and impacts*. Earth-Science Reviews 85, 23-46.
[37] Howie F.M.P., **2009**. *Beachrock development along the North coast of Cornwall*. Geoscience in South-West England 12, 85-94.
[38] Vincent C., **2011**. *Contrasted textural and taphonomic properties of high-energy wave deposits cemented in beachrocks (St. Bartholomew Island, French West Indies)*. Sedimentary Geology 237, 189-208.
[39] Arrieta N., Goienaga N., Martínez-Arkarazo I., Murelaga X., Baceta J.I., Sarmiento A., Madariaga J.M., **2011**. *Beachrock formation in temperate coastlines: Examples in sand-gravel beaches adjacent to the Nerbioi-Ibaizabal Estuary (Bilbao, Bay of Biscay, North of Spain)*. Spectrochimica Acta Part A 80, 55-65.
[40] Erginal A.E., Kıyak N.G., Ozturk M.Z., Avcioglu M., Bozcu M., Yiğitbaş E., **2012**. *Cementation characteristics and age of beachrocks in a fresh-water environment, Lake İznik, NW Turkey*. Sedimentary Geology 243-244, 148-154.
[41] Lau A.Y.A., Terry J.P., Switzer A.D., Pile J., **2015**. *Advantages of beachrock slabs for interpreting high-energy wave transport: evidence from Ludao Island in south-eastern Taiwan*. Geomorphology 228, 263-274.

1.1.3 Speed of cementation and age

The cementation of beach sediments can generally be very rapid, taking place in a time range of months to years[42-44]. For instance, it has been reported that Indian Ocean natives would collect beachrocks as building materials and new cemented structures would form within a year[45]. Usually, the materials incorporated within the beachrock formations, such as recent or modern man-made vestiges allow testifying the rapidity of the cementation[46]. For instance, Emery et al. (1954)[47] described the presence of World War II reminders in beachrocks from the Marshall Islands.

Some beachrock formations can belong to the Pleistocene epoch (from 2.600.000 to 12.000 years ago, approximately)[46], however, the greater number of beachrocks are predominantly originated during the Holocene era (from nearly 12.000 years ago till current times). Indeed, although not many of the documented beachrocks have been subjected to radiocarbon dating, the majority of them can have been formed in the last 1000-5000 years, and few of them are far more recent (Figure 1.4). Nevertheless, this information has to be taken with caution, because apart from carbonate cements, beachrocks incorporate more aged biogenic compounds or carbonate clasts, and thus, carbon dating results can be biased to older dates[48].

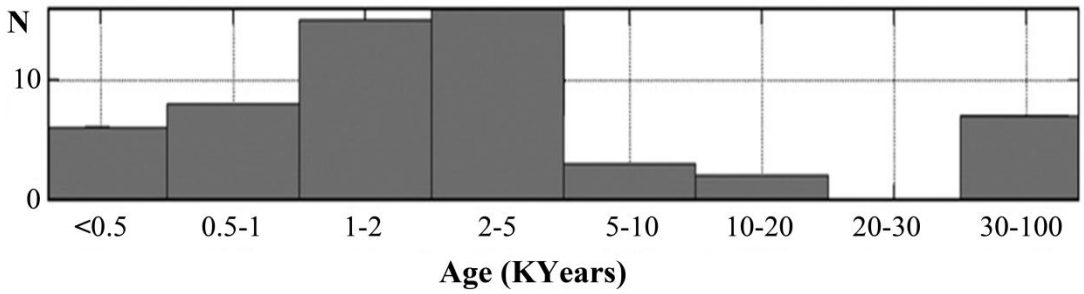

Figure 1.4. Age (KYears, years x 10^3) of beachrock occurrences (N) reported in the literature. Source: Vousdoukas (2007)[48].

[42] Frankel E., **1968**. *Rate of formation of beachrock*. Earth and Planetary Science Letters 4, 439-440.
[43] Easton W.H., **1974**. *An unusual inclusion in beachrock*. Journal of Sedimentary Petrology 44, 693–694.
[44] Eberli G.P., Baechle B., Anselmetti F, Incze M., **2003**. *Factors controlling elastic properties in carbonate sediments and rocks*. The Leading Edge 22, 654-660.
[45] Moresby R., **1835**. *Extracts from commander Moresby's report on the northern atolls of the Malvides*. Journal of the Royal Geographical Society 5, 398-404.
[46] Turner R.J., **2005**. *Beachrock*. In: Schwartz M.L. (Ed.), Encyclopaedia of Coastal Science. Kluwer Academic Publishers, The Netherlands, pp. 183-186.
[47] Emery K.O., Tracey J.I.J., Ladd, H.S.A., **1954**. *Geology of Bikini and nearby atolls*. U.S. Geological Survey Proffesional Paper 260 (260A), 265.
[48] Vousdoukas M.I., Velegrakis A.F., Plomaritis T.A., **2007**. *Beachrock occurrence, characteristics, formation mechanisms and impacts*. Earth-Science Reviews 85, 23-46.

1.1.4 Modern marine carbonate cements

1.1.4.1 Most common carbonate cements

Carbonate minerals include the anionic complex CO_3^{2-} as essential composite of their structure, associated to one or more cations that configure diverse carbonate minerals. The most common carbonates in ancient carbonate rocks are calcite and specially dolomite, whilst in modern sediments and marine cements the calcium carbonate polymorphs aragonite and calcite are more usual[49]. As in modern marine environments aragonite and HMC metastable phases are common (alternated coatings of both of them can co-occur[50]), their main characteristics will be described.

Aragonite ($CaCO_3$) contains an orthorhombic crystal system and that arrangement favours the incorporation of cations larger than 1 Å, such as Sr^{2+}, Pb^{2+} and Ba^{2+}, mainly. Among them, the most important trace element is Sr and marine aragonite usually contains around 5.000-10.000 ppm of this element. In contrast, Mg can be found in the aragonite lattice in a very low concentration[51]. The preference of Sr incorporation and the low content of Mg can help distinguishing aragonite from calcite. Aragonite is common in modern marine sediments as part of skeletal constituents or cements[49].

Calcite ($CaCO_3$) includes a rhombohedral (trigonal) crystal system and usually tends to incorporate cations smaller than 1 Å, like Mg^{2+}, Fe^{2+}, Mn^{2+} and Zn^{2+}, in its lattice[52]. In this case, it is particularly usual the substitution of Ca^{2+} by Mg^{2+}, and depending on the $MgCO_3$ content, different types of calcite can be found: low magnesian calcite (LMC) and high magnesian calcite (HMC), being the threshold between them usually 4 mole % of $MgCO_3$ [53,54]. The lower the temperature, the less $MgCO_3$ mol % can be included in the calcite crystal, therefore, the Mg content of calcites usually tends to decrease from tropical warm waters to high latitude colder areas[50]. In modern marine environments, magnesian calcites can be found in skeletal grains, ooids or cements[55].

[49] Flügel E., **2004**. *Microfacies of Carbonate Rocks*. Springer Science & Business Media, New York, 976 pp.
[50] Opdyke B.N., Wilkinson B.H., **1990**. *Paleolatitude distribution of Phanerozoic marine ooids and cements*. Palaeogrography, Palaeoclimatology, Palaeoecology 78, 135-148.
[51] Boggs S., **2009**. *Petrology of Sedimentary Rocks*. Cambridge University Press, UK, 600 pp.
[52] Hanken N-M., Bjorlykke K., Nielsen J.K., **2010**. *Carbonate Sediments*. In: Bjorlykke K. (Ed.), Petroleum Geoscience: From sedimentary environments to rock physics. Springer-Verlag, Germany, pp. 141-200.
[53] Andersson A.J., Mackenzie F.T., Bates N.R., **2008**. *Life on the margin: implications of ocean acidification on Mg-calcite, high latitude and cold-water marine calcifiers*. Marine Ecology Progress Series 373, 265-273.
[54] Morse J.W., Arvidson R.S., Lüttge A., **2007**. *Calcium carbonate formation and dissolution*. Chemical Reviews 107, 342-381.
[55] Morse J.W., **2003**. *Formation and diagenesis of carbonate sediments*. In: Mackenzie F.T. (Ed.), Sediments, Diagenesis and Sedimentary Rocks 7. Treatise on Geochemistry (Hollan H.D., Turkeian K.K., Eds.). Elsevier, Oxford, pp. 67-86.

1.1.4.2 Factors controlling the precipitation of carbonates

In spite of all the research performed about beachrocks in the last decades, the prevailing factors that control the characteristics of the carbonate cements are not well understood yet. However, some chemical, physical and sedimentological properties seem to influence in the precipitation of the carbonate cements[56,57].

a) Chemical conditions

The mineral calcium carbonate ($CaCO_3$) has a crystal lattice containing one calcium ion (Ca^{2+}) ionically linked to one carbonate ion (CO_3^{2-}), and it can conform diverse polymorphs, like calcite (with a trigonal structure) or aragonite (with an orthorhombic structure)[58].

As specified by Morse and Mckenzie (1990)[59], one of the most relevant and interesting attributes that characterizes the geochemistry of sedimentary carbonates, is that the anion CO_3^{2-} is involved in the intricate carbonate system. Accordingly, to understand the formation of beachrock through the precipitation of carbonates, the marine carbonate system, as well as calcium carbonate precipitation and dissolution should be taken into account. When atmospheric CO_2 comes into contact with seawater, it can become dissolved into the water, where depending on the pH, bicarbonate and carbonate ions can be formed (Eq. 1.1). This dissociation is a process that strongly depends on pH[60].

$$CO_2 + H_2O \leftrightarrow H_2CO_3 \leftrightarrow HCO_3^- + H^- \leftrightarrow CO_3^{2-} + 2H^+ \qquad \text{(Eq. 1.1)}$$

The alkalinity of seawater is determined by the concentration of bicarbonate ions (HCO_3^-) and carbonate ions (CO_3^{2-}), as well as boric acid (HBO_3^-) in a lesser extent. However, carbonates alkalinity is a function of the bicarbonate and carbonate ions[59,60].

[56] Molenaar N., Venmans A.A.M., **1993**. *Calcium carbonate cementation of sand: a method for producing artificially cemented samples for geotechnical testing and a comparison with natural cementation processes*. Engineering Geology 35, 103-122.
[57] Vousdoukas M.I., Velegrakis A.F., Plomaritis T.A., **2007**. *Beachrock occurrence, characteristics, formation mechanisms and impacts*. Earth-Science Reviews 85, 23-46.
[58] Ridgwell A., Zeebe R.E., **2005**. *The role of the global carbonate cycle in the regulation and evolution of the Earth system*. Earth and Planetary Science Letters 234, 299-315.
[59] Morse J.W., Mackenzie F.T., **1990**. *Geochemistry of Sedimentary Carbonates*. Elsevier, The Netherlands, 707 pp.
[60] Gischler E., Lomando A.J., **2007**. *Beachrock and Intertidal Precipitates*. In: Nash D.J., McLaren S.J. (Eds.), Geochemical Sediments and Landscapes. Wiley-Blackwell, UK, pp. 365-390.

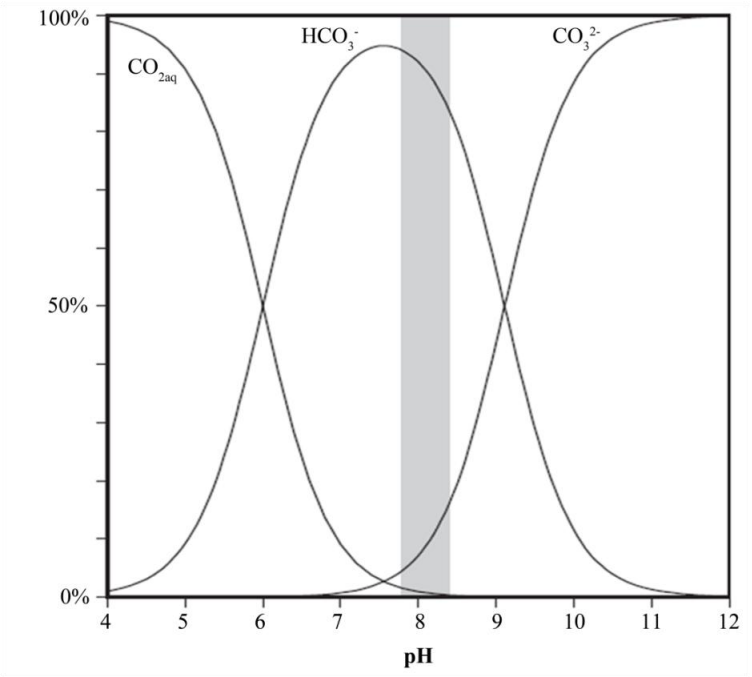

Figure 1.5. Speciation diagram of the carbonic acid system in seawater as a function of pH. The grey coloured area indicates the typical pH value of modern seawater. Source: Neumeier (1998)[61].

The three inorganic carbonate species (CO_2, HCO_3^- and CO_3^{2-}) can co-exist in seawater, but under normal marine conditions, and thus in a pH around 8, bicarbonate ions prevail (Figure 1.5). Indeed, bicarbonate ions, formed upon the dissolution of CO_2 gas, are ubiquitous in seawater. In addition, Ca^{2+} is naturally abundant in seawater, being among the ionic species with highest concentration in the ocean (after Cl^-, Na^+, Mg^{2+} and SO_4^{2-})[62,63]. Therefore, under normal marine conditions, Ca^{2+} and HCO_3^- can react to form calcium carbonate (Eq. 1.2).

$$Ca^{2+} + 2HCO_3 \leftrightarrow CaCO_3 + H_2O + CO_2 \qquad \text{(Eq. 1.2)}$$

In relation with the precipitation of carbonates, apart from pH, there are also other factors that can influence in the equilibrium of the three inorganic carbon species, such as, temperature, salinity and partial pressure of CO_2 (P_{CO2})[64,65]. Similarly to pH,

[61] Neumeier U., **1998**. *Le role de l'activite microbienne dans la cimentation precoce des beachrocks (sediments intertidaux)*. PhD Thesis, University of Geneva. 183 pp.
[62] Ridgwell A., Zeebe R.E., **2005**. *The role of the global carbonate cycle in the regulation and evolution of the Earth system*. Earth and Planetary Science Letters 234, 299-315.
[63] Kortazar L., Saez J., Astigarraga E., Goienaga N., Fernandez L., **2013**. *Chemometrics for the classification and calibration of seawater using the H+ affinity spectrum*. Talanta 116, 108-114.
[64] Millero F.J., **1995**. *Thermodynamics of the carbon dioxide system in the oceans*. Geochimica et Cosmochimica Acta 59, 661-677.
[65] Vousdoukas M.I., Velegrakis A.F., Plomaritis T.A., **2007**. *Beachrock occurrence, characteristics, formation mechanisms and impacts*. Earth-Science Reviews 85, 23-46.

increasing temperature and salinity stimulate the precipitation of carbonates, and on the contrary, a P_{CO2} increase will give rise to the dissolution of carbonates[66].

As just mentioned, an increase of temperature yields a decrease in the solubility of CO_2 and thus of $CaCO_3$ formation[67]. As such, the latitudinal temperature gradient implies that saturation of seawater with respect to $CaCO_3$ increases from polar regions to the Equator[66]. Therefore, it can be presumed that the preferential beachrock formation is manifested in areas with increasing temperatures[68]. This could be one of the differences between tropical areas, where high temperatures are common and beachrocks are quite usual and temperate zones, where colder temperatures are regularly found and beachrocks are rather uncommon. Nevertheless, the role of the temperature in carbonate precipitation could have more implications, especially nowadays that rising temperatures are related with the increasing atmospheric CO_2 concentrations occurred over the past two centuries, promoting a greater CO_2 uptake by the oceans with the consequent marine acidification[69,70]. The lower pH values can lead to the dissolution of carbonates, affecting to the formation and preservation of beachrocks. Thus, in the future, as affirmed by Vousdoukas et al. (2007)[68], various feedback mechanisms related with temperature can be involved in beachrock formation, which can be difficult to predict.

Regarding the salinity, which promotes the precipitation of carbonates, it should be remarked that meteoric waters usually contain much lower ion concentrations than marine waters. As a consequence, carbonates precipitation rates should be much lower in a meteoric environment and the precipitation would mainly depend on the availability of meteoric fluids, which would be a function of rainfall rates[66,71,72].

In addition, rising of P_{CO2} near the surface of Earth, increases the amount of CO_2 that could become dissolved in water, consequently increasing the solubility of

[66] Gischler E., Lomando A.J., **2007**. *Beachrock and Intertidal Precipitates*. In: Nash D.J., McLaren S.J. (Eds.), Geochemical Sediments and Landscapes. Wiley-Blackwell, UK, pp. 365-390.
[67] Molenaar N., Venmans A.A.M., **1993**. *Calcium carbonate cementation of sand: a method for producing artificially cemented samples for geotechnical testing and a comparison with natural cementation processes*. Engineering Geology 35, 103-122.
[68] Vousdoukas M.I., Velegrakis A.F., Plomaritis T.A., **2007**. *Beachrock occurrence, characteristics, formation mechanisms and impacts*. Earth-Science Reviews 85, 23-46.
[69] Feely R.A., Sabine C.L., Lee K., Berelson W., Kleypas J., Fabry J., Millero F.J., **2004**. *Impact of anthropogenic CO_2 on the $CaCO_3$ system in the oceans.* Science 305, 362-366.
[70] Chierici M., Fransson, **2009**. *Calcium carbonate saturation in surface water of the Artic Ocean: undersaturation in freshwater influenced shelves*. Biogeosciences 6, 2421-2432.
[71] Morse J.W., Mackenzie F.T., **1990**. *Geochemistry of Sedimentary Carbonates*. Elsevier, The Netherlands, 707 pp.
[72] Tucker M.E., **1990**. *Dolomites and dolomitization models*. In: Carbonate sedimentology (Eds. Tucker M.E., Wright V.P.). Blackwell Science Ltd., Oxford, 482 pp.

carbonate minerals. Anyway, the effect of P_{CO2} by itself does not affect the solubility of carbonates as much as the effect of temperature. Nonetheless, at great P_{CO2} conditions, for example, in deep sea, its effect alone can significantly increase the solubility of carbonates[73].

Despite the factors that control the precipitation of carbonates are quite known, upon the influence of parameters like temperature, salinity and P_{CO2}. In contrast, the controls on the mineralogy are not that clear. Apparently, Mg/Ca ratios of pore waters as well as supply rates of CO_3^{2-} could explain the different mineralogy of marine carbonates. In this sense, usually, aragonite is the predominant carbonate phase precipitated from seawater, because Mg^{2+} and SO_4^{2-} inhibit the growth of calcite crystals. Besides, when the precipitation rate is very fast, the supersaturation degree is high or temperature is high, calcium carbonate would precipitate as aragonite; otherwise, under less favouring conditions, calcite would be formed[74]. Therefore, the high water agitation that normally occurs in the intertidal zone, promote CO_2 degassing and the subsequent acidity decrease that results on a higher carbonate concentration. This way, supply rates of CO_3^{2-} can be high in the intertidal zone, encouraging the precipitation of aragonite instead of (magnesian) calcite[75,76].

b) Physical conditions

The cementation is inevitably associated to the hydrodynamic conditions undergoing in the depositional environment[77]. This way, one of the physical conditions that apparently control the formation of the cements is the magnitude and distribution of the wave energy alongside the coast[78]. Indeed, the main vector of the dissolved cementing material through the sand is seawater and the driving forces of water circulation through sediments are waves, tides, currents and evaporation. Therefore, high wave energy conditions and the subsequent constant supply of seawater can favour

[73] Krauskopf K.B., Dennis K. Bird, **1995**. *Introduction to Geochemistry*. McGraw-Hill, Inc., New York, 647 pp.
[74] Folk R.L., **1974**. *The natural history of crystalline calcium carbonate; effect of magnesium content and salinity*. Journal of Sedimentary Petrology 44, 40-53.
[75] Gischler E., Lomando A.J., **2007**. *Beachrock and Intertidal Precipitates*. In: Nash D.J., McLaren S.J. (Eds.), Geochemical Sediments and Landscapes. Wiley-Blackwell, UK, pp. 365-390.
[76] Given R.K., Wilkinson B.H., **1985**. *Kinetic control of morphology, composition and mineralogy of abiotic sedimentary carbonates*. Journal of Sedimentary Petrology 55, 109-119.
[77] Molenaar N., Venmans A.A.M., **1993**. *Calcium carbonate cementation of sand: a method for producing artificially cemented samples for geotechnical testing and a comparison with natural cementation processes*. Engineering Geology 35, 103-122.
[78] Vousdoukas M.I., Velegrakis A.F., Plomaritis T.A., **2007**. *Beachrock occurrence, characteristics, formation mechanisms and impacts*. Earth-Science Reviews 85, 23-46.

the cementation of the sediments. Indeed, in many cases, the higher frequency and degree of cementation is found on seaward areas[79].

Furthermore, areas preferentially facing the predominant wind and, as a consequence, more exposed to wave action, receive great amounts of seawater spray, promoting the formation of beachrock cement in that windward zone[75]. It is not surprising then that the presence of beachrock has been often related with high energy environments, in areas with high exposition to waves and tides[79-81].

Anyway, some counterarguments have been raised in this sense, because, although preferential beachrock formation can be found at high energy conditions, the greater agitation of the beach sediments, as well as the higher grain size of the sediments commonly characterizing high energy shallow marine environments, could limit the sediments stabilization and thus, the development of the cementation[79,82]. Indeed, the cemented layers are more discontinuous and less extensive in beachrocks found in low energy environments[84].

c) Sedimentological conditions

The sedimentological characteristics of the sediments that compose the beachrock can also control the cementation phenomenon. For the lithification to occur, it is required the introduction of fluids that would supply with the compounds and transformations that lead the cementation process.

Thus, well-washed sediments with high permeability and high porosity, that can provide sufficient vertical water circulation to supply the cementing materials, enable the formation of beachrock[79,83]. Those conditions generally converge in the intertidal zone and in the uppermost subtidal zones of high energetic environments[79].

[79] Molenaar N., Venmans A.A.M., **1993**. *Calcium carbonate cementation of sand: a method for producing artificially cemented samples for geotechnical testing and a comparison with natural cementation processes*. Engineering Geology 35, 103-122.
[80] Gischler E., Lomando A.J., **1997**. *Holocene cemented beach deposits in Belize*. Sedimentary Geology 110, 277-297.
[81] Howie F.M.P., **2009**. *Beachrock development along the North coast of Cornwall*. Geoscience in South-West England 12, 85-94.
[82] Vousdoukas M.I., Velegrakis A.F., Plomaritis T.A., **2007**. *Beachrock occurrence, characteristics, formation mechanisms and impacts*. Earth-Science Reviews 85, 23-46.
[83] Guerra N.C., Kiang C.H., Sial A.N, **2005**. *Carbonate cements in contemporaneous beachrocks, Jaguaribe Beach, Itamaraca Island, northeastern Brazil: petrographic, geochemical and isotopic aspects*. Anais da Academia Brasileira de Ciencias 77, 343-352.

Controls on cementation can be also related with the grain size of the sediments. For instance, the strength of the cemented sediments can be related with the number of cemented contact points per volume unit, which will be conditioned by the grain size distribution as well as the thickness and texture of the cement bridges between the grains. This way, fine grained sand provides more contact points per volume than coarse grained sand[84]. However, coarse grains can be also vulnerable to cementation[85], and provide adequate permeability and porosity conditions to ensure sufficient volumes of supersaturated water circulation within the pore system, and thus, succeed in the cementation[86].

Generally, the composition of the grains does not influence in the cementation process; it could take place either with carbonate grains, siliciclastic grains, or a mixture of both. Nevertheless, some authors state that in those cases in which the environmental and sedimentary characteristics are not propitious for the cementation, the composition and concentration of the grains do matter. This is likely to happen for example in temperate and sub-tropical locations, as well as in deep-water marine sedimentary environments[84].

In addition, the commencement of the cementation needs a moderate stabilization of the sediments, as it has been previously mentioned. Sediments can be somewhat immobilized for instance during a recess of the sedimentation process[84]. However, that stabilization of the sediments can be mainly induced by biologic-physical interactions, due to the presence of sea grasses and algal mats or other microbial mat assemblages[84,87,88]. For example, biofilms derived from cyanobacterial colonisations can coat diverse grains and bind them together, generating the stabilization of the sediments[89].

[84] Molenaar N., Venmans A.A.M., **1993**. *Calcium carbonate cementation of sand: a method for producing artificially cemented samples for geotechnical testing and a comparison with natural cementation processes*. Engineering Geology 35, 103-122.
[85] Longman M.W., **1980**. *Carbonate diagenetic textures from nearsurface diagenetic environments*. AAPG Bulletin 64, pp. 461-487.
[86] Moore C.H., **1997**. *Carbonate diagenesis and porosity*. Developments in Sedimentology 46, Elsevier, Amsterdam, 338 pp.
[87] Grant J., Gust G., **1987**. *Prediction of coastal sediment stability from photopigment content of mats of purple sulphur bacteria*. Nature 330, 244-246.
[88] Paterson D.M., Black K.S., **2000**. *Silicaltic Intertidal Microbial Sediments*. In: Riding R.E., Awramik S.M. (Eds.), Microbial Sediments. Springer-Verlag, Germany, pp. 217-225.
[89] Taher A.G., Abdel-Motelib A., **2013**. *Microbial stabilization of sediments in a recent Salina, Lake Aghormi, Siwa Oasis, Egypt*. Facies 60, 45-52.

1.1.5 Beachrock formation theories

1.1.5.1 Theoretical formation and evolution stages

There is a general agreement in the overall formation and evolution of beachrocks, which could consist in the following stages, as described by Turner (1999)[90] and Rey et al. (2004)[91]:

- At first, an initial cementation occurs in subsurface (under the uncemented sand) of the intertidal zone.

- Then, the outcropping of the cemented sand takes place, apparently enhanced by high energy events and the subsequent beach sand removal. The exhumation of the beachrocks leaves them exposed to wave action, shaping the cemented structures. This process could take from weeks to months.

- Once they are exposed during several weeks, beachrock outcrops are hardened and colonized by epilithic biota (microorganism and algae). That colonization gives a typical greenish coloration, indeed, Rey et al. (2004)[91] affirms that the greener it is, the more time it has been exposed. In this step, the cemented structures are consolidated and it could take from months to decades.

- If it is exposed for various decades with no relevant cementation, Turner (1999)[90] describes that beachrock units can disintegrate into blocks and slabs, and be moved or buried under the unconsolidated sediment. Besides, Rey et al. (2004)[91] explained that at favourable weather conditions, unconsolidated sand can progressively cover the cemented structures and if the cementation was efficient enough, the beachrock can remain until the next winter, when it could be exposed again.

[90] Turner R.J., **1999**. *The evolution of beachrock morphology and its influence on beach morphodynamics*. In: The non-steady-state of the inner shelf and shoreline: coastal change on the time scale of decades to millennia in the Late Quaternary. The University of Hawaii, pp. 185-190.
[91] Rey D., Rubio B., Bernabeu A.M., Vilas F., **2004**. *Formation, exposure, and evolution of a high-latitude beachrock in the intertidal zone of the Corrubedo complex (Ria de Arousa, Galicia, NW Spain)*. Sedimentary Geology 169, 93-105.

1.1.5.2 Mechanisms of formation

Although the just mentioned general stages of beachrock formations are widely accepted, the processes that lead to the initial cementation itself are not very well understood yet and they are rather diverse and a matter of debate. The different theories recorded in the literature in this regard, will be mentioned in the following lines.

a) Physicochemical processes

Direct cement precipitation

This is a theory explained in many some studies dealing with the origin of beachrock. It refers to the precipitation of cements from meteoric water (also known as fresh water) or marine water (seawater), which would be influenced by the temperature of the groundwater and the local lithology[92,93].

According to the literature, the meteoric water (that is, fresh water) as a sole source of cements is quite controversial, because beachrock formations have been recognized either in dry areas (such as the ones found in the Red Sea[94]) or throughout coasts that are too small to have a constant fresh water table. In addition, there are scarce evidences, from the geochemical and mineralogical point of view, about cements commonly related to meteoric waters in beachrock formations (calcite and LMC)[93,95].

In contrast, the prevailing origin attributed to beachrock occurrences is related to precipitation of cements from marine waters. This would be enhanced by the alternation of wet and dry periods, as well as the rising of temperature of interstitial fluids after diurnal solar heating. In other words, the seawater would soak the beach face, the sediments of the beach act as the nuclei required for the beginning of the cementation, and the process would progress thanks to the CO_2 degassing and evaporation of water films originated after low tides and backwash[95,96].

[92] Morse J.W., Mackenzie F.T., **1990**. *Geochemistry of sedimentary carbonates*. Developments in Sedimentology 48, 707 pp.
[93] Vousdoukas M.I., Velegrakis A.F., Plomaritis T.A., **2007**. *Beachrock occurrence, characteristics, formation mechanisms and impacts*. Earth-Science Reviews 85, 23-46.
[94] Friedman G.M., Gavish E., **1971**. *Mediterranean and Red Sea (Gulf of Aqaba) beachrocks*. In: Bricker O.P. (Ed.), Carbonate Cements. The Johns Hopkins Press, Baltimore, M.D., pp. 13-16.
[95] Gischler E., Lomando A.J., **2007**. *Beachrock and Intertidal Precipitates*. In: Nash D.J., McLaren S.J. (Eds.), Geochemical Sediments and Landscapes. Wiley-Blackwell, UK, pp. 365-390.
[96] Tietz, G., Muller, G., **1971**. *High-magnesian calcite and aragonite cementation in recent beachrocks, Fuerteventure, Canary Island, Spain*. In: Bricker, O.P. (Ed.), Carbonate Cement. Johns Hopkins Press, Baltimore, pp. 4-8.

This theory (soaking of the beach during high tides and evaporation after low tides) gains strength, first because of the fact that beachrocks are mainly formed in the intertidal zone and second, because marine cements (aragonite and HMC) have been frequently identified in beachrock occurrences[97]. Nevertheless, it has also some weaknesses and there are authors who believe that it might not be enough to explain the cementation phenomenon[98].

Mixing of meteoric and marine waters

There are some studies that have identified the co-occurrence of marine and meteoric cements in the same beachrock formations. Thus, it leads to believe that a mixture of both, marine and meteoric waters can influence in the cement precipitation. For instance, Schmalz (1971)[99] studied beachrocks from the Marshall Islands (Eniwetok Atoll), or Moore (1973)[100] analysed beachrocks from the intertidal zone of Grand Cayman, suggesting both of them mixed meteoric-marine conditions for the precipitation of the cements.

Degassing of CO_2 from groundwater

This theory was firstly presented by Hanor (1978)[101], concluding that CO_2 degassing from groundwater in a marine phreatic context (where fresh groundwater and marine water are moved by wave pumping) can induce the precipitation of carbonates. Binkley et al. (1980)[102] proposed this origin also for vadose cements composing beachrocks from Ore Lake (Michigan).

It is believed that precipitates formed upon supersaturation of mixed fresh and seawater groundwater can change the time of the commencement of the process, as well as the amount, size and morphology of the cements. Indeed, as the cementation progresses, the porosity of the sediments is reduced, and consequently, decreases also the capacity of the groundwater to degas and generate new cements[101]. The CO_2 degassing from groundwater could be somewhat appropriate to explain the beachrock

[97] Vousdoukas M.I., Velegrakis A.F., Plomaritis T.A., **2007**. *Beachrock occurrence, characteristics, formation mechanisms and impacts*. Earth-Science Reviews 85, 23-46.
[98] Neumeier U., **1999**. *Experimental modeling of beachrock cementation under microbial influence*. Sedimentary Geology 126, 35-46.
[99] Schmalz R.F., **1971**. *Formation of beachrock at Eniwetok Atoll*. In: Bricker O.P. (Ed.), Carbonate Cements. Johns Hopkins Press, Baltimore, pp. 17-24.
[100] Moore C.H., **1973**. *Intertidal carbonate cementation Grand Cayman, West Indies*. Journal of Sedimentary Petrology 43, 591-602.
[101] Hanor J.S., **1978**. *Precipitation of beachrock cements: mixing of marine and meteoric waters vs CO_2-degassing*. Journal of Sedimentary Petrology 48, 489-501.
[102] Binkley K.L., Wilkinson B.H., Owen R.M., **1980**. *Vadose beachrock cementation along a southeastern Michigan Marl Lake*. Journal of Sedimentary Petrology 50, 953-961.

phenomenon in tropical and subtropical climates; to enable the cementation process, sufficient groundwater flow and prolonged water residence is needed, circumstances that tend to result from seasonal rainfalls, characteristic of those climates[103].

b) Biological processes

It has been already mentioned the key role that microorganisms can play in the stabilization of the sediments to further enable the lithification process. However, the microbial-mineral interaction can go beyond the purely stabilizer function and it can be fundamental for the formation of carbonates[104]. Microbes (also named as microscopic organisms or microorganisms) include principally bacteria, fungi, small algae and protozoan. Many research works dealing with microbial carbonates focus principally on the role of bacteria (specifically, cyanobacteria[105,106]), while small algae and protozoan are mainly referred because of their involvement in the stabilization process. In any case, microbes are ubiquitous organisms that can be associated to diverse processes regarding the production, accumulation and diagenesis of sediments[104].

Indeed, in recent years there are more and more evidences suggesting that processes once considered merely physicochemical, result to have a biological and/or organic origin, either in terrestrial or marine environments[107-109]. For instance, the microbial mediation on the precipitation of carbonates can be found in diverse depositional settings such as marine reefs, lacustrine whitings, cave crusts, or even in grains and cements found in sedimentary materials[105]. Special mention should be given to the many studies attributing a biologic origin to stromatolitic beachrock (i.e., is a sedimentary rock formation containing laminated structures of probable biological origin, usually representing biosedimentological remains of biofilms and microbial mats)[110,111] or

[103] Vousdoukas M.I., Velegrakis A.F., Plomaritis T.A., **2007**. *Beachrock occurrence, characteristics, formation mechanisms and impacts*. Earth-Science Reviews 85, 23-46.
[104] Riding R., Awramik S.M., **2000**. *Microbial Sediments*. Springer-Verlag, Germany, 331 pp. In: Millenium Reviews (Eds.: Best J.L., Fielding C., Jarvis I., Mozley P.). Millenium Reviews, Sedimentology 47, 179-214.
[105] Díez B., Bauer K., Bergman B., **2007**. *Epilithic cyanobacterial communities of a marine tropical beachrock (Heron Island, Great Barrier Reef): Diversity and Diazotrophy*. Applied and Environmental Microbiology 73, 3656-3668.
[106] Kamennaya N.A., Ajo-Franklin C.M., Northen T., Jansson C., **2012**. *Cyanobacteria as biocatalysts for carbonate mineralization*. Minerals 2, 338-364.
[107] Dupraz C., Visscher P.T., Baumgartner L.K., Reid R.P., **2004**. *Microbe-mineral interactions: early carbonate precipitation in a hypersaline lake (Eleuthera Island, Bahamas)*. Sedimentology 51, 745-765.
[108] Freytet P., Verrecchia E.P., **1998**. *Freshwater organisms that build stromatolites: a synopsis of biocrystallization by prokaryotic and eukaryotic algae*. Sedimentology 45, 535-563.
[109] Reitner J., Arp G., Thiel V., Gautret P., Galling U., Michaelis W. **1997**. *Organic matter in Great Salt Lake ooids (Utah, USA): first approach to a formation via organic matrices*. Facies 36, 210-219.
[110] Krumbein, W.E., **1979**. *Photolithotropic and chemoorganotrophic activity of bacteria and algae as related to beachrock formation and degradation (Gulf of Aqaba, Sinai)*. Geomicrobiology Journal 1, 139-203.
[111] Reitner J., Quéric N-V., Arp G., **2010**. *Advances in Stromatolite Geobiology*. Lecture Notes in Earth Sciences. Springer-Verlag, London, 559 pp.

even more to the contemporary believe regarding the biologically derived formation of beachrocks[112,113].

To better understand the possible biological processes involved in beachrock formation, it has to be remarked that for the precipitation of carbonates to take place, the availability of free calcium and carbonate alkalinity needs to be promoted[114]. Alkalinity conditions could be reached by physicochemical processes, as it has been described in the previous section (e.g. degassing of CO_2 and evaporation), or it could also be mediated by microorganisms. The latter, could be either microbially-induced (active precipitation) or microbially-influenced (passive precipitation). On this basis, the term "organomineralization", proposed by Dupraz et al. (2009)[114], will be used to refer to those microbially mediated processes. In any case, diverse microbial components participate to reach the alkalinity conditions required for organomineralization processes. Among those components, the metabolic pathways followed to obtain energy and carbon and the role of organic matrix have to be cited[114].

Certainly, diverse metabolic mechanisms or physiological activities developed by a wide array of microorganisms can stimulate carbonate precipitation[114,115]. It can be cited for instance, the ammonification of amino acids, urea hydrolysis and sulphate reduction occurring in the degradation of organic matter[116-118], especially in areas exposed to light[113,119]. In addition, anoxygenic bacteria have been also considered to be relevant in the beachrock biology[114,120].

[112] Webb G.E., Jell J.S., Baker J.C., **1999**. *Cryptic intertidal microbialites in beachrock, Heron Island, Great Barrier Reef: implications for the origin of microcrystalline beachrock cement*. Sedimentary Geology 126, 317-334.
[113] Neumeier U., **1999**. *Experimental modeling of beachrock cementation under microbial influence*. Sedimentary Geology 126, 35-46.
[114] Dupraz C., Reid R.P., Braissant O., Decho A.W., Norman R.S., Visscher P.T., **2009**. *Processes of carbonate precipitation in modern microbial mats*. Earth-Science Reviews 96, 141-162.
[115] Buczynski C., Chafetz H.S., **1991**. *Habit of bacterially induces precipitates of calcium carbonate and the influence of medium viscosity on mineralogy*. Journal of Sedimentary Petrology 61, 226-233.
[116] Berner R.A., **1968**. *Calcium Carbonate concretions formed by the decomposition of organic matter*. Science 159, 195-197.
[117] Krumbein, W.E., **1979**. *Photolithotropic and chemoorganotrophic activity of bacteria and algae as related to beachrock formation and degradation (Gulf of Aqaba, Sinai)*. Geomicrobiology Journal 1, 139-203.
[118] Ehrlich H.L.,1996. *Geomicrobiology*. Marcel Dekker, New York, 800 pp.
[119] Vousdoukas M.I., Velegrakis A.F., Plomaritis T.A., **2007**. *Beachrock occurrence, characteristics, formation mechanisms and impacts*. Earth-Science Reviews 85, 23-46.
[120] Díez B., Bauer K., Bergman B., **2007**. *Epilithic cyanobacterial communities of a marine tropical beachrock (Heron Island, Great Barrier Reef): Diversity and Diazotrophy*. Applied and Environmental Microbiology 73, 3656-3668.

The various metabolic pathways directly influence in the geochemistry of the fluids in the vicinity of the living cells, altering the redox and saturation states of that surrounding microenvironment[121,122]. Therefore, the microenvironment around each bacterium can be different from the bulk aqueous environment, and as a result, it can allow the formation of mineral phases that would not be expected from the bulk fluid[122]. For instance, in the cyanobacteria (Figure 1.6A), uptake of the bicarbonate anion causes the release of OH^-, which changes the alkalinity and inorganic carbon speciation around the cell surface. Calcification can be encouraged by the production of carbonate anions and the preadsorption of calcium cations to the cell. Similarly, In the Fe(III)-reducing bacterium (Figure 1.6B), liberation of Fe(II) from the ferric hydroxide substratum can stimulate magnetite formation on the pre-existing mineral surfaces, but also on the cell surface if deprotonated ligands had adsorbed ferric iron[122].

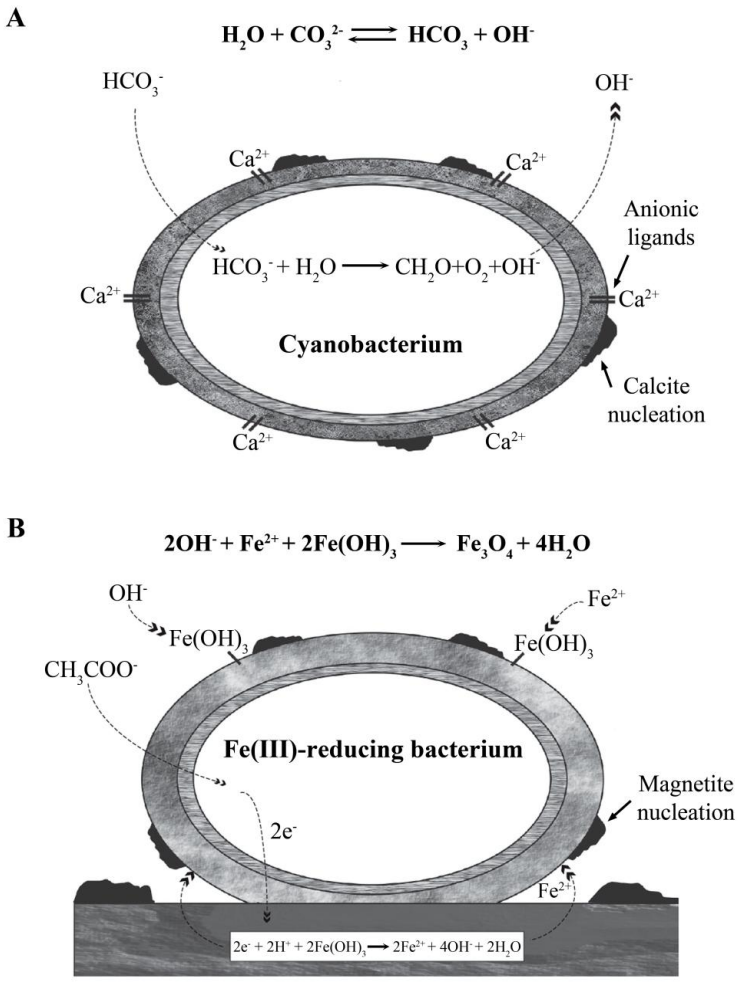

Figure 1.6. Representation of metabolically-induced biomineralization in (A) cyanobacteria and (B) Fe(III)-reducing heterotrophs. Source: Konhuaser and Rifing (2012)[122].

[121] Perito B., Mastromei G., **2011**. *Molecular basis of bacterial calcium carbonate precipitation*. In W.E.G. Müller (Ed.), Molecular biomineralization: aquatic organisms forming extraordinary materials. Springer-Verlag, Germany, pp. 113-140.
[122] Konhauser K., Riding R. **2012**. *Bacterial biomineralization*. In: Knoll A.H., Canfield D.E., Konhauser K. O. (Eds.), Fundamentals of Geobiology. John Wiley & Sons, Chichester, UK, pp. 105-130.

Concerning the role of the organic matrix, the extracellular polymeric substances (EPS) need to be mentioned. This high molecular weight polysaccharide matrix is generated by bacteria and microalgae, and it can be composed of protein and peptides, noncarbohydrate acidic compounds, and inorganic compounds, such as sulphates and phosphates, and even extracellular DNA[123]. The EPS is the predominant component of biofilms[124] and helps microbial communities to attach to surfaces especially in the high-energy environments (e.g., waves, tidal currents) that they commonly live. Indeed, EPS various functional groups involved in the EPS are capable of binding and concentrating Ca^{2+} and Mg^{2+} ions from surrounding seawater[123,125]. Moreover, recently the potential function of heterotrophic bacteria, such as sulphate-reducing bacteria, in the production of the extracellular matrix has been evidenced[126].

In relation with the organomineralization processes, the EPS can provide the nucleation sites for the growing of carbonates[127]. In essence, it has been demonstrated that a biofilm containing certain microorganisms and the extracellular polysaccharide substances secreted by them, can have a key role in the precipitation, trapping, and binding of carbonate crystals[128]. Furthermore, negatively charged functional groups possibly existing in the biofilm (like carboxyl, phosphate, amine, and hydroxyl groups) can absorb Ca^{2+} ions and favour the precipitation of carbonates[129] (see Figure 1.7).

In this sense, according to some authors[126,130,131], the action of certain organic macromolecules, specially rich in carboxylic compounds containing amino acids like aspartic and glutamic acid, could be particularly relevant in the morphology, formation and growth of carbonate crystals.

[123] Dupraz C., Reid R.P., Braissant O., Decho A.W., Norman R.S., Visscher P.T., **2009**. *Processes of carbonate precipitation in modern microbial mats*. Earth-Science Reviews 96, 141-162.
[124] Allison D.G., **1998**. Exoplysaccharide production in bacterial biofilms. Biofilm Journal 3, paper 2 (BF98002). Online Journals-http://www.bdt.org.br/bioline/bf.
[125] Decho A.W., Visscher P.T., Reid R.P., **2005**. *Production and cycling of natural microbial exopolymers (EPS) within a marine stromatolite*. Palaeogeograohy, Palaeocliamtology, Palaeoecology 219, 71-86.
[126] Braissant O., Decho A.W., Dupraz C., Glunk C., Przekop K.M., Visscher P.T., **2007**. *Exopolymeric substances of sulfate-reducing bacteria: interactions with calcium at alkaline pH and implication for formation of carbonate minerals*. Geobiology 5, 401-411.
[127] Castanier S., Le Métayer-Levrel G., Perthuisot J.P., **2000**. *Bacterial role in the precipitation of carbonate minerals*. In: Riding R.E., Awramik S.M. (Eds.), Microbial Sediments. Springer-Verlag, Germany, pp. 32-39.
[128] Winsborough B.M., **2000**. *Diatoms and benthic Microbial carbonates*. In: Riding R.E., Awramik S.M. (Eds.), Microbial Sediments. Springer-Verlag, Germany, pp. 76-83.
[129] Zhu T., Dittrich M., **2016**. *Carbonate precipitation through microbial activities in natural environment, and their potential in biotechnology: a review*. Frontiers in Bioengineering and Biotechnology 4, 1-21.
[130] Reitner J., **1993**. *Modern cryptic microbialite/metazoan facies from Lizard Island (Great Barrier Reef, Australia): formation and concepts*. Facies 29, 3-40.
[131] Manoli F., Dalas E., **2001**. *Calcium carbonate crystallization in the presence of glutamic acid*. Journal of Crystal Growth 222, 293-297.

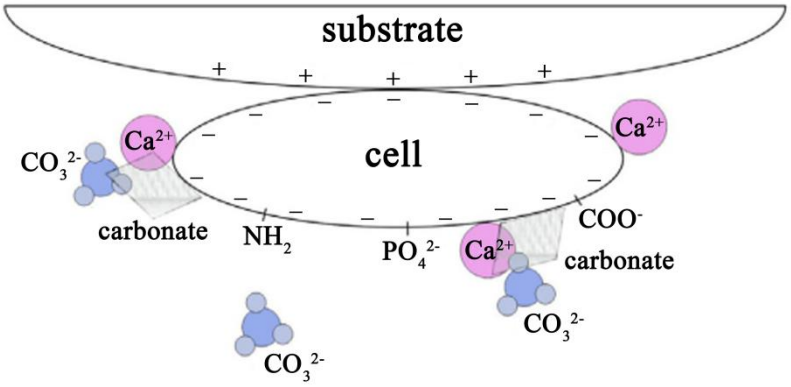

Figure 1.7. Representation of a cell wall containing negatively charged functional groups, like carboxyl, phosphate and amine, which can absorb Ca^{2+} ions. When carbonate ions are available, carbonates can precipitate in the cell surface. Source: Zhu and Dittrich (2016)[132].

Beachrock, similarly to other rock surfaces, can accommodate biofilms in their structure[133]. In addition, bacterial populations are particularly large and productive in the intertidal zone, an area where beach lithification tends to occur[134]. Nevertheless, often microbial activity leaves no traces or the microbial mediated crystals are altered during the diagenetic process, making difficult the recognition of biosignatures that would evidence the source of the original carbonate material[135,136].

However, frequently, microbially derived mineral growth generates the initial formation of amorphous solid phases and then, their respective crystalline equivalents nucleate slowly at ambient temperatures. The transition from amorphous to crystalline phases can involve the precipitation of metastable phases[137-138]. Besides, spherule-shaped precipitates are also common in microbially-mediated carbonate formation[139,140].

[132] Zhu T., Dittrich M., **2016**. *Carbonate precipitation through microbial activities in natural environment, and their potential in biotechnology: a review*. Frontiers in Bioengineering and Biotechnology 4, 1-21.
[133] Gorbushina A.A., Krumbein E.E., **2000**. *Subaerial microbial mats and their effects on soil and rock*. In: Riding R.E., Awramik S.M. (Eds.), Microbial Sediments. Springer-Verlag, Germany, pp. 161-170.
[134] Turner R.J., **2005**. *Beachrock*. In: Schwartz M.L. (Ed.), Encyclopaedia of Coastal Science. Kluwer Academic Publishers, The Netherlands, pp. 183-186.
[135] Buczynski C., Chafetz H.S., **1991**. *Habit of bacterially induced precipitates of calcium carbonate and the influence of medium viscosity on mineralogy*. Journal of Sedimentary Petrology 61, 226-233.
[136] Castanier S., Le Métayer-Levrel G., Perthuisot J.P., **2000**. *Bacterial role in the precipitation of carbonate minerals*. In: Riding R.E., Awramik S.M. (Eds.), Microbial Sediments. Springer-Verlag, Germany, pp. 32-39.
[137] Konhauser K., Riding R. **2012**. *Bacterial biomineralization*. In: Knoll A.H., Canfield D.E., Konhauser K. O. (Eds.), Fundamentals of Geobiology. John Wiley & Sons, Chichester, UK, pp. 105-130.
[138] Addadi L., Raz S., Weiner S., **2003**. *Taking advantage of disorder: amorphous calcium carbonate and its roles in biomineralization*. Advanced Materials 15, 959-970.
[139] Tourney J., Ngwenya B.T., **2009**. *Bacterial extracellular polymeric substances (EPS) mediate CaCO3 morphology and polymorphism*. Chemical Geology 262, 138-146.
[140] Braissant O., Cailleau G., Dupraz C., Verrecchia E.P., **2003**. *Bacterially induced mineralization of calcium carbonate in terrestrial environments: the role of exoplysaccharides and amino acids*. Journal of Sedimentary Research 73, 485-490.

Furthermore, one of the characteristics commonly related to biological intermediation in beachrock is the presence of micritic cement[141-144]. The majority of microbial micrite does not usually compose a whole grain or an external cement, but it represents the initial internal stages where the calcification of organic tissue (biofilm) is encouraged by metabolic activity and environmentally enhanced[145]. These micritic crystals could also serve as nuclei for physic-chemically precipitated overgrowth of prismatic crystals[146].

As an example of the relevance that biological processes could have in the formation of beachrocks, a study carried out by Neumeier (1998)[146] has to be cited, who concluded that, although physicochemical mechanisms interfere in beachrock formation, microbial activity is the main driving force.

Finally, concerning the biological processes likely to be involved in beachrocks, it has to be highlighted also the difference between tropical areas and temperate areas in terms of metabolic rates, which according to Riding et al. (2004)[145] is:

- Fast in the intertidal and tropical rain forest areas, where the occurrence of beachrock is common.

- Peculiarly expressive in Mediterranean and dry arid zones.

- Slower, but marked, in temperate and cold arid zones, where this phenomenon seems to be rather scarce.

[141] Bathurst R.G.C., **1975**. *Carbonate sediments and their diagenesis*. Developments in sedimentology 12, Elsevier, Amsterdam, 658 pp.
[142] Webb G.E., Jell J.S., Baker J.C., **1998**. *Cryptic intertidal microbialites in beachrock, Heron Island, Great Barrier Reef: implications for the microcrystalline beachrock cement*. Sedimentary Geology 126, 317-334.
[143] Vousdoukas M.I., Velegrakis A.F., Plomaritis T.A., **2007**. *Beachrock occurrence, characteristics, formation mechanisms and impacts*. Earth-Science Reviews 85, 23-46.
[144] Turner R.J., **2005**. *Beachrock*. In: Schwartz M.L. (Ed.), Encyclopaedia of Coastal Science. Kluwer Academic Publishers, The Netherlands, pp. 183-186.
[145] Riding R., Awramik S.M., **2000**. *Microbial Sediments*. Springer-Verlag, Germany, 331 pp. In: Millenium Reviews (Eds.: Best J.L., Fielding C., Jarvis I., Mozley P.). Millenium Reviews, Sedimentology 47, 179-214.
[146] Neumeier U., **1999**. *Experimental modeling of beachrock cementation under microbial influence*. Sedimentary Geology 126, 35-46.

1.1.6 Diagenesis: environments and characteristic cements

The diagenesis involves all the physical, chemical or biological processes (occurring separately or simultaneously in time) that affect the sediments after deposition and during the conversion into a sedimentary rock[147]. For instance, the principal diagenetic process influencing carbonate sediments is the progressive cementation[148].

In this context, diagenetic environments refer to surface or subsurface areas where specific diagenetic processes occur, and they are typified by certain characteristics that allow somehow recognising them. Commonly, the most decisive diagnostic criteria indicative of a certain diagenetic environment, are the cement mineralogy and morphology[149,150].

Depending on the fluid chemistry and the distribution of fluids in the pores diverse diagenetic environments can be distinguished. The fluid chemistry would mark whether the environment is marine or meteoric (freshwater), while the distribution of the fluids would evidence a phreatic (pores completely filled with water) or a vadose zone (pores partly filled with water and air). The normal diagenetic sequence for a marine sediment during a relative lowering of sea level would be to go from the marine phreatic zone through the mixing zone into the meteoric phreatic and finally into the vadose environment[151]. On this basis, three main diagenetic environments will be described, depending on a marine (mainly phreatic) environment, meteoric (either phreatic or vadose) environment, or a mixture of both of them (Figure 1.8A).

[147] Tucker M., **1990**. *Diagenetic processes, products and environments*. In: Tucker M.E., Wright V.P., (Eds.), Carbonate sedimentology. Blackwell Scientific Publications, Oxford, pp. 314-364.
[148] Mohamad A.H., Tucker E.V., **1976**. *Diagenetic history of the Aymestry limestone beds (High Gorstian Stage), Ludlow Series, Welsh Borderland, U.K*. In: Chilingarian G.V., Wolf K.H. (Eds.), Diagenesis III. Elsevier, Amsterdam, pp. 317-385.
[149] Flügel E., **2004**. *Microfacies of Carbonate Rocks*. Springer Science & Business Media, New York, 976 pp.
[150] Gischler E., Lomando A.J., **2007**. *Beachrock and Intertidal Precipitates*. In: Nash D.J., McLaren S.J. (Eds.), Geochemical Sediments and Landscapes. Wiley-Blackwell, UK, pp. 365-390.
[151] Longman M.W., **1980**. *Carbonate diagenetic textures from nearsurface diagenetic environments*. AAPG Bulletin 64, pp. 461-487.

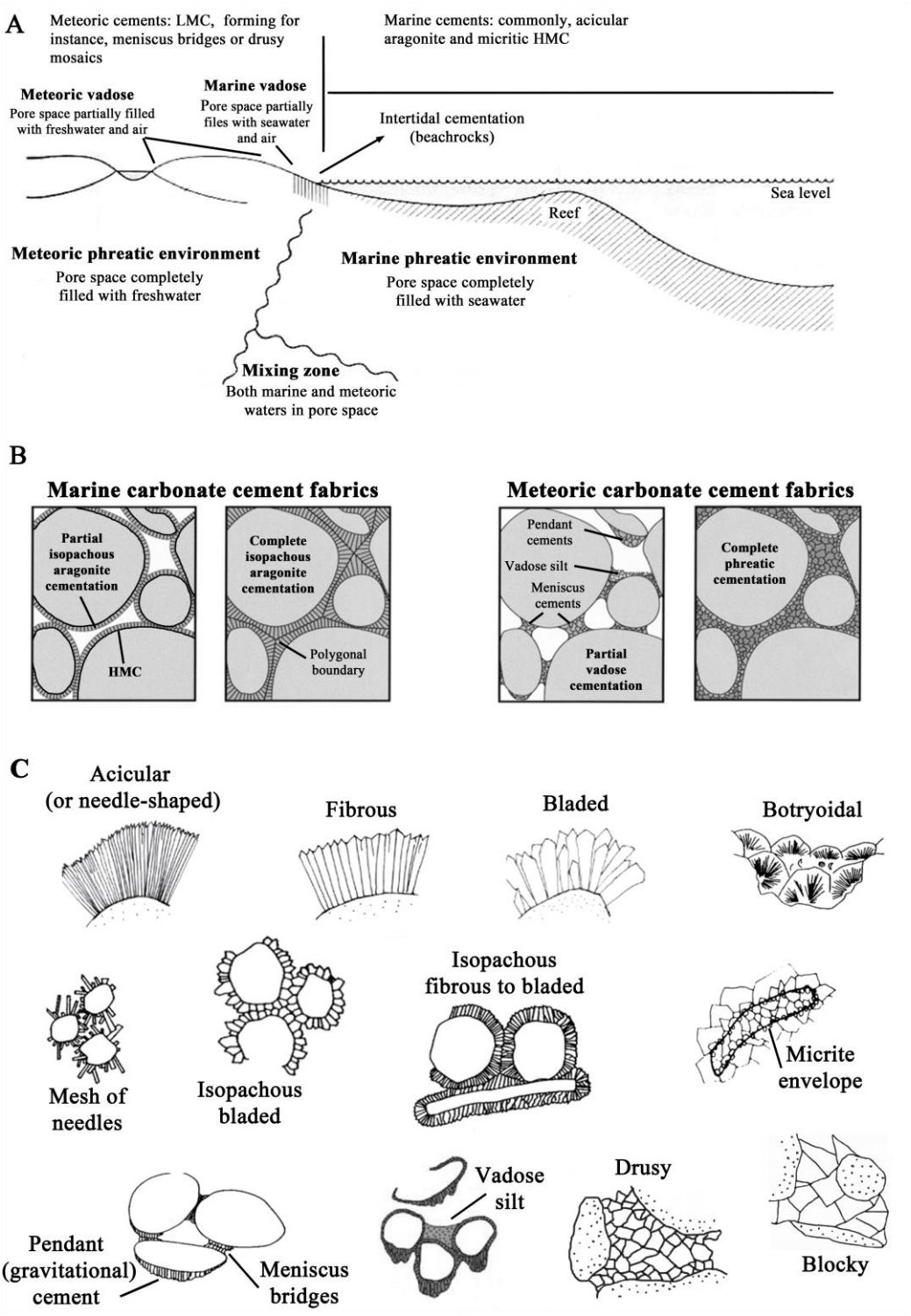

Figure 1.8. A) Schematic beach profile showing the main diagenetic environments[152]. B) Representation of typical shallow marine and meteoric carbonate cement fabric examples found in modern sediments[153]. C) Cement types and fabrics commonly formed in carbonate rocks, either in marine and/or meteoric environments[154,155]. LMC: Low Magnesium Calcite. HMC: High Magnesium Calcite.

[152] Tucker M.E. **1981**. *Sedimentary petrology, an introduction*. Blackwell, Oxford, 252 pp.
[153] Scholle P.A., Ulmer-Scholle D.S., **2003**. *Cements and cementation*. In: Middleton G.V. (Ed.), Encyclopaedia of Sediments and Sedimentary Rocks: Boston, Kluwer Academic Publishers, pp. 110-119.
[154] Boggs S., **2009**. *Petrology of Sedimentary Rocks*. Cambridge University Press, UK, 600 pp.

1.1.6.1 Marine environment

Most carbonates are deposited in marine environments, and therefore, their diagenetic history starts here[156]. The beach is an ideal setting for the precipitation of marine cements and the two major sites of marine cementation are the high-energy intertidal zone and the shelf-margin reef (Figure 1.8A). Their typical high-energy conditions (in terms of wave and tidal activity), and coarse-grained sediments that provide high porosity and permeability, can ensure a high rate of fluid flow and the elevated saturation state required for cementation[157,158].

Furthermore, although cementation can be enhanced by several biological, chemical and physical factors, marine cementation generally takes place very near the sediment-water interface upon active water circulation. Even in the sea waters that tend to be supersaturated with respect to calcium carbonate, sea water needs to circulate easily through the sediments for a significant marine cementation, and this takes place in the active marine phreatic zone. However, cementation could also take place at stagnant conditions also[156].

In those cases in which all pore spaces in a sediment or rock are completely filled with normal marine water, they are considered to be representative of the marine-phreatic diagenetic environment[156]. Although marine vadose cements can be formed in areas of relatively high tidal range, most cementation in the beach shoreface certainly occurs in a marine phreatic environment[157]. Therefore, the description of the marine zone will mainly focus on phreatic conditions, and vadose conditions will be explained when describing the meteoric zone.

The prevailing cements precipitated in the marine phreatic environment are high magnesium calcite and aragonite. Mg-calcite usually precipitates in the form of micritic (i.e. microcrystalline), with an isopachous disposition around the grains (Figure 1.8B and Figure 1.9). Occasionally, Mg-calcite micritic crystals can gather to form pseudopellets or Mg-calcite rhombs can form a thick coating of fibrous to bladed isopachous cement

[155] Flügel E., **2004**. *Microfacies of Carbonate Rocks*. Springer Science & Business Media, New York, 976 pp.
[156] Longman M.W., **1980**. *Carbonate diagenetic textures from nearsurface diagenetic environments*. AAPG Bulletin 64, pp. 461-487.
[157] Moore C.H., **1997**. *Carbonate diagenesis and porosity*. Developments in Sedimentology 46, Elsevier, Amsterdam, 338 pp.
[158] Moore C.H., **2001**. *Carbonate reservoirs. Porosity evolution and diagenesis in a sequence stratigraphic framework*. Developments in sedimentology 55. Elsevier, Amsterdam, 444 pp.

(Figure 1.8C)[159]. These cement types have been found in beachrocks formed under a marine phreatic context suggested to be derived from an organic source[160].

Regarding the marine aragonite cement, frequently forms fibrous crystals growing outwards tangentially from the grain (Figure 1.9). Aragonite crystals can also show other dispositions such as a loose mesh of crystals, coarse botryoids or micrite (Figure 1.8C). In addition, there have been described other characteristics, like polygonal boundaries formed by the intersection of the isopachous fibrous cements, which could be indicative of early diagenesis occurred in the phreatic environment[159-162] (Figure 1.8B).

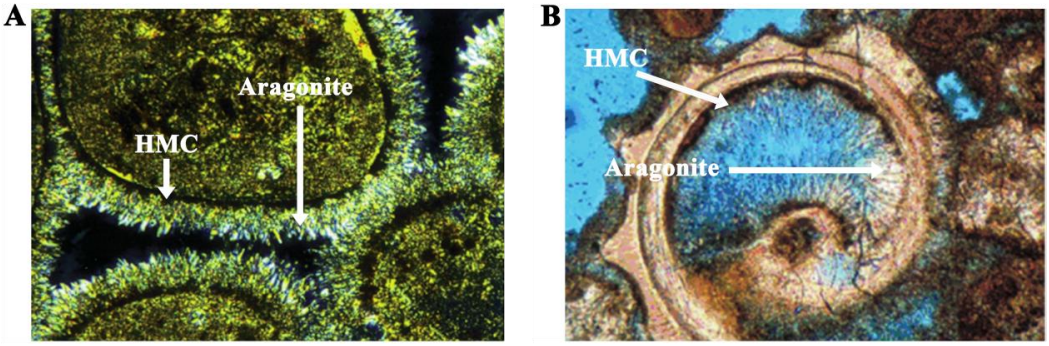

Figure 1.9. Thin section microphotographs showing recent sediments cemented with high magnesian calcite (HMC) and aragonite. A) Modern beachrock at Salt Cay (Bahamas Islands)[163]. B) Recent sediment from Grand Cayman (Cayman Islands)[164].

1.1.6.2 Meteoric environment

Meteoric waters, although they can show a wide variety of carbonate saturation states, at first are usually undersaturated with respect to most carbonate mineral phases (due in part to atmospheric CO_2) and they can be strongly aggressive towards those minerals. Moreover, most shallow marine carbonate sequences are affected by the influence of meteoric diagenesis[165,166]. For instance, the modern carbonate phases that

[159] Longman M.W., **1980**. *Carbonate diagenetic textures from nearsurface diagenetic environments*. AAPG Bulletin 64, pp. 461-487.
[160] Moore C.H., **1977**. *Beach rock origin: some geochemical, mineralogical and petrographic considerations*. Geoscience and man 18, pp. 155-163.
[161] Howie F.M.P., **2009**. *Beachrock development along the North coast of Cornwall*. Geoscience in South-West England 12, 85-94.
[162] Kindler P., Hearty P.J., **2000**. *Elevated marine terraces from Eleuthera (Bahamas) and Bermuda: sedimentological, petrographic and geochronological evidence for important deglaciation events during the middle Pleistocene*. Global and Planetary Change 24, 41-58.
[163] Scholle P.A., Ulmer-Scholle D. S, **2003**. *Cements and cementation*. In: Middleton G.V. (Ed.), Encyclopedia of Sediments and Sedimentary Rocks: Boston, Kluwer Academic Publishers, pp., 110-119.
[164] Scholle P.A., Ulmer-Scholle D.S., **2003**. *A color guide to the petrography of carbonate rocks: grains, textures, porosity, diagenesis*. American Association of Petroleum Geologists Memoir 77, 474 pp.
[165] Moore C.H., Wade W.J., **2013**. *Carbonate reservoirs. Porosity and diagenesis in a sequence stratigraphic framework*. El Sevier, The Nertherlands, 392 pp.
[166] Land L.S., **1986**. *Limestone diagenesis-some geochemical considerations*. In: Mumpton F.A. (Ed.), Studies in Diagenesis. U.S. Geological Survey Bulletin, pp. 129-137.

consist mainly on metastable HMC and aragonite can be easily altered by meteoric waters or mixtures of meteoric and marine waters, in surface and shallow subsurface conditions[167,168]. Meteoric diagenesis begins with the loss of magnesium from HMC (becoming into LMC), then a progressive disappearance of aragonite occurs and the replacement of aragonite by calcite (LMC)[169].

Meteoric diagenesis takes place in the vadose zone and the phreatic zone, as well as the shallow subsurface (Figure 1.8A). Those zones comprise subenvironments distinguished by differences in water movement (active circulation or stagnant conditions), solution as well as precipitation processes and resulting cements and porosity type[171]. This way, two different hydrologic regimes will be considered in the meteoric diagenetic: the vadose and the phreatic zone.

a) Meteoric vadose cements

The vadose diagenetic environment is the subaerial zone located under the land surface and above the zone of saturation or water table (Figure 1.8A). Water in the vadose zone is generally meteoric (rain) water, wetting and drying periods can be frequent in the vadose zone, depending on the evaporation or precipitation amounts[170]. Thus, the pore space might be filled with both air and water. As this zone is not water saturated, water tends to be held by capillarity between the grains and specific cement types can be developed from that irregular distribution of the water. Cements precipitated in vadose conditions can be small equant shaped crystals, but they frequently form meniscus bridges, an arrangement clearly indicative of the vadose zone, either in meteoric or vadose conditions[171-174] (Figure 1.8B and Figure 1.8C).

As mentioned, one of the major controls on the amount of water that passes through the vadose zone is climate and the nature of the rainfall (e.g. seasonal or

[167] Longman M.W., **1980**. *Carbonate diagenetic textures from nearsurface diagenetic environments*. AAPG Bulletin 64, pp. 461-487.
[168] James N.P., Choquette P.W., **1984**. *Diagenesis 9-Limestones.The meteoric diagenetic environment*. Geoscience Canada 11, 161-194.
[169] Flügel E., **2004**. *Microfacies of Carbonate Rocks*. Springer Science & Business Media, New York, 976 pp.
[170] Moore C.H., **1997**. *Carbonate diagenesis and porosity*. Developments in Sedimentology 46, Elsevier, Amsterdam, 338 pp.
[171] Halley R.B., Harris P.M., **1979**. *Fresh-water cementation of a 1,000 year-old oolite*. Journal of Sedimentary Petrology 49, pp. 969-988.
[172] James N.P., Choquette P.W., **1984**. *Diagenesis 9-Limestones.The meteoric diagenetic environment*. Geoscience Canada 11, 161-194.
[173] Meyers J.H., **1987**. *Marine vadose beachrock cementation by cryptocrystalline magnesian calcite-Maui, Hawaii*. Journal of Sedimentary Petrology 57, 558-570.
[174] Ozturk M.Z., Erginal A.E., Kiyak N.G., Ozturk T., **2015**. *Cement fabrics and optical luminescence ages of beachrock, North Cyprus:implications for Holocene sea-level changes*. Quaternary International (In Press).

torrential and scarce or gentle)[175]. In this sense, well-cemented beachrock can show silt-sized sediments which were infiltrated at vadose conditions and deposited in the intergranular space, for instance after storm events[176].

b) Meteoric phreatic cements

Freshwater phreatic zone is located between the vadose and mixed marine phreatic-freshwater zones (Figure 1.8A). Here the pore space is fully filled with meteoric water containing variable amounts of dissolved carbonate. Much of the meteoric water may enter the phreatic zone directly through the vadose zone.

Meteoric phreatic intergranular cements generally occur in a more homogeneous distribution than their vadose analogues (Figure 1.8B). The most characteristic criteria to recognise cements precipitated in this zone consist of blocky or drusy calcite crystals forming isopachous rims and even mosaics in the intergranular space (Figure 1.8C)[177,178]. However, the morphology of the cements can be rather variable, although phreatic cements are generally larger than vadose cements[173,179].

Regardless of the particularities of the marine and meteoric environments, it has to be cited that specific diagenetic conditions characterised by mixing of meteoric and marine waters may exist in shallow subsurface near-coastal settings (mixing zone) and at the coastal interface of land and sea (marine beaches, shoreface), characterised by rapidly changing conditions (marine vadose environment).

Mixtures of salt water and fresh water contribute significantly to the dissolution of carbonate rocks on coasts. The mixing of waters found in this zone may also be partly responsible for the precipitation of aragonite and dolomite cementation for instance in vugs and in the dolomitization process. The diagenetic criteria of the marine vadose zone are similar to those of the meteoric vadose zone, but the cementation is more rapid[180].

[175] Longman M.W., **1980**. *Carbonate diagenetic textures from nearsurface diagenetic environments*. AAPG Bulletin 64, pp. 461-487.
[176] Marques Vieira M., De Ros L.F., **2006**. *Cementation patterns and genetic implications of Holocene beachrocks from northeastern Brazil*. Sedimentary Geology 192, 207-230.
[177] Melim L.A., Westphal H., Swart P.K., Eberli G.P., Munnecke A., **2002**. *Questioning carbonate diagenetic paradigm: evidence from the Neogene of the Bahamas*. Marine Geology 185, 27-53.
[178] Boggs S., **2009**. *Petrology of Sedimentary Rocks*. Cambridge University Press, UK, 600 pp.
[179] Moore C.H., **1997**. *Carbonate diagenesis and porosity*. Developments in Sedimentology 46, Elsevier, Amsterdam, 338 pp.
[180] Flügel E., **2004**. *Microfacies of Carbonate Rocks*. Springer Science & Business Media, New York, 976 pp.

Indeed carbonate platforms remaining near sea level for extended periods, can be subjected to the flushing of sea water into the platforms, resulting in diagenetic processes. The high chemical reactivity of carbonates yields extensive early carbonate diagenesis including marine cementation in the environment of deposition, and dissolution and cementation under meteoric water influences[180], as it has been found in various beachrocks[181-185].

1.1.7 Implications of beachrock formations

The presence of beachrocks in a certain setting can cause diverse alterations, especially from the mophodynamical and ecological point of view, as described in detail by Vousdoukas et al. (2007)[186] and briefly mentioned herein.

Beachrocks interact with the predominant wave regime and tidal range[187,188] and the subsequent morphodynamic modifications likely to be produced are rather complex and even unpredictable[188]. However, it seems that, especially in small islands and atolls[189], the presence of beachrock can promote the wave dissipation and thus, reduce the erosion affecting the beach[186,188]. Moreover, these structures can be like a natural coastal defence towards wave energy and could modify the nearshore dynamics[188].

It has to be mentioned also that they can alter the sediment composition and movement, as well as the porous character of the beach[190]. In this context, it has been

[181] Beier J.A., **1985**. *Diagenesis of Quaternary Bahamian beachrock: petrographic and isotopic evidence*. Journal of Sedimentary Petrology 55, 755-761.
[182] Chowdhury S.Q, Fazlul A.T.M., Hasan H.K., 1997. *Beachrock in St. Martin's Island, Bangladesh: Implications of sea level changes on beachrock cementation*. Marine Geodesy 20, 89-104.
[183] Rey D., Rubio B., Bernabeu A.M., Vilas F., **2004**. *Formation, exposure, and evolution of a high-latitude beachrock in the intertidal zone of the Corrubedo complex (Ria de Arousa, Galicia, NW Spain)*. Sedimentary Geology 169, 93-105.
[184] Erginal A.E., Kiyak N.G., Ozturk M.Z., Avcioglu M., Bozcu M., Yigitbas E., **2012**. *Cementation characteristics and age of beachrocks in a fresh-water environment Lake Iznik, NW Turkey*. Sedimentary Geology 243-244, 148-154.
[185] Arrieta N., Iturregui A., Martínez-Arkarazo I., Olazabal M.A., Murelaga X., Baceta J.I., Madariaga J.M., **2015**. *Multianalytical X-ray based micro-spectroscopic approach for the analysis of carbonates in beachrock cements.* Analytical Methods 7, 8865-8876.
[186] Vousdoukas M.I., Velegrakis A.F., Plomaritis T.A., **2007**. *Beachrock occurrence, characteristics, formation mechanisms and impacts*. Earth-Science Reviews 85, 23-46.
[187] Cooper J.A.G., **1991**. *Beachrock formation in low latitudes: implications for coastal evolutionary models*. Marine Geology 98, 145-154.
[188] Alexandrakis G., Ghionis G., Poulos S., **2013**. *The effect of beach rock formation on the morphological evolution of a beach. The case study of an eastern Mediterranean beach: Ammoudara, Greece*. Journal of Coastal Research 69, 47-59.
[189] Dickinson W.R., **1999**. *Holocene sea-level record on Funafuti and potential impact of global warming on Central Pacific Atolls*. Quaternary Research 51, 124-132.
[190] Karambas T., **2003**. *Modelling of infiltration-exfiltration effects of cross-shore sediment transport in the swash zone*. Coastal Engineering 45, 63-82.

mentioned that the overall long-term effect of all those processes could lead to a loss of sediment and the outcropping or exhumation of buried beachrocks[191].

From an ecological perspective, the formation of beachrocks implies that what once was a mobile beach now is a rocky shore, and this change can certainly cause diverse alterations[192]. For instance, persisting exposure of intertidal beachrocks can completely modify the ecology of the sandy beach, as the hard substrate can accommodate a great diversity of animal and plant species[193], gradually replacing the ones found in loose sand[191,194,195]. In this sense, irregular beachrock surfaces can involve safety risks because of the slippery biological mats that can be found on the surface of the outcrops. Thus, the presence of beachrocks can have implications in the functional area and the aesthetics of the beach[191].

1.1.8 Interests of the study of beachrock formations

1.1.8.1 Biotechnological applications

Now that recently is raising awareness about the possible biological influence in the origin of the cementation, the examination of these processes might positively contribute in diverse research lines. Indeed, bacterially induced precipitation of carbonates has gained importance in the scientific community as it may have diverse applications[196], for instance, in the atmospheric CO_2 fixation through carbonate sediment formation and lithification[197], in the investigation of alternative construction materials[198], the comprehension of the origin of carbonates found in Martian meteorites[199] or on the surface of Mars (remotely recognized)[200], and even in the solid phase trapping of

[191] Vousdoukas M.I., Velegrakis A.F., Kontogianni A., Makrykosta E.N., **2009**. *Implications of the cementation of beach sediments for the recreational use of the beach*. Tourism Management 30, 544-552.
[192] McLean R., **2011**. *Beachrock*. In: Hopley D. (Ed.), Encyclopaedia of Coral Reefs. Springer, The Netherlands, pp. 107-111.
[193] Turner R.J., **2005**. *Beachrock*. In: Schwartz M.L. (Ed.), Encyclopaedia of Coastal Science. Kluwer Academic Publishers, The Netherlands, pp. 183-186.
[194] Bain R.J., **1988**. *Exposed beachrock: its influence on beach processes and criteria for recognition*. Proceeddings of the 4th Symposium on Geology of the Bahamas, San Salvador, pp. 33-44.
[195] Brattström, H., **1992**. *Marine biological investigations in the Bahamas. 22. Littoral zonation at three Bahamian beachrock localities*. Sarsia 77, 81-109.
[196] Sánchez-Román M., Romanek C.S., Fernández-Remolar D.C, Sánchez-Navas A., Mckenzie J.A., Pibernat R.A., Vasconcelos C., **2011**. *Aerobic biomineralization of Mg-rich carbonates: Implication for natural environments*. Chemical Geology 281, 143-150.
[197] Chafetz, H.S., Buczynski, C., **1992**. *Bacterially induced lithification of microbial mats*. Palaios 7, 277–293.
[198] De Muynck W., De Belie N., Verstraete W., **2010**. *Microbial carbonate precipitation in construction materials: A review*. Ecological Engineering 36, 118-136.
[199] McKay D.S., Gibson E.K., Thomas-Keprta K.L., Vali H., Romanek C.S., Clement S., Chillier X.D.F., Maechling C.R., Zare R.N., **1996**. *Search for past life on Mars: possible relic biogenic activity in Martian meteorite ALH84001*. Science 273, 924-930.
[200] Morris R.V., Ruff S.W., Geller R., Ming D.W., Arvidson R.E., Clark B.C., Golden D.C., Siebach K., Klingelhöfer G., Schröderm C., Fleischer I., Yen A.S., Squyres S.W., **2010**. *Identification of carbonate-rich outcrops on mars by the spirit rover*. Science 329, 421-424.

inorganic contaminants[201] or medical pathologies like the formation of kidney stones in humans[202]. Therefore, the understanding of microbially induced precipitation of calcium carbonate, could offer several prospective biotechnological applications[203]. Likewise, the research of beachrock formations could help in the investigation of diagenetic controls in porosity and permeability, and therefore, have applications in the study of reservoir and aquifer properties[204].

1.1.8.2 Archaeological interest and construction material

Diverse references relate beachrocks with construction materials. For instance, apparently beachrocks made up of scoria slabs gave an idea to Roman engineers about which materials to use in their buildings[205]. In addition, some geoarchaeological studies revealed that beachrock materials were associated to temple constructions[206] and used in tomb construction dated at 1800 B.C.[207] in Greek settlements as well as in ancient tombs placed in the kingdom of Tonga[208] (Figure 1.10A). Besides, it has been discussed the possibility of beachrocks been used in the construction of the Bimini Road, which some authors believed to be part of the legendary Atlantis[209] (Figure 1.10B).

[201] Warren L.A., Maurice P.A., Parmar N., Ferris F.G., **2001**. *Microbially mediated calcium carbonate precipitation: implications for interpreting calcite precipitation and for solid-phase capture of inorganic contaminants*. Geomicrobiology Journal 18, 93-115.
[202] Connolly J.M., Jacskon B., Rothman A.P., Klapper I., Gerlach R., **2015**. *Estimation of a biofilm-specific reaction rate: kinetics of bacterial urea hydrolysis in a biofilm*. Biofilms and Microbiomes 1, 1-8.
[203] Zhu T., Dittrich M., **2016**. *Carbonate precipitation through microbial activities in natural environment, and their potential in biotechnology: a review*. Frontiers in Bioengineering and Biotechnology 4, 1-21.
[204] Gonzalez L.A., Roberts J., Tsoflias G., Zhang C., Villaneda Van Vloten I., **2015**. *Carbonate cementation in meteoric-marine shoreline systems: revisiting beachrock cementation processes*. Annual Review Meeting of the Kansas Interdisciplinary Carbonates Consortium (KICC). The University of Kansas, pp. 140-141.
[205] Siddall R. **2000**. *The use of volcaniclastic material in Roman hydraulic concretes: a brief review*. In: The Archaeology of Geological Catastrophes (Eds. McGuire W.G., Griffiths D.R., Hancock P.L., Stewart I.S.), Geological Society, London, pp. 339-344.
[206] Stanley J., Bernasconi M.P., Toth T., Mariottini S., Iannelli M.T., **2007**. *Coast of Ancient Kaulonia (Calabria, Italy): its submergence, lateral shifts and use as a major source of construction material*. Journal of Coastal Research 23, 15-32.
[207] Goudie A., **1969**. *A note on Mediterranean beachrock: its history*. Atoll Research Bulletin 126, 11-14.
[208] Clark G., Burley D., Murray T., **2008**. *Monumentality and the development of the Tongan maritime chiefdom*. Antiquity *82*, 994.
[209] Shinn E.A., **2009**. *The Mystique of Beachrock*. In: Swart P.K., Eberli G.P., McKenzie J.A., Jarvis I., Stevens T., (Eds.), Perspectives in Carbonate Geology: A Tribute to the Career of Robert Nathan Ginsburg. John Wiley & Sons, Ltd, Chichester, West Sussex, pp. 19-28.

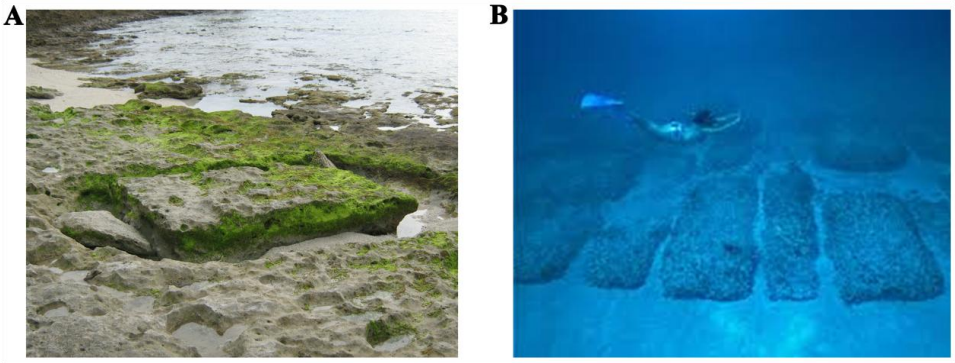

Figure 1.10. A) Beachrock found in many Tongan islands, which was used as a building material in ancient tombs[210]. B) Natural submerged beachrock in the Bimini Road (Bahamas), that some authors consider to be ruins from the Atlantis[210].

Furthermore, some early studies pointed out the use of beachrocks as construction material and its related economic value. Emery and Cox (1956)[210] for instance, explained that beachrocks located in various settings of Hawaii, were quarried and used for construction purposes or decorative uses in buildings. But the author also suggested that "the economic value, however, is not great because the cut stone probably would have an appearance very similar to concrete made from loose beach sand". However, he also mentioned that beachrock could be a good constituent of aggregate for concrete[210,211]. In fact, more recently, it has been also found to be related with limestones used for road building[212]. Not only that, if the processes that lead to beachrock formation are understood, it is believed that could set a model to produce environmental friendly artificial materials that would be potentially useful in coastal infrastructures made for erosion control purposes, like coastal walls[213].

1.1.8.3 Use as a sea-level indicator

Considering that beachrocks are mainly formed in the intertidal zone, and thus its vertical range is limited to between tide marks, several studies have used exposed or submerged beachrock as a sea level indicator[214-216]. Beachrocks can be exposed or exhumed due to the erosion prompted by sea level rise or a negative sediment budget.

[210] Emery K.O., Cox D.C., **1956**. Beachrock in the Hawaiian Islands. Pacific Science 10, 382-402.
[211] Narver D.L., **1954**. *Good concrete made with coral and sea wate*r. Civil Engineering 24, 49-52.
[212] Emery S., Cocks G., Keeley R., **2007**. *Selection and use of locally available pavement materials for low-volume roads in Western Australia*. In: 9th International Conference on Low Volume Roads (Austin).Transportation Research Record 1989. Washington, 194-200.
[213] Danjo, T., Kawasaki, S., **2014**. *Characteristics of Beachrocks: A Review*. Geotechnical and Geological Engineering 32, pp. 215-246.
[214] Hopley D., **1986**. *Beachrock as a sea level indicator*. In: Van de Plassche O. (Ed.). Sea-level Research: A Manual for the Collection and Evaluation of Data. Norwich, Geo Books, pp. 157-173.
[215] Goodwin I.A., **2009**. *Beachrock*. In: Gornitz V. (Ed.), Encyclopedia of Paleoclimatology and Ancient Environments. Springer, The Netherlands, pp. 89-90.
[216] McLean, R., **2011**. *Beachrock*. In: Hopley D. (Ed.), Encyclopaedia of Coral Reefs. Springer, The Netherlands, pp. 107-111.

Those beachrocks that persist after the erosion would represent the original intertidal zone (i.e., the area between tide marks), so if dated, they can allow sea level reconstructions of interest from the paleoenvironmental point of view[217]. However, the use of beachrocks as palaeo-sea level indicators can be rather controversial because of the radiocarbon dating problem that has been already mentioned[218] and because upper limit of beachrock formation might not be accurate[219].

1.1.9 Techniques of study

Many studies about beachrock formation have focused on the examination of the cements, because their mineralogy and morphology can be indicative of the depositional environment in which they were formed. Some early studies dealing with this phenomenon were assisted mainly by field observations and thin section examinations under light microscopy together with carbonate geochemical analyses[220,221]. Thin section analysis, sometimes aided by staining techniques to facilitate the recognition of carbonates[222], is certainly a valuable tool for petrographic analyses and it has been used to estimate the features and cementation pattern of beachrock formations.

However, as shown by Alexanderson (1972)[223] for the first time, and as attested by authors like Jorgensen (1976)[224] or Meyers (1987)[225], higher magnifications as provided by scanning electron microscopy (SEM), proved to be an essential tool to decipher relevant characteristics of the cements[226]. Since then, thin section inspections with light microscopy and/or SEM analyses of beachrock fragments are being common and greatly

[217] Desruelles S., Fouache E., Ciner A., Dalongeville R., Pavlopoulos K., Kosun E., Coquinot Y., Potdevin J.L., **2009**. *Beachrocks and sea level changes since Middle Holocene: Comparison between the insular group of Mykonos-Delos-Rhenia (Cyclades (Greece) and the southern coast of Turkey*. Global and Planetary Change 66, 19-33.
[218] Vousdoukas M.I., Velegrakis A.F., Plomaritis T.A., **2007**. *Beachrock occurrence, characteristics, formation mechanisms and impacts*. Earth-Science Reviews 85, 23-46.
[219] McLean, R., **2011**. *Beachrock*. In: Hopley D. (Ed.), Encyclopaedia of Coral Reefs. Springer, The Netherlands, pp. 107-111.
[220] Ginsburg R.N., **1954**. *Early diagenesis and lithification of shallow-water carbonate sediments in South Florida*. In: Leblanc R.J., Breeding J.G. (Eds.). Regional aspects of carbonate sedimentation.Society of Economic Paleontologists and Mienralogists Special Publications 5, pp. 80-100.
[221] Bain R.J., **1988**. *Exposed beachrock: its influence on beach processes and criteria for recognition*. Proceedings of the 4th Symposium on Geology of the Bahamas, San Salvador, pp.33-44.
[222] Dickson J.A.D., **1966**. *Carbonate identification and genesis as revealed by staining*. Journal of Sedimentary Petrology, 36, 491-505.
[223] Alexandersson T., **1972**. *Intragranular growth of marine aragonite and Mg-calcite: evidence of precipitation from supersaturated seawater*. Journal of Sedimentary Petrology 42, 441-460.
[224] Jorgensen N.O., **1976**. *Recent high magnesian calcite/aragonite cementation of beach and submarine sediments from Denmark*. Journal of sedimentary Petrology 46, 940-951.
[225] Meyers J.H., **1987**. *Marine vadose beachrock cementation by cryptocrystalline magnesian calcite-Maui, Hawaii*. Journal of Sedimentary Petrology 57, 558-570.
[226] Bathurst R.G.C., **1974**. *Marine diagenesis of shallow water calcium carbonate sediments*. Annual Review of Earth and Planetary Sciences, 257-274.

appropriate methods for the study of cementation sequences and the morphology of the crystals in beachrock cements[227-232]. To further elucidate the composition of the cements, information about the elemental geochemistry can be estimated using SEM coupled with energy dispersive X-ray spectroscopy (SEM-EDS) and also using the electron microprobe analysis, as demonstrated by Schroeder (1979)[233] or Calvet et al. (2003)[234]. Moreover, elemental analyses have been performed by means of inductively coupled plasma (ICP) techniques as well[235].

From the molecular point of view, X-ray diffraction (XRD) analyses are commonly employed to distinguish among the diverse carbonate phases that could be present within the cements, being especially relevant for the estimation of the Mg content that would lead the recognition of HMC[232,236,237]. Other techniques that would provide molecular information, such as Raman spectroscopy and Infrared spectroscopy, have been scarcely used in the study of beachrocks[237,238].

Another important tool is the stable isotopes analysis in carbonates (generally, $\delta^{13}C$ and $\delta^{18}O$), which is widely employed as it helps in determining the characteristics of the

[227] Font Y., Calvet F., **1997**. *"Beachrocks" Holocenos de la Isla de La Reunion, Oceano Indico*. Cuadernos de Geologia Iberica 22, 87-102.
[228] Webb G.E., Jell J.S., Baker J.C., **1999**. *Cryptic intertidal microbialites in beachrock, Heron Island, Great Barrier Reef: implications for the origin of microcrystalline beachrock cement*. Sedimentary Geology 126, 317-334.
[229] Kneale D., Viles H.A., **2000**. *Beach cement: incipient CaCO3-cemented beachrock development in the upper intertidal zone, North Uist, Scotland*. Sedimentary Geology 132, 165-170.
[230] Marques Vieira M., De Ros L.F., **2006**. *Cementation patterns and genetic implications of Holocene beachrocks from northeastern Brazil*. Sedimentary Geology 192, 207-230.
[231] Moissette P., Koskeridou E., Cornée J-J., André J-P., **2013**. *Fossil assemblages associated with submerged beachrock beds as indicators of environmental changes in terrigenous sediments: Examples from the Gelasian (Early Pleistocene) of Rhodes, Greece*. Palaeogeograohy, Palaeoclimatology, Palaeoecology 369, 14-27.
[232] Arrieta N., **2014**. *The study of an unusual temperate latitude beachrock formation. Characterization of Azkorri beach and Tunelboka cove locations*. PhD Thesis, University of the Basque Country.
[233] Schroeder J.H., **1979**. *Carbonate diagenesis in Quaternary beachrock of Uyombo, Kenya: seuqences of processes and coexistence of heterogenic products*. Geol Rundsch 68, 894-919.
[234] Calvet F., Cabrera M.C., Carracedo J.C., Mangas J., Perez-Torrado F.J., Recio C., Trave A., **2003**. *Beachrocks from the island of La Palma (Canary Islands, Spain)*. Marine Geology 197, 75-93.
[235] Howie F.M.P., **2009**. *Beachrock development along the North coast of Cornwall*. Geoscience in South-West England12, 85-94.
[236] Flügel E., **2004**. *Microfacies of Carbonate Rocks*. Springer Science & Business Media, New York, 976 pp.
[237] Arrieta N., Iturregui A., Martínez-Arkarazo I., Olazabal M.A., Murelaga X., Baceta J.I., Madariaga J.M., **2015**. *Multianalytical X-ray based micro-spectroscopic approach for the analysis of carbonates in beachrock cements.* Analytical Methods 7, 8865-8876.
[238] Bernier P., Guidi J.B., Bottcher M.E., **1997**. *Coastal progradation and very early diagenesis of ultramafic sands as a result of rubble discharge from asbestos excavations (northern Corsica, western Mediterranean)*. Marine Geology 144, 163-175.

environment of formation[239-241]. Frequently, isotope analyses are combined with radiocarbon dating[242,243] or OSL[244]. However, caution is required with the interpretation of radiocarbon dating (of bulk samples or cements) results obtained from beachrocks because, as previously mentioned, apart from carbonate cements, beachrock outcrops usually contain older biogenic material and detritic material, that might interfere in the dating results[240,244].

Regardless of the analysis of cements, there are other research lines concerning beachrock that focus on morphologic[245-247], topographic, bathymetric[240] and geophysical[248] characteristics related with these structures, to explore sea-level fluctuations or variations in coastal erosion and morphodynamics. Interestingly, beachrock has been also the basis for social studies, to assess the general viewpoint of beach users in terms of recreational affections[249]. Finally, although they are rather scarce in the analysis of beachrocks, there are other techniques, such as, fluorescence, cathodoluminiscence, and fluid inclusion microscopy as well as backscattered electron microscopy which are regularly used in carbonate systems[250], and could have the potential for being used in the analysis of beachrock formations.

[239] Chaves N.S., Sial A.N., **1998**. *Mixed oceanic and freshwater depositional conditions for beachrocks or Northeast Brazil: evidence from carbon and oxygen isotopes*. International Geology Review 40, 748-754.
[240] Erginal A.E., Kıyak N.G., Ozturk M.Z., Avcioglu M., Bozcu M., Yiğitbaş E., **2012**. *Cementation characteristics and age of beachrocks in a fresh-water environment, Lake İznik, NW* Turkey. Sedimentary Geology 243-244, 148-154.
[241] Avcioglu M., Yigitbas E., Erginal A.E., **2015**. *Beachrock formation on the coast of Gokceada Island and its relation to the active tectonics of the region, northern Aegean Sea, Turkey*. Quaternary International (In Press). doi:10.1016/j.quaint.2015.10.108.
[242] Spurgeon D., Davis J.R.A., Shinn E.A., **2003**. *Formation of beach rock at Siesta Key, Florida and its influence on barrier island development*. Marine Geology 200, 19-29.
[243] Desruelles S., Fouache E., Ciner A., Dalongeville R., Pavlopoulos K., Kosun E., Coquinot Y., Potdevin J.-L., **2009**. *Beachrocks and sea level changes since Middle Holocene: Comparison between the insular group of Mykonos-Delos-Rhenia (Cyclades, Greece) and the southern coast of Turkey.* Global and Planetary Change 66, 19-33.
[244] Tatumi S.H., Kowata E.A., Gozzi G., Kassab L.R.P., Suguio K., Barreto A.M.F., Bezerra F.H.R., **2003**. *Optical dating results of beachrock, eolic dunes and sediments applied to sea-level changes study*. Journal of luminescence 102-103, 562-565.
[245] Rey D., Rubio B., Bernabeu A.M., Vilas F., **2004**. *Formation, exposure, and evolution of a high-latitude beachrock in the intertidal zone of the Corrubedo complex (Ria de Arousa, Galicia, NW Spain)*. Sedimentary Geology 169, 93-105.
[246] Vousdoukas M.I., Velegrakis A.F., Karambas T.V., **2009**. *Morphology and sedimentology of a microtidal beach with beachrocks: Vatera, Lesbos, NE Mediterranean*. Continental Shelf Research 29, 1937-1947.
[247] Caron V., **2011**. *Contrasted textural and taphonomic properties of high-energy wave deposits cemented in beachrocks (St. Bartholomew Island, French West Indies)*. Sedimentary Geology 237, 189-208.
[248] Erginal A.E, Ekinci Y.L, Demirci A., Bozcu M., Ozturk M.Z., Avcioglu M., Oztura E., **2013**. *First record of beachrock on Black Sea coast of Turkey: Implications for Late Holocene sea-level fluctuations*. Sedimentary Geology 294, 294-302.
[249] Vousdoukas M.I., Velegrakis A.F., Kontogianni A., Makrykosta E-F., **2009**. *Implications of the cementation of beach sediments for the recreational use of the beach*. Tourism Management 30, 1-9.
[250] Flügel E., **2004**. *Microfacies of Carbonate Rocks*. Springer Science & Business Media, New York, 976 pp.

1.2 Beachrock in temperate coastlines: the case of the Nerbioi-Ibaizabal estuary

In view of the scarce occurrences documented in reference to beachrocks located in temperate zones, this section will be dedicated to them, with particular emphasis on beachrock formations located in the vicinity of Nerbioi-Ibaizabal estuary, case of study of this thesis.

To mention some examples of cold-temperate regions, Siesser (1974)[251] found beachrock formations dominated by LMC in a temperate zone of South Africa (34.1º latitude) suggested to be relict fortuitous formations. Similarly, Binkley et al. (1980)[252] also described LMC cemented beachrocks in a marl lake of Michigan (42.3º latitude), probably formed upon the degassing of CO_2 from groundwater. Acicular aragonite cemented beachrocks have been documented by Sellwood (1994)[253] in Clew Bay, Ireland (53.9º latitude). More recently, Kneale and Viles (2000)[254] studied an occurrence of the phenomenon in North Uist, Scotland (57.7º latitude), formed with HMC and aragonite cements, proposing that biological factors and physicochemical mechanisms (like the degassing of CO_2 from beach groundwater) might be related with the cementation. Continuing with the journey in the United Kingdom, Howie (2009)[255] detailed diverse beachrocks from the North Coast of Cornwall, England (50.5º latitude), composed with LMC cements, indicative of a freshwater phreatic environment.

In relation to the Iberian Peninsula, and coming closer to our area of study, Rey et al. (2004)[256] examined exposed beachrocks from the southern Galician coastline (42.6º latitude), predominantly cemented with LMC, suggesting that they were formed through the contribution of carbonate-enriched meteoric waters in the intertidal zone. Additionally, although there have not been found any research studies on this regard, apparently it is

[251] Siesser W.G., **1974**. *Relict and recent beachrock from Southern Africa*. Geological Society of American Bulletin 85, 1849-1854.
[252] Binkley K.L., Wilkinson B.H., Owen R.M., **1980**. *Vadose beachrock cementation along a Southeastern Michigan marl lake*. Journal of Sedimentary Petrology 50, 953-962.
[253] Sellwood, B.W. **1994**. *Principles of carbonate diagenesis*. In: Parker A., Sellwood B. (Eds), *Quantitative Diagenesis: Recent Developments and Applications to Reservoir Geology, NATO Advanced Study Institute Series C, Mathematical and Physical Sciences*. Kluwer Academic, Dordrecht, 1-32.
[254] Kneale D. and Viles H.A., **2000**. *Beach cement: incipient $CaCO_3$-cemented beachrock development in the upper intertidal zone, North Uist, Scotland*. Sedimentary Geology 132, 165-170.
[255] Howie F.M.P., **2009**. *Beachrock development along the North coast of Cornwall*. Geoscience in South-West England 12, 85-94.
[256] Rey D., Rubio B., Bernabeu A.M., Vilas F., **2004**. *Formation, exposure, and evolution of a high-latitude beachrock in the intertidal zone of the Corrubedo complex (Ria de Arousa, Galicia, NW Spain)*. Sedimentary Geology 169, 93-105.

known that cemented beaches exist also in other areas or Northern Spain, like in Asturias and in the west side of the estuary of Avilés, close to a zinc-smelting factory[257].

An outstanding example of cementation in temperate coastlines associated to an industrialized estuarine area might be the beachrock formations existing around the Nerbioi-Ibaizabal estuary, more specifically in these settings: Arrigunaga beach, Tunelboka cove, Alpenarri cove, Azkorri beach and La Salvaje beach (Figure 1.11). Some of them have been already studied as part of a previous PhD thesis, which was mainly focused on Tunelboka cove and Azkorri beach. To cite some concluding remarks of that work, four cement generations were identified, formed with HMC and aragonite indicative of a marine-phreatic context, as well as ferruginous cements and LMC cements, related with vadose-meteoric environs[258]. Biological and physicochemical factors were apparently involved in the cementation phenomenon, possibly controlled by the presence of organic matter and the proliferation of microorganisms; the sediment accumulation rates and the high wave energy conditions characteristic of this coastline; and the characteristic heterogeneous nature of the constituent sediments, especially related with the industrial wastes disposed into the estuary[259].

Certainly, not long ago, the beachrock from Tunelboka, Azkorri and Arrigunaga, have been considered to be formed during the *Anthropocene*[260,261]. The term *Anthropocene* has been recently proposed[262] and it is still a matter of debate, but it is informally used to refer to diverse geological, ecological, sociological, and anthropological modifications in recent Earth history[263].

[257] Flor G., Martínez Cedrún P., Flor Blanco G., **2011**. *Los campos dunares de Asturias, Cantabria y País Vasco*. In: Sanjaume Saumell E., Gracia Prieto F.J. (Eds.), Las dunas en España. Sociedad Española de Geomorfología, pp. 127-159.
[258] Arrieta N., Goienaga N., Martínez-Arkarazo I., Murelaga X., Baceta J.I., Sarmiento A., Madariaga J.M., **2011**. *Beachrock formation in temperate coastalines: examples in sand-gravel beaches adjacent to the Nerbioi-Ibaizabal Estuary (Bilbao, Bay of Biscay, North of Spain)*. Spectrochimica Acta Part A: Molecular and Biomolecular spectroscopy 80, 55-65.
[259] Arrieta N., **2014**. *The study of an unusual temperate latitude beachrock formation. Characterization of Azkorri beach and Tunelboka cove locations*. PhD Thesis, University of the Basque Country.
[260] Irabien M.J., García-Artola A., Cearreta A., Leorri E., **2015**. *Chemostratigraphic and lithostratigraphic signatures of the Anthropocene in estuarine areas from the eastern Cantabrian coast*. Quaternary International 364, 196-205.
[261] Pujalte V., Astibia H., Aizpiri F., Payros A., **2015**. *Las playas cementadas del "Antropoceno" de Bizkaia: origen y degradación*. Geogaceta 57, 123-126.
[262] Zalasiewicz J., Williams M., Smith A., Barry T.L., Coe A.L., Bown P.R., Brenchley P., Cantrill D., Gale A., Gibbard P., Gregory F.J., Hounslow M., Kerr A.C., Pearson P., Knox R., Powell J., Waters C., Marshall J., Oates M., Rawson P., Stone P., **2008**. *Are we now living in the Anthropocene?*. Geological Society of America Today 18, 4-8.
[263] Waters C. N., Zalasiewicz J., Summerhayes C., Barnosky A.D., Poirier C., Gałuszka A., Cearreta A., Edgeworth M., Ellis E.C., Ellis M., Jeandel C., Leinfelder R., McNeill J. R., deB. Richter D., Steffen W., Syvitski J., Vidas D., Wagreich M., Williams M., Zhisheng A., Grinevald J., Odada E., Oreskes N., Wolfe A.P., **2016**. *The Anthropocene is functionally and stratigraphically distinct from the Holocene*. Science 351, 137-147.

Figure 1.11. General view of the settings in the vicinity of the Nerbioi-Ibaizabal estuary where beachrock formations can be found. A) Arrigunaga beach (43º21'19'' N - 3º01'09'' W, area of study of this work). B) Tunelboka cove (43º 22'31'' N - 3º01'58'' W). C) Alpenarri cove (43º22'39'' N - 3º01'50'' W). D) Azkorri beach (43º22'47'' N - 3º00'59'' W). E) La Salvaje beach (43º22'59'' N - 3º00'20'' W, area of study of this work).

In this context, following with the study of the cementation phenomenon that occurs in the area, this PhD will deal with the beachrocks existing in Arrigunaga beach (although it was regenerated in the late 90s, as it will be further detailed) and La Salvaje beach (which to the best of our knowledge, will be documented for the first time). Alpenarri cove has not been studied because of the difficulties to access to the cove, which can only be reached by rappelling down the cliff or by sea at very low spring tides.

Before going into details about the beachrocks under study, the geographic and oceanographic setting as well as the historical background of the area will be described, in an attempt to better understand their particular characteristics and influences, as well as the results that will be presented throughout this work.

1.2.1 Geographic and oceanographic context

An estuary, as defined by Pritchard (1967)[264], is *a semi-enclosed coastal body of water, which has a free connection with the open sea, and within which sea water is measurably diluted with fresh water derived from land drainage*.

This configuration is typical in the northern coast of the Iberian Peninsula, where sand bars or beach deposits separate estuaries from the open sea. The morphology and extension of these transition areas between land and sea, is determined by the erosion and sedimentation events as well as tides[265].

The Nerbioi-Ibaizabal estuary (also called “estuary of Bilbao”) is located in the southeastern Bay of Biscay as part of the Basque-Cantabrian Basin, between the coordinates 43º23'N to 43º14'N and 03º07'W to 02º55'W, with a NW-SE orientation, surrounding the city of Bilbao (in Northern Spain, Basque Country, province of Biscay).

Nowadays, the estuary is 15 km in length and is a system formed by the low course (the tidal part) of the Nerbioi-Ibaizabal river (although other tributaries like Kadagua, Asua, Galindo and Gobelas, discharge into the river) and the area called “Abra” bay or “Abra of Bilbao”[265,266] (Figure 1.12). The later is a natural basin, with an average width of 3.5 km and a maximum depth of 30 m, located in the mouth of the

[264] Pritchard D.W., **1967**. *What is an estuary: physical viewpoint*. American Association for the Advancement of Science 83, 3-5.
[265] Arranz S., **2012**. *Contaminación por metales pesados. El caso de la ría de Bilbao*. Itsas Memoria. Revista de Estudios Marítimos del País Vasco 7. Untzi Museoa-Museo Naval, Donostia-San Sebastián, pp. 265-282.
[266] Cearreta A., Leorri E., **2000**. *La transformación ambiental reciente de la Ría de Bilbao: indicadores micropaleontológicos en el registro sedimentario estuarino*. Naturalia Cantabricae 1, 21-31.

estuary and is influenced by the diverse anthropogenic activities carried out in the vicinity[267], as it will be later described.

This area is characterised by a temperate-oceanic climate with moderate winters and warm summers[268]. Likewise, the average temperature lies around 15ºC and the total annual precipitation in the city of Bilbao can reach 1200 mm[269].

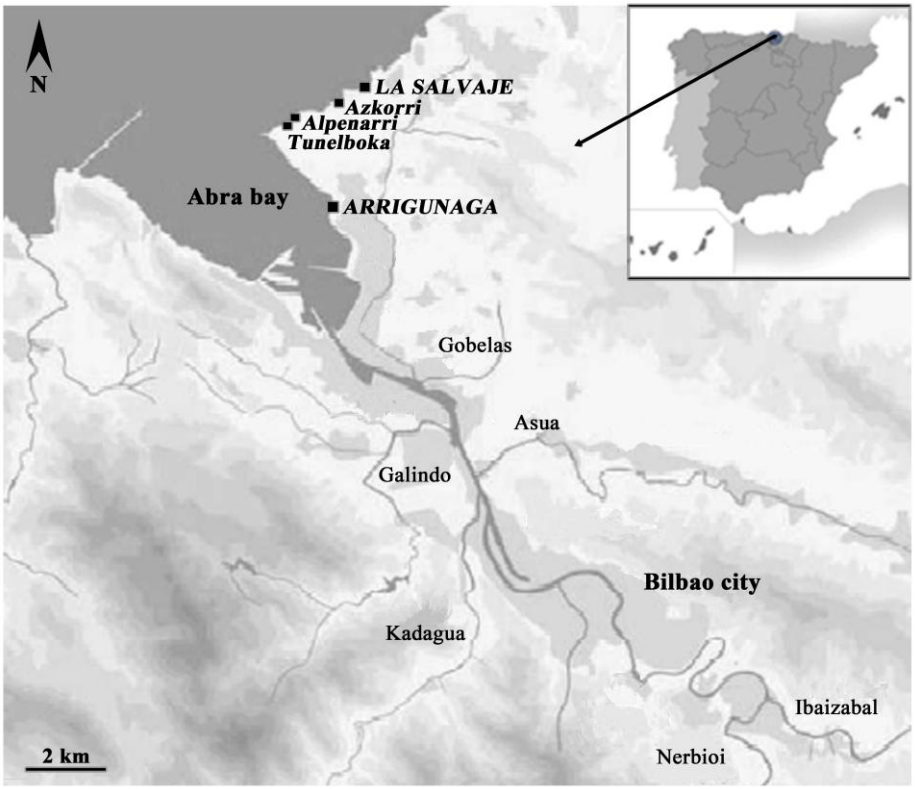

Figure 1.12. Location map of the Nerbioi-Ibaizabal estuary, including the areas showing beachrock formations: Arrigunaga beach, Tunelboka cove, Alpenarri cove, Azkorri beach and La Salvaje beach. Modified from García-Barcina et al. (2002)[270].

Regarding the marine dynamics, this high energy coastline has a semidiurnal tidal cycle and therefore, there are two high tides and two low tides each day. In addition, it constitutes a macro-mesotidal system, with tides ranging from 1 m at neap tide to 4-6 m

[267] Marigómez I., Soto M., Orbea A., Cancio I., Cajaraville M.P., **2004**. *Biomonitoring of environmental pollution in the Basque coast using molecular, cellular and tissue-level biomarkers: an integrative approach.* In: Borja A., Colllins M. (Eds.), Oceanography and Marine Environment of the Basque Country. Elsevier Oceanography Series 70, Amsterdam, The Netherlands, pp. 335-364.
[268] Usabiaga J.I., Sáenz J., Valencia V., Borja Á., **2004**. *Climate and Meteorology: variability and its influence on the Ocean.* In: Borja A., Collins M. (Eds.), Oceanography and Marine Environment of the Basque Country. Elsevier Oceanography Series 70, Amsterdam, The Netherlands, pp. 75-95.
[269] Lugaresaresti Bilbao J.I., **2002**. *Cambio ambiental reciente en el territorio de Bizkaia*. Lurralde 25, pp. 141-162.
[270] García-Barcina J.M., Oteiza M., de la Sota A., **2002**. *Modelling the faecal colliform concentrations in the Bilbao estuary*. Hydrobiologia 475/476, 213-219.

at spring tide[271,272]. Moreover, due to its location and orientation, this part of the coast is exposed to large storms from the NW and strong NW swell waves are predominant; however, they are less intense during the summer[273]. Thus, concurring with the northwest direction of prevailing winds, tide comes from the west, advancing then northwards along the eastern coastline[274].

Away from the estuaries, the tidal currents decrease and water circulation is principally dependent on wind forcing variations. Nevertheless, these currents do not have the capacity of producing littoral sediment transport alongside the Basque coast[274-276].

1.2.2 Geologic context

The entire Basque coastline is included within the Basque Arc Domain and the area of study comprises the region characterized by the syncline of Bizkaia[273,277], whose core is noticeable from the sea in Punta Galea cliff. This cliff exposes different sections constituted by carbonate turbidite layers from the Middle Eocene of the deep Basque Arc domain[278] (Figure 1.13A).

The section in Arrigunaga (Figure 1.13B), placed in the southwestern side of the syncline, is formed with materials belonging to the Lower Eocene composed of limestones and marls, other part to the Middle Eocene that includes a continuous alternation of calcarenites and calcareous sandstones, as well as marly Lower

[271] Cearreta A., Irabien M.J., Leorri E., Yusta I., Croudace I.W., Cundry A.B., **2000**. *Recent anthropogenic impacts on the Bilbao estuary, Northern Spain: geochemical and microfaunal evidence*. Estuarine. Coastal and Shelf Science 50, 571-592.
[272] Valencia V., Franco J., Borja A., Fontán A., **2004**. *Hydrography of the southeastern Bay of Biscay.* In: Borja A., Collins M. (Eds.), Oceanography and Marine Environment of the Basque Country. Elsevier Oceanography Series 70, Amsterdam, The Netherlands, pp. 159-194.
[273] Galparsoro I., Borja A., Legorburu I., Hernández C., Chust G., Liria P., Uriarte A., **2010**. *Morphological characteristics of the Basque continental shelf (Bay of Biscay, northern Spain); their implications for Integrated Coastal Zone Management*. Geomorphology 118, 314-329.
[274] González M., Uriarte A., Fontán A., Mader J., Gyssels P., **2004**. *Marine Dynamics.* In: Borja A., Collins M. (Eds.), Oceanography and Marine Environment of the Basque Country. Elsevier Oceanography Series 70, Amsterdam, The Netherlands, pp. 133-157.
[275] Halverson M.J., Pawlowicz R., **2008**. *Estuarine forcing of a river plume by river flow and tides*. Journal of Geophysical Research 113, C09033, doi:10.1029/2008JC004844.
[276] Fernández-Salas L. M., Durán R., Mendes I., Galparsoro I., Lobo F. J., Bárcenas P., Rosa F., Ribó M., García-Gil, S., Ferrín A., Carrara G., Roque C., Canals M. **2015**. *Shelves of the Iberian Peninsula and the Balearic Islands (I): Morphology and sediment types*. Boletín Geológico y Minero 126, 2-3, 327-376.
[277] Pascual A., Cearreta A., Rodriguez Lázaro J., Uriarte A., **2004**. *Geology and Palaeoceanography*. In: Borja A., Collins M. (Eds.), Oceanography and Marine Environment of the Basque Country. Elsevier Oceanography Series 70, Amsterdam, The Netherlands, pp. 53-73.
[278] Soraluce J., Ordiales A., Uriel Z., Nuñez J., Castilla H., Gallo L., Pastor N., Elorza J., **2012**. *Turbiditas carbonatadas del Eoceno medio en Punta Galea, Arco Vasco: contenidos de $CaCO_3$, presencia de restos vegetales continentales y silicificaciones selectivas*. Geogaceta 52, 69-72.

Maastrichtian materials and alternation of marl and marly limestones from the Middle Maastrichtian[279].

The section of La Salvaje (Figure 1.13B), located in the north of the syncline of Bizkaia, is composed of materials of the Lower Eocene, outcropping between the east of the beach (Solondotas headland), where it contacts with rocks from the Upper Cretaceous (Upper Maastrichtian), extending along the beach towards Azkorri. It is formed by a random alternation of limestone and hemipelagic marls, fine siliciclastic turbidites and mixed turbidites (calciclastic and siliciclastic) that can reach 100 cm of thickness[280].

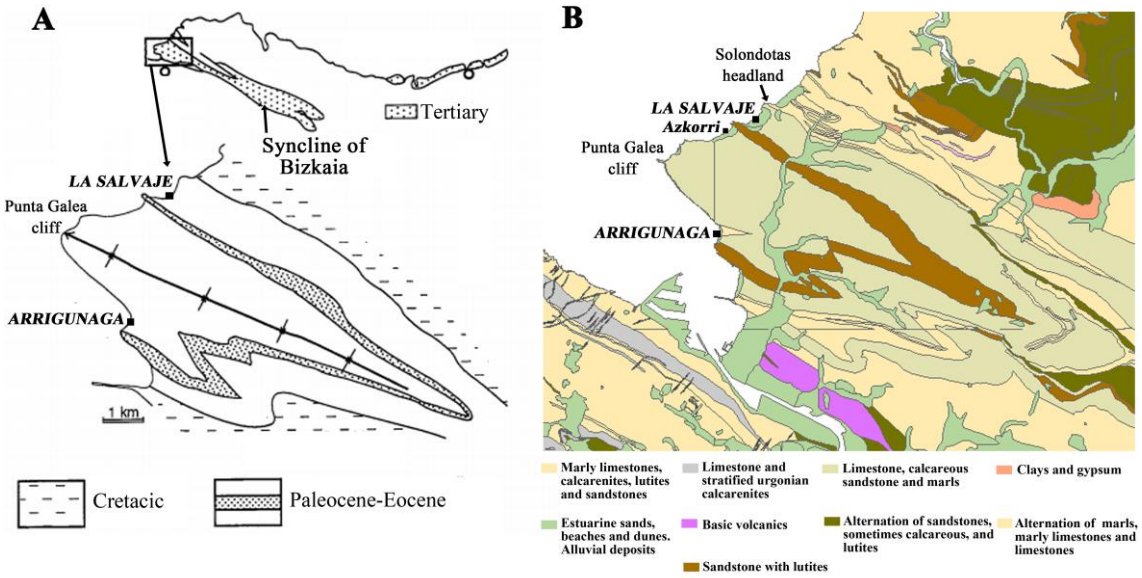

Figure 1.13. A) Geologic setting and B) lithologic characteristics of the area of study. Source A: Pujalte et al. (1997)[281]. Source B: Gobierno Vasco-Eusko Jaurlaritza (2016)[282].

Besides, it must be highlighted that this part of the Atlantic basin is especially rich in iron-ore, which contributed to heavy mining exploitation[283] and subsequent economic and social changes, as well as human derived physical modifications in the area, as it will be outlined in the next section.

[279] Rodríguez Lázaro J., Elorza J., Orue-Etxebarria X., Aguirre J., **1989**. *Materiales de edad Maastrichtiense en la serie eocénica del flanco-SW del sinclinorio de Bizkaia (Arrigunaga, N de Bilbao)*. Kobie (Serie Ciencias Naturales) 18, 105-114.
[280] Bernaola G., Nuño-Arana, Payros A., **2006**. *Análisis bioestratigráfico del Eoceno Inferior de la sección de Barinatxe (Pirineos Occidentales) mediante nanofósiles calcáreos*. Geogaceta 40, 175-178.
[281] Pujalte V., Payros A:, Orue-Etxebarria X., Baceta J.I., **1997**. *Secuencia evolutiva de los depósitos resedimentados eocenos de Punta Galea, Bizkaia: relevancia para determinación del sentido de transporte en láminas "slump"*. Geogaceta 22, 169-172.
[282] Gobierno Vasco-Eusko Jaurlaritza, **2016**. Visor GeoEuskadi. http://www.geo.euskadi.net.
[283] Belzunce M.J., Solaun O., Valencia V., Pérez V., **2004**. *Contaminants in estuarine and coastal waters*.In In: Borja, A., Collins, M. (Eds.), Oceanography and Marine Environment of the Basque Country. Elsevier Oceanography Series, 70. Elsevier, Amsterdam, pp. 233–251.

1.2.3 Evolution of the anthropic influence

With regard to estuaries, they include a wide variety of systems (such as, beaches and dunes, marshlands, intertidal zones or deep water areas) and they hold a high biological productivity, actually, the highest among all the ecosystems of temperate zones[284]. But the coastal environment, being the interface between the land and the ocean, is a particularly dynamic and fragile realm exposed to threats from human activities [284,285].

The eastern Cantabrian area, where the estuary of Bilbao is located, is characterized by an abrupt coast with cliffs, and estuaries may play an important role because, for instance, they are the main systems that allow nutrient exchange between the land and the coast[284]. However, natural processes may be conditioned, masked or enhanced by the anthropogenic influence[284,286,287].

To understand the human pressure experienced in the estuary of Bilbao, a brief historical background will be outlined. In coastal communities of the Cantabrian coast in general, the main economic sustenance was provided by fishing, trading and agricultural activities until the 19th century. In addition, preliminary industrial activities were also being developed basing on tidal mills as well as foundries and shipyards. The most intense commercial trading with Europe was focused on the Port of Bilbao. Therefore, the channelling and conditioning of the navigation area was required in the river, invading more than a half of the original surface. However, the influence of social and economic factors gets more intense in the second half of the 19th century and beginning of the 20th century, prompted my diverse technological innovations (like the train and development of steam engines) and the richness of the mines from Biscay, allowing the expansion of mining activities and giving rise to an industrial revitalization[284] (Figure 1.14).

The estuary of Bilbao was a pivotal element in that Industrial Revolution occurred in the region during the late 19th century, being one of the economic engines of the

[284] Rivas Mantecon V., Cendrero Uceda A., **1992**. *Análisis histórico de la evolución superficial de los estuarios del País Vasco*. Lurralde 15, 199-227.
[285] Crain C.M., Halpern B.S., Beck M.W, Kappel C.V., **2009**. *Understanding and managing human threats to the coastal marine environment*. Annals of the New York Academy of Sciences 1162, 39-62.
[286] Eyre B., Balls P., **1999**. *A comparative study of nutrient behavior along the salinity gradient of tropical and temperate estuaries*. Estuaries 22, 313-326.
[287] Méndez Martínez G., Pérez-Arlucea M., González-Villanueva R., Ovejero Campos A., **2011**. *Anthropogenic influence on the Holocene sedimentation process along the Atlantic coast of Galicia (NW Iberian Peninsula)*. Journal of Coastal Research, Special Issue 64, 1788-1792.

country[288]. At that time many infrastructures were created and several modifications were performed in the estuary. Certainly, an expansion of mining activities as well as iron- and steel-making industries was being appreciated and incipient shipping businesses were established. Soon, the value of the mining sites increased exceptionally because of their richness, ease of extraction, closeness to the river and their adequate adaptation to the requirements of the technological advances like the Bessemer process[289,290]. Therefore, the iron ore exploitation was intensified for its commercialization and exportation, allowing the creation of a whole net of industries around the estuary[288]. Consequently, the need of supplying coal for the metalworking industries, the transport of final products and mainly the exportation of iron ore to European ports, encouraged the development of the shipping industries, constituting another prosperous sector in the new economical situation of the area [289,291].

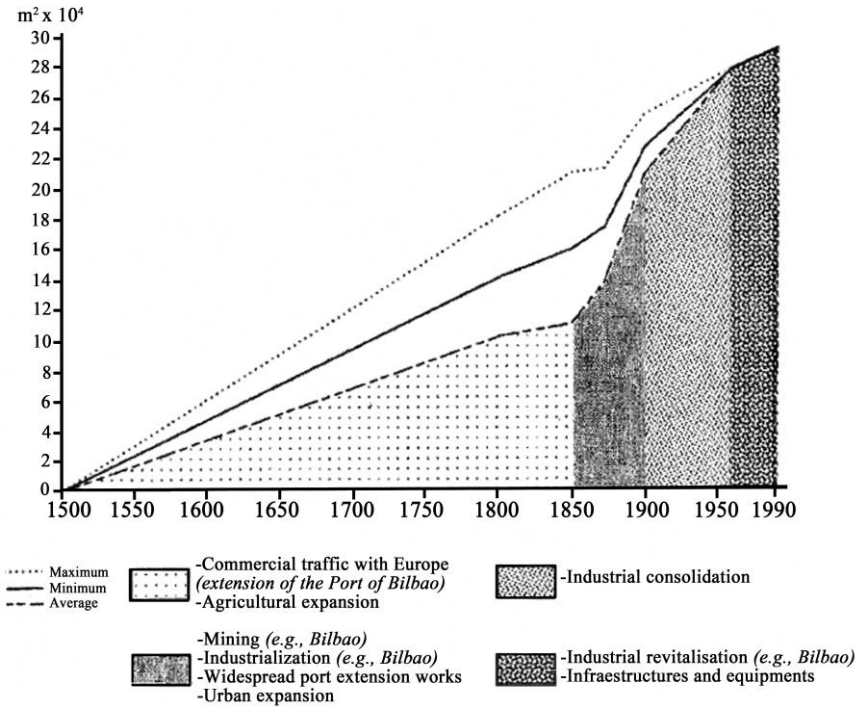

Figure 1.14. Chronological evolution of the human occupation in the estuaries of the Basque Country. Modified from Rivas and Cendrero (1992)[292].

[288] Arranz S., **2012**. *Contaminación por metales pesados. El caso de la ría de Bilbao*. Itsas Memoria. Revista de Estudios Marítimos del País Vasco 7. Untzi Museoa-Museo Naval, Donostia-San Sebastián, pp. 265-282.
[289] González Portilla M.M., Beascoechea Gangoiti J.M., Novo López P.A., Pareja Alonso A., Serrano Abad S., Zárraga Sangróniz K., **2001**. *Los orígenes de una metrópoli industrial: la Ría de Bilbao.I-Modernización y mestizaje de la ciudad industrial*. Fundación BBVA, Editorial Nerea, Bilbao.
[290] Bessemer H., **1860**. *On the manufacture of malleable iron and steel*. Journal of the Franklin Institute 69, 193-199.
[291] Ibañez I., Erkoreka A., **2009**. *Vida a bordo en los barcos de la flota de Altos hornos de Vizcaya en la década de 1950*. Itsas Memoria. Revista de Estudios Marítimos del País Vasco 6, Untzi-Museoa-Museo Naval, Donostia-San Sebastián, pp. 499-520.
[292] Rivas Mantecon V., Cendrero Uceda A., **1992**. *Análisis histórico de la evolución superficial de los estuarios del País Vasco*. Lurralde 15, 199-227.

The earliest iron and steel industry was established in the mid part of the estuary in 1854[293]. It was a time of industrial, economical and social progressions, and among them, a company known as *Altos Hornos de Vizcaya* (AHV) has to be cited, due to its significance in the economy and society of the region throughout the 20th century. AHV was established in 1902, after the union of three former steel-making companies (*Altos Hornos de Bilbao, La Vizcaya* and *La Iberia*)[294] and led to consider this region as the main producer of soft iron and steel in the country during the first two decades of the century[295]. Before long, a whole set of port equipment, boats, cranes and other facilities were commonly assembled in the estuary of Bilbao[296] (Figure 1.15). After almost 100 years of history, and an intense industrial trajectory behind it, the AHV company closed in 1996, although steel working remained in the area.

Figure 1.15. View of the estuary of Bilbao in 1961. Source: Mas Serra (2012)[297].

But in relation with the industrial and urban development, the natural layout of the estuarine system has been strongly modified to adapt it to industrial and navigation necessities. As a consequence, the configuration that the estuary shows nowadays is far from the original one back in the 1300s when the city of Bilbao was founded[298].

[293] Cearreta A., Irabien M.J., Leorri E., Yusta I., Croudace I.W., Cundry A.B., **2000**. *Recent anthropogenic impacts on the Bilbao estuary, Northern Spain: geochemical and microfaunal evidence*. Estuarine, Coastal and Shelf Science 50, 571-592.
[294] Ibañez I., Erkoreka A., **2009**. *Vida a bordo en los barcos de la flota de Altos hornos de Vizcaya en la década de 1950*. Itsas Memoria. Revista de Estudios Marítimos del País Vasco 6, Untzi-Museoa-Museo Naval, Donostia-San Sebastián, pp. 499-520.
[295] Asociación Vasca de Patrimonio Industrial y Obra Pública (AVPIOP-IOHLEE), **2012**. *Patrimonio Industrial en el País Vasco*. Volumen I. Colección de Patrimonio Cultural Vasco (EKOB). Gobierno Vasco-Eusko Jaurlaritza, 676 pp.
[296] Villar Ibáñez J.E., **1998**. *Embarcaciones portuarias y de tráfico interior en los puertos de Bilbao y Pasajes*. Itsas Memoria. Revista de Estudios Marítimos del País Vasco 2, Untzi Museoa-Museo Naval, Donostia-San Sebastián, pp. 407-416.
[297] Mas Serra E., **2012**. *Soporte territorial e identidad urbana: el caso de la comarca de la Ría de Bilbao*. Scripta Nova. Revista Electrónica de Geografía y Ciencias Sociales XVI, pp. 1-16.
[298] Arranz S., **2012**. *Contaminación por metales pesados. El caso de la ría de Bilbao*. Itsas Memoria. Revista de Estudios Marítimos del País Vasco 7. Untzi Museoa-Museo Naval, Donostia-San Sebastián, pp. 265-282.

The anthropic modifications of the estuary started with diverse works to reroute tributaries like Gobelas river, construct dykes, open bifurcations, or perform dredging activities, with the aim of facilitating the navigation and even to avoid floods that were affecting the city. By the year 1844, the river was completely channelled, but as some problems persisted, new modifications were commissioned by private mining industries to channel specific areas of the river, and complementarily, establish railroads that would allow the transport of iron ore[299].

Along the years, more changes have been performed, such as the extension of existing docks, new dredging actions, widening of certain parts of the river as well as the construction of ports and breakwaters (compare Figure 1.16A and Figure 1.16B). Many of these infrastructures are located in the Abra bay, in the vicinity of Arrigunaga beach (Figure 1.16B).

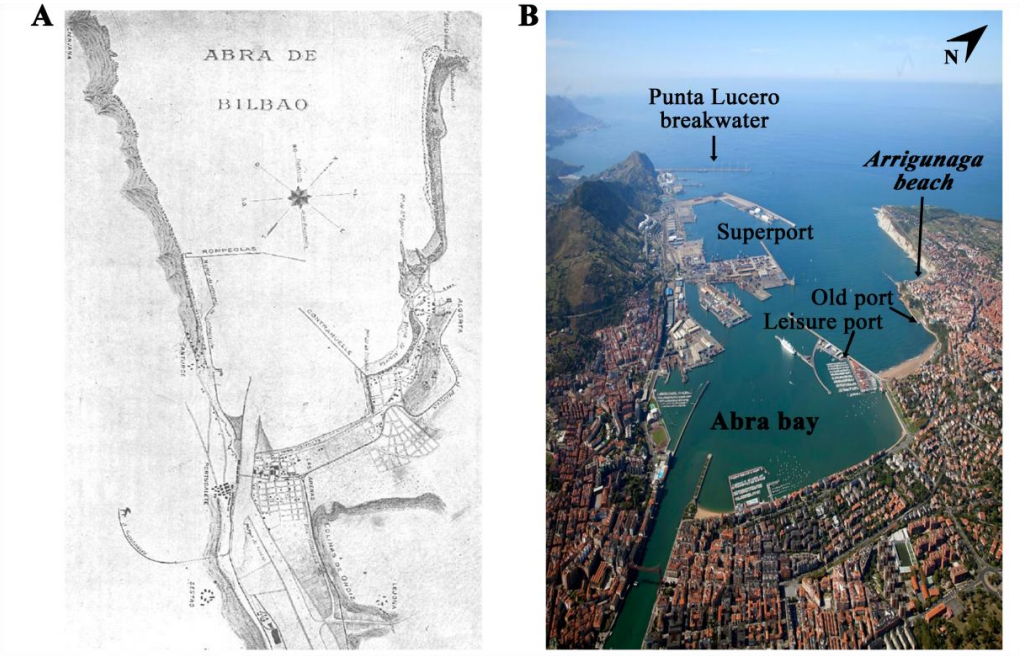

Figure 1.16. A) Fragment of the plane where some works performed on the river and Abra bay can be observed (year 1916). B) Actual view of the Abra bay, detailing various infrastructures established along the years in the vicinity of Arrigunaga beach.

[299] Arranz S., **2012**. *Contaminación por metales pesados. El caso de la ría de Bilbao*. Itsas Memoria. Revista de Estudios Marítimos del País Vasco 7. Untzi Museoa-Museo Naval, Donostia-San Sebastián, pp. 265-282.

Under these circumstances, nowadays, it is estimated that the actual surface of the Nerbioi-Ibaizabal estuary constitutes the 68.7% of the original area[300]. Moreover, the greatest population density of the Basque Country is concentrated around this estuary (2250 inhabitants/km^2, approximately)[301], with the legacy of the industrial epoch that characterizes the area.

1.2.4 Environmental alterations

The industrialization developed in the Nerbioi-Ibaizabal estuary since the 19th century yielded economical and social advances in the area as it has been described in the previous section. But, in turn, throughout the last 150 years, the system received loads of wastes from diverse sources like chemical and metal working industries, mining activities, and even domestic effluents[302]. According to some studies performed to assess the affections of the industrial wastes, the river would receive every day 900 tons of solid wastes derived from mining activities, 400 tons of acid wastes, 80 tons of metals, 1 ton of cyanide compounds, 600 tons of chemical oxygen demand and so on[303].

Therefore, all the intense activities occurring around the estuary completely occupied the intertidal zones and produced dramatic affections from the environmental point of view, leading to consider this estuary as the most polluted coastal zone in the north of Spain[304,305]. The environmental effects included a drastic oxygen deficiency as well as high concentrations of organic contaminants and metals in sediments, mainly in the middle part of the estuary (which was the most industrialized zone)[306]. It is not surprising then that the estuary was commonly considered as a sewer going towards the sea. Therefore, the following lines will deal with the possible impacts that the stress of the estuary might have had in the adjacent coast, with special interest in Arrigunaga beach and La Salvaje beach.

[300] Franco J., Borja A., Valencia V., **2004** . *Overall assessment-human impacts and quality status*. In: Borja A., Collins M. (Eds.), Oceanography and Marine Environment of the Basque Country. Elsevier Oceanography Series 70, Amsterdam, The Netherlands, pp. 581-597.
[301] Belzunce M.J., Solaun O., Valencia V., Pérez V., **2004**. *Contaminants in estuarine and coastal waters*. In: Borja A., Collins M. (Eds.), Oceanography and Marine Environment of the Basque Country. Elsevier Oceanography Series 70, Amsterdam, The Netherlands, pp. 233-251.
[302] Cearreta A., Irabien M.J., Leorri E., Yusta I., Croudace I.W., Cundry A.B., **2000**. *Recent anthropogenic impacts on the Bilbao estuary, Northern Spain: geochemical and microfaunal evidence*. Estuarine, Coastal and Shelf Science 50, 571-592.
[303] Barreiro P.M., Aguirre J.J., **2005**. *25 años del Plan Integral de Saneamiento de la Ría de Bilbao*. Dyna, pp.25-30.
[304] Cearreta A., Leorri E., **2000**. *La transformación ambiental reciente de la Ría de Bilbao: indicadores micropaleontológicos en el registro sedimentario estuarino*. Naturalia Cantabricae 1, 21-31.
[305] Franco J., Borja A., Valencia V., **2004**. *Overall assessment-human impacts and quality status*. In: Borja A., Collins M. (Eds.), Oceanography and Marine Environment of the Basque Country. Elsevier Oceanography Series 70, Amsterdam, The Netherlands, pp. 581-597.
[306] Saiz-Salinas J.I., González-Oreja J.A., **2000**. *Stress in estuarine communities: lessons from the highly-impacted Bilbao estuary (Spain)*. Journal of Aquatic Ecosystem Stress and Recovery 7, 43-55.

1.2.4.1 The estuary plume: industrial and urban pressure

The Metropolitan area of Bilbao has one of the largest concentration of industry and inhabitants on the Atlantic coast of Spain[307]. Consequently, the industrial and urban pressure developed throughout the years contributed in the impoverishment of the environmental conditions of the estuary[308]. For instance, Gobelas river is among the most highly contaminated emplacements in the estuary, not only due to loads of industrial but also urban wastes disposed in the river. Discharges from the river into the estuary are particularly remarkable in floods season[309-311], leading to the input of diverse contaminants[312].

As defined by Morris W.A. et al. (1995)[313], an estuarine plume is mainly *a coastal sea region which is significantly influenced by land-derived discharge emanating from an estuary*. In this sense, in the coastal zone of the Basque country, and in the Nerbioi-Ibaizabal estuary in particular, river plumes are associated with high concentrations of dissolved heavy metals. A dilution of the metals occurs along the coast, but the remnants of dissolved metals together with particulate metals and precipitates are still subjected to coastal transport[314]. This way polluted waters coming from the Nerbioi-Ibaizabal estuary (Figure 1.17) are usually directed eastwards by currents formed under the influence of the northwest winds, driving the estuary plume towards the eastern adjacent coast[315-317].

[307] García-Barcina J.M., Oteiza M., de la Sota A., **2002**. *Modelling the faecal colliform concentrations in the Bilbao estuary*. Hydrobiologia 475/476, 213-219.
[308] Franco J., Borja A., Valencia V., **2004**. *Overall assessment-human impacts and quality status*. In: Borja A., Collins M. (Eds.), Oceanography and Marine Environment of the Basque Country. Elsevier Oceanography Series 70, Amsterdam, The Netherlands, pp. 581-597.
[309] Seebold I., Labarta C., Amigo J.M., **1983**. *Heavy metals in the sediments of the Bilbao estuary*. Analytical Techniques in Environmental Chemistry. Pergamon Press. pp. 459-464.
[310] Gartzia de Bikuña B., Arrate J., Luján S., Moso M., **2008**. *Monografía sobre la Calidad del Agua en Bizkaia, 2009*. Informe no publicado de Anbiotek SL, para Diputación Foral De Bizkaia, 126 pp.
[311] Gredilla A., Fdez-Ortiz de Vallejuelo S., Arana G., de Diego A., Madariaga J.M., **2013**. *Long-term monitoring of metal pollution in sediments from the estuary of the Nerbioi-Ibaizabal River (2005-2010)*. Estuarine, Coastal and Shelf Science 131, 129-139.
[312] Fernández S., Villanueva U., de Diego A., Arana G., Madariaga J.M., **2006**. *Monitoring trace elements (Al, As, Cr, Cu, Fe, Mn, Ni and Zn) in deep and surface waters of the estuary of the Nerbioi-Ibaizabal River (Bay of Biscay, Basque Country)*. Journal of Marine Systems 72, 332-341.
[313] Morris A.W., Allen J.I., Howland R.J.M., Wood R.G., **1995**. *The estuary plume zone: source or sink land-derived nutrient discharges?*. Estuarine, Coastal and Shelf Science 40, 387-402.
[314] Belzunce M.J., Solaun O., Valencia V., Pérez V., **2004.** *Contaminants in estuarine and coastal waters*. In: Borja A., Collins M. (Eds.), Oceanography and Marine Environment of the Basque Country. Elsevier Oceanography Series 70, Amsterdam, The Netherlands, pp. 233-251.
[315] Díez I., Secilla A., Santolaria A., Gorostiaga J.M., **1999**. *Phytobenthic intertidal community structure along an environmental pollution gradient*. Marine Pollution Bulletin 38, 463-472.
[316] Bald J., Borja A., Muxika I., Franco J., Valencia V., **2005**. *Assessing reference conditions and physico-chemical status according to the European Water Framework Directive: a case-study from the Basque Country (Northern Spain)*. Marine Pollution Bulletin 50, 1508-1522.
[317] Legorburu I., Galparsoro I., Larreta J., Germán Rodríguez, Borja A., **2013**. *Spatial distribution of metal accumulation areas on the continental shelf of the Basque Country (Bay of Biscay): A GIS-based approach*. Estuarine, Coastal and Shelf Science 134, 162-173.

Figure 1.17. Old view of the Abra Bay, where it can be observed the estuary plume.

Thus, several studies have been carried out to evaluate the impacts of the highly altered estuarine waters in the nearby littoral realm. Those studies commonly examine benthic marine communities, as they are believed to have the potential of indicating the environmental conditions influenced by the stress of polluted coastal waters. Generally, the consequences recognised in the most altered areas were a reduction of species richness, the proliferation of opportunistic and ephemeral species tolerant to pollution as well as the general simplification of the communities caused by the high turbidity, high sedimentation level and high amounts of suspended particles coming from the river mouth[318,319].

Arrigunaga is a beach sheltered in the Abra bay, thus, it has been usually considered in the mentioned studies. As a result, based on the characteristics of the benthic communities, it has been usually recognised among the most degraded areas, suffering a direct impact of the pollution coming from the estuary[318-320].

[318] Gorostiaga J.M., Díez I., **1996**. *Changes in the sublittotal benthic marine macroalgae in the polluted area of Abra de Bilbao and proximal coast (Northern Spain)*. Marine Ecology Progress Series 130, 157-167.
[319] Pagola-Carte S., Saiz-Salinas J.I., **2001**. *Changes in the sublittoral faunal biomass induced by the discharge of a polluted river along the adjacent rocky coast (N. Spain)*. Marine ecology progress series 212, 13-27.
[320] Díez I., Bustamante M., Santolaria A., Tajadura J., Muguerza N., Borja A., Muxika I., Saiz-Salinas J.I., Gorostiaga J.M., **2012**. *Development of a tool for assessing the ecological quality status of intertidal coastal rocky assemblages, within Atlantic Iberian coasts*. Ecological Indicators 12, 58-71.

However, a gradient of decreasing pollution existed from the source of the pollution, towards the eastern open coast[318-321]. That way, the disturbance caused by the polluted plume decreased in the sites located in the open coast, although alterations of the benthic communities were also appreciated. In contrast to Arrigunaga beach, La Salvaje has been rarely considered for the examination of benthic communities. Nevertheless, areas close to La Salvaje beach like La Galea, Azkorri or other further zones, showed lower degradation levels than Arrigunaga[318,320], therefore, it can be inferred that La Salvaje might be influenced by the estuary plume similarly to those open coast areas.

In any case, it has to be mentioned that many industrial activities ceased, waste water treatments improved and environmental protective policies were applied. As such, a cleaning up programme commenced also in 1979, with the aim of guaranteeing aquatic life in the fluvial system, recover the coastline and beaches for bathing and recreational use, reach acceptable aesthetic conditions in the water and drastically reduce the toxic discharges derived from industrial activities[322]. Thus, a considerable environmental improvement has been recognised in the estuarine system and in the degraded adjacent coast[319,320,323]. Despite the recovery, pollutants are still retained in the sediments of the estuary, which upon physical reworking like dredging activities for example, can be liberated to the water column; therefore, the quality of the estuary remains as a matter of concern[324,325].

1.2.4.2 Discharge points of urban effluents

There are several points around the estuary particularly known because of being discharge points of urban inputs. As it was previously mentioned, one of them is related with Gobelas river, which discharges into a beach named as “La Bola” (Figure 1.18A). But perhaps the greatest exponent of the influence of sewage waters might be found in the Tunelboka cove, where the output point (Figure 1.18B) of the first sewage treatment plant of Bilbao is located.

[321] Franco J., Borja A., Valencia V., **2004**. *Overall assessment-human impacts and quality status*. In: Borja A., Collins M. (Eds.), Oceanography and Marine Environment of the Basque Country. Elsevier Oceanography Series 70, Amsterdam, The Netherlands, pp. 581-597.
[322] Barreiro P.M., Aguirre J.J., **2005**. *25 años del Plan Integral de Saneamiento de la Ría de Bilbao*. Dyna, pp.25-30.
[323] García-Barcina J.M., Oteiza M., de la Sota A., **2002**. *Modelling the faecal colliform concentrations in the Bilbao estuary*. Hydrobiologia 475/476, 213-219.
[324] Cearreta A., Irabien M.J., Leorri E., Yusta I., Croudace I.W., Cundry A.B., **2000**. *Recent anthropogenic impacts on the Bilbao estuary, Northern Spain: geochemical and microfaunal evidence*. Estuarine, Coastal and Shelf Science 50, 571-592.
[325] Leorri E., Cearreta A., Irabien M.J., Yusta I., **2008**. *Geochemical and microfaunal proxies to assess environmental quality conditions during the recovery process of a heavily polluted estuary: The Bilbao estuary case (N. Spain)*. Science of the Total Environment 396, 12-27.

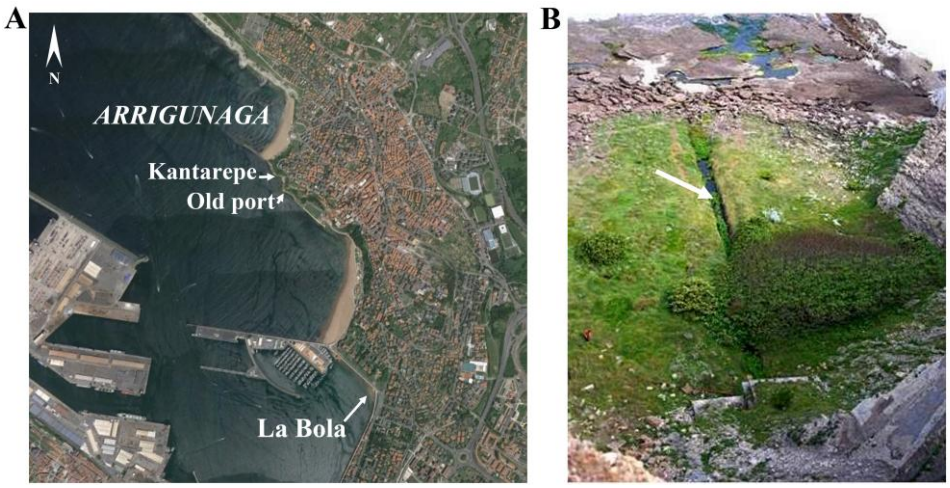

Figure 1.18. A) Location of Arrigunaga beach, as well as Kantarepe cove, the Old Port and the beach known as "La Bola". B) Detailed image of the sewage waters´ discharge point in Tunelboka cove.

The Nerbioi-Ibaizabal river provided the main water supply for the inhabitants settled around the estuary. In 1885, the cholera epidemic was originated and the industrial as well as mining activities were knocked out. Furthermore, the excessive mortality aroused the first concerns about public health and new water treatment mechanisms were pursued. This way, in 1891, the engineer Recaredo de Uhagón (1848-1912) won a public contest with a sanitation plan called *Mens sana in corpore sano*. This project comprised the first advanced and innovative sanitation system of Spain and it consisted on a dual separative circuitry to isolate rainwater from sewage waters; rainwaters were dumped directly into the river using the existent sanitation network, while a new sewerage system was built to collect exclusively the sewage waters and conduct them, directly and without treatment, to the open sea. With this new sewerage system, wastewaters were collected in a great deposit of 12.000 m^3 located in Zorrozaurre (Bilbao), and pumped (in the Elorrieta Pump House) towards the sea through a 10 km long pipe that would finish in Tunelboka cove, where the non-treated sewage waters were dumped[326].

The construction works of this sanitation system started in 1895, when there was a population of 63.900 inhabitants, and finished in 1903 when the population reached the 90.200 inhabitants. The system had the capacity to serve to 100.000 inhabitants, but the urban development proceeded faster than expected and the system became obsolete.

[326] Cárcamo J., **1996**. *Bombeadora de Elorrieta*. Colección Patrimonio Industrial de Bizkaia, nº 3. Diputación Foral de Bizkaia. Bilbao, 11 pp.

Therefore, in the 20s the area had already 150.000 inhabitants and wastes disposal into the estuary was occurred commonly again[327,328].

However, since 1995, as part of the cleaning up program established to improve the environmental conditions of the area, sewage waters coming from the metropolis of Bilbao, including the town of Getxo (where Arrigunaga beach and part of La Salvaje beach are located) and Sopelana (where part of La Salvaje is located) among other urban areas, would be treated in the waste water treatment plant of Galindo[329].

With reference to the locations of interest, it must be remarked that in Arrigunaga, despite the aforementioned direct impact of the estuary, the influence of the Gobelas river and the Tunelboka cove have been also recognized as sources of contamination[343]. Furthermore, apart from Tunelboka, it has been documented another place close to Arrigunaga, particularly known because of the accumulation of urban wastes. That place was apparently located in the Old Port (Figure 1.18A) at the sea, and it received the faecal waters coming from Algorta, but it disappeared when it was filled up with soil[330].

Regarding La Salvaje beach, Tunelboka cove is again a source of contamination, but also the sanitation coming from the adjacent urbanization, whose collector discharges in the east edge of the beach[329].

1.2.4.3 The slag disposal

The highly polluted estuarine plume was not the only side-effect of the frenetic activity developed in the riverbanks. The water body also received overwhelming amounts of wastes, such as slag, derived from steel manufacturing and mining activities.

In this context, many metallurgical industries would use port vessels, like hoppers, to transport their residues. The hoppers are a special type of boat that contains a central deposit whose walls are sealed from the rest of the hull. That deposit had a bottom gate that could be opened from the deck; when the deposit was full of wastes, slag or dredged materials, it was emptied into the river by opening the gate. The previously

[327] Cárcamo J., **1996**. *Bombeadora de Elorrieta*. Colección Patrimonio Industrial de Bizkaia, nº 3. Diputación Foral de Bizkaia. Bilbao, 11 pp.
[328] Barreiro P.M., Aguirre J.J., **2005**. *25 años del Plan Integral de Saneamiento de la Ría de Bilbao*. Dyna, pp.25-30.
[329] Gobierno Vasco-Eusko Jaurlaritza, **2000**. *Calidad del agua de baño de las playas del País Vasco: 1985-1998. Análisis de series temporales*. Vitoria-Gasteiz, 175 pp.
[330] Gorrotxategi Nieto M., **2000**. *Getxoko izenak. Aldeetxe eta leku izenak. Nombres de caseríos y lugares.* Getxoko Udala.

mentioned AHV company, for instance, by the year 1916 had its own fleet of hoppers to transport their wastes. Among them, the hooper called "Portu" can be cited (Figure 1.19A), which was constructed in 1902 and remained active during 65 years[331,332].

This way, metal-rich blast furnace slag were regularly dumped at the sea and, as a witness, heavy metal enriched coarse particles have been recently found in the estuary mixed with fine sediments[333]. Furthermore, an open sea slag disposal was established 4 miles away from the coast, in the area located at 43º 25.5' N - 3º 3' W and 43º 26.5' N - 3º 1,7' W (Figure 1.19B).

That dumping site was authorized by the Ministry of Public Works and Urban Development, and slag and other steelwork wastes were disposed there during the 20th century. Indeed, apparently between 1980 and 1995, the disposal is said to have accumulated a maximum of 225.000 tons of inert slag and 14.000 tons of steel mill powder every year[334].

That official dumping site has an extension of 7.4 km^2, in a depth ranging from 62 to 80 m. However, it has been suggested that the dumped materials might have been dispersed and even disintegrated, being transported outside the official dumping site or incorporated into the sea bed materials[335]. Indeed, high concentrations of Fe, Mn, Cu, Pb, Zn and Hg, have been found in the nearby water body[336] (Figure 1.19C). Nevertheless, in spite of the high concentration of metals that compose the by-products deposited in that area, referred to be mainly non bioavailable and no relevant disturbances have been found yet in the benthic communities, being considered mainly inert wastes[335,336].

[331] Llarena Mármol J., **2004**. *Restauración de embarcaciones preservando el futuro*. Kobie (Serie Anejos) 6, 745-750. Diputación Foral de Bizkaia. Bilbao.
[332] Ruigómez Matxin J., **2014**. *Activities Report 2003-2014.* Ría de Bilbao Maritime Museum Foundation, 188 pp.
[333] Cundy A.B., Croudace I.W., Cearreta A., Irabien M.J., **2003**. *Reconstructing historical trends in metal input in heavily-disturbed, contaminated estuaries: studies from Bilbao, Southampton Water and Sicily*. Applied Geochemistry 18, 311-325.
[334] Borja A., Tueros I., Belzunce M.J., Galparsoro I., Garmendia J.M., Revilla M., Solaun O., Valencia V., **2008**. *Investigative monitoring within the European water Framework Directive: a coastal blast furnace slag disposal, as an example*. Journal of Environmental Monitoring 10, 453-462.
[335] Borja A., Galparsoro I., Garmendia J.M., Revilla M., Tueros I., Valencia V., **2006**. *Caracterización de la antigua zona de vertidos de "Altos Hornos de Vizcaya" y evaluación del riesgo actual para la biota*. Informe final para Dirección de Aguas Departamento de Medio Ambiente y Ordenación del Territorio del País Vasco.
[336] Tueros I., Borja A., Larreta J., Rodríguez J.G., Valencia V., Millán E., **2009**. *Integrating long-term water and sediment pollution data, in assessing chemical status within the European Water Framework Directive*. Marine Pollution Bulletin 58, 1389-1400.

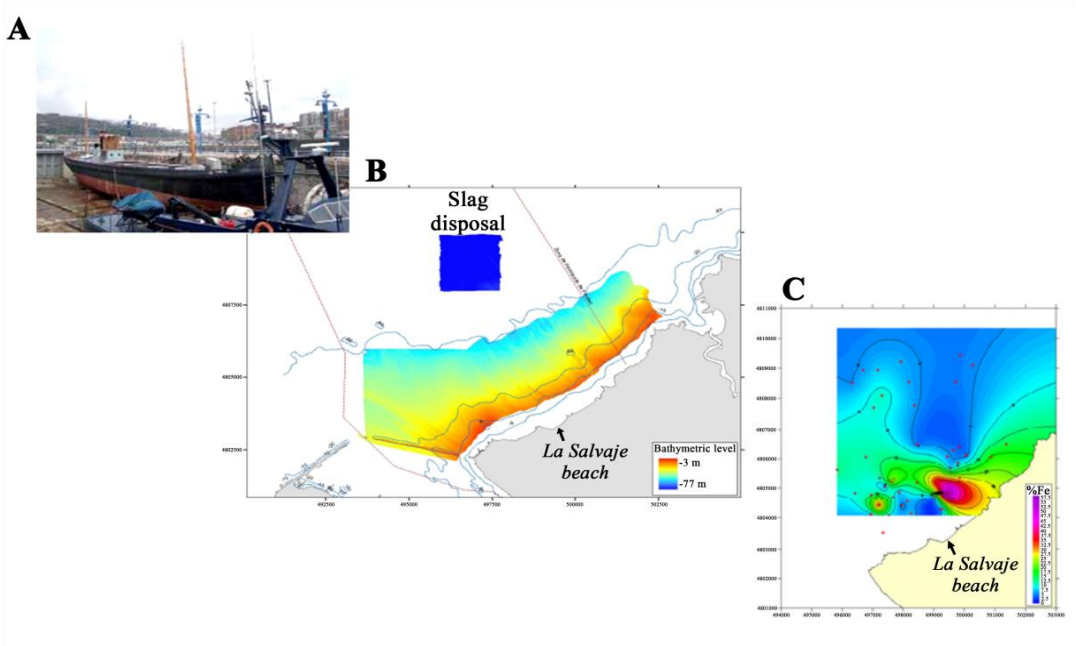

Figure 1.19. A) View of the Hopper called "Portu". Source: Ruigómez Matxin (2014)[337]. B) Location of the slag disposal. C). Iron concentration in the area near La Salvaje beach. Source: Borja et al. (2006)[338].

Although no relevant adverse effects have been found yet, other consequences might be occurring nowadays. For instance, in some beaches facing that slag disposal, like La Salvaje beach, the loose sand is becoming blacker, probably due to the iron-rich particles that reached the shore helped by tidal currents[339,340]. In addition, some authors also suggested that one of the effects of the slag disposal is the deposition and accumulation of slag and other industrial wastes in the coast, forming cemented dark sands[341]. Indeed, the beachrocks around the estuary of Bilbao have been often associated with the massive amounts of slag dumped into the system[342-345]. In this sense, some authors suggested that due to the expected shoreline retreat that might

[337] Ruigómez Matxin J., **2014**. *Activities Report 2003-2014.* Ría de Bilbao Maritime Museum Foundation, 188 pp.
[338] Borja A., Galparsoro I., Garmendia J.M., Revilla M., Tueros I., Valencia V., **2006**. *Caracterización de la antigua zona de vertidos de "Altos Hornos de Vizcaya" y evaluación del riesgo actual para la biota*. Informe final para Dirección de Aguas Departamento de Medio Ambiente y Ordenación del Territorio del País Vasco.
[339] Tueros I., **2010**. *Bizkaiko Labe Garaien lorratzak Sopelako hondartzetan*. Elhuyar Zientzia eta Teknologia 264, 12-15.
[340] Pérez F.P., **2004**. *Playas del País Vasco*. ADEVE (Cristina Ruiz Urionabarrenetxea). Editor Petronor, 293 pp.
[341] Lugaresaresti Bilbao J.I., **1994**. *Aspectos de clima marítimo y morfodinámica en el Puerto Exterior de Bilbao*. Kobie (Serie Ciencias Naturales) 22, 24-32. Diputación Foral de Bizkaia. Bilbao.
[342] Lugaresaresti Bilbao J.I., **2002**. *Cambio ambiental reciente en el territorio de Bizkaia*. Lurralde 25, pp. 141-162.
[343] Arrieta N., Goienaga N., Martínez-Arkarazo I., Murelaga X., Baceta J.I., Sarmiento A., Madariaga J.M., **2011**. *Beachrock formation in temperate coastlines: Examples in sand-gravel beaches adjacent to the Nerbioi-Ibaizabal Estuary (Bilbao, Bay of Biscay, North of Spain)*. Spectrochimica Acta Part A 80, 55-65.
[344] Arranz S., **2012**. *Contaminación por metales pesados. El caso de la ría de Bilbao*. Itsas Memoria. Revista de Estudios Marítimos del País Vasco 7. Untzi Museoa-Museo Naval, Donostia-San Sebastián, pp. 265-282.
[345] Astibia H., **2012**. *Tunelboka y Gorrondatxe (Getxo, Bizkaia), fósiles humanos para el Antropoceno.* Euskonews, 640.

occur soon, and the subsequent erosion of these deposits, beachrocks could be secondary potential sources of contaminants for the coast realm[346].

1.2.5. Description of the beachrock formations under study

1.2.5.1. Arrigunaga beach

This 628 km long beach is placed in the town of Getxo, around 17 km far from Bilbao (43º 21' N – 3º 01' W), and it is bordered on the north with the Punta Galea Cliff. On the top of the cliff this place is characterized by the presence of a windmill known as "Aixerrota", an iconic building of the town of Getxo, built around the 18th century. To the west of the cliff, getting closer to the ocean, it can be found also the best example of the military construction of the 18th century conserved in Bizkaia, "La Galea Fort".

Until the 90s, this beach was notoriously characterized by the presence of dark and dirty sand, cementation and high presence of gravels. But after its regeneration in the late 90s, it was replaced by the fine sands of Bakio beach (43º 25' N – 2º 48' W). This process will be explained more in depth in the following section.

- **Adaptation actions for functional improvement**

Arrigunaga beach is located in the right bank of the mouth of the Nerbioi-Ibaizabal estuary, inside the Abra bay, and as it suffered a strong degradation and alteration, the Provincial Council of Bizkaia contemplated its regeneration in the early 90s, mainly due to these problems:

-Presence of gravels.
-Presence of cemented sand that made bathing very difficult or even impossible.
-Existence of dark and dirty sand.

In an attempt to solve those functional and aesthetical problems, the *Leonardo Torres Quevedo Foundation* of the University of Cantabria performed a thorough study of the situation and proposed the possible alternatives to regenerate the beach[347]. In order to understand the evolution of the beach, some relevant aspects collected in that study will be highlighted herein.

[346] Irabien M.J., García-Artola A., Cearreta A., Leorri E., **2015**. *Chemostratigraphic and lithostratigraphic signatures of the Anthropocene in estuarine areas from the eastern Cantabrian coast*. Quaternary International 364, 196-205.
[347] Losada M.A., Medina R., Baquerizo A., Silva R., Tomillo C., Foyo A., Sagaseta C., Polanco J.A., Canteras J.C., **1993.** *Estudio de la playa de Arrigunaga. Situación actual y alternativas de regeneración*. Fundación Torres Quevedo. Diputación Foral de Bizkaia. Universidad de Cantabria (Inédito).

At first, some peculiarities dealing with marine dynamics will be remarked. The tidal action produces a movement of the water body that in the rising tide runs upstream of the Nerbioi river and in contrast, during falling tide, is moved towards the sea. This water flow and reflow is known as tidal currents. In the specific case of Arrigunaga beach, according to the previously mentioned study, it was observed that the water flow going from the river towards the beach (Figure 1.20A) and the water flow moving in the opposite direction (1.20B) were unbalanced, with a net balance towards Arrigunaga. As such, the possible contaminants transported with the tidal currents or floodings, tend to go towards Arrigunaga and would be directed to the beach by wave action (Figure 1.20A). In any case, it should be remarked also that, as mentioned before, the sewage waters discharged in Tunelboka cove could influence in Arrigunaga beach, possibly facilitated by tidal currents (Figure 1.20B).

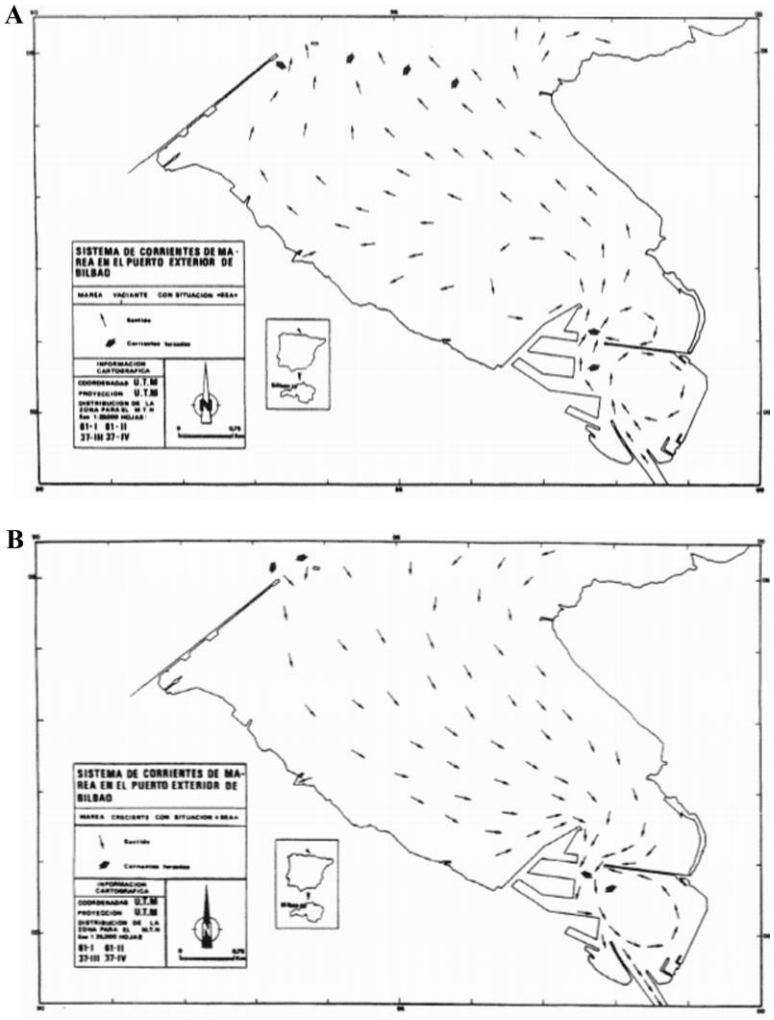

Figure 1.20. Tidal currents in the Abra bay. Source: Lugaresaresti (1994)[348].

[348] Lugaresaresti Bilbao J.I., **1994**. *Aspectos de clima marítimo y morfodinámica en el Puerto Exterior de Bilbao*. Kobie (Serie Ciencias Naturales) 22, 24-32. Diputación Foral de Bizkaia. Bilbao.

Knowing that characteristic of the marine dynamics in the area of study, it could be interesting to pay attention also to the morphodynamic features. The profile of a beach is mainly conditioned by the currents associated to wave breaking and the existent materials or sediments. In those cases in which waves reach the shore with parallel wave fronts, negligible alongshore currents are generated. On the contrary, if waves approach the shore with a certain obliquity, a wave driven alongshore current can be formed[349], with the subsequent potential capacity for sediment transport. In the case of Arrigunaga, the orientation of the beach is quite parallel to the wave fronts. However, in the area next to the cliff (the northern part of the beach), the wave obliquity is quite remarkable (around 70º-80º) and therefore, there was a higher sediment input in that zone.

From the sedimentological perspective, as previously mentioned, the beach was characterized by the high presence of gravel, coming mainly from the erosion of certain parts of the Punta Galea cliff. Likewise, apparently, the beach was just a tidal plain, and the sand might have been derived from the massive disposal of blast furnace slag; they were transported by the tidal currents towards the beach and reduced to sand-size by wave action, progressively forming dark sands in the beach. As the slag input was decreased and the sand of beach eroded, the gravels were again visible as well as the structures of cemented sand.

In view of these problems, diverse actions were taken in an attempt to solve the functionality and aesthetic characteristics of the beach. This project included the following actions[350,351]:

- Construction of three breakwaters (40, 55 and 75 m long) in the north of the beach, perpendicularly to the cliff.
- Extension of the breakwater (240 m long) in the southern area.
- Removal of (cemented) sand (excavation of around 27.000 m^3), and the subsequent filling of the intertidal and supratidal zones with around 200.000 m^3 of loose sand.
- Definition of accesses to the beach and urbanization.

[349] Den Heijer C., **2013**. *The role of bathymetry, wave obliquity and coastal curvature in dune erosion prediction*. PhD thesis, Delft University of Technology, 172 pp.
[350] SENER, **1994**. *Proyecto de regeneración de la Playa de Arrigunaga. Proyectos de emisarios submarinos, estudios de dispersión de contaminantes y dinámica litoral*.
[351] Lugaresaresti Bilbao J.I., **2002**. *Cambio ambiental reciente en el territorio de Bizkaia*. Lurralde 25, pp. 141-162.

After those actions, the current view of the beach can be observed in Figure 1.21, which is compared with the aspect of the area in the early 80s.

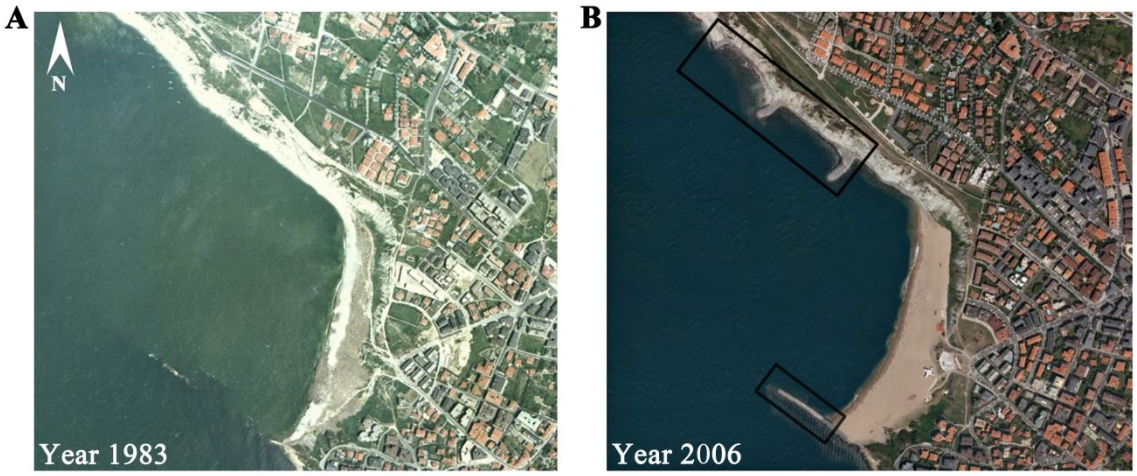

Figure 1.21. Comparison between orthophotos of Arrigunaga beach in A) 1983 (before the regeneration) and B) 2006 (indicating the infrastructures established after the regeneration). Source: Diputación Foral de Bizkaia (2016)[352].

However, probably due to the erosion of the sand occurred along the years, nowadays cemented sands, or beachrocks, are again visible in Arrigunaga beach, specially at low spring tides (Figure 1.22), as it will be described in the next section.

Figure 1.22. General views of Arrigunaga beach A) before the regeneration (later 90´s). B) Nowadays. C) Nowadays, but at low spring tide, where beachrock outcrops can be observed (marked with the black line).

- **Beachrock of Arrigunaga**

Beachrock sediments occur there overlying a wave-cut platform carved onto indurated Palaeogene deep marine deposits (turbidites, limestones and marls), in the form of sand to gravel sized heterolithic sediments accumulated in subhorizontal to slightly inclined dm-thick graded beds (foreshore facies). According to the literature and pictures of the beach before the regeneration, it can be deduced that beachrock was well

[352] Diputación Foral de Bizkaia, **2016**. Planos y ortofotos. http://www.bizkaia.eus.

stratified in thin beds (Figure 1.23), indicative of different episodes of cementation, exposure or even material arrivals[353,354].

Figure 1.23. Photograph of a beachrock in Arrigunaga previously to the regeneration. Source: García Garmilla (1990)[353].

After the regeneration, remnants of these facies can also be seen at low tide along the present beach intertidal zone, forming some kind of indurated and isolated residual platform and benches. Beachrocks are generally found in the mid-intertidal zone of the northern area, but at low spring tides, more cemented beds that are usually under water, are exposed also along the beach (figure 1.24A). Furthermore, diverse stages of the evolution of beachrocks can be observed throughout the year. Sometimes it might not be visible, as it is covered by a layer of unconsolidated sand, occasioned by beach accretion events (Figure 1.24B). But, after the beach erosion and low tides, the unconsolidated sand is retired and beachrock formations exhumed. If the beachrock has been exposed long enough (e.g., three months), cemented bodies are greatly noticeable, colonized by epilithic biota (compare Figure 1.22.B vs 1.22C and see 1.24B and 1.24J). The influence of the regeneration works and the action of waves, have favoured the development of cavities, furrows and discontinuities in their original structure (Figure 1.24F).

Additionally, diverse human artefacts can be visualized within the cemented bodies, with a great abundance of industrial residues like mm- to cm-sized slag and

[353] García Garmilla F., **1994**. *Diagenesis de las arenitas: ejemplos del Cretácico, Terciario y Cuaternario de la zona de Bilbao*. Kobie (Serie Ciencias Naturales) 19, 85-103.
[354] Leorri E., Cearreta A., **2009**. *El registro geológico de la transformación ambiental de la ría de Bilbao durante el Holoceno y Antropoceno*. Munibe, Suplemento 26. Sociedad de Ciencias Aranzadi, 192 pp.

other components like refractory bricks (Figure 1.24G-I). Many of them can co-exist with local clasts and even with typical intertidal species, like limpets and molluscs. The human-derived materials are nowadays especially visible in the northern area of the beach, were due to the obliquity of the incident waves, external inputs tended to deposit previously to the regeneration of the beach. It is presumed that the nature and abundance of the man-derived remains was possibly more diverse and greater before the removal of the cemented sand; in any case, their presence nowadays is evident enough to testify the material arrival from nearby anthropogenic sources, and simultaneously, the recent genesis of the cemented bodies.

Figure 1.24. A) General view of Arrigunaga beach at low tide, where beachrock outcrops can be observed in the north and the mid part of the beach. B) Beachrock outcrop colonized by a green mat of epilithic biota. C) Example of an outcrop viewed in the north. D-E) Examples of the outcrops observed along the mid part. F) Outcrops with cavities formed through the erosion or regeneration actions. G-I) Materials that can be found cemented within the beachrock, including human derived materials like slag and bricks. J) Detail of local clasts, slag and intertidal species.

1.2.5.2 La Salvaje beach

La Salvaje beach is also known with other names like “Barinatxe” or “Solondotas”, and it is located on the boundaries of the towns of Getxo and Sopelana, 22 km far from Bilbao (43º 23’ N – 3º 00’ W). With an extension of around 752 m, it is oriented towards the open sea and although its slope is very steep especially in the upper zone, is quite flat in the baseline of the coast; indeed, the extension of the beach during low tides triples the one at high tides, making this beach one of the most extensive beaches in the Basque Country[355].

It is mainly formed with bioclastic sands provided by alongshore currents. However, it is also characterized by fine and dark sands especially in the central and right parts of the beach and it has been considered to be rather dusty, as the sand can be mixed with the powder derived from industrial residues[356].

As a curiosity, in this completely open beach, waves can usually arrive with great force on the shore, and moreover, it can be a quite windy beach. Thus, these characteristics make the place to be very frequented for diverse recreational uses like surfing or paragliding. Indeed, the rate of users that come to this beach is very high[357].

- **Beachrock of La Salvaje**

After the strong storm events occurring in the winter of 2014, the presence of beachrock in La Salvaje beach was confirmed and evidences of intertidal cementation were found. As in the case of Arrigunaga beach, the cemented bodies were more prominent at low spring tides. Moreover, they also show subhorizontal to slightly seaward-dipping dm-thick beds (Figure 1.25A-B) as well as isolated benches (Figure 1.25C). They are mainly found in the mid-intertidal zone of the beach, although beachrock outcrops could also be found in the upper intertidal zone of that zone (Figure 1.25D). They mainly accumulate fine sized sediments, although heterolithic fine to gravel sized sediments could be found cemented especially in the southwestern area.

[355] Pérez F.P., **2004**. *Playas del País Vasco*. ADEVE (Cristina Ruiz Urionabarrenetxea). Editor Petronor, 293 pp.
[356] Pujalte V., Astibia H., Aizpiri F., Payros A., **2015**. *Las playas cementadas del “Antropoceno” de Bizkaia: origen y degradación*. Geogaceta 57, 123-126.
[357] Gobierno Vasco-Eusko Jaurlaritza, **2000**. *Calidad del agua de baño de las playas del País Vasco: 1985-1998. Análisis de series temporales*. Vitoria-Gasteiz, 175 pp.

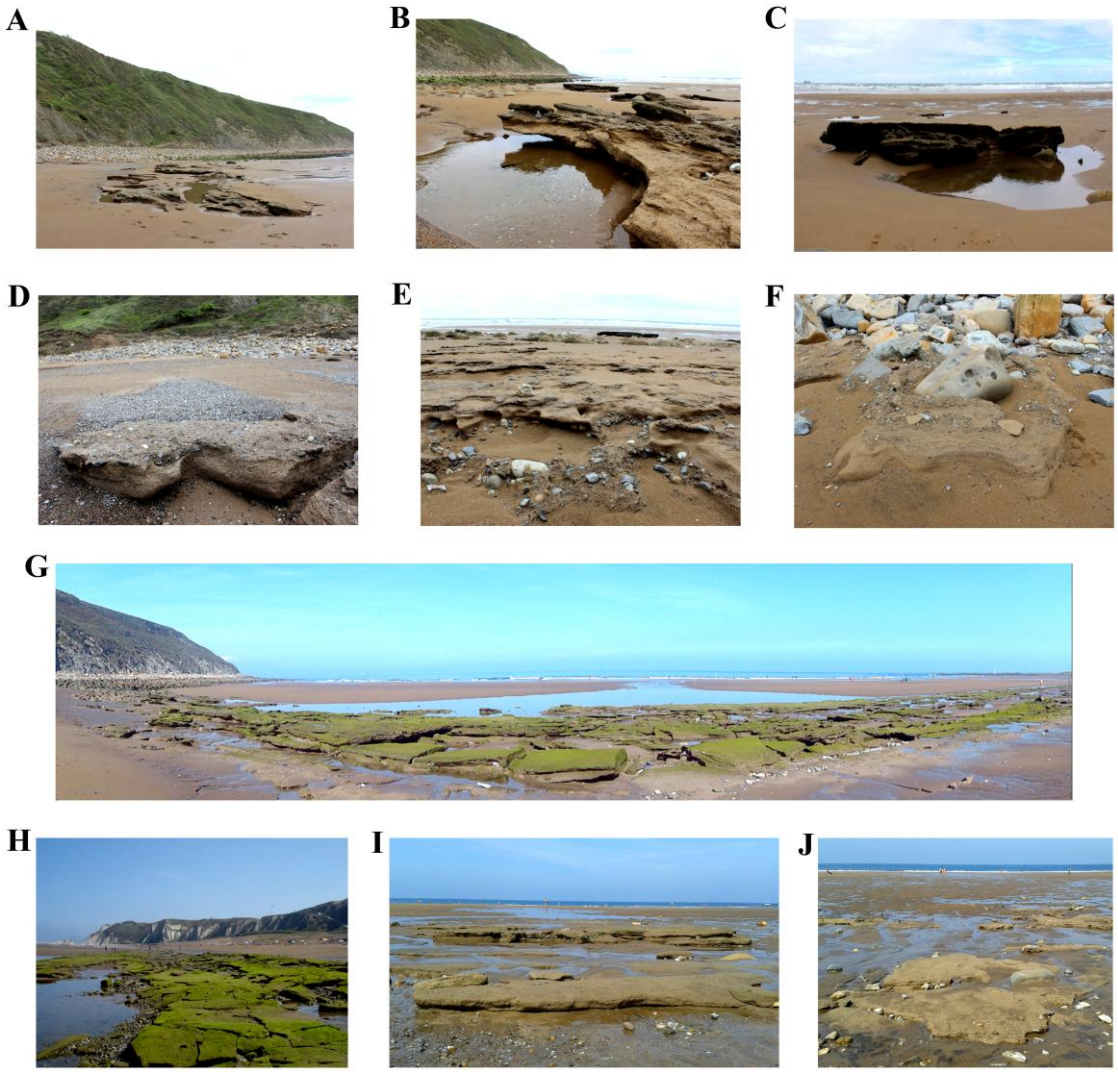

Figure 1.25. A-B) Subhorizontal to slightly seaward-dipping dm-thick beds. C) Image of an isolated bench. D) Example of an outcrop found in the upper intertidal zone. E) Cavities and F) flutings observed as a result of the erosion. G) General view of the outcrops found in the southwestern area of the beach. H) Detail of the contiguous broken slabs, sectioned through a set of fissures. I-J) Isolated outcrops found going towards the mid part of the beach.

Indeed, the first outcrops found in the year 2014, were identified in that southwestern area. Erosional features modelled by wave action, like cavities and wave induced flutings, can be observed similarly to other beachrocks[358] (Figure 1.25B-E). After a few months, they generally formed contiguous broken slabs, sectioned through a set of fissures (probably formed after strong wave erosion) and united through polygonal and orthogonal connections (Figure 1.25G-H), as it has been described in some beachrocks[359]. Going towards the mid part, the outcrops were more isolated, lacked in

[358] Howie F.M.P., **2009**. *Beachrock development along the North coast of Cornwall*. Geoscience in South-West England 12, 85-94.
[359] Erginal A.E, Ekinci Y.L, Demirci A., Bozcu M., Ozturk M.Z., Avcioglu M., Oztura E., **2013**. *First record of beachrock on Black Sea coast of Turkey: Implications for Late Holocene sea-level fluctuations*. Sedimentary Geology 294, 294-302.

epilithic biota, denoting that they were in a different evolution stage, as they might be less consolidated or just exposed to open air (Figure 1.25I-J).

From the observations of the beachrock from La Salvaje, it can be said that the presence of slag within the cemented deposits is not that apparent and notorious. But, the presence of wastes within the beachrocks in the form of fine sized grains is not discarded, because for instance, unconsolidated iron particles are noticed especially in the mid part of the beach (Figure 1.26A-C). Moreover, non-cemented wastes can be found dispersed along the shore (Figure 1.26D-E).

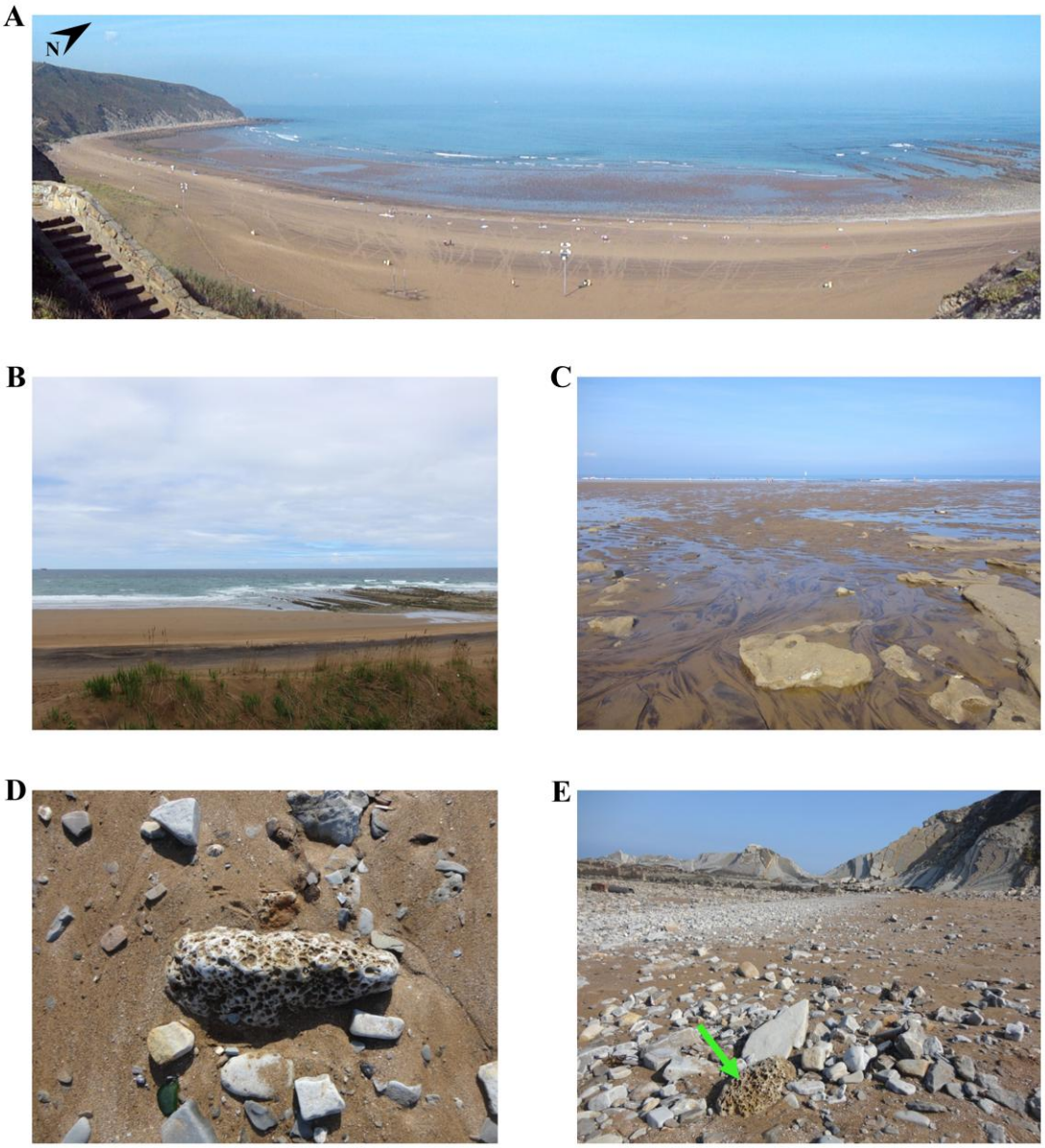

Figure 1.26. A) General view of La Salvaje beach. B) Detail of the blackening of the unconsolidated sand. C) Image of the dark sand and a beachrock outcrop. D-E) Non-cemented wastes found dispersed along the beach.

Chapter 2

Objectives

This PhD is part of a research program started in 2010 dealing with the study of the processes involved in the formation of rather uncommon beachrocks set in a particularly altered estuarine area located in a temperate zone. The analyzed area belongs to the Nerbioi-Ibaizabal Estuary (Bilbao, North of Spain) and covers beachrocks located in two beaches, Arrigunaga (inside the estuary) and La Salvaje (outside the estuary).

The inherent complexity of this cementation phenomenon and the disturbances occurred in the area of study during the recent past decades will go hand in hand along this work, in an attempt to recognize the underlying characteristics of the studied beachrock outcrops.

On that basis, this PhD work pursues these main objectives:

1) To examine the main physical and compositional characteristics of the beachrock outcrops.

2) To quantitatively estimate the metal content of the cemented bodies and assess the possible contamination trapped in them.

3) To determine the characteristics of the cements and that way, estimate the diagenetic environment and/or processes involved in the cementation.

With those principal aims in mind, diverse operational objectives were followed:

- To gather information about the main constituents of the deposits and their possible weathering compounds.
- To study, for the first time, the feasibility of Raman spectroscopy to perform field analysis.
- To estimate the metal content of the studied beachrock outcrops in relation with the possible environmental alterations that affected each setting.
- To use standard environmental indexes for the contamination assessment.
- To visualize the characteristics of the beachrocks, with especial focus on the cements, using, as a breakthrough, varied and complementary microscopic imaging tools.
- To identify the composition disposition and morphology of the various cements that bind the diverse grains together.
- To propose the main factors involved in the beachrock formation of Arrigunaga and La Salvaje beach, being the first record of the phenomenon in the latter one.

Overall, after explaining the details of the techniques used (Chapter 3), the results are integrated in diverse chapters (Chapter 4, 5 and 6) that would lead to the conclusions explained in Chapter 7.

Chapter 3

Experimental procedure

This chapter describes the experimental procedures followed to meet the objectives of the research. First of all, the diverse sampling campaigns will be explained in order to understand the basis of each stage of the work. As it will be exposed throughout the thesis, the results derived from the different samplings will demonstrate the significance of the sampling strategies. Regarding the utilised analytical tools and instruments, it is worth mentioning that the order in which the techniques are explained in this section does not correspond accurately with the order of appearance in the results (Chapters 4, 5 and 6). However, herein it is pursued the understanding of the complementarities among the selected techniques for the target challenges in each phase of the work.

In that context, subsequently to sample collection, the pretreatment procedure will be described, including the sieving of the samples and the thin section preparation (followed by the staining method applied to the thin sections). In both cases, preliminary to any analysis, it was essential the microscopic examination of the samples of interest. Overall, polarized light microscopy was used as a first step, but fluorescence microscopy and electronic microscopy were also applied in an attempt to better understand the underlying characteristics of the beachrock outcrops, with special interest in the cements. Regarding the electronic microscopy, two kinds of imaging techniques were applied: secondary electron imaging (SE) and backscattered electron imaging (BSE), complementary to the previous microscopic information. In addition, electronic imaging could be accompanied by Energy Dispersive X-Ray Spectroscopy (EDS) analysis, to determine the elemental distribution of the selected areas. With regard to the compositional characteristics, Raman spectroscopy was also used as a molecular fingerprint of both, the framework grains and the cements. The former include *in situ* analyses, while the analysis of the latter was completed with X-Ray Diffraction (XRD). Additionally, stable isotope analyses ($\delta^{13}C$ and $\delta^{18}O$) greatly contributed in the understanding of the origin of the carbonate cements. Besides, Inductively Coupled Plasma-Mass Spectroscopy (ICP-MS) in conjunction with total carbonate quantification provided the preliminary information about the element concentration of the beachrock units. Moreover, ICP-MS also helped in the comparison of the different sites of study, always complemented by statistical analyses.

3.1 Sampling procedure

The sampling plan varied depending on the aims behind each main phase of the research. Some phases were focused on the analyses of different strata, others in the examination of diverse materials trapped within the beachrocks, while some were mostly dedicated to the comparison of outcrops located at different tidal levels in Arrigunaga and La Salvaje beach. In any case, samples were regularly collected under low tide conditions to ensure the visibility of the outcrops. The sample collection was aided by a stainless steel chisel and a hammer, and samples were subsequently transported to the laboratory in properly labelled zip bags. To guarantee the representativeness of the analyses, convenient and sufficient quantities were sampled. The specifications of the main sampling plans are explained in the following lines.

3.1.1 Stratigraphic sampling of beachrock outcrops in Arrigunaga beach

As explained before, Arrigunaga was at first the main research focus, as there were not found yet sufficient evidences of the presence of beachrocks in La Salvaje. In contrast, in Arrigunaga, despite the regeneration process performed in the late 90´s, many beachrock outcrops are still mostly located in the northernmost part (left side of the beach). In fact, that part might be the area with the higher abrasive seawater influence, due to the morphodynamic characteristics of the beach.

Among the diverse outcrops observed, in October 2010 representative samples were obtained from a 1.40 m high stratified bed (Figure 3.1). It was located in the higher intertidal zone and it was sampled in the initial stages of the research, because it was believed to resemble the cemented beds existing in the beach previous to the regeneration. Therefore, following the steps succeed in previous work of the adjacent coast[1], the interest of this outcrop laid on the screening of the main characteristics of the cements and the materials composing the matrix of the beachrock, as well as on establishing possible trends of the components at different heights (work described in Chapter 4). Following the procedure used in those locations, 10 different samples were collected along the outcrop (S1-S10), representing the various exposed strata. It must be mentioned that at first sight, the strata were not as well defined as in the adjacent beaches, except from the intermediate part of the outcrop, where the limits of the strata seem to be more noticeable.

Figure 3.1. A) The vertical outcrop considered for this study, including the ten samples collected (S1-S10). Details of the vertical outcrop, where the differences of the stratification level can be appreciated between the upper (B), intermediate (C) and lower (D) part of the beachrock.

[1] Arrieta N., **2014**. *The study of an unusual temperate latitude beachrock formation. Characterization of Azkorri beach and Tunelboka cove locations*. PhD Thesis, University of the Basque Country.

The results achieved through the investigation of this outcrop, gave some basic information about the cements and the possible anthropogenic nature of some of the cemented materials. Thus, this preliminary study led somehow the course of the following sampling strategies and analyses, to further explore the cements and the anthropogenic materials.

Focusing on the anthropogenic materials, detailed analyses were mainly focused on the slag trapped within various outcrops. In an attempt to better determine their composition, a Raman spectroscopic study was carried out, combining *in situ* and laboratory analyses (results explained in Chapter 4). Overall, 29 samples were considered for these analyses. However, it is worth mentioning that laboratory analyses were mainly based on representative samples collected according to the variability observed during *in situ* analyses at different low tidal periods, from the indurated and isolated residual platform and benches present in the northernmost and the middle part of the beach (Figure 3.2).

Figure 3.2. A) Overview of the indurated and isolated residual platform and benches. B) Example of the area examined with *in situ* Raman spectroscopy in the northernmost part of the beach. C) Detail of a brick trapped in the beachrock. D) Exemplar of a typical slag found in the beach. E) *In situ* Raman spectroscopy analysis being carried out in the beachrock. F-H) Wastes that can be found cemented in Arrigunaga beach.

3.1.2 Sampling areas in Arrigunaga and La Salvaje beach

The possible influence of the anthropogenic alterations was also investigated through the quantitative determination of the metal content, in beachrock outcrops belonging to both settings. For that purpose, diverse areas were considered for sample collection.

- **Arrigunaga beach**

Regarding Arrigunaga beach, as the majority of the outcrops were accumulated in the northernmost part of the beach, under the cliff, we selected that area to perform the transverse sampling (Figure 3.3A). It must be clarified that ART5 is slightly displaced from the rest of the samples, but resulted of interest as it was part of a highly cemented seaward pavement found along the shore (Figure 3.3A and Figure 3.3B).

Some visual features can be discerned in the samples, although all of them show randomly trapped greater grains, probably coming from cliff derived materials, it can also be distinguished that the seaward samples, especially ART4, retain a more and greater variety of grains, possibly reflecting the onshore increasing material arrival (Figure 3.3D).

Figure 3.3. A) The area where the transverse transect was performed in Arrigunaga beach (marked with the white box). B) Location of the sampled spots (ART1-ART4). C). Spatial location of all the sampling points (ART1-ART5). D) Detailed view of some sample fragments.

On the other hand, as shown in Figure 3.4, three sites were sampled in the longitudinal sampling (ARL1-ARL3) in Arrigunaga beach (Figure 3.4A). Attending to the visual characteristics of the samples (Figure 3.4B), it can be said that the sample closer to the cliff (ARL1) seems to have a greater content of gravels and boulders than the rest, probably due to the entrapment of materials coming from the cliff. These cemented

deposits are believed to be generally submerged but the strong spring tides unfolded their presence and allowed their visualization.

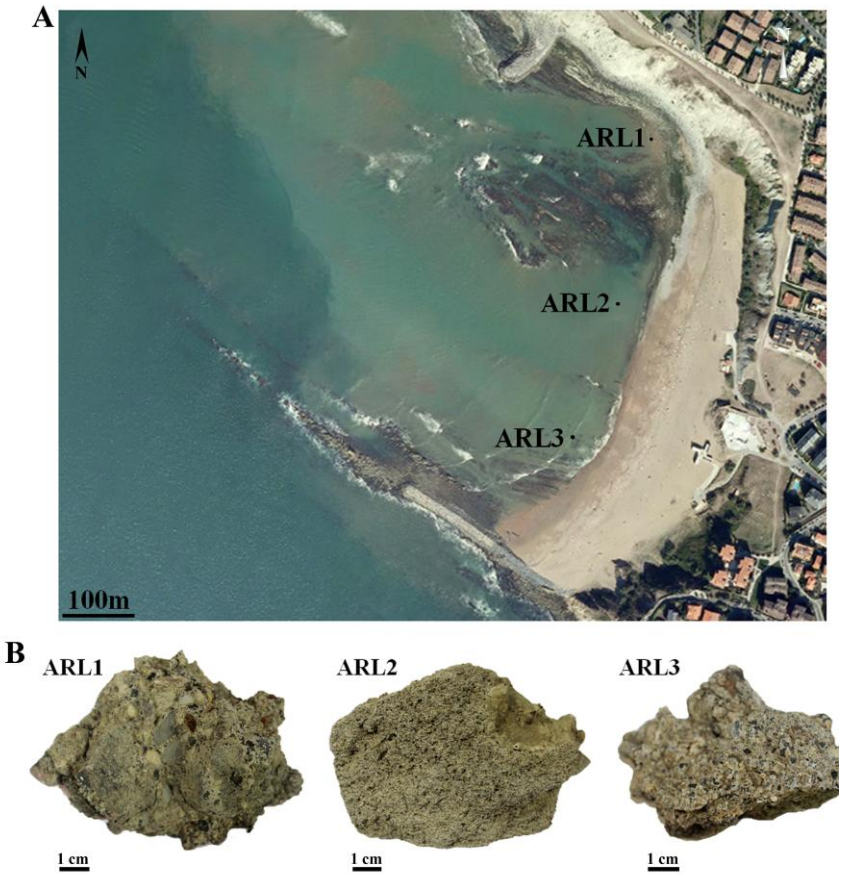

Figure 3.4. A) Location of the areas considered in the longitudinal transect carried out in Arrigunaga beach. B) Detailed view of some sample fragments.

- **La Salvaje beach**

The following images show the sampling carried out in La Salvaje beach. With reference to the transverse sampling, in this beach also, the outcrops are generally more dispersed along the intertidal level in the area next to the cliff (southeastern part of the beach). Therefore, the transverse sampling (LST1-LST4) was carried out in that region (Figure 3.5A and Figure 3.5B). It should be noted that the sample LST1, was part of the inner outcrop and showed a smaller grain size, in contrast to the variety of sizes amalgamated in the other samples (Figure 3.5C). As mentioned before, that difference in the cemented grain sizes might be induced by the increasing material arrival.

Finally, the points sampled longitudinally (LSL1-LSL5) can be recognised in Figure 3.6. Similarly to the sampling performed in Arrigunaga beach, the aim was to sample the most extreme areas where the outcrops would be found, as well as a middle point. However, in La Salvaje, two parts could be differentiated during the longitudinal

sampling; one of them showing decimetric cemented outcrops colonized with intertidal vegetation, possibly reflecting a longer exposure time (Figure 3.6B), while the zone shown in Figure 3.6C, was composed of discontinuous bare cemented beds. It should be highlighted that mostly LSL2 showed a higher integrity, leading to believe that it was better cemented, as the rest of the specimens were more friable (Figure 3.5C).

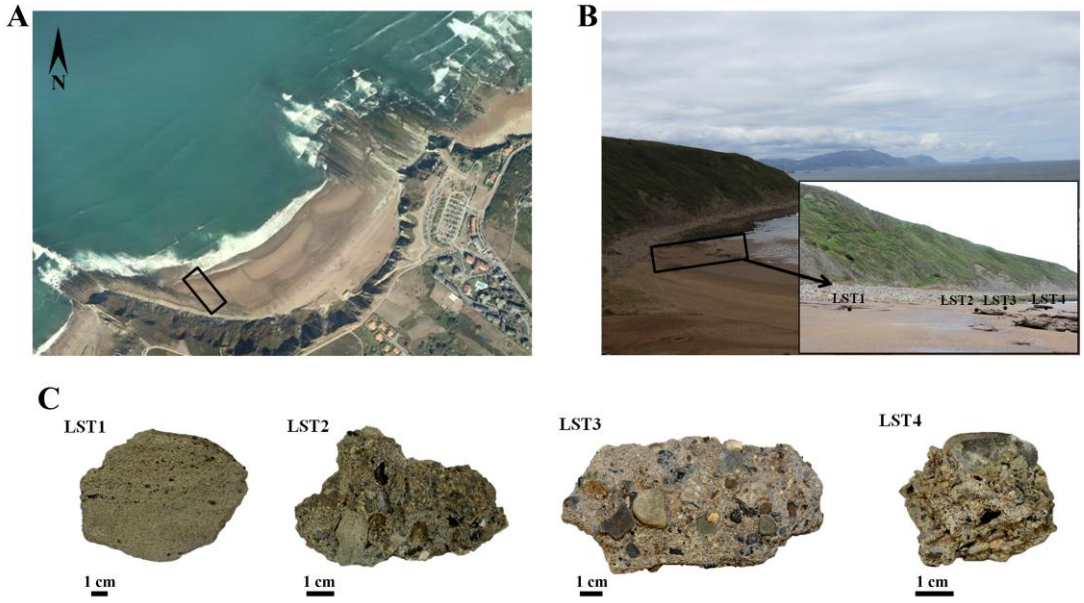

Figure 3.5 A) Area of La Salvaje beach where the transverse transect was performed in (marked with the black box). B) Location of the sampling points. D) Detailed view of sample fragments.

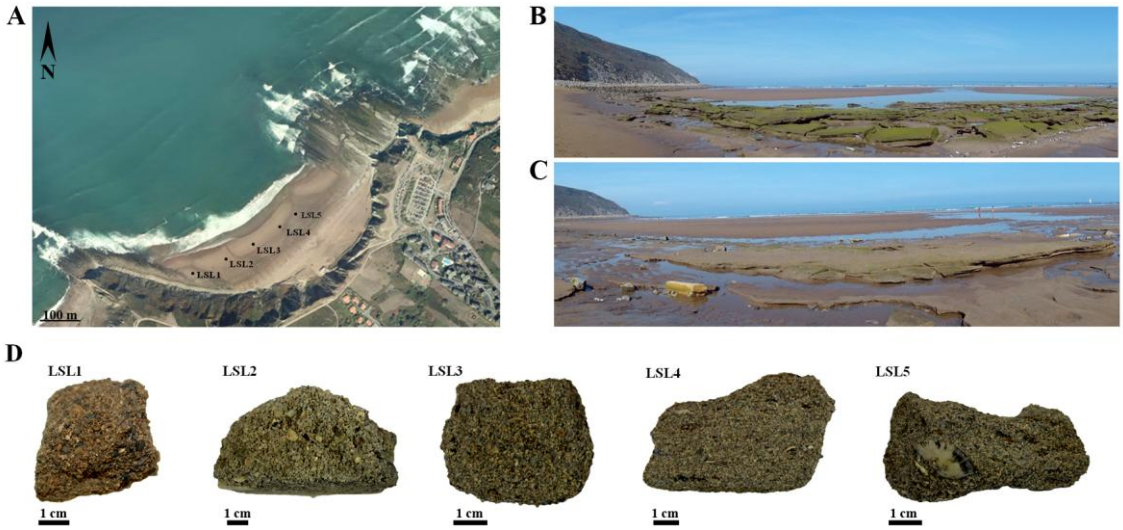

Figure 3.6. A) Location of the areas considered in La Salvaje beach during the longitudinal sampling. B-C) Images of some sampled outcrops. D) Detailed view of some sample fragments.

3.1.3 Random sampling in the selected areas

In relation with the areas described in the previous section, and considering that the visibility of the outcrops is rather diverse depending on the period of the year or the weather, among other factors, random samples could be gathered throughout those areas. On the whole, an average of four samples was collected in each of the areas of Arrigunaga and La Salvaje beach, gathering overall, 27 and 30 samples respectively. The gathering of diverse samples of the same area resulted essential especially for the analysis of the cements, by the examination of thin sections or the cements themselves, by diverse microscopic and analytic techniques. For instance, as it will be explained later, cements were removed from the sample using a microdrill or a scalpel, so as to get powdered samples required for the target analyses. But, the presence and accessibility of that cement is greatly variable in the beachrock samples, and sometimes even unfeasible to get enough amount of cement to be analysed. Thus, this random sampling allowed having a wide variety of beachrock samples representative of an area, providing especially more chances to get the needed amount of cements for the expected analyses (work described in Chapter 6).

3.2 Sample pretreatment

After their collection, the samples were air dried till constant weight and depending on the target aim in each of the stages of the work, a different treatment was required previous to the analyses: particle size separation for quantitative analyses through ICP-MS or preparation of thin sections for the petrographic examination of the samples.

3.2.1 Particle size separation

Samples were sieved in an Octagon digital sieve shaker (Endecotts, London, UK) mounted with laboratory test sieves (Figure 3.7A) and then ground in a planetary ball mill Pulverisette 6 (Fritsch, Indar-Orberstein, Germany) during 15-30 minutes at a speed of 400-500 rpm. Diverse grain sizes were obtained depending on the target aim in each stage of the research. At first (Chapter 4), four different particle size ranges or fractions (>2mm, 250µm-2mm, 75-250µm and <75µm) were acquired on 10 cm^3 sample volumes (Figure 3.7B) in an attempt to have a screening of the compositional characteristics of the framework grains and the cements, through the geochemical study of its grain size[2].

[2] Iturregui A., Arrieta N., Murelaga X, Baceta J.I., Olazabal M.A., Martínez-Arkarazo I., Madariaga J.M., **2014**. *The relevance of the analytical methodology in the geochemical characterization of beachrock*

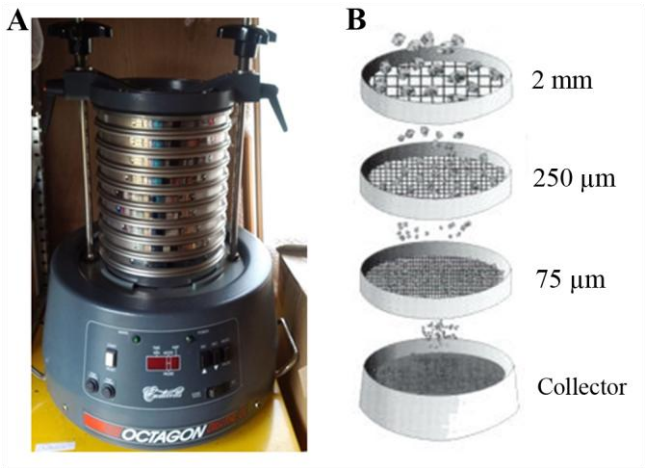

Figure 3.7. A) Image of the sieve shaker used for the sieving of the samples. B) Illustration of the proceeding followed during the particle size separation to obtain four different size ranges or fractions (>2mm, 250µm-2mm, 75-250m and <75µm).

That process helped in deciding the most appropriate particle size required for the following stage of the work. In fact, as it will be explained in Chapter 5, subsequently, the <2mm particle size was considered to examine more in detail the metal content within the beachrock outcrops.

3.2.2 Preparation of thin sections

The production of the thin sections was commissioned to the general services associated to the Department of Mineralogy and Petrology of the University of the Basque Country (SGiker, UPV/EHU).

As showed in Figure 3.8, the realisation of the thin section includes the cutting of the sample to an approximate size of 0.5 x 2.5 x 4 cm, which is then polished and stuck onto a glass slide with epoxy resin. Subsequently, the sample is thinned to a thickness of 0.03mm. It is worth mentioning that when the sample is not very well cemented, before starting the thin section preparation process, sample needs to be given cohesion. For that purpose, a polyester resin is used to produce a hardened and compact block, without altering the sample.

outcrops: Arrigunaga beach inside the Nerbioi-Ibaizabal estuary (Getxo, Basque Country). Analytical Methods, *6*, 8247-8257.

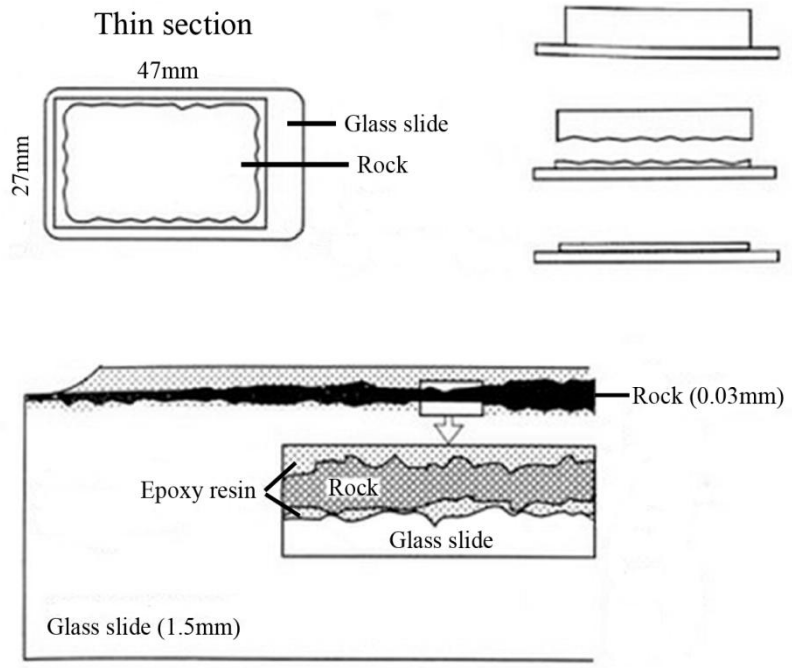

Figure 3.8. Illustration that summarises the preparation of the thin sections (modified from Hibbard, 1995[3]).

3.3 Analytical techniques

3.3.1 Staining: Alizarin red S and potassium ferricyanide

During the PhD stay carried out in the University of Kansas (KU), a staining method was applied on the thin sections in an attempt to recognise textural and compositional characteristics of the carbonate cements. For that purpose, a mixture of Alizarin red S and potassium ferricyanide dissolved in a dilute hydrochloric acid solution was employed. These are one of the most generally used dyes for carbonates[4].

The Alizarin red S, or 1,2-dihydroxy-9,10-anthraquinonesulfonic acid sodium salt, is also known as sodium alizarin sulphonate ($C_{14}H_7O_7SNa$).This organic dye will stain pink to red (depending on the crystallographic orientation) any carbonate that reacts with the dilute acid. The staining depends on the degree of reaction with the acid: the more reactive minerals, like calcite and aragonite, stain red while the less reactive ones, such as dolomite and siderite, are not stained[4,5].

[3] Hibbard M. J., **1995**. *Petrography to Petrogenesis*. Prentice-Hall, New Jersey.
[4] Dickson J.A.D., **1966**. *Carbonate identification and genesis as revealed by staining*. Journal of Sedimentary Petrology, 36, 491-505.
[5] Oakley L.M., 2013. Enhanced resolution of the palaeoenvironmental and diagenetic features of the Silurian Brassfiel formation. PhD Thesis, Wright State University, Ohio, p.9.

Potassium ferricyanide with the formula $K_3[Fe(CN)_6]$, yields a blue precipitate in carbonates with ferrous iron (Fe^{2+}). Minerals like calcite, magnesite or ankerite can be stained blue in cold solution. Nevertheless, in the case of siderite and usually dolomites, the staining solution needs to be heated to around 60ºC to assure the reaction between the carbonates and the acid media[4].

The stain was prepared by the Department of Geology of KU as follows basing on the procedure described by Friedman (1959)[6]:

-A*lizarin red S:* dissolve 0.1gr of alizarin red S in 100ml of 0.2% cold HCl. The 0.2% HCl was prepared by adding 0.2ml of concentrated HCl to 998ml distilled water.

-*Potassium ferricyanide:* add one or two drops of potassium ferricyanide to diluted HCl (1:50-100).

-Mix the two solutions: three parts of alizarin red S and two parts of the potassium ferricyanide.

Afterwards, the thin section was immersed in the stain during 50 seconds. Finally, the slide was removed from the stain and gently washed with water.

3.3.2 Optical microscopy

The visual inspection of the samples intended to give a general insight of the samples of interest. Two types of optical microscopy (commonly known also as *light microscopy*) were used: polarized light microscopy and fluorescence microscopy.

3.3.2.1 Polarized light microscopy

This kind of microscope is also known as *polarizing microscope* or *petrographic microscope* and it is commonly used for the investigation of rocks and minerals. In fact, this tool allows changing the light source (natural light to polarized light) thanks to two polarizing filters integrated in the microscope: a polarizer (located between the light source and the sample) and an analyzer (positioned between the sample and the observer). Two kinds of observations can be made: with plane polarized light (PPL, or parallel nicols) and with crossed polarized light (XPL, or crossed nicols). In PPL, the

[6] Friedman G.M. **1959**. *Identification of carbonate minerals by staining methods*. Journal of Sedimentary Petrology, 29, 87-97.

polarizer is only used and in XPL, both the analyzer and the polarizer are crossed (Figure 3.9).

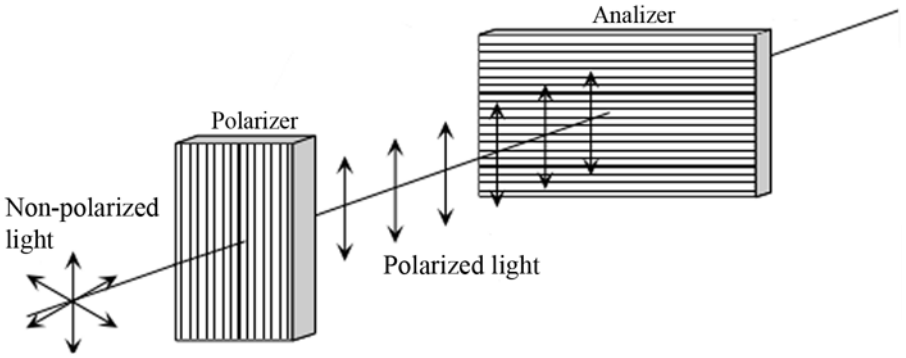

Figure 3.9. Scheme of the two polarizing filters (polarizer and analyzer) fitted in the polarized light microscope. When the non-polarized light crosses through the polarizer, the light coming out on the other side will then be plane polarized. If another polarizer with its polarization direction oriented perpendicular to the first polarizer is activated, crossed polarized light will be produced.[7]

3.3.2.2 Fluorescence microscopy

Fluorescence is a kind of luminescence occurring when a material emits light after being excited with a high energy source such as ultraviolet radiance. Thus, in this type of microscope imaging, in contrast to polarized microscopy, the light source is not natural light but ultraviolet light provided by a mercury vapour lamp, that yields an image in the visible region.

From the geological point of view, it is widely used for the examination of thin sections (or highly polished slices) in the petrographic study of sediments with a high organic content or with organic origin. In the case of carbonate rocks, the specific causes that yield the fluorescence are not well known. However, fluorescence microscopy can be used in the study of carbonates for instance to identify microfabrics that might be out of sight, to study organic components or to comprehend biomineralization processes[8].

3.3.2.3 Instruments

Two different devices were employed for these analyses. One of the equipments belongs to the Department of Geology of the Basque Country (UPV/EHU), while the other one was used in the Department of Geology of the University of Kansas (KU).

[7] Nelson S.A, **2014**. *Properties of light and examination of isotropic substances*. Tulane University, New Orleans.
[8] Flügel E., **2014**. *Microfacies of Carbonate Rocks*. Springer Science & Business Media, New York.

- Nikon SMZ-U 1500 polarizing microscope

In the early stages of the thesis, the optical examinations were performed in the Department of Geology of the UPV/EHU by means of a Nikon SMZ-U 1500 stereo microscope (Japan) coupled to a digital camera (DS-5 Megapixels). The images were obtained using 0.75x, 2x, 4x and 8x objective lenses. It was used for the visualization of different particle sizes and for the examination of thin sections through polarized light.

- Olympus BX51 fluorescence microscope

During the research carried out in the Department of Geology of the University of Kansas (KU), a more in detail examination of the thin sections was performed using an Olympus BX51 microscope (Figure 3.10A), which was equipped with a DP73 digital camera (17.3 Megapixels and Peltier cooling system). The system is equipped with polarizing filters and a vertical illuminator that contains a turret of filter cubes (Figure 3.10B) and it is coupled to a high-pressure mercury vapor lamp (U-HGLGPS, Olympus) (Figure 3.10C) for fluorescence microscopy.

For the fluorescence image acquisition, natural light needed to be switched off to avoid interferences, the mercury bulb activated and the fluorescence mirror unit engaged with the adequate filter cube (WBV). The images were obtained using 4x, 10x, 20x and 50x objective lenses and the Olympus Stream Image Analysis Software was used for image capturing and processing.

Fluorescence microscopy was used to obtain complementary information after the observation of the thin sections through polarized light, in order to check the possible presence of organic compounds associated to the cements. Therefore, to maximise the information about the areas of interest in the thin sections, as a general rule, the same region was captured with both light sources: at first, once the area was selected, polarized light microscopic images were obtained, and then the same spot was retained for fluorescence images.

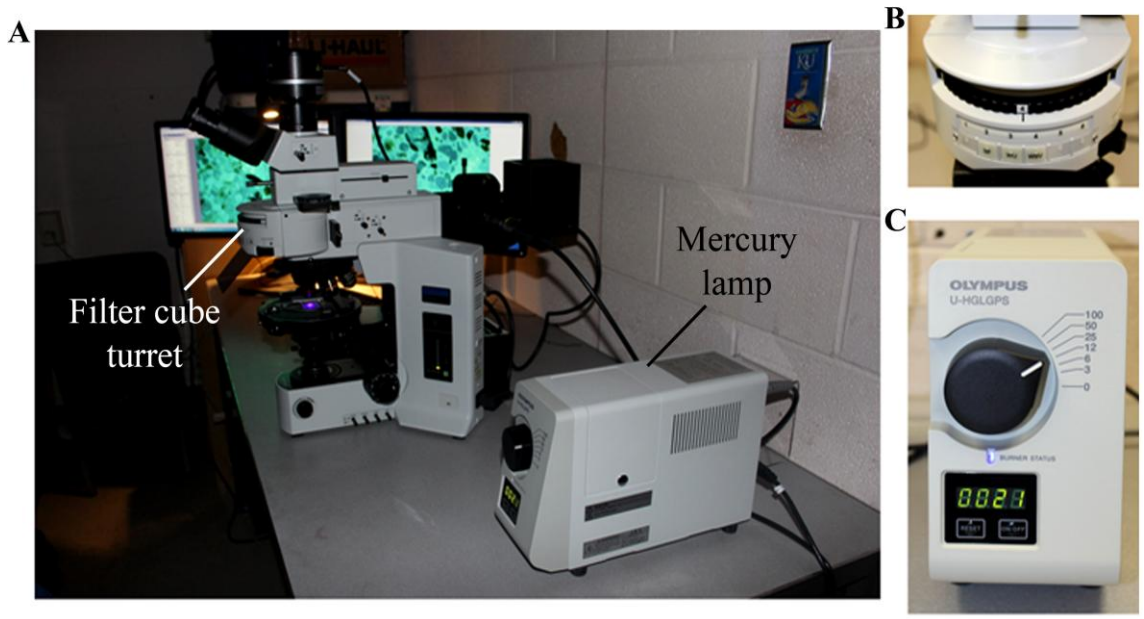

Figure 3.10. A) The Olympus BX51 fluorescence microscope used in the Department of Geology of the University of Kansas (KU). B) Close view of the filter cube turret positioned in the WBV filter cube for fluorescence imaging. C) The mercury lamp used as a light source for fluorescence imaging.

3.3.3 Scanning electron microscopy – Energy Dispersive X-Ray Spectroscopy (SEM-EDS)

After the examinations carried out by optical microscopy, SEM was applied to delve further into the microstructure of the samples of interest.

To understand the combination of light and electron microscopy techniques, their differences will be mentioned in the following lines. The main similarity is that both instrumental techniques are used for visualizing objects and details that are too small to be discerned at naked eye[9]. However, each device uses a different radiation type for imaging, as light microscopy employs photons (light rays) focused through various lenses (usually made of glass) while electron microscopy uses a beam of electrons focused by a set of electromagnets, having more resolution than light microscopy and providing higher magnifications. Therefore, electron microscopy allows unravelling structural details not visible with the light microscope. In addition, the higher resolution provides electron microscopy with a greater depth of field than in light microscopy[10,11].

[9] Abramovitz M., **2003**. *Microscope; Basics and Beyond*.Olympus America, New York, USA, 50pp.
[10] Murphy D.B., **2001**. *Fundamentals of light microscopy and electronic imaging*. John Wiley&Sons, New York, USA, 385pp.
[11] *Electron Microscopes vs. Optical (Light) microscopes*, **2009**. In: Microscopy Basics, Theory (MicrobeHunter Microscopy Magazine). Retrieved from http://www.microbehunter.com/electron-microscopes-vs-optical-light-microscopes/

As the magnification and depth achievable by SEM is higher than in optical microscopy, complementary information could be obtained using both tools.

In addition, the coupling with an EDS allowed determining the elemental distribution of the analysed areas. These examinations were performed over freshly broken fragments of the samples (mainly to observe the morphology of the cements) as well as thin sections (especially to characterise the areas previously recognised through optical microscopy).

In SEM a high energy primary electrons beam is focused towards a specimen causing an interaction that can yield the emission of secondary electrons, backscattered electrons, characteristic x-rays as well as other photons of diverse energy. In this case, two of the most interesting signals were considered for the imaging of the samples: secondary electrons (SE) and backscattered electrons (BSE)[12].

3.3.3.1 Secondary electron imaging (SE)

The image is formed from the secondary electrons emitted by the sample, through inelastic scattering interactions. The low energy of the secondary electrons (usually <50KeV), cannot provide much information about the inner parts of the sample so they represent the three dimensional appearance of the fine surface. This kind of images were realised over freshly broken fragments previously coated with gold.

3.3.3.2 Backscattered electron imaging (BSE)

In contrast to SE, the image is based on the elastically scattered electrons (>50KeV) emitted from the sample after the interaction with the primary electrons beam. Those elements with higher atomic number backscatter more electrons than “light” elements, so they produce brighter spots in the image. This creates contrast between areas representing dissimilarities in the chemical composition. Therefore, this technique was especially used for imaging ferruginous cements previously recognised through optical microscopy over thin sections, which were not coated with gold prior to the BSE imaging.

[12] Reimer L., **1998**. *Scanning electron microscopy. Physics of Image formation and Microanalysis*. Springer Series in Optical Sciences. New York.

3.3.3.3 Instruments

Prior to the examination, samples needed to be properly prepared for imaging. For that purpose, at first the specimen was mounted onto a stud using a conductive graphite paint to fix the sample to a stable surface during the analysis. Then, when broken fragments were analysed, a coat of conductive material was applied over the specimen to facilitate the electron beam to be transferred to the sample. In that case, samples were coated with gold (thickness <20μm) using an Emitech K550X sputter coater vacuum chamber (Quorum Technologies LTD., Sussex, UK). It is worth mentioning that thin sections were not coated with gold previously to their analysis.

To obtain the electron images and determine the elemental composition of the samples, two different installations were used: the Coupled Multispectroscopy Singular Laboratory (LASPEA) associated to the General Services of the University of the Basque Country (SGiker-UPV/EHU) as well as services of the Microscopy and Analytical Imaging Laboratory (MAI) located in the University of Kansas (KU). The particularities of the instruments used in each of them will be explained herein.

- EVO®40 Scanning Electron Microscope

In the UPV/EHU, an EVO®40 Scanning Electron Microscope (Carl Zeiss NTS GmbH, Oberkochen, Germany) (Figure 3.11A) was used coupled to an Oxford INCA 350 X-Max Energy-Dispersive X-ray Spectroscopy system (Oxford Instruments, Oxfordshire, UK) (Figure 3.11B).This equipment is settled on an antivibration table in a temperature controlled room. The acquisition of the images was performed at high vacuum with an acceleration voltage of 20kV. Through this instrument, two types of images were captured: SE images and BSE images. SE images were obtained mainly in the broken fragments while BSE were primarily used to image ferruginous cements in thin sections.

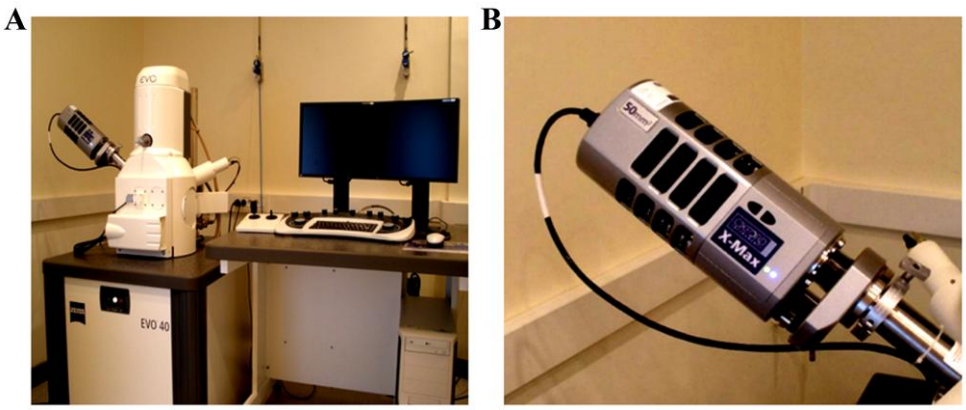

Figure 3.11. A) The SEM-EDS equipment. B) Detailed view of the EDS instrument Oxford INCA 350 X-Max.

- FEI Versa 3D Dual Beam Electron Microscope

During the research performed in the University of Kansas, SE images were obtained using a FEI Versa 3D Dual Beam electron microscope (FEI, Hillsboro, Oregon, USA) (Figure 3.12).This equipment is also coupled to an EDS for the identification of the main elements composing the samples. The data acquisition was provided by the AZtec Microanalysis software (Oxford Instruments, Oxfordshire, UK).

It is worth mentioning that this instrument combines high and low vacuum for processing uncoated, non-conductive or natural state samples. When running the low vacuum SEM, the electron column and electron gun remain at the regular high vacuum but the sample chamber is at a low vacuum[13]. That way it is possible to compensate for charge build up in non conductive samples even at the high accelerating voltages required for analysis techniques, like the EDS. In fact, the FEI Versa 3D Dual Beam was used to determine the elemental distribution in areas previously selected through optical microscopy, and for that purpose, EDS analyses were performed at low vacuum, at high voltage (20kV) and making use of the 500µm X-ray cone. This way, in contrast to the previously described instrument, EDS mappings could be realised at high magnifications without the risk of charge build up in the samples.

[13] Petruk W., **2010**. *Applied Mineralogy in the Mining Industry*. Elsevier, The Netherlands.

Figure 3.12. The FEI Versa 3D Dual Beam electron microscope.

3.3.4 Raman spectroscopy

As the Raman spectroscopy gives unique information for each compound, it allows characterising the cements, with the ability of distinguishing between polymorphic compounds, and it also contributes in identifying the molecular composition of the framework grains.

This technique was used for different purposes, such as *in situ* examinations and laboratory analyses, and three different equipments were used depending on the aims. However, some generalities can be mentioned, common when using any of the Raman instruments, such as the fact that prior to the analyses, the equipments were daily calibrated with the 520.5cm^{-1} silicon band. Moreover, the Omnic 7.2 software (Thermo-Nicolet, Madison, USA) was used for data processing and the identification of the spectra was based on the comparison with e-VISART, e-VISNICH spectra databases[14,15]

[14] Castro K., Pérez-Alonso M., Rodríguez-Laso M.D., Fernández L.A., Madariaga J.M., **2005**. *On-line FT-Raman and dispersive Raman spectra database of artists' materials (e-VISART database)*. Analytical and Bioanalytical Chemistry 382, 248-258.

[15] Maguregui M., Prieto-Taboada N., Trebolazabala J., Goienaga N., Arrieta N., Aramendia J., Gómez-Nubla L., Sarmiento A., Olivares M., Carrero J., Martinez-Arkarazo I., Castro K., Arana G., Olazabal M.A., Fernández L.A., Madariaga J.M., **2010**. *Dispersive Raman spectra database of original and decayed materials belonging to the Natural, Industrial and Cultural Heritage (e-VISNICH database)*. ChemCH, first International Congress Chemistry for Cultural Heritage, Ravenna, Italy, p. 168. http://158.227.5.164/RamanDB/.

and the RUFF online database[16]. In the following lines, the main characteristics of the three instruments used will be specified:

- B&WTek InnoRam spectrometer

The Raman spectra were obtained *in situ* by means of a portable InnoRam spectrometer (B&WTek^{INC}, Newark, USA) equipped with a diode 785nm laser (Figure 3.13). The acquisition of the spectra was carried out with a hand-held microprobe (150µm spot size) coupled to a 5 metres long optic fiber, which allowed reaching the spots closest to the seashore, avoiding contact between the instrument and the water. Generally, the measurement conditions consisted in 1-5 seconds and 5-20 accumulations, and usually no more than 20% of the laser power was used to prevent laser induced alterations. The spectra were obtained in a range around 100 to 3000cm^{-1}, with a resolution of 3.5cm^{-1}. Data acquisition was carried out with the BWSpecTM software version 3.26 (B&WTek^{INC}, Newark, USA).

Figure 3.13. The InnoRaman^{TM} B&WTek^{INC} spectrometer.

- Renishaw RA100 spectrometer

The laboratory examination of the samples was performed using a Renishaw RA 100 Raman spectrometer (Renishaw, Gloucestershire, UK), equipped with a 785nm excitation laser and a Peltier cooled CCD detector (Figure 3.14). The nominal laser

[16] Downs R.T, **2006**. *The RRUFF Project: an integrated study of the chemistry, crystallography, Raman and infrared spectroscopy of minerals*. Program and Abstracts of the 19th General Meeting of the International Mineralogical Association in Kobe, Japan. O03-13. http://rruff.info/.

power is 150mW at the source and it can be controlled to use the 1%, 10% or 100% of the power in order to avoid laser induced transformations in the sample.

The objective lens of 20x and 50x magnifications were mainly used (with a 10μm spot size) and a video-camera controlled by a joystick to focus on the areas of interest. Spectra were generally collected in the range between 100 and 3000cm^{-1} with a resolution of 2cm^{-1}, aided by the Wire 3.2 software (Renishaw, Gloucestershire, UK) package for data obtaining.

The number of accumulations and the measuring time to accomplish well-resolved Raman spectra varied depending on the pinpointed area, verifying that no sample alteration was generated with the laser to get a good signal to noise ratio. The identification of the spectra was carried out by the aforementioned spectra databases.

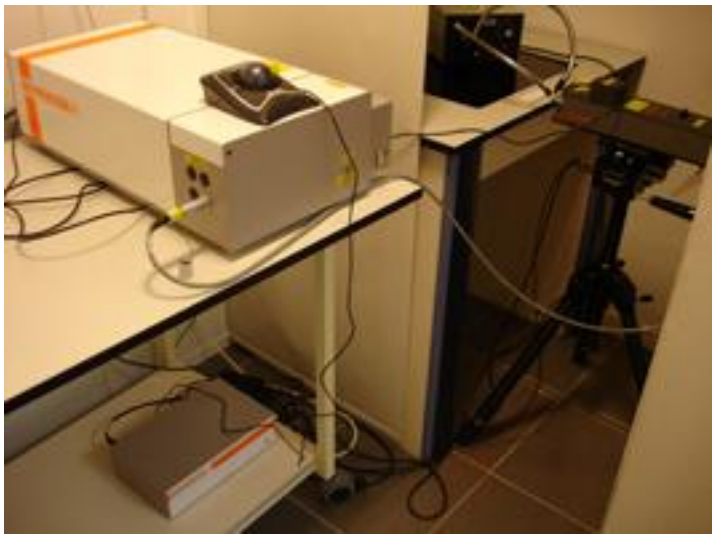

Figure 3.14. The Renishaw RA 100 Raman spectrometer.

- Renishaw InVia confocal micro spectrometer

This instrument was employed for a more detailed analysis of the samples in the laboratory. It consists on a Renishaw InVia confocal micro Raman spectrometer (Renishaw, Gloucestershire, UK) with a Peltier cooled CCD detector (Figure 3.15). The excitation wavelengths of the available lasers are 514nm (green) and 785nm (red), which depending on the matrix allows the analysis to be carried out with two different energies,

aiding to avoid the fluorescence. The spectrometer has two different modular optics depending on the laser used, in any case, it can provide a spectral resolution of $1cm^{-1}$. The equipment is coupled to a DMLM Leica microscope (Bradford, UK) and 5x N PLAN, 20x N PLAN EPI, 50x N PLAN objectives were mainly used. The microscope is equipped with a Prior Scientific motorized XYZ positioning stage controlled by a joystick and connected with a microcamera. The spectral range was 100-$4000cm^{-1}$ the software Wire 3.2 (Renishaw, Gloucestershire, UK) was used for data obtaining.

This instrument is settled on an optical table for vibration isolation in a temperature controlled room, inside the Coupled Multispectroscopy Singular Laboratory (LASPEA, SGiker, UPV-EHU) (Figure 3.15). It is remarkable that this Raman spectrometer can be connected to the SEM instrument through the Structural and Chemical analyser (SCA). This interface among both techniques enables laser light to be focused on a micrometric spot projected onto the sample surface in the SEM image. This way, when confusing areas were found, the imaging power of the SEM was used to identify certain points of interest on samples to be afterwards analysed by Raman spectroscopy.

Figure 3.15. The SEM-EDS (left) and the Raman equipment (right). Both of them can be coupled through the SCA device.

3.3.5 X-Ray Diffraction (XRD)

The results obtained by this technique provided information about the structural characteristics of the crystalline materials. Thus, it was used to corroborate the composition of the cements. To this end, cements were isolated from the bulk sample using an electric micro drill or an scalpel and a magnification lamp for the proper visualization of the samples.

The analyses were commissioned to the General X-Ray Service of the UPV/EHU (Molecules and Material Unit, SGiker, UPV-EHU). There, XRD analyses were carried out with a PANalytical Xpert PRO (Toronto, Canada) powder diffractometer, which integrates a copper tube (λCuKαaverage= 1.5418A, λCuKα1= 1.54060A, λCuKα2= 1.54439A), vertical goniometer (Bragg-Brentano geometry), programmable divergence aperture, automatic interchange of samples, secondary graphite monochromator and PixCel detector. The measurement conditions for the Cu tube were 40kV and 40mA, with an angular range (2θ) scanned between 5 and 70°. Data processing and the identification of the mineral phases was performed with the PANalytical X`pert HighScore software package combined with the specific Powder Diffraction File (PDF-2) database 7bvc (International Centre for Diffraction Data - ICDD, Pennsylvania, USA) and Miller indexing (hkl) of the observed maxima.

The relative proportions of the main carbonate cement forms were semi-quantitatively estimated based on the Relative Intensity Ratio (RIR) values. As the relative proportions of carbonates were only considered, the carbonates necessarily add to 100% ignoring the other possible minerals and amorphous phases present in the sample. With regard to the Mg content, the stoichiometry of the calcites was estimated following the equation of Lumsden (1979)[17] which relates the molar content % $MgCO_3$ of calcite with the displacement of the (104) peak. For that purpose, silicon was added as an internal standard in the sample to correct the position of reflections. The precision of the measurements was ± 0.25mol%.

3.3.6 Stable isotope analysis ($\delta^{13}C$ and $\delta^{18}O$)

Isotopes are one or more species of the same chemical element (as such, they have the same number of protons in the nucleus) that have dissimilar atomic weights (containing different number of neutrons). The differences in the atomic weight can cause remarkable diversities in the distribution for the isotope during natural processes like evaporation, or phase transformations. Therefore, the analysis of stable isotopes can provide valuable information about the diagenetic environment. Oxygen (isotopes ^{18}O and ^{16}O) and carbon (isotopes (^{13}C and ^{12}C) isotope analyses can provide relevant information about carbonate cements and the diagenetic environment of formation[18,19].

[17] Lumsden D.N., **1979**. *Discrepancy between Thin Section and X-Ray Estimates of Dolomite in Limestone*, Journal of Sedimentary Petrology, 49, 429-436.
[18] Moore C.H., **1997**. *Carbonate diagenesis and porosity*. Elsevier, Amsterdam, 338 pp.
[19] Flügel E., **2014**. *Microfacies of Carbonate Rocks*. Springer Science & Business Media, New York, 975 pp.

These analyses were performed at the Keck Paleoenvironmental and Environmental Stable Isotope Laboratory (KPESIL) of the University of Kansas.

3.3.6.1 Sample preparation

First, samples of interest were cleaned with compressed air to avoid as much as possible the presence of impurities. Powdered carbonate samples ranging from 0.1 to 0.4 mg were extracted with a Nikon SMZ800 microscope-mounted drill assembly (Figure 3.16) using a 0.5 mm-diameter tungsten carbide dental burr, similarly to other studies[20]. To be more accurate on the cement isolation, samples could also be acquired using a scalpel. Samples were collected in FisherbrandTM low-nitrogen weighing paper 6" x 6" (Thermo Fisher Scientific Inc., USA) and then transferred to metallic boats, to be weighed in a XP2U ultra micro balance (Mettler Toledo, Ohio, USA).

Figure 3.16. Image of the microscope-mounted drill assembly used for the collection of cement samples.

3.3.6.2 Instruments

Samples were roasted in vacuum at 200 °C for 1 h to remove volatile organic contaminants. Then, the samples were analyses in a Kiel IV carbonate device coupled to a ThermoFinnigan MAT 253 mass spectrometer setup (Thermo Scientific, Bremen, Germany) (Figure 3.17). The carbonate device converts carbonate samples to CO_2, which is then analyzed on the mass spectrometer.

[20] Ludvigson G.A., Jacobson S.R., Witzke B.J., González L.A., **1996**. *Carbonate component chemostratigraphy and depositional history of the Ordovician Decorah Formation, Upper Mississipi Valley*. Geological Society of America, Special Paper 306, pp. 67-86.

Figure 3.17. The Kiel IV carbonate device coupled to a ThermoFinnigan MAT 253 mass spectrometer.

Once roasted, samples are transferred to glass vials and loaded into a carousel, to introduce them in the Kiel's temperature regulated chamber (70ºC). After atmospheric gases are evacuated from the vials, three drops of orthophosphoric acid (H_3PO_4) are added to the samples. Then, CO_2 and water are cryogenically isolated on a trap at 170ºC and non condensable gases are pumped away. CO_2 is cryogenically transferred to a second trap, leaving the water on the first trap and the purified CO_2 is introduced in the mass spectrometer for measurement.

Regarding the conditions used for the ThermoFinnigan MAT 253, mass 44 voltage from the standard gas, as measured with the MAT 253 collectors, is balanced with the mass 44 voltage measured from the sample gas. The isotopic composition of the sample is determined from the average of 8 cycles of standard gas/sample gas measurements of 8 seconds each (i.e. isotopic composition is measured and integrated for 8 seconds on the standard gas followed by the sample gas). The delta values are calibrated using 3 working and international standards of known isotopic composition. Analytical precision is monitored by daily analysis of NBS-19 and NBS-18 limestone standards, which are run at the beginning, middle, and end of a 40 sample cue. All results are reported relative to the Peedee belemnite (PDB) standard and a precision better than ±0.1‰ was reported for both carbon and oxygen.

Stable isotope ratios are usually reported through the delta value (δ) given in per mill (‰), which is obtained by:

$$\delta = \frac{R_x - R_{std}}{R_{std}} \times 1000$$

where *R* is the measured ratio between the heavy and the light isotope, *x* the sample and *std*, the standard sample. $\delta^{13}C$ values are referred to $^{13}C/^{12}C$ ratios and $\delta^{18}O$ values to $^{18}O/^{16}O$ ratios. If $\delta A > \delta B$, it can be said that sample A is enriched in the heavy isotope, compared to B[21-22].

3.3.7 Inductively Coupled Plasma-Mass Spectroscopy (ICP-MS)

The microscopic examinations together with Raman spectroscopy, provided valuable information about the cements, but they also illustrated and helped in determining the composition of framework grains, with special interest in those believed to have an anthropogenic origin. Consequently, to complement that information, the metal content was quantitatively measured based on a procedure that first requires a microwave-assisted acid digestion to be followed by the quantification of the elements through ICP-MS.

3.3.7.1 Reagents and materials

Previously to any step, the plastic and glassware used for sample treatment or preparation of ICP-MS solutions were cleaned with tap water and soap, rinsed with Milli-Q water (<18.2MΩ/cm, Millipore, USA), immersed afterwards in a 10% HNO_3 (69%, Merck) bath for 24h, exhaustively rinsed twice with Elix quality water and finally soaked again with Milli-Q water (Millipore, USA) , to be finally dried in a laminar airflow hood inside a class 100 clean room. The nitric acid (HNO_3, 69%) and hydrochloric acid (HCl, 37%) used during the extraction step are both of Tracepur grade and supplied by Merck (Darmsdt, Germany).

[21] Sharp Z., **2007**. *Principles of Stable Isotope Geochemistry*. Pearson Prentice Hall, Upper Saddle River NJ, USA, 344 pp.
[22] Hoefs J., **2009**. *Stable Isotope Geochemistry*. Springer-Verlag, Germany, 285 pp.

3.3.7.2 Microwave-assisted acid digestion

This step was performed following the U.S. Environmental Protection Agency (USEPA) EPA 3051A method, modified by Carrero et al.[23,24], which is commonly applied in the research group to process a wide variety of samples like sediments, slag, mine wastes soils and even beachrock samples[25-28]. A Multiwave 3000 (Anton Paar, Graz, Austria) system (Figure 3.18A) was used for the extraction of non siliclastic compounds. This tool is equipped with a 8XF-100 microwave digestion rotor and 100mL fluorocarbon polymer microwave vessels (Figure 3.18B).

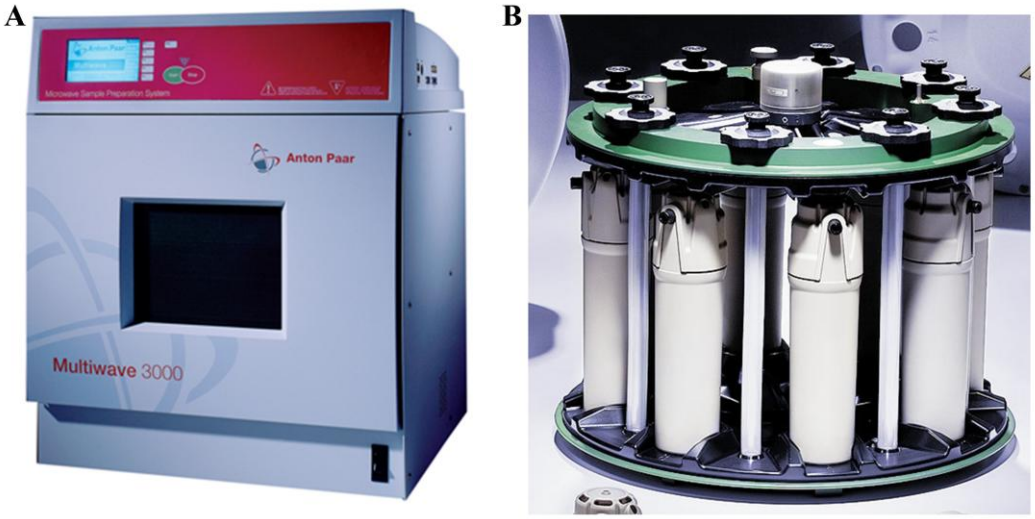

Figure 3.18. A) The Multiwave 3000 system. B) The 8XF-100 microwave digestion rotor.

Prior to the extraction, the sample pretreatment described in section 3.2.1 was performed. Subsequently, 0.5g of the samples of interest were weighted (in an AJ150 Mettler-Toledo analytical balance, ± 0.0001g) and mixed in the vessels with a 9:3 of nitric acid (HNO_3, 69%) and hydrochloric acid (HCl, 37%) mixture. Two samples (three

[23] EPA Method 3051A, **2007**. *Microwave assisted acid digestion of sediments, sludges, soils and oils*. United States Environmental Protection Agency (USEPA).
[24] Carrero J.A., **2011**. *Evaluación del Impacto del Tráfico Rodado en Suelos y Plantas de Margen de Carretera*. PhD Thesis. University of the Basque Country.
[25] Carrero J.A., Goienaga N., Fdez-Ortiz de Vallejuelo S., Arana G., Madariaga J.M., **2010**. *Classification of archaeological pieces into their respective stratum by a chemometric model based on the soil concentration of 25 selected elements*. Spectrochimica Acta Part B 65, 279-286.
[26] Carrero J.A., Arrizabalaga I., Bustamante J., Goienaga N., Arana G., Madariaga J.M., **2013**. *Diagnosing the traffic impact on roadside soils through a multianalytical data analysis of the concentration profiles of traffic-related elements*. Science of the Total Environment 458-460, 427-434.
[27] Iturregui A., Arrieta N, Murelaga X, Baceta J. I., Olazabal M.A., Martínez-Arkarazo I., Madariaga J.M., **2014**. *The relevance of the analytical methodology in the geochemical characterization of beachrock outcrops: Arrigunaga beach inside the Nerbioi-Ibaizabal estuary (Getxo, Basque Country)*. Analytical Methods, 6, 8247-8257.
[28] Arrieta N., **2014**. *The study of an unusual temperate latitude beachrock formation. Characterization of Azkorri beach and Tunelboka cove locations*. PhD Thesis, University of the Basque Country.

replicates from each) and two blanks (Milli-Q water, <18.2 ΩM/cm, Millipore, USA) were simultaneously prepared for every round. The blanks were used in order to detect possible solvent or impurities contaminations that may affect to the analysis. After that, the vessels were inserted counterbalanced in the rotor, entered into the microwave and the above mentioned method programmed. This method consists on applying at first enough power (1000W to 800W), that would allow reaching 170ºC during 4.5 minutes. Finally, a cooling ramp is programmed that would last 15 minutes, a period of time in which the application of power ceases and the ventilation system is activated. After digestion and cooling, the vessels were removed from the rotor. Once cooled at room temperature, the extracts were filtered through 0.45mm PVDF syringe filters and weighed into 50mL polypropylene tubes. All the solutions required during the procedure were prepared with Milli-Q water.

3.3.7.3 ICP-MS instruments

Before the elemental measurement, the acidic concentration of the extracts was reduced to 1% HNO_3 to avoid damage to the equipment. To ensure the reduction of the acidity, the obtained extracts were gravimetrically diluted with Milli-Q water (1:12.5). Then, two different devices were used for the elemental analysis due to technical advances of the research group. In any case, the analyses were carried out inside a clean room (class 100) and ICP-MS standard solutions were based on Alfa Aesar (Specpure®, Plasma Germany) commercial solutions. Be^{9}, Sc^{45}, In^{115} and Bi^{209} solutions (1000mg/L in 5% HNO3) (Specpure®, Alfa Aesar, USA) were added to blank, calibrates and sample solutions as internal standard to yield a 10µg/l concentration level. Argon (99.999%, Praxair, Spain) was used for plasma generation.

At first, an ELAN 9000 mass spectrometer (Perkin Elmer, Ontario, Canada) was employed. The operating conditions consisted on nebuliser, plasma and auxiliary flow rates of $0.9L/min^{-1}$, $15L/min^{-1}$ and $1L/min^{-1}$, respectively, as well as a radiofrequency power of 1100W. Three replicates were measured per sample with a $1mL/min^{-1}$ sample flux and one sweep per replicate.

At later stages of the thesis, samples were analysed by means of a NexION 300 ICP-MS spectrometer (PerkinElmer, Ontario, Canada). In this case, the nebuliser, plasma and auxiliary flow rates were of $0.98L/min^{-1}$, $18.0L/min^{-1}$ and $1,20L/min^{-1}$ respectively. This time also three replicates were measured per sample with a

300µL/min^{-1} sample flux and one sweep per replicate and a radiofrequency power of 1600W was applied.

On the whole, twenty-six elements were generally quantified: Ca, Mo, Sr, Cd, Ni, Ag, As, Cr, Na, Tl, Ba, K, Co, Mg, Ti, Al, V, Pb, Cu, Mn, Zn, Sn, Fe, Hg, Sb and Se. Considering the different concentration ranges of the elements analysed in the cemented outcrops, the major elements (Ca, Fe, Al, Mg, Mn, Na and K) were out of the calibration range, so a second dilution (1:100) was necessary to determine their concentration.

3.3.8 Acid-base backward titration

This technique was used to determine the total carbonate content of the different particle size ranges considered for the granulometric analyses (250 mm to 2 mm, 75-250 mm and <75 mm). The total carbonate content of the selected fractions was determined to procure a more comprehensive characterization of the constituent particles and, particularly, the cements. Therefore, carbonate quantification was performed based on backward acid-base titration.

For that purpose, 0.5 g of the fractions (weighted in a AJ150 Mettler-Toledo analytical balance, ± 0.0001 g) were reacted with 0.5mol/L HCl added in excess (prepared from 37% HCl by Panreac and previously standardized with Na_2CO_3 99.5%, Merck) (Eq. 3.1). Carbonate ions in the sample reacted with HCl and produced CO_2, which was removed by heating the solution prior to boiling. The excess amount was then titrated with 0.25mol/L NaOH (prepared from 98%, J.T. Baker, and previously standardized with the 0.5mol/L HCl) (Eq. 3.2). Phenolphthalein was used as the indicator of the endpoint in every step.

$$CaCO_{3\,(s)} + 2HCl_{(aq)}\,(\text{in excess}) \rightarrow CaCl_{2\,(aq)} + CO_{2\,(g)} + HCl_{(exc)} + H_2O_{(l)} \quad \text{(Eq. 3.1)}$$

$$HCl_{(exc)} + NaOH_{(aq)} \rightarrow NaCl_{(aq)} + H_2O_{(l)} \quad \text{(Eq. 3.2)}$$

To determine the repeatability of the titration process, three replicates of each sample were analysed. Titrations were carried out with a 725 Dosimat autoburette (Metrohm Ltd., Herisau Switzerland) and an Asincro magnetic stirrer (JP Selecta S.A.®, Barcelona, Spain) was used to homogenize the solutions.

3.3.9 Statistical analyses

To better understand the results obtained in the aforementioned quantitative, correlation analyses and principal component analysis (PCA) were carried out. Through the correlation analyses, the Pearson correlation coefficient (r) was estimated basing on the t-statistic at a confidence level of 95% ($p < 0.05$) and 99% ($p < 0.01$) for a 2-tailed test, in order to better understand the relation between the variables considered. Regarding the PCA, this tool is frequently used in environmental studies as it facilitates the interpretation of high dimensional data. Often that kind of data contains smaller inherent dimensionality, which is relevant enough to understand the underlying meaning of the data set. In this sense, PCA is among the most popular methods for dimensionality reduction, trying to catch the maximum information out of the original data identifying more basic components, named principal components (PC), that will represent most of the variance of the original variables[29,30].

On this basis, the principal component analysis was developed in order to visualise and interpret the possible differences among the data set obtained for the different samples. For the statistical treatment The Unscrambler® 9.2 software[31] (Camo Asa, Trodheim, Norway) was used and all the data were normalized, centred and auto-scaled (1/SDev) to develop PCA analysis.

[29] Esbensen K.H., Guyot D., Westad F., Houmoller L. P., **2002**.*Multivariate Data Analysis- in Practice: An Introduction to Multivariate Data Analysis and Experimental Design*. CAMO ASA, Norway.
[30] Demsar U., Harris P., Brunsdon C., Fotheringham A.S., McLoone S., **2013**. *Principal components analysis on spatial data: an overview.* Annals of the Association of American Geographers 103, 106-128.
[31] CAMO ASA, **2005**. *The Unscrambler User Manual, Version 9.2.* Norway.

Chapter 4

In situ and laboratory analyses over beachrock outcrops of Arrigunaga beach

This chapter is focused on the analyses performed in Arrigunaga beach, a work that has been divided in two sections. It starts with the description of a geochemical study performed over different grain sizes. As it will be detailed herein, among other preliminary notions about the compositional characteristics, the grain size fractionation of the samples allows us estimating the presence of anthropogenic materials. In order to delve further into that matter, the following section deals with the characterisation of the human derived materials through a Raman spectroscopic examination, including *in situ* and laboratory measurements, demonstrating, as a novelty, the feasibility of the *in situ* Raman analysis in this field.

In order to understand the circumstances that led to design those analyses, it is worth emphasising that, as mentioned in the first chapter, originally the phenomenon of beachrock formation has been thought to be restricted to tropical and subtropical coasts, nonetheless, even though it is far less usual, there are studies confirming the presence of beachrock in temperate coasts[1], providing a glimpse of its incidence in that latitude. This is the case of beachrocks placed in the vicinity of the Nerbioi-Ibaizabal estuary, and specifically the outcrops found in the Arrigunaga beach.

In that context, it must be kept in mind that the local abundance of ores especially rich in iron prompted the establishment of the first iron and steel industry in 1854 in the main channel of the estuary. Subsequently, the largest blast furnace steel factory was active until the late 20th century. During that period, throughout 50 years from 1940 on, the slags coming from the blast furnace were disposed at the sea[2]. Moreover as a consequence of the industrial and urban growth developed since the mid 19th century, severe environmental alterations occurred around the estuary, such as a strong oxygen depletion and high content of organic matter together with abundant heavy metals in the river water and sediments[3-5]. Despite the improvement of the environmental status of the system in the last two decades[2], the materials cemented in the beachrocks might reflect the industrial past of the estuary, because the predominant eastwards winds led to the transport of contaminants and wastes towards the right sandbanks of the mouth of the estuary, which include the sceneries where the beachrocks are present. On account of that background, two types of studies were performed: geochemical studies based on grain size fractionation and Raman spectroscopic analyses (on site and off site), as explained in already published works[6,7].

[1] Vousdoukas M.I., Velegrakis A.F., Plomaritis T.A., **2007**. *Beachrock occurrence, characteristics, formation mechanisms and impacts*. Earth-Science Reviews 85, 23-46.
[2] Borja A., Tueros I., Belzunce M.J., Galparsoro I., Garmendia J.M., Revilla M., Solaun O., Valencia V., **2008**. *Investigative monitoring within the European Water Framework Directive: a coastal blast furnace slag disposal, as an example*. Journal of Environmental Monitoring 10, 453-462.
[3] Cearreta A., Irabien M.J., Leorri E., Yusta I., Croudace I.W., Cundy A.B., **2000**. *Recent Anthropogenic Impacts on the Bilbao Estuary, Northern Spain: Geochemical and Microfaunal Evidence*. Estuarine, Coastal and Shelf Science 50, 571-592.
[4] Leorri E., Cearreta A., Irabien M.J., Yusta I., **2008**. *Geochemical and microfaunal proxies to assess environmental quality conditions during the recovery process of a heavily polluted estuary*: *The Bilbao estuary case (N. Spain)*. Science of the Total Environment 396, 12-27.
[5] Gredilla A., Fdez-Ortiz de Vallejuelo S., Arana G., de Diego A., Madariaga J.M., **2013**. *Long-term monitoring of metal pollution in sediments from the estuary of the Nerbioi-Ibaizabal River (2005–2010).* Estuarine, Coastal and Shelf Science 131, 129-139.
[6] Iturregui A., Arrieta N., Murelaga X., Baceta J.I., Olazabal M.A., Martínez-Arkarazo I., Madariaga J.M., **2014**. *The relevance of the analytical methodology in the geochemical study of beachrock outcrops: Arrigunaga Beach inside the Nerbioi-Ibaizabal estuary (Getxo, Basque Country)*. Analytical Methods 6, 8247-8257.
[7] Iturregui A., Arrieta N., Aramendia J, Arrizabalaga I., Murelaga X, Baceta J.I., Olazabal M.A., Martínez-Arkarazo I., Madariaga J.M., **2015**. *In-situ and laboratory Raman spectroscopic analysis on beachrock deposits: characterisation of the trapped materials*. Journal of Raman Spectroscopy, DOI 10.1002/jrs.4815.

4.1 Geochemical study based on grain size fractionation

The mentioned context and the unusual temperate latitude of the location make the beachrock of the Nerbioi-Ibaizabal estuary a challenging object of study. Indeed, sediment transport processes occurring in marine environments, such as local fluvial discharge, wave currents, storm currents and littoral currents, promote depositional mechanisms that lead to complex sedimentation processes mainly in estuaries and coastal environments where most of these materials and pollutants arrive, due to the interactions with other environmental variables, like current velocities, water chemistry, water circulation and sediment grain size. Therefore, particles could act as sediment grains and metals usually are adsorbed onto particles, integrating them into the sedimentary record. The latter is a grain size dependent process, as trace metals are commonly associated with clay and silt particles because their larger surface-volume ratio makes them more capable of adsorbing higher metal contents[8-11].

In the area of study, apart from beach grains such as bioclasts or cliff-derived clasts, anthropogenic vestiges like gravel-sized pieces of slag and bricks are commonly appreciated trapped within the beachrock outcrops, a fact that added to the mentioned historical framework might require grain size effect corrections in the study of these sedimentary structures. Apart from the relevance that particles and trace metals could have in this study, the examination of carbonates is fundamental as the cements responsible for the coalescence of the grains during intertidal cementation are mainly calcium carbonates[12]. The characteristics of the cements depend on the surrounding physicochemical conditions and certainly it is widely believed that aragonite and high-magnesium calcite (HMC) are the most common cements in early marine cementation[12,13], as found in Azkorri beach and Tunelboka cove[14].

[8] Murray K.S., Cauvet D., Lybeer M., Thomas J.C., **1999**. *Particle size and chemical control of heavy metals in bed sediment from the Rouge River, Southeast Michigan*. Environmental Science and Technology 33, 987-992.
[9] French P., **2002**. *Coastal and estuarine management*. Routledge Environmental Managment Series, London, 272 pp.
[10] Syvitski J.P.M., **2007**. *Principles, methods and application of particle size analysis.* Cambridge University Press, UK, 388 pp.
[11] Frankowski M., Siepak M., Ziola A., Novotny K., Vaulovic T., Siepak J., **2008**. *Vertical distribution of heavy metals in grain size fractions in sedimentary rocks: Mosina-Krajkowo water well-field, Poland*. Environmental Monitoring and Assessment, 155, 493-507.
[12] Vousdoukas M.I., Velegrakis A.F., Plomaritis T.A., **2007**. *Beachrock occurrence, characteristics, formation mechanisms and impacts*. Earth-Science Reviews 85, 23-46.
[13] Folk R.L., **1974**. *The natural history of crystalline calcium carbonate; effect of magnesium content and salinity*. Journal of Sedimentary Petrology 44, 40-53.
[14] Arrieta N., Goienaga N., Martínez-Arkarazo I., Murelaga X., Baceta J.I., Sarmiento A., Madariaga J.M., **2011**. *Beachrock formation in temperate coastlines: Examples in sand-gravel beaches adjacent to the Nerbioi-Ibaizabal Estuary (Bilbao, Bay of Biscay, North of Spain)*. Spectrochimica Acta Part A 80, 55-65.

In view of the heterogeneity that the wide variety of grains together with the cements provide to the beachrocks, a grain size separation was considered convenient, to simultaneously obtain a first notion of the characteristics of both, the constituent particles and the cements in an attempt to isolate them.

The methodology followed for the granulometric analysis, as explained in Iturregui et al (2014)[15], was based on a grain size fractionation of the samples. Representative samples were obtained from the 1.40 m high stratified bed, where 10 exposed strata were sampled and named as S1-S10 (see Figure 3.1 in Chapter 3). At first, 10 cm^3 volume samples were ground and sieved to get different grain sizes (Ø>2 mm, 250µm<Ø<2mm, 75<Ø<250µm, Ø<75 µm). All samples were weighed before and after the sieving, to estimate the percentage of each fraction and the associated material recovery. Afterwards, a microscopic examination of the four grain sizes was carried out to predict the composition of each fraction and that visual inspection was complemented with Raman spectroscopic molecular analyses. Those qualitative analyses were quantitatively corroborated with ICP-MS and total carbonate quantification supported by chemometric analyses.

4.1.1 Microscopic examination

As mentioned before, the samples of the strata found in the vertical outcrop (Fig.1A) were divided in different size fractions (Ø>2mm, 250µm<Ø<2mm, 75<Ø<250µm, Ø<75µm). The Ø<2mm fraction was automatically discarded to separate boulders and gravels that were out of the aim of the study (see Figure 4.1A).

With regard to the rest of the fractions, after the sieving, between 94 and 97% of the initial mass of the samples was recovered in every sieving round. As a result, according to the size scales described by Blott & Pye[16], it can be observed that the column was characterized by medium to very coarse sands (250µm<Ø<2mm) accounting for the 93-97% of the samples mass (Table 4.1).

[15] Iturregui A., Arrieta N., Murelaga X., Baceta J.I., Olazabal M.A., Martínez-Arkarazo I., Madariaga J.M., **2014**. *The relevance of the analytical methodology in the geochemical study of beachrock outcrops: Arrigunaga Beach inside the Nerbioi-Ibaizabal estuary (Getxo, Basque Country)*. Analytical Methods 6, 8247-8257.

[16] Blott S.J, Pye K., **2001**. *Gradistat: a grain size distribution and statistics package for the analysis of unconsolidated sediments.* Earth Surface Processes and Landforms 26, 1237-1248.

Table 4.1. Mass percentage for each particle size (250µm<Ø<2mm, 75<Ø<250µm, Ø<75µm) in the ten strata (S1-S10) of the vertical column. Uncertainty lower than 3% at the 95% confidence level.

Sample	250µm<Ø<2mm	75<Ø<250µm	Ø<75µm
S1	97	2	0.8
S2	97	1	1
S3	97	2	0.7
S4	96	2	0.9
S5	97	2	0.6
S6	97	2	0.8
S7	95	4	0.4
S8	93	3	3
S9	96	1	2
S10	94	2	3

Table 1 also shows that the 75<Ø<250µm fraction contains the 1.3-3.8% of the total mass, while the Ø<75µm fraction involves the 0.4-2.7%. In addition, it is remarkable that the lowest strata, which were considered harder during the acquisition of the samples, contained by far the highest percentage of the Ø<75µm grain size.

Regarding the microscopic composition of the samples (Figure 4.1B-D), the heterogeneity of the 250µm<Ø<2mm size range was clearly distinguished, where diverse siliceous beach grains, slag, gravels and bioclasts were present (Figure 4.1B). In contrast, there seemed to be a higher content of particulate metallic material in the 75<Ø<250µm fraction, where small fragments that could be related with cement remains were observed around the grains (Figure 4.1C). Furthermore, the whitish colour of the Ø<75µm particle size denoted a higher concentration of cements, although some impurities were also appreciated within this fraction (Figure 4.1D).

In fact, it is believed that during the sieving, the particles are subjected to a grain-to-grain superficial abrasion, promoting the detachment of the cements that could be first powdered and transferred to the fraction with the smallest grain size.

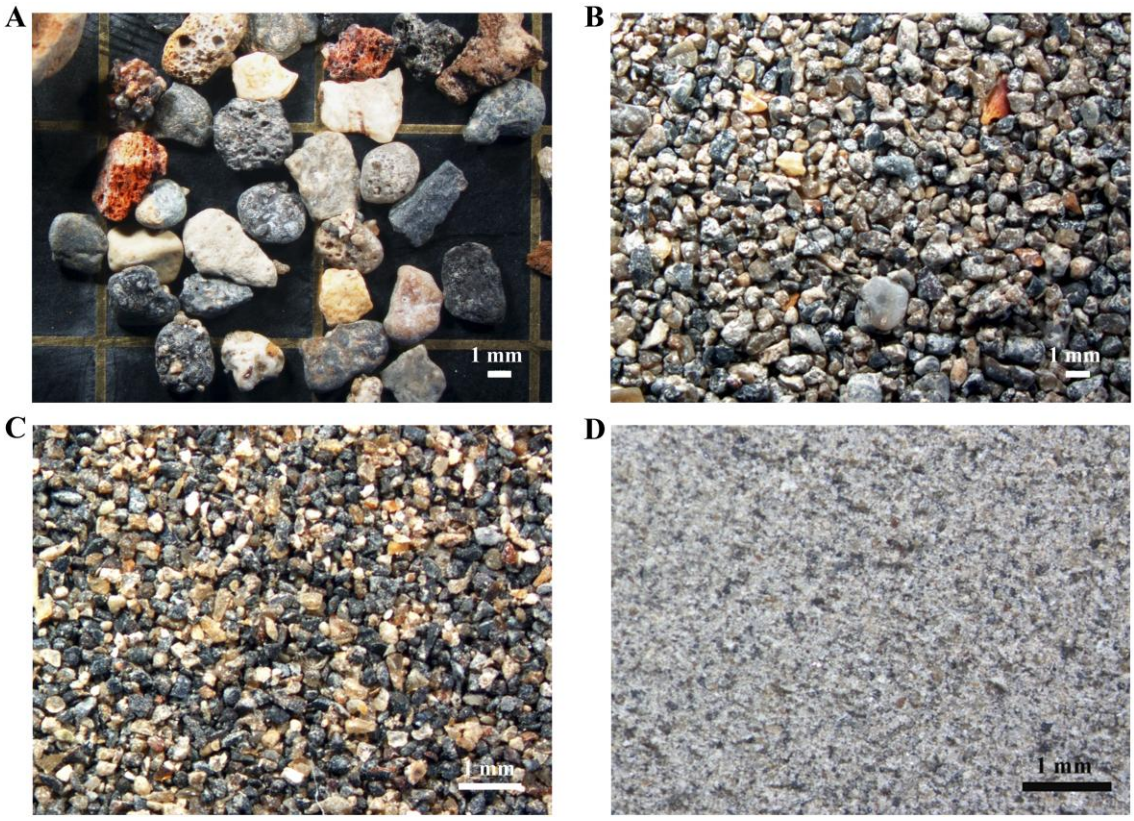

Figure 4.1. Microphotographs of the obtained particle sizes: A) Ø<2mm (0.75x), B) 250µm<Ø<2mm (0.75x), C) 75<Ø<250µm (2x) and D) Ø<75µm (2x).

In view of the main components of the particle sizes, as the 250µm<Ø<2mm size was considerably heterogeneous, it was inferred that the 75<Ø<250µm fraction might be mainly composed of metallic material. Moreover, it was possible to estimate that apparently the cement might be accumulated in the Ø<75µm fraction, with some remainders in the 75<Ø<250µm grain size. To confirm this concern, the 75<Ø<250µm (henceforth also known as the coarser fraction) and Ø<75µm (henceforth known as the finest fraction) grain sizes were analysed by means of Raman spectroscopy.

4.1.2 Estimation of the molecular composition by Raman spectroscopy

The composition of the 75<Ø<250µm and Ø<75µm grain sizes was determined through Raman spectroscopy, to have an idea of the mineral phases included in each fraction. This way, as shown in figure 4.2, in the 75<Ø<250µm size range, different iron compounds were identified, such as hematite (α-Fe_2O_3, with Raman bands at 227, 293, 410 and 612 cm^{-1}) and lepidocrocite (γ-FeO(OH), with Raman bands at 249, 379 and 522 cm^{-1}). Taking into consideration the iron abundance of the Basque-Cantabrian basin, the identified minerals might have a natural origin.

As a matter of fact, in a research work related with the sediments of the vicinity of the Nerbioi-Ibaizabal estuary, hematite was found considering it as a natural mineral phase[17]. However, in a study focused on the slag from different locations of Biscay, hematite was also detected[18]. Thus, it is not clear whether the origin of the hematite is natural or anthropogenic. In any case, the presence of this mineral is likely to be enhanced due to the anthropogenic influence mostly promoted by the diverse industrial activities developed around the estuary, such as mining exploitation and steelmaking industry. Moreover, hematite and lepidocrocite, both were also detected trapped within an adjacent beachrock. There, the formation of the lepidocrocite was ascribed to the solubilisation of iron rich compounds, which enhance the reaction between the iron trivalent cation and seawater derived hydrogen-carbonates, giving rise to a new compound, more exactly, the lepidocrocite[19]. Therefore, these facts evidenced the presence of iron compounds in the 75<Ø<250µm grain size.

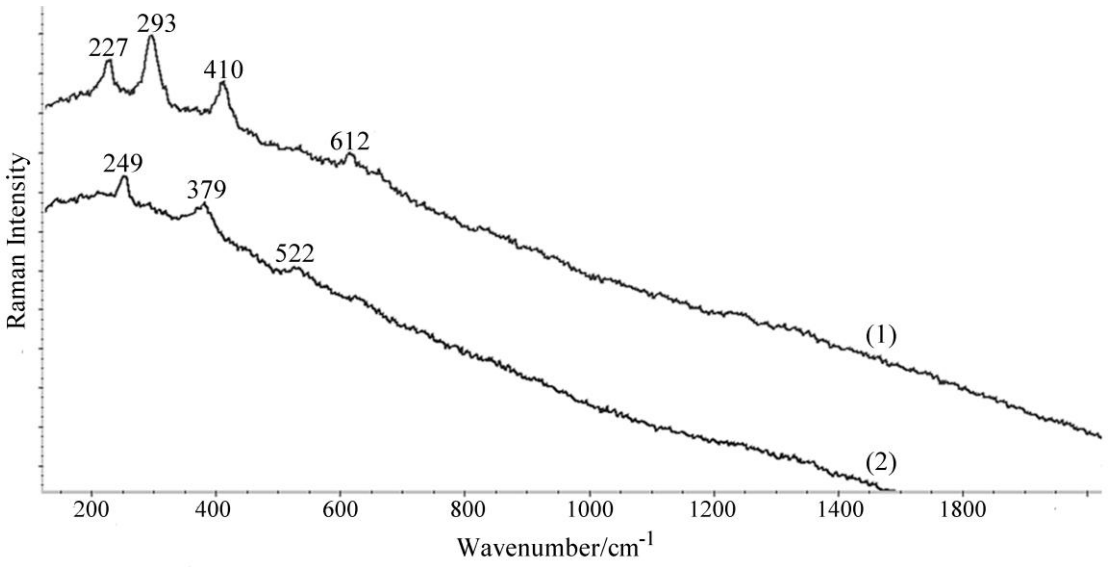

Figure 4.2. Raman spectra of hematite (1) and lepidocrocite (2), both found in the 75<Ø<250µm size fraction.

[17] Villanueva U., Raposo J.C., Castro K., de Diego A., Arana G. and Madariaga J.M., **2008**. *Raman spectroscopy speciation of natural and anthropogenic solid phases in river and estuarine sediments with appreciable amount of clay and organic matter*. Journal of Raman Spectroscopy 39, 1195-1203.
[18] Gomez-Nubla L., Aramendia J., Fdez-Ortiz de Vallejuelo S., Castro K. and Madariaga J.M., **2013**. *From Portable to SCA Raman devices to characterize harmful compounds contained in used black slag produced in Electric Arc Furnace of steel industry*. Journal of Raman Spectroscopy 44, 1163-1171.
[19] Arrieta N., Goienaga N., Martínez-Arkarazo I., Murelaga X., Baceta J.I., Sarmiento A., Madariaga J.M., **2011**. *Beachrock formation in temperate coastlines: Examples in sand-gravel beaches adjacent to the Nerbioi-Ibaizabal Estuary (Bilbao, Bay of Biscay, North of Spain)*. Spectrochimica Acta Part A 80, 55-65.

With regards to the cement remains contained in both fractions, high magnesium calcite (HMC, $Ca(Mg)CO_3$) was identified mainly in the Ø<75µm fraction, and occasionally in the 75<Ø<250µm. This is a common marine carbonate containing more than 4% of $MgCO_3$ randomly replacing the $CaCO_3$ in the calcite lattice[20,21]. Indeed, it is recognisable due to the displacement of the peaks to higher wavenumber with respect to the calcite Raman spectrum[22], as it occurred in this case at 150, 279, 714 and 1086 cm^{-1} Raman bands (Figure 4.3). HMC could arise accompanied by amorphous carbon with Raman bands at 1307 and 1591 cm^{-1}.

Nevertheless, in the Ø<75µm fraction, apart from quartz, aragonite ($CaCO_3$) was the identified main compound due to its Raman bands at 153, 205, 704 and 1085 cm^{-1}. However, it is remarkable a finding in the 1200-1800 cm^{-1} region, where together with the aragonite Raman bands (Figure 4.3), different peaks were repeatedly obtained at 1210, 1239, 1313, 1333 and 1863 cm^{-1}. According to the literature, various organic and biological systems provide a Raman response around that region. For instance, between 1000 and 1200 cm^{-1} C-C single bond stretching vibrations and contributions from C-N and C-O vibrations could be found. Furthermore, the range of 1238-1350 cm^{-1} could be related with amide III, including overlapping of C-H bending modes and CH_2 twisting vibrations[23,24]. Therefore, these facts suggested that the group of bands between 1210 and 1333 cm^{-1} showed in Figure 4.3 represent some kind of organic compound. The presence of these kind of compounds within carbonate crystals would not be surprising, because many authors[21,25,26] described that certain organic macromolecules, especially rich is aspartic acid ($C_4H_7NO_4$) and glutamic acid ($C_5H_9NO_4$), could be relevant in the morphology, formation and growth of carbonate crystals. However, we shall be turning to this matter in Chapter 6, exclusively dedicated to the investigation of the cements, where more analyses will be described in an attempt to delve further into this hypothesis.

[20] Vousdoukas M.I., Velegrakis A.F., Plomaritis T.A., **2007**. *Beachrock occurrence, characteristics, formation mechanisms and impacts*. Earth-Science Reviews 85, 23-46.
[21] Urmos J., Sharma S.K., Mackenzie F.T., **1991**. *Characterization of some biogenic carbonates with Raman Spectroscopy*. American Mineralogist 76, 641-646.
[22] Bischoff W.D., Sharma S.K., Mackenzie F.T., **1985**. *Carbonate ion disorder in synthetic and biogenic magnesian calcites: A Raman spectral study*. American Mineralogist 70, 581-589.
[23] Sánchez Román M., Fernández-Remolar D., Amils R., Sánchez-Navas, Schmid T., San Martin-Uriz P., Rodríguez N., McKenzie J.A., Vasconcelos C., **2014**. *Microbial mediated formation of Fe-carbonate minerals under extreme acidic conditions*. Scientific Reports 4, 1-7.
[24] Edwards H.G.M, Moody C.D., Newton E.M., Jorge Villar S.E., Russell M.J., **2005**. *Raman spectroscopic analysis of cyanobacterial colonization of hydromagnesite, a putative martian extremophile*. Icarus 175, 372-381.
[25] Reitner, J., **1993**. *Modern cryptic microbialite/metazoan facies from Lizard Island (Great Barrier Reef, Australia): formation and concepts*. Facies 29, 3-40.
[26] Braissant O., Cailleau G., Dupraz C., Verrecchia E.P., **2003**. *Bacterially induced mineralization of calcium carbonate in terrestrial environments: the role of exopolysaccharides and amino acids*. Journal of Sedimentary Research 73, 485-490.

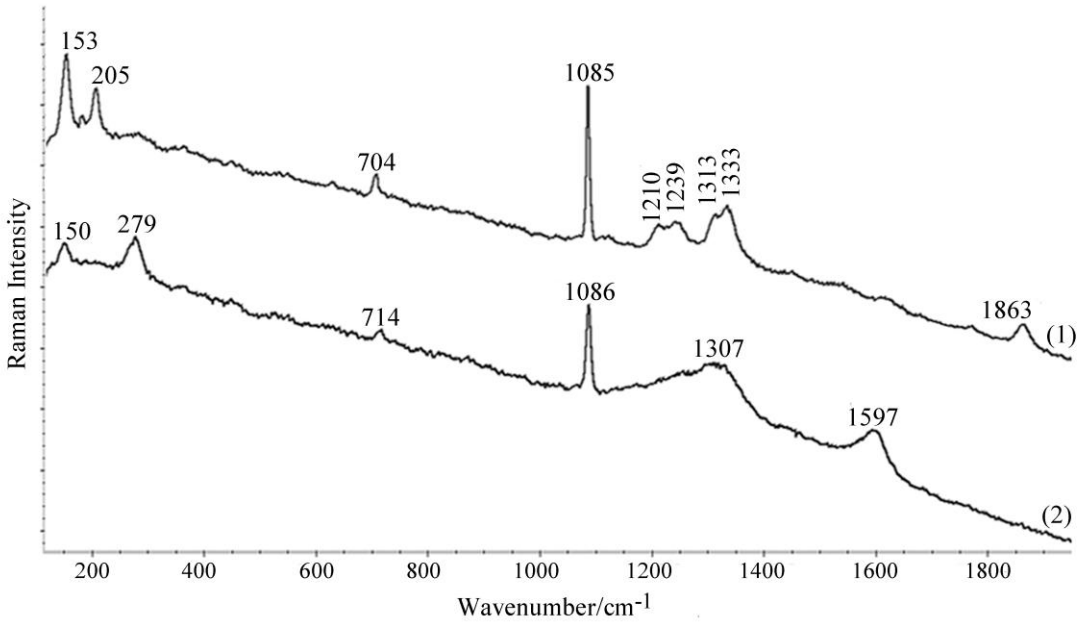

Figure 4.3. Raman spectrum of aragonite (1) and high magnesium calcite (2), mainly identified in the Ø<75µm fraction.

In view of these results, it might be assumed that there seem to be at least two types of cements composed of HMC and aragonite. The fact of having found HMC also in the 75<Ø<250µm could indicate that it might remain fixed in the grains after the sieving process, in contrast to the aragonite cement which would have been detached from the grains and transferred completely to the Ø<75µm test sieve. That presumption led to believe that possibly two phases are present bonding the grains, coinciding with studies in adjacent beaches, where a sequence constituted by HMC and aragonite as the main carbonate cement phases has been found in the beachrock outcrops[27].

Thus, Raman spectroscopy also suggests that the 75<Ø<250µm and Ø<75µm fractions contain mainly metallic particulates and cements, respectively. In any case, in order to characterise more in detail the powdered samples, it was decided to quantitatively verify the composition of the different grain sizes.

[27] Arrieta N., Goienaga N., Martínez-Arkarazo I., Murelaga X., Baceta J.I., Sarmiento A., Madariaga J.M., **2011**. *Beachrock formation in temperate coastlines: Examples in sand-gravel beaches adjacent to the Nerbioi-Ibaizabal Estuary (Bilbao, Bay of Biscay, North of Spain)*. Spectrochimica Acta Part A 80, 55-65.

4.1.3 Elemental quantification by ICP-MS

The outcomes explained along these lines complement the premises figured out after the microscopic and Raman spectroscopic examinations. Thereby, metal characterisation helped in verifying if the metal content was higher in the 75<Ø<250µm size range, as well as in identifying the major elements present in the fraction Ø<75µm, to see whether they were associated to the cements that presumably are compiled there.

The only three elements that showed concentration values lower than the detection limits (calculated as three times the standard deviation of the blanks, considering also the slope and intercept of the calibration) were Se, Hg and Sb. Table 4.2 and Table 4.3 summarise the mean concentration values and relative standard deviation (RSD) of the other measured elements in the ten strata. The RSD resulted lower than 20% in most of the cases, even though some elements showed higher RSD values at the mg/kg concentration levels in the 75<Ø<250µm fraction, providing an insight of the heterogeneity of the coarser particle size fraction.

In general terms, taking into consideration both fractions, the major elements present in the ten strata were Fe, Ca, Mg, Al as well as Mn, Na and K, which represent more than the 95% of the total metallic content in both fractions as it can be appreciated in Figure 4.4. There, it can also be estimated the distribution of the major elements within the strata. The Fe is mainly accumulated in the strata between S3 and S7, in the intermediate ones. This metal could be representative of many of the analysed elements because Mn, Zn, Cu, Pb, Cr, As, Ni, Mo, Ag, Cr, Co and Ba, showed a similar trend along the stratigraphic column. Conversely, an inverse distribution is observed in Ca, as strata S1, S2, S8, S9 and S10 showed the highest content. Ca exemplifies also the tendency of elements like Na, Sr, Cd and Mg. The rest of the elements (Al, Ti, Tl and K) showed a fairly homogeneous concentration.

Table 4.2a. Mean concentration (g/kg) and RSD (%) values of the major elements measured in the 75<Ø<250µm particle size.

	S1		S2		S3		S4		S5		S6		S7		S8		S9		S10	
	Mean	RSD	Mean	RSD	Mean	RSD	Mean	RSD	Mean	RSD	Mean	RSD	Mean	RSD	Mean	RSD	Mean	RSD	Mean	RSD
Fe	210	5	117	2	402	6	222	7	213	8	288	17	169	5	95	11	54	10	122	9
Ca	83	2	92	3	56	3	58	2	79	3	59	5	80	3	55	12	117	5	60	2
Al	21	3	23	3	17	6	16	18	24	5	17	13	23	7	19	9	17	10	10	7
Mg	20	5	22	1	20	7	19	13	22	3	19	12	20	6	31	8	27	8.4	15	6
Mn	7	3	6	3	9	6	8	15	8	3	8	13	7	3	5	13	4	2	3	5
Na	2	3	3	1	2	7	2	12	3	2	2	15	2	9	4	10	2	12	2	8
K	2	5	3	4	1	3	1	4	2	5	2	9	2	5	1	15	2	11	1	2

Table 4.2b. Mean concentration (mg/kg) and RSD (%) values of the minor elements measured in the 75<Ø<250µm particle size.

	S1		S2		S3		S4		S5		S6		S7		S8		S9		S10	
	Mean	RSD	Mean	RSD	Mean	RSD	Mean	RSD	Mean	RSD	Mean	RSD	Mean	RSD	Mean	RSD	Mean	RSD	Mean	RSD
Zn	984	9	603	10	2550	12	1612	11	1146	4	2137	15	1447	3	553	4	483	14	344	15
Ba	693	15	645	19	801	2	1003	8	741	14	486	5	633	6	595	7	595	16	647	9
Sr	624	2	770	4	353	7	433	9	632	3	414	12	586	4	656	19	1001	2	508	4
Ti	267	4	317	6	254	3	217	14	339	1	243	11	326	3	372	12	340	9	242	2
Cu	212	18	100	14	369	24	244	10	143	24	240	15	147	16	69	18	52	12	54	16
Pb	146	17	164	10	606	11	404	10	254	23	368	21	240	3	110	24	99	9	60	7
Cr	47	1	29	2	79	6	48	3	48	6	56	12	38	6	24	10	19	13	23	4
Sn	49	27	53	6	186	4	49	20	46	19	91	11	62	11	28	18	30	28	10	24
As	30	4	20	3	40	9	42	5	30	8	39	8	24	8	13	7.8	16	4	21	12
Ni	30	4	20	3	50	10	35	4	32	14	35	4	27	5	13	15	13	19	15	14
V	27	2	21	7	33	3	29	18	28	2	32	10	25	4	17	12	17	2	26	6
Co	13	6	8	2	23	3	16	2	14	13	16	16	10	6	5	17	5	5	7	8
Mo	3	9	2	2	4	10	2	2	3	10	3	11	2	8	1	3	2	5	1	7
Tl	0.5	1	0.4	5	0.3	3	0.3	19	0.7	20	0.3	11	0.3	7	0.2	7	0.2	7	0.2	7
Cd	0.5	24	0.3	23	0.3	13	0.3	19	0.5	11	0.3	19	0.3	9	0.2	13	0.4	13	0.2	7
Ag	0.2	5	0.2	7	0.3	11	0.2	4	0.2	4	0.2	3	0.2	8	0.2	14	0.2	3	0.1	14

Table 4.3a. Mean concentration (g/kg) and RSD (%) values of the major elements measured in the Ø<75µm particle size.

	S1		S2		S3		S4		S5		S6		S7		S8		S9		S10	
	Mean	RSD	Mean	RSD	Mean	RSD	Mean	RSD	Mean	RSD	Mean	RSD	Mean	RSD	Mean	RSD	Mean	RSD	Mean	RSD
Ca	186	2	183	2	129	15	166	2	144	10	140	4	123	2	100	4.0	197	3	174	2
Fe	41	4	37	2	74	5	69	5	55	3	55	2	60	7	17	5	18	3	21	1
Mg	146	2	17	2	15	3	16	4	18	1	17	5	17	3	38	2	23	8	17	2
Al	124	1	13	3	12	4	12	7	16	3	14	5	17	4	17	2	11	11	9	3
Mn	4	2	4	3	4	3	4	4	5	3	4	6	5	2	3	2	2	5	2	1
Na	2	3	3	3	2	3	2	3	3	3	2	4	3	4	4	3	2	11	2	4
K	2	4	2	3	2	7	2	16	2	5	2	5	2	2	1	7	2	12	1	2

Table 4.3b. Mean concentration (mg/kg) and RSD (%) values of the minor elements measured in the Ø<75µm particle size.

	S1		S2		S3		S4		S5		S6		S7		S8		S9		S10	
	Mean	RSD	Mean	RSD	Mean	RSD	Mean	RSD	Mean	RSD	Mean	RSD	Mean	RSD	Mean	RSD	Mean	RSD	Mean	RSD
Sr	810	2	895	3	770	8	873	2	892	3	829	4	781	2	1132	4	1547	2	1073	2
Ba	469	2	397.3	1	800	2	858	1	803	3	932	14	941	4	891	7	292	1	430	4
Zn	548	4	356.5	1	461	2	479	6	406	3	423	7	522	6	261	4	312	1	285	2
Ti	160	9	179.9	4	185	5	193	16	289	2	261	5	358	2	356	4	197	16	136	2
Pb	129	2	113.2	2	224	7	234	3	200	2	225	5	214	15	108	4	91	3	67	2
Cu	80	6	64.0	3	171	2	175	5	120	4	131	6	110	6	29	3	39	3	36	6
Cr	39	11	39.9	3	47	11	43	4	81	5	49	7	76	2	18	12	25	7	21	7
Ni	41	10	33.0	4	56	8	52	6	65	7	44	9	60	3	12	16	22	4	21	11
As	27	6	18.28	1	64	2	59	6	34	5	30	6	26	4	10	4	16	8	19	2
V	15	5	14.76	3	22	6	22	6	20	2	23	4	19	4	13	4	14	3	15	6
Sn	14	6	12.9	9	18	3	19	17	19	5	20	13	22	14	9	9	7	10	5	9
Co	10	2	7.92	2	21	2	19	5	13	6	11	7	10	2	3	4	7	5	6	2
Mo	3	18	4.08	4	4	8	5	7	9	5	5	10	9	4	1	17	3	16	2	13
Cd	0.8	10	0.449	5	0.5	9	0.6	3	0.5	8	0.4	7	0.5	6	0.3	6	0.6	5	0.5	5
Tl	0.5	3	0.403	5	0.4	6	0.4	2	0.4	2	0.3	4	0.4	2	0.2	3	0.3	6	0.2	4
Ag	0.2	6	0.1952	8	0.4	11	0.3	3	0.3	4	0.3	3	0.3	3	0.2	7	0.2	7	0.2	3

In spite of the general distribution of the elements, differences among the 75<Ø<250µm and Ø<75µm fractions are worth mentioning. In fact, taking into consideration all the samples, the concentration of Ca ranges around 11-52% in the coarser fraction (Figure 4.4A); in contrast to the 53-77% found in the finest particle size (Figure 4.4B). On the contrary, metals are more concentrated in the 75<Ø<250µm particle size, especially Fe, which constitutes the 24-78%, while a 7-31% was detected in the finest fraction. In addition, it is worth highlighting that overall it can be appreciated in both particle sizes that Ca and Fe seem to have an opposite trend; the higher the concentration of Ca, the lower is the concentration of Fe, and *vice versa*.

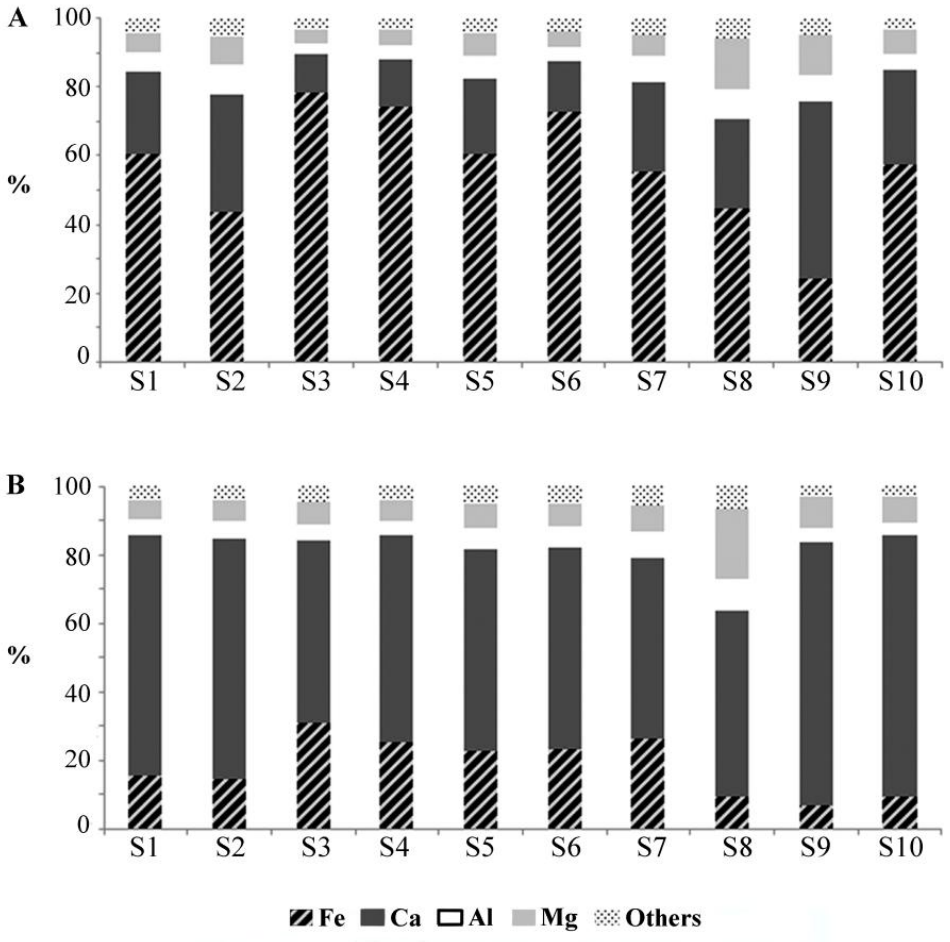

Figure 4.4. Percentage of Fe, Ca, Al, Mg and the rest of the analysed elements in the A) 75<Ø<250µm and B) Ø<75µm fractions.

In order to observe more in detail the differences among the two fractions, the metal content of each of them was compared calculating the ratio between the concentration of the analysed metals in the 75<Ø<250µm fraction and the Ø<75µm fraction (Figure 4.5).

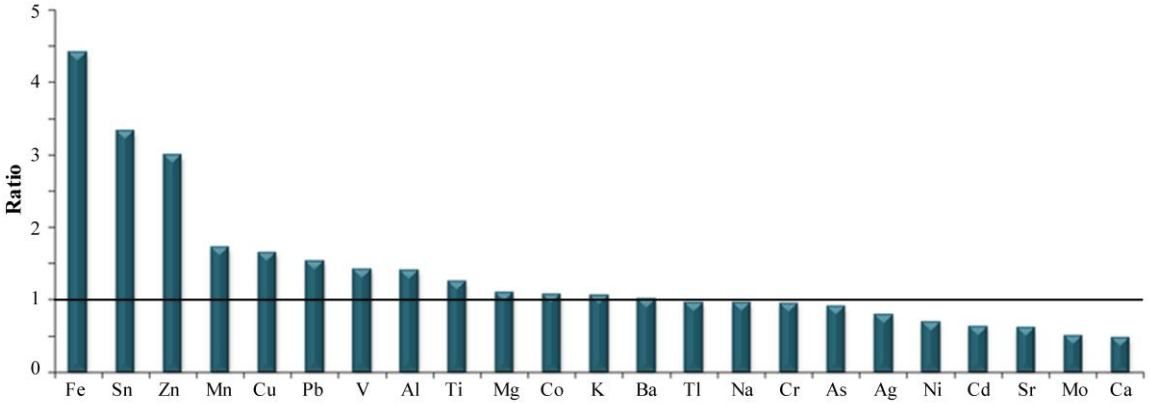

Figure 4.5. Representation of the ratio between the concentration of the metals in the 75<Ø<250µm and Ø<75µm particle sizes. The horizontal line indicates the ratio equal to 1. Ratio>1: elements that have a higher concentration in the coarser fraction. Ratio~1: elements that have a similar concentration in both fractions. Ratio<1: elements that have a higher concentration in the finest fraction.

Hence, through this ratio between the concentration in 75<Ø<250µm and Ø<75µm, it was found that the majority of the metals (Fe, Sn, Zn, Mn, Cu, Pb, V, Al, Ti, Mg, Co) present a higher concentration in the greatest fraction. Among those elements, Fe is the one with the higher ratio value which, by the way is believed to be the major constituent of many slag and trapped materials in the beachrock, a fact supported by the Raman spectroscopic results explained before and also by the high presence of iron oxides and oxyhydroxides found among the anthropogenic materials found within the adjacent beachrock[28].

Besides, K, Ba, Tl, Na and Cr present almost similar concentration in both fractions. However, some other elements like As, Ni, Cd, Ni and Mo that are predominant in the Ø<75µm fraction, possibly represent the compounds mainly contained in the finest fraction. But the most remarkable fact of the finest fraction might be the higher ratio value of Ca and Sr, two elements regularly associated to marine carbonate cements, especially the Ca. Thus, it seems that the elements commonly associated to carbonate cements are more abundant in the finest fraction.

In general terms it must be remarked that, when studying the metal concentrations of different grain sizes, it is commonly considered that the finest the fraction the higher is the metal content, because, among other reasons, the larger surface to volume ratio of

[28] Arrieta N., Goienaga N., Martínez-Arkarazo I., Murelaga X., Baceta J.I., Sarmiento A., Madariaga J.M., **2011**. *Beachrock formation in temperate coastlines: Examples in sand-gravel beaches adjacent to the Nerbioi-Ibaizabal Estuary (Bilbao, Bay of Biscay, North of Spain)*. Spectrochimica Acta Part A 80, 55-65.

the clays enhances the binding with the metals. But in this case, the highest metallic content was found in the coarser fraction, which is likely produced by an external anthropogenic income. Indeed, some authors suggest that an increased concentration of metals in coarse fractions might be a result of the presence of mining wastes in the system due to the limited transport and higher residence time of those anthropogenic remains[29]. In contrast, the finest fraction, although it might contain remainders of sediments, it seems to be more related with the cements responsible of the coalescence of the grains. In any case, the carbonate quantification might shed new light on this hypothesis.

4.1.4 Total carbonate quantification

By virtue of this analysis, it was tried to estimate the amount of carbonates associated to the cements in three of the size classes: 250µm<Ø<2mm, 75<Ø<250µm, Ø<75µm.

Attending to the samples of the different strata, the ones on the top (S1 and S2) and in the lowest side of the outcrop (S9 and S10) present the higher quantity of carbonates. In the first ones, considering the proximity to a cliff of a calcareous nature, the origin of the extra carbonates might be lixiviation waters coming from there. In contrast, the downward slope of the outcrop might promote an accumulation of the carbonates in its base after the percolation of carbonate-rich waters.

Besides, the relation between carbonates and grain size must be highlighted. The 250µm<Ø<2mm and 75<Ø<250µm particle sizes showed similar carbonates concentration, 29% and 26% w/w, respectively. Nevertheless, under the optic microscope it was observed that in the largest particle size limestone and biological fragments are accumulated, which could presumably be dissolved during the acid attack performed in the titration. The 75<Ø<250µm fraction, in contrast, is principally composed of particulate metallic remainders.

Indeed, the highest concentration of carbonates, 45% w/w, was found in the Ø<75µm particle size. Even though some rests were assumed in the 75<Ø<250µm fraction, the concentration of carbonates found in all the strata ranges from 130 to 268 g kg^{-1} (equivalent to 2.2 to 4.5 mol kg^{-1}), while the finest fraction contains a total carbonate concentration between 277 and 373 g kg^{-1} (equivalent to 4.6 and 6.2 mol kg^{-1}, see Figure

[29] Singh A.K., Hasnain S.I., Banerjee D.K., **1999**. *Grain size and elemental partitioning of heavy metals in sediments of the Damodar River a tributary of the lower Ganga, India*. Environmental Geology 39, 90-98.

4.6). These facts are in tune with the presumption of the accumulation of the cements in the finest particles, so further examinations were basically founded on Ø<75µm. Assuming that the most common minerals in intertidal cementation are calcium carbonates[30], the results obtained at different strata about Ca and carbonates concentration were compared in Figure 4.6. A very similar tendency is perceived among them but there is still a spare content of carbonates that, seemingly, is not associated with Ca. Carbonates could also be linked to other elements, like Sr and Mg, as the former is commonly included in the aragonite structure and the latter is part of the high magnesium calcite[31]. Nevertheless, the highest amount of Sr was found in S9, being around 18 mmol, so scarcely contribute in the comparison. In contrast, Mg marked a greater difference equalising even more the tendencies, which could evidence again the presence of HMC within the cements.

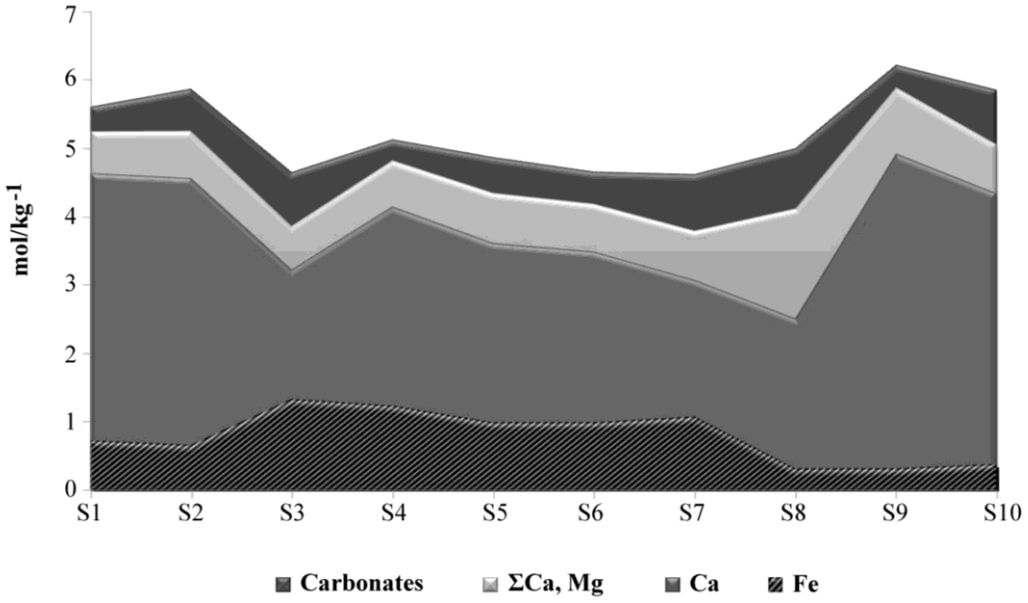

Figure 4.6. Comparison of the data obtained in the <75µm fraction: carbonates, calcium and magnesium (ΣCa, Mg), calcium (Ca) and iron (Fe) concentration.

Although the contribution of magnesium stands out in some strata, concretely in S8, there is still an excess of carbonates not explained. To shed some light on this, it was contrasted with the concentration of metals and, not only there were not in concordance, but an opposite trend was identified, above all between carbonates and iron as those strata with the maximum values of metals (S3, S4, S5, S6 and S7) confine the lowest carbonate concentration (Figure 4.6). That content of carbonates that

[30] Gischler E., Lomando A.J., **2007**. *Beachrock and Intertidal Precipitates*. In: Nash D.J., McLaren S.J. (Eds.),*Geochemical Sediments and Landscapes*. Wiley-Blackwell, UK, pp. 365-390.
[31] Folk R.L., **1974**. *The natural history of crystalline calcium carbonate; effect of magnesium content and salinity*. Journal of Sedimentary Petrology 44, 40-53.

apparently is not associated with Ca and Mg is possibly related with other carbonates that could be contained in a lesser extent in the finest fraction, or with the oxidation of organic matter, redox processes and other interferences that might occurred during the titration. However, thanks to this comparative approximation, it was possible to explain the 85-95% of the measured carbonates (take in mind that the RSD ranges from 1 to 5%) just confronting it mainly with the content of Ca and Mg found in each stratum, giving and idea of the composition of the cements, that could mainly consist of calcium carbonate solely and also with higher amounts of Mg probably constituting HMC cement.

4.1.5 Statistical analysis

Relying on the granulometric characterization followed by metal and carbonate quantification, Ø<75µm and 75<Ø<250µm fractions seemed to have a dissimilar composition. To better understand the differences among both grain sizes, the results were subjected to different statistical examinations.

Pearson´s correlation coefficients were calculated at a confidence level of 95% ($p<0.05$, $r < 0.55$) and 99% ($p<0.01$, $r <0.71$) for the elements and carbonates quantified in both fractions of the ten samples. The results revealed that there is no correlation between Ca and carbonates in the 75<Ø<250µm size fraction (see Table 4.4). In contrast, a high correlation coefficient can be observed (see Table 4.5) among those two constituents in the Ø<75µm fraction. Thus, Ca and carbonates are more related between them in the finest grain size, which supports the idea that the calcium carbonate cements can be accumulated there. Furthermore, the carbonates are also correlated with Sr in the finest fraction, probably because Sr is a common element involved in the aragonite lattice[32].

Besides, Fe, Mn, Zn, Ba, Cu, Cr, Ni, Pb, As, V, Co, Sn and Mo are positively correlated especially in the 75<Ø<250µm grain size, suggesting that those elements have a common origin. In fact, the correlation coefficients are higher in the coarser fraction, probably, as remarked in section 4.1.3, due to the presence of anthropogenic inputs, such as mining wastes[33].

[32] Folk R.L., **1974**. *The natural history of crystalline calcium carbonate; effect of magnesium content and salinity*. Journal of Sedimentary Petrology 44, 40-53.
[33] Singh A.K., Hasnain S.I., Banerjee D.K., **1999**. *Grain size and elemental partitioning of heavy metals in sediments of the Damodar River – a tributary of the lower Ganga, India*. Environmental Geology 39, 90-98.

Table 4.4. Pearson´s correlation matrix of the 75<Ø<250µm fraction (n=10). Significant positive correlations are coloured in green and negative correlations in red. Underlined coefficients are significant at a 99% confidence level (p<0.01, r>0.71); in the rest of them, correlation is significant at a 95% confidence level (p<0.05, r>0.55).

	Ca	Fe	Mg	Al	Na	Mn	K	Sr	Zn	Ba	Ti	Cu	Cr	Ni	Pb	As	V	Co	Sn	Mo	Cd	Tl	Ag	Carbonates
Ca	1.00																							
Fe	-0.58	1.00																						
Mg	0.28	-0.43	1.00																					
Al	0.41	0.02	0.31	1.00																				
Na	0.20	-0.48	0.78	0.55	1.00																			
Mn	-0.24	0.84	-0.18	0.48	-0.19	1.00																		
K	0.61	-0.15	0.12	0.90	0.46	0.28	1.00																	
Sr	0.89	-0.81	0.59	0.31	0.51	-0.52	0.46	1.00																
Zn	-0.50	0.94	-0.27	0.06	-0.47	0.84	-0.15	-0.73	1.00															
Ba	-0.65	0.82	-0.17	-0.03	-0.32	0.39	-0.10	-0.36	0.67	1.00														
Ti	0.47	-0.57	0.81	0.56	0.85	-0.27	0.45	0.70	-0.49	-0.42	1.00													
Cu	-0.49	0.98	-0.32	0.05	-0.47	0.87	-0.11	-0.73	0.96	0.46	-0.60	1.00												
Cr	-0.50	0.99	-0.36	0.11	-0.43	0.90	-0.06	-0.76	0.93	0.83	-0.51	0.98	1.00											
Ni	-0.49	0.98	-0.39	0.10	-0.47	0.91	-0.14	-0.72	0.92	0.39	-0.55	0.97	0.99	1.00										
Pb	-0.46	0.91	-0.26	0.05	-0.37	0.82	-0.15	-0.69	0.94	0.48	-0.48	0.93	0.97	0.91	1.00									
As	-0.47	0.88	-0.56	-0.06	-0.67	0.81	-0.17	-0.77	0.87	0.53	-0.75	0.90	0.88	0.92	0.85	1.00								
V	-0.54	0.92	-0.72	-0.13	-0.71	0.72	-0.20	-0.85	0.83	0.37	-0.76	0.85	0.69	0.89	0.77	0.92	1.00							
Co	-0.48	0.99	-0.43	0.04	-0.51	0.88	-0.11	-0.76	0.92	0.49	-0.59	0.97	0.99	0.99	0.92	0.93	0.91	1.00						
Sn	-0.37	0.78	-0.17	0.10	-0.27	0.73	-0.04	-0.55	0.87	0.19	-0.32	0.87	0.89	0.84	0.86	0.64	0.64	0.80	1.00					
Mo	-0.26	0.91	-0.34	0.24	-0.42	0.89	0.13	-0.51	0.82	0.36	-0.40	0.89	0.95	0.94	0.81	0.80	0.83	0.92	0.84	1.00				
Cd	0.53	0.10	0.07	0.50	-0.07	0.41	0.53	0.37	0.05	0.03	0.14	0.11	0.20	0.23	0.02	0.16	-0.16	0.18	0.05	0.49	1.00			
Tl	0.25	0.20	-0.11	0.69	0.15	0.53	0.70	0.07	0.07	0.07	0.17	0.15	0.29	0.32	0.07	0.22	0.25	0.28	0.07	0.48	0.66	1.00		
Ag	-0.02	0.58	0.27	0.63	0.17	0.85	0.38	-0.16	0.63	0.34	0.16	0.63	0.68	0.69	0.71	0.48	0.33	0.65	0.67	0.72	0.43	0.51	1.00	
Carbonates	0.15	-0.16	-0.11	-0.32	-0.01	-0.37	-0.09	0.17	-0.39	-0.25	-0.14	-0.15	-0.19	-0.24	-0.44	-0.29	-0.14	-0.23	-0.15	-0.10	0.15	-0.10	-0.49	1.00

Table 4.5. Pearson´s correlation matrix of the Ø<75µm fraction (n=10). Significant positive correlations are coloured in green and negative correlations in red. Underlined coefficients are significant at a 99% confidence level (p<0.01, r>0.71); in the rest of them, correlation is significant at a 95% confidence level (p<0.05, r>0.55).

	Ca	Fe	Mg	Al	Na	Mn	K	Sr	Zn	Ba	Ti	Cu	Cr	Ni	Pb	As	V	Co	Sn	Mo	Cd	Tl	Ag	Carbonates
Ca	1.00																							
Fe	-0.28	1.00																						
Mg	0.47	-0.59	1.00																					
Al	-0.75	0.21	0.44	1.00																				
Na	-0.78	-0.17	0.78	0.86	1.00																			
Mn	-0.56	0.81	-0.24	0.71	0.33	1.00																		
K	0.05	0.60	-0.51	0.42	-0.03	0.74	1.00																	
Sr	0.35	-0.76	0.53	-0.30	-0.06	-0.75	-0.58	1.00																
Zn	0.01	0.76	-0.65	0.19	-0.21	0.70	0.72	-0.71	1.00															
Ba	-0.86	0.62	0.15	0.71	0.54	0.76	0.21	-0.55*	0.33	1.00														
Ti	-0.79	0.07	0.55	0.93	0.84	0.55	0.17	-0.08	-0.01	0.70*	1.00													
Cu	-0.23	0.97	-0.55	0.12	-0.24	0.72	0.50	-0.66	0.70	0.60*	-0.02	1.00												
Cr	-0.22	0.70	-0.47	0.48	0.04	0.81	0.86	-0.59	0.68	0.46	0.32	0.59*	1.00											
Ni	-0.21	0.91	-0.63	0.29	-0.18	0.81	0.77	-0.70	0.75	0.53	0.16	0.84	0.91	1.00										
Pb	-0.44	0.94	-0.39	0.40	0.01	0.87	0.55	-0.66	0.68	0.78	0.32	0.94	0.72	0.85	1.00									
As	-0.13	0.88	-0.51	-0.10	-0.35	0.48	0.30	-0.53	0.58	0.42	-0.23	0.93	0.36	0.69	0.77	1.00								
V	-0.33	0.90	-0.49	0.16	-0.20	0.69	0.39	-0.59	0.55	0.69	0.14	0.93	0.62	0.79	0.95	0.79	1.00							
Co	-0.06	0.91	-0.60	-0.10	-0.41	0.54	0.42	-0.55	0.64	0.38	-0.23	0.95	0.46	0.76	0.80	0.98	0.82	1.00						
Sn	-0.40	0.91	-0.45	0.52	0.16	0.95	0.70	-0.76	0.77	0.70	0.38	0.85	0.84	0.90	0.95	0.62	0.84	0.52	1.00					
Mo	-0.25	0.62	-0.42	0.51	0.08	0.76	0.79	-0.47	0.57	0.47	0.47	0.52	0.98	0.86	0.67	0.27	0.58	0.37	0.78	1.00				
Cd	0.72	0.05	-0.53	-0.42	-0.62	-0.14	0.33	0.06	0.54	-0.50	-0.53	0.07	0.04	0.20	-0.07	0.14	-0.10	0.21	-0.01	0.01	1.00			
Tl	0.37	0.50	-0.69	-0.04	-0.36	0.45	0.78	-0.58	0.83	-0.11	-0.33	0.44	0.43	0.58	0.34	0.38	0.22	0.48	0.50	0.32	0.69	1.00		
Ag	-0.41	0.93	-0.35	0.34	0.03	0.79	0.54	-0.71	0.70	0.72	0.18	0.94	0.60	0.82	0.92	0.88	0.84	0.87	0.85	0.51	0.01	0.43	1.00	
Carbonates	0.84	-0.72	0.01	-0.66	-0.44	-0.84	-0.31	0.66	-0.44	-0.96	-0.63	-0.67	-0.61	-0.63	-0.83	-0.50	-0.75	-0.48	-0.80	-0.55	0.43	-0.03	-0.77	1.00

Regarding the principal component analysis, in Figure 4.7 is exposed the PCA model for the normalized and centred data set of both fractions, where scores (samples) and loadings (measured elements) are projected. The model explains the 64% of the total variance with the first two principal components (PC1, 41% and PC2, 23%). Two main groups are visualized according to the grain size, confirming that the 75<Ø<250µm fraction, collected in the positive side of the *y* axis (PC2), is more related to the great majority of the metals that might be clustered due to their anthropogenic origin. There is an exception with the Ø<75µm fraction of the stratum S8, which contains greater amounts of Mg, being more similar to the values of the larger fraction than to the rest of the samples of its grain size. The concentration of K, Ba, as well as Pb and Cu, is alike in both particle sizes so those elements are slightly distanced from the group. The Ø<75µm fraction, contrarily reflected in the negative side, of the y axis (PC2) is more associated to carbonates, Ca and Sr, even though elements like Mo, Cd, Ni and Ag are gathered in this as well, indicating a natural source for those elements.

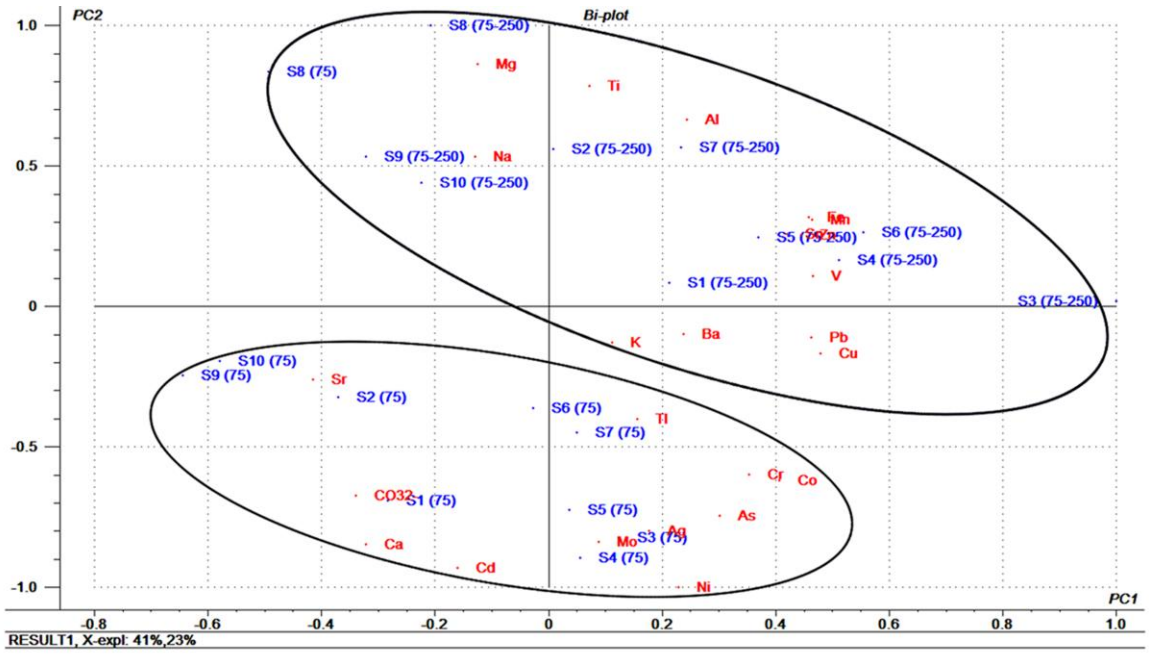

Figure 4.7. Display of the PCA model defined by two principal components including the 75<Ø<250µm and Ø<75 µm particle sizes (scores) and the analysed metals (loadings).

All in all, it has been possible to statistically confirm what the foregoing analyses have demonstrated. Indeed, there is an implicit difference between the examined grain sizes regarding the composition of them. Hence, it can be asserted that the majority of the metals are concentrated in the 75<Ø<250µm size range suggesting an external input. In contrast, the carbonates associated to the cements are mainly accumulated in the Ø<75µm particle size as evidenced by its relation with Ca, Mg and Sr.

4.1.6 General remarks of the analysis based on the grain size fractionation

In this study, the microscopic visualization and Raman spectroscopic analyses of the particle sizes carried out as a first step were successfully complemented by metal and carbonates quantification, a procedure where statistical analyses helpfully contributed.

In general terms, the major elements present in the outcrop were Fe, Ca, Mg, Mn, Al and K, but resulted essential to detect their distribution in the fractions of interest. Thanks to the size fractionation of the samples, an anthropogenic input of metals was evidenced because, in contrast to the inherited tendency of the increasing metal content in the finest particles, metals are more concentrated in the 75<Ø<250µm particle size, as corroborated by PCA. Raman spectroscopy helped in that premise as iron particulates like hematite and lepidocrocite were found within the 75<Ø<250µm fraction. In fact, Fe was the main component in this fraction, which showed high positive correlations with other metals like Mn, Zn, Cu, Cr, Ni, Pb, As, Sn and Co, suggesting a common origin probably derived from industrial wastes. Furthermore, the lack of association among the metals and carbonates, minimize the importance of the cement remainders present in the 75<Ø<250µm particle size. On the contrary, the higher amount of carbonates and Ca in the Ø<75µm fraction, added to their similar tendencies, as well as their positive correlation and their clustering in PCA analysis, showed that through this procedure, cements might have been mostly isolated in the Ø<75 µm particle size. In fact, in view of the Raman spectroscopic results, HMC and aragonite might be composing the cements.

Overall, the joint use of the analytical tools employed in this study resulted particularly successful for the examination of such a heterogeneous beachrock, as it was possible to hypothesise about the composition of the cements that might be responsible for the aggregation of the grains. Furthermore, the grain size based methodology allowed evidencing an external income of anthropogenic wastes; the slag and rubble dumped from mining and industrial activities occurring nearby, might have been subjected to mechanical abrasion promoted by wave forcing an, as a consequence, might caused the fractionation of the wastes resulting on particulate metallic materials.

4.2 *In situ* and laboratory Raman spectroscopic study

Among the wastes commonly found trapped in the studied beachrocks, the presence of slag is noticeable. Slag is a solid waste by-product derived from metallurgical processes of smelting ore. Millions of tons of slag are globally produced every year and the study of these materials has considerably increased in the last decades, to assess their possible reuse or environmental hazards[34-36]. In any case, in order to evaluate those inherent properties and the evolution under certain environmental conditions, their composition needs to be determined. The constituents of the slag can vary depending on the raw ore, smelting process, or the kind of furnace employed during the metallurgical processing. Generally, the major compounds consist on a mixture of silicates, as Ca-rich silicates in the olivine and pyroxenes group, oxides based on Fe, Ca or Mg, polymorphs of quartz and other minor compounds and impurities coming from the ore or the furnace lining[36,37]. Due to their mineral and chemical features, slag have cementitious properties analogous to construction materials. Likewise, when exposed to seawater and sulphate environments, they can suffer different physical and chemical alterations, such as sulphate attack and hydration[38].

Raman spectroscopy has been a convenient technique in various studies concerning slag and related cement materials to ascertain not only the composition, but also their possible weathering products in order to assess the alterations in the materials and their long-term durability[37-39]. Furthermore, previous works evidenced that Raman spectroscopy can provide an accurate and accessible identification of mineral phases in a geological context, even in field conditions[40]. Indeed, when the first *in situ* Raman study was carried out more than a decade ago, laboratory equipments were regarded as a better option. However, the technological developments achieved during the last years,

[34] Barca C., Meyer D., Liira M., Drissen P., Comeau Y., Florent Chazaren A., **2014**. *Steel slag filters to upgrade phosphorus removal in small wastewater treatment plants*: Removal mechanisms and performance. Ecological Engineering 68, 214-222.
[35] Schöler A., Lothenbach B., Winnefeld F., Zajac M., **2015**. *Hydration of quaternary Portland cement blends containing blast-furnace slag, siliceous fly ash and limestone powder*. Cement and Concrete Composites *55*, 374-382.
[36] Piatak N.M., Parsons M.B., Seal II R.R., **2015**. *Characteristics and environmental aspects of slag: A review*. Applied Geochemistry *57*, 236-266.
[37] Gomez-Nubla L., Aramendia J., Fdez-Ortiz de Vallejuelo S., Castro K. and Madariaga J.M., **2013**. *From Portable to SCA Raman devices to characterize harmful compounds contained in used black slag produced in Electric Arc Furnace of steel industry*. Journal of Raman Spectroscopy 44, 1163-1171.
[38] Kourounis S., Tsivilis S., Tsakiridis P.E., Papadimitriou G.D., Tsibouki Z., **2007**. *Properties and hydration of blended cements with steelmaking slag*. Cement and Concrete Research 37, 815-822.
[39] Martinez-Ramirez S., Frías M., Domingo C., **2006**. *Micro-Raman spectroscopy in white portland cement hydration: long-term study at room temperature.* Journal of Raman Spectroscopy 37, 555-561.
[40] Jehlička J., Vitek P., Edwards H.G.M., Heagraves M., Čapoun T., **2009**. *Application of portable Raman instruments for fast and non-destructive detection of minerals on outcrops.* Spectrochimica Acta, Part A 73, 410-419.

have allowed expanding the benefits of this technique in small and convenient equipments for analyses on site. Although the resolution of the portable Raman spectrometers is lower than those designed for the laboratory, nowadays portable and laboratory equipments are considered to be comparable and used in a wide variety of fields of interest[41-44].

However, very few works have deal with the study of beachrock outcrops through Raman spectroscopy[46-48]. Previous research carried out in Azkorri beach and Tunelboka cove, evidenced its usefulness in ascertaining the main compositional characteristics not only of cements but also of the trapped materials of beachrock outcrops[40]. Nevertheless, to our knowledge, *in situ* analyses have never been performed over beachrock deposits. Also, there is a lack of knowledge about the possible interactions that the cemented materials might have with different environmental factors, like those affecting in the Arrigunaga beach; the urban-industrial atmosphere and/or seawater.

Thus, this section describes *in situ* and laboratory Raman spectroscopic examinations carried out in beachrock outcrops of Arrigunaga beach (see Figure 3.2 in Chapter 3) not only to gather information about the main constituents of the deposits and their possible weathering compounds, but also, to study the viability of the field study through Raman spectroscopy.

[41] Sharma S.K., Lucey P.G., Ghosh M., Hubble H.W., Horton K.A., **2003**. *Stand-off Raman spectroscopic detection of minerals on planetary surfaces*. Spectrochimica Acta Part A 59, 2391-2407.
[42] Colomban P., **2012**. *The on-site/remote Raman analysis with mobile instruments: a review of drawbacks and success in cultural heritage studies and other associated fields.* Journal of Raman Spectroscopy 43, 1529-1535.
[43] Aramendia J., Gomez-Nubla L., Castro K., Martinez-Arkarazo I., Vega D., Sanz López de Heredia A., García Ibáñez de Opakua A., Madariaga J. M., **2012**. *Portable Raman study on the conservation state of four CorTen steel-based sculptures by Eduardo Chillida impacted by urban atmospheres*. Journal of Raman Spectroscopy 23, 1111-1117.
[44] Gómez-Laserna O., Olazabal M.A., Morillas H., Prieto-Taboada N., Martinez-Arkarazo I., Arana G., Madariaga J.M., **2013**. *In-situ spectroscopic assessment of the conservation state of building materials from a Palace house affected by infiltration water.* Journal of Raman Spectroscopy 44, 1277-1284.
[45] Veneranda M., Irazola M., Pitarch A., Olivares M., Iturregui A., Castro K., Madariaga J.M., **2014**. *In-situ and laboratory Raman analysis in the field of cultural heritage: the case of a mural painting*. Journal of Raman Spectroscopy 45, 228-237.
[46] Bernier P., Guidi J., Böttcher M.E, **1997**. *Coastal progradation and very early diagenesis of ultramafic sands as a result of rubble discharge from asbestos excavations (northern Corsica, western Mediterranean).* Marine Geology 144, 163-175.
[47] Arrieta N., Goienaga N., Martínez-Arkarazo I., Murelaga X., Baceta J.I., Sarmiento A., Madariaga J.M., **2011**. *Beachrock formation in temperate coastlines: Examples in sand-gravel beaches adjacent to the Nerbioi-Ibaizabal Estuary (Bilbao, Bay of Biscay, North of Spain)*. Spectrochimica Acta Part A 80, 55-65.
[48] Iturregui A., Arrieta N., Murelaga X., Baceta J.I., Olazabal M.A., Martínez-Arkarazo I., Madariaga J.M., **2014**. *The relevance of the analytical methodology in the geochemical study of beachrock outcrops: Arrigunaga Beach inside the Nerbioi-Ibaizabal estuary (Getxo, Basque Country)*. Analytical Methods 6, 8247-8257.

4.2.1 *In situ* Raman spectroscopic analysis

At first, an attempt was made to determine the composition of the cements, but although aragonite was identified (with characteristic Raman bands at 151, 704 and 1085 cm^{-1}), it was not possible to ensure at naked eye if the laser beam was focused on the cement or, in contrast, on other grains such as shell fragments. The work of N. Arrieta et al. demonstrated that the aragonite of the cement and the aragonite coming from a gastropod shell can be easily distinguished by Raman spectroscopy basing on the *β*-carotene bands of the shell[49]. However, in this case the *in situ* aragonite spectra obtained were not well resolved enough to make that differentiation. Thus, the *in situ* analyses aimed mainly to identify the composites of the slag and some of the mineral phases identified are detailed in Table 4.6.

Table 4.6. Summary of the compounds detected *in situ* by Raman spectroscopy.

Compound	Formula	*In situ* Raman bands (cm^{-1})
Amorphous carbon	C	1300br, 1550br
Quartz	SiO_2	207*m, 357*w, 395*vw, 464m, 700*vw, 1158*vw
Hematite	α-Fe_2O_3	226*vw, 298m, 410w, 499vw, 612br, 1311*br
Cristobalite	SiO_2	231s, 414s
Tephroite	Mn_2SiO_4	809m, 839m
Rhodonite	$MnSiO_3$	258*m, 332w, 366w, 680vs, 974*w, 993*w
Labradorite	$(Ca,Na)(Si,Al)_4O_8$	275br, 485sh, 504m, 560*m, 777*br
C-S-H	$Ca_3Si_2O_7 \cdot 3H_2O$	665w, 1072vw
Gypsum	$CaSO_4 \cdot 2H_2O$	414*m, 492*m, 617*m, 670*w, 1006w, 1134*m
Portlandite	$Ca(OH)_2$	357s

*Raman bands detected in the laboratory
vw: very weak, w:weak, m:medium, s:strong, sh:shoulder, br: broad

Among the analysed slag, hematite (α-Fe_2O_3) was very common, together with other phases such as amorphous carbon (C) or quartz (SiO_2) (see spectrum 1 in Figure 4.8). The hematite was identified through its main characteristic Raman bands at 298, 410 and 612 cm^{-1}. The amorphous carbon presented its main features at 1300 an 1550 cm^{-1}, while quartz was discernible through the main Raman band at 464 cm^{-1}.

[49] Arrieta N., Goienaga N., Martínez-Arkarazo I., Murelaga X., Baceta J.I., Sarmiento A., Madariaga J.M., **2011**. *Beachrock formation in temperate coastlines: Examples in sand-gravel beaches adjacent to the Nerbioi-Ibaizabal Estuary (Bilbao, Bay of Biscay, North of Spain)*. Spectrochimica Acta Part A 80, 55-65.

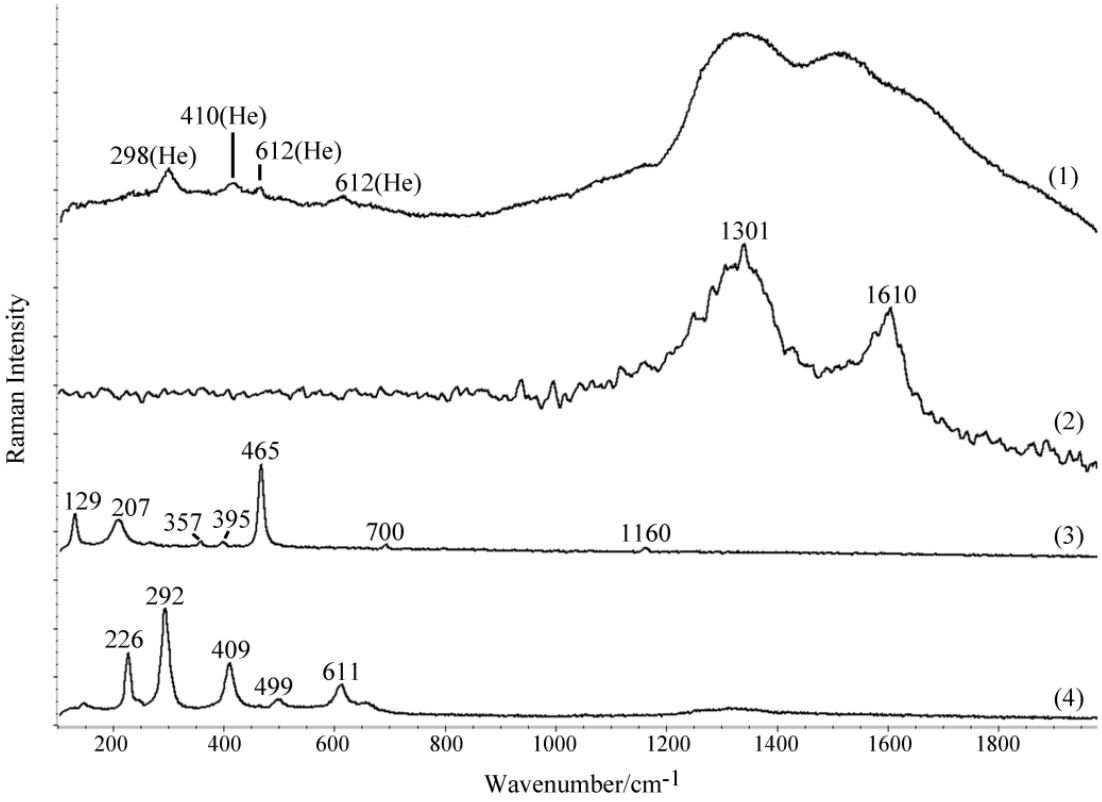

Figure 4.8. 1) *In situ* spectrum of hematite (He), quartz (Q) and amorphous carbon. Laboratory spectra of 2) amorphous carbon, 3) quartz and 4) hematite.

Some slag were composed of a high temperature quartz polymorph, more specifically the cristobalite (SiO_2) with Raman bands at 231 and 414 cm^{-1}, along with tephroite (Mn_2SiO_4) with characteristic Raman bands at 809 and 839 cm^{-1} (see spectrum 1 in Figure 4.9). Both compounds have been reported as constituents of slag derived from steelmaking industry[50]. Indeed, cristobalite is the second most common crystalline form of silica but its existence in nature is quite rare. Besides, tephroite is a manganese silicate mineral included in the olivine group and it can be a refractory material from blast furnace structures[51].

[50] Gomez-Nubla L., Aramendia J., Fdez-Ortiz de Vallejuelo S., Castro K. and Madariaga J.M., **2013**. *From Portable to SCA Raman devices to characterize harmful compounds contained in used black slag produced in Electric Arc Furnace of steel industry*. Journal of Raman Spectroscopy 44, 1163-1171.
[51] Hubble D.H., **1999.** *Steel Plant Refractories*. In: Wakelin D.A. (Ed.), *The Making, Shaping, and Treating of Steel: Ironmaking volume.*The AISE Steel Foundation, Pittsburgh, pp.161-228.

The spectra obtained in the same slag indicate also the presence of rhodonite ($MnSiO_3$), a Mn-rich silicate belonging to the pyroxenoid group. The characteristic bands of this mineral phase can slightly vary conditioned through the substitutions of Mn by Ca, Mg or Fe^{2+}. However, the strong band at 680 cm^{-1} and two lower peaks at 332 and 366 cm^{-1}, correspond to the ones reported in the literature[52]. Other weaker bands are also mentioned in the low wavenumber region, but that area is usually considered quite complex and in this case it would also be difficult to decipher due to the signal of the cristobalite.

The spectrum (1) shown in Figure 4.9 is an example of the well resolved Raman spectrum that can be obtained *in situ* with the portable instrument, indicating clearly the simultaneous presence of three different mineral phases.

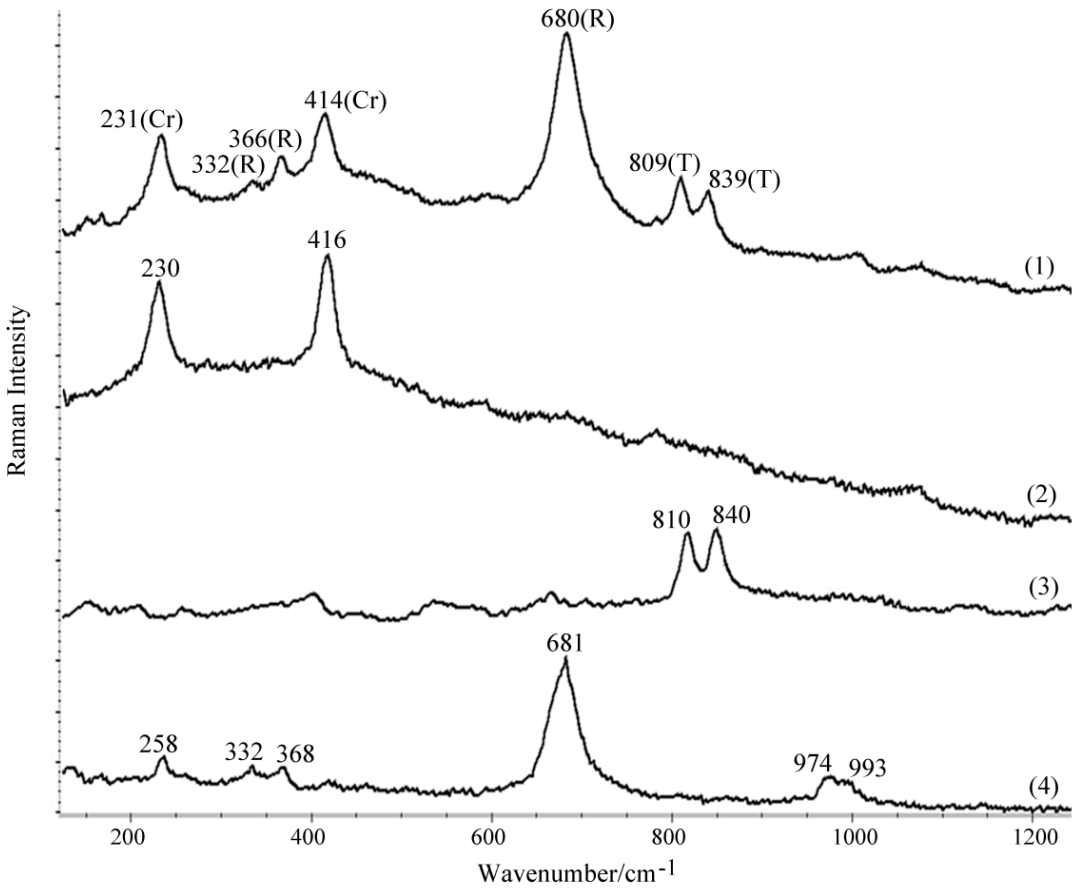

Figure 4.9. 1) *In situ* spectrum of cristobalite (Cr), tephroite (T) and rhodonite (R). Laboratory spectra of 2) cristobalite, 3) tephroite and 4) rhodonite.

[52] Mills S.J., Frost R.L., Kloprogge J.T., Weier M.L., **2005**. *Raman spectroscopy of the mineral rhodonite.* Spectrochimica Acta Part A 62, 171-175.

Other slag do not show such a mixture of minerals, and they can be mainly composed of feldspars such as labradorite $(Ca,Na)(Si,Al)_4O_8$, which is considered an intermediate member between albite ($NaAlSi_3O_8$) and anorthite ($CaAl_2Si_2O_8$) in the plagioclase group[53]. Labradorite was identified thanks to its Raman peaks at 275, 485 and 504 cm^{-1} (see spectrum 1 in Figure 4.10). At higher wavenumbers, some other bands were found around 1290 and 1460 cm^{-1}, which could be assigned to the matrix effects of black slag when excited with the 785 nm laser[54]. Indeed, some authors state that the bands in that spectral region might be a result of the luminescence emission phenomenon triggered by the presence of siliceous materials containing rare earth elements[55].

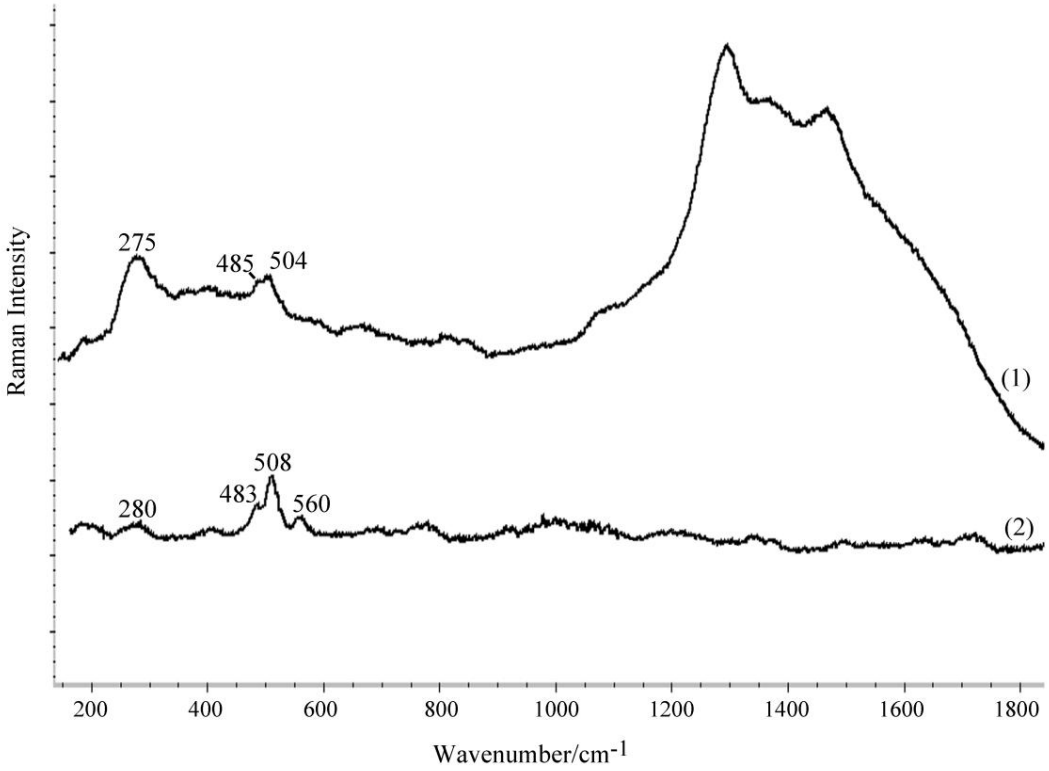

Figure 4.10. 1) *In situ* spectrum of labradorite and 2) the laboratory result.

[53] Harker A., **2011**.*The Natural History of Igneous Rocks*. Cambridge University Press, Cambridge, 408 pp.
[54] Gomez-Nubla L., Aramendia J., Fdez-Ortiz de Vallejuelo S., Castro K. and Madariaga J.M., **2013**. *From Portable to SCA Raman devices to characterize harmful compounds contained in used black slag produced in Electric Arc Furnace of steel industry*. Journal of Raman Spectroscopy 44, 1163-1171.
[55] Lenz C., Talla D., Ruschel K., Škoda R., Götze J., Nasdala L., **2013**. *Factors affecting the Nd^{3+} (REE^{3+}) luminescence of minerals.* Mineralogy and Petrolology 107, 415-428.

The mentioned constituents include mixtures of oxides, silica polymorphs, diverse silicates and eventually, a variety of compounds related with the iron and steel making industry. Many of them can be refractory materials, denoting that they are chemically stable and resistant to high temperatures and pressures, thus, they can be considered as original constituents. Nevertheless, some other compounds were detected, likely to be formed upon the environmental exposure of the slag.

To better understand that fact, some particularities found along the trapped materials have to be mentioned. Indeed, it is remarkable the colour differences that some slag had at first glance, possibly reflecting the influence of atmospheric and/or seawater weathering processes. For instance, Figure 4.11 shows an example of a slag where in the darkest area hematite was identified, likely to be a original compound, together with portlandite ($Ca(OH)_2$) and tricalcium silicate hydrate (C-S-H), phases commonly related to the hydration of cementitious materials[56].

The presence of portlandite is deduced from the band at 357 cm^{-1}, usually attributed to the bending vibration mode[57]. Regarding the C-S-H, Bensted et al.[58] referred to this phase also with the formula $Ca_3Si_2O_7 \cdot 3H_2O$, only as an approximation because this poorly ordered phase is non stoichometric and in addition, different kinds of C-S-H can be formed as a result of the hydration. In any case, the band at 665 cm^{-1} showed in Figure 4.11 (see spectrum 1), coincides with the characteristic Si-O-Si bending region described in the literature for this phase. In addition, the 1072 cm^{-1} band might support the presence of C-S-H, as it corresponds to the symmetric C-O stretching of carbonates impurities possibly associated to C-S-H[59,60]. Finally, the band at 785 cm^{-1} is usually related with the Si-O-Si stretching mode, evidencing the existence of a compound of siliceous nature[61].

[56] Prusinski J.R., **2006**. *Slag as cementitious materials.* In: Lamond J.F. and Pielert J.H. (Eds), *Significance of Tests and Properties of Concrete and Concrete-making Material.* ASTM International, Pennsylvania, USA, pp. 512-532.
[57] Chollet M., Horgnies M., **2011***. Analyses of the surfaces of concrete by Raman and FT-IR spectroscopies: comparative study of hardened samples after demoulding and after organic post-treatment.* Surface and Interface Analysis 43, 714-725.
[58] Bensted J. ***2002****. Hydration of Portland cement.* In: Ghosh S.N. and Saketharaman J. (Eds.), *Advances in Cement Technology: Chemistry, Manufacture and Testing.* Tech Books International, New Delhi, India, pp. 31-86.
[59] Kirkpatrick R. J., Yarger J. L., Macmillan P. F., Yu P., Cong X., **1997**. *Raman spectroscopy of C-S-H, Tobermorite and Jennite.* Advanced Cement Based Materials 5, 93-99.
[60] Tarrida M., Madon M., Le Rolland B., Colombet P., **1995**. *An in-situ Raman spectroscopy study of the hydration of tricalcium silicate*.Advanced Cement Based Materials *2*, 15-20.
[61] Davidson G., **2000**. *Spectroscopic Properties of Inorganic and Organometallic Compounds*. Royal Society of Chemistry, Cambridge, 382 pp.

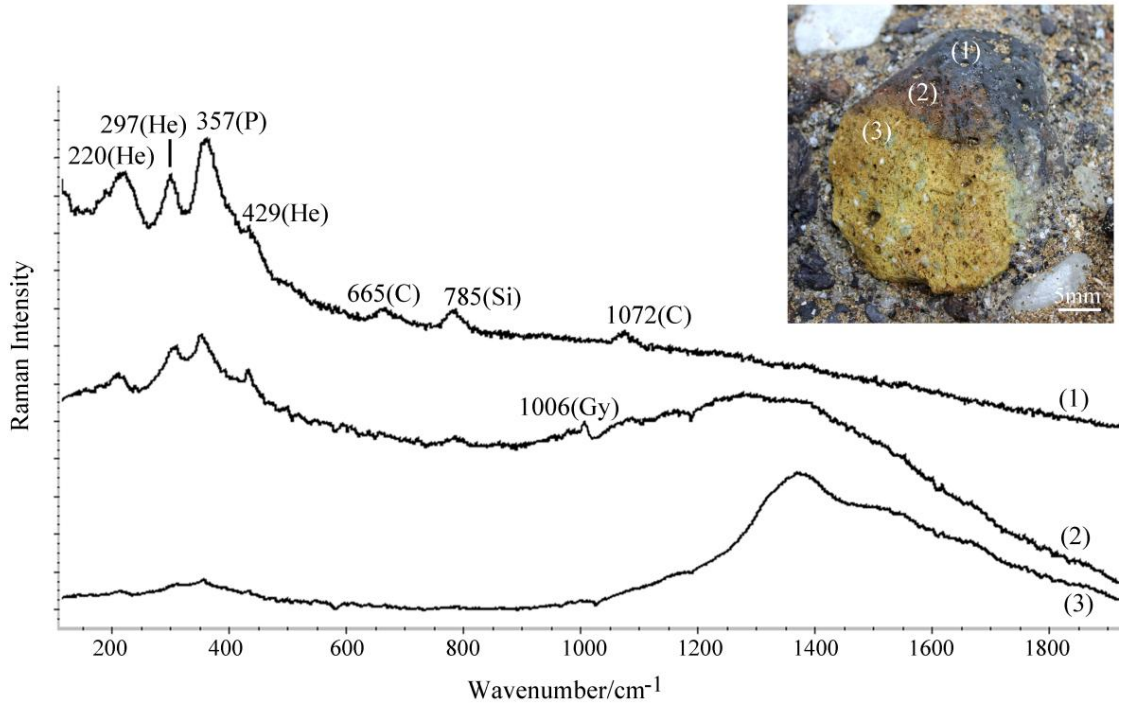

Figure 4.11. Colour changes appreciated *in situ* in some slag: 1) a black area composed of hematite (He), portlandite (P) and C-S-H (C), where the Si-O-Si stretching mode (S) is also present; 2) a reddish area where similar compounds are found as well as gypsum (Gy); 3) yellowish area where other signs derived from the matrix of the slag are mostly observed.

In a reddish colour of that slag, hematite and portlandite could be discerned again. However, the main difference with the previously described section is that instead of the C-S-H, gypsum ($CaSO_4 \cdot 2H_2O$) was detected through its main Raman peak at 1006 cm^{-1} (see spectrum 2 in Figure 4.12). This compound can also be considered a hydration product, but taking into account the phases mentioned so far, it might be also a sulphate attack product. For example, it is believed that materials analogous to slag containing portlandite and C-S-H, when exposed to a sulphate rich solution, like seawater, can trigger the formation of gypsum[62]. Another possible sulphate attack product is the ettringite ($3CaO \cdot Al_2O_3 \cdot 3CaSO_4 \cdot 32H_2O$) and occasionally, some weak bands were also found around 980 and 1087 cm^{-1} probably representing that compound, but the spectra were not well resolved enough to assure its presence.

[62] Odler I., **2003**. *Special Inorganic Cements*. E&FN Spon, London, 416 pp.

Finally, a yellowish area was recognisable and there, although signs of hematite and portlandite apparently remain, the most remarkable bands were found in the 1370-1620 cm^{-1} region (see spectrum 3 in Figure 4.11), that might derive from the matrix of the slag through the luminescence emission of rare earth elements, as mentioned above[63,64].

Apart from the screening performed from the compositional point of view, this analysis allowed to have an idea of the kind of the secondary compounds that could be found among the slag embedded in the analysed beachrocks. For instance, portlandite and C-S-H could be a result of hydration mechanisms, while the attack of SO_2 acid gases in high humidity conditions could explain also the formation of the gypsum compound, triggered by seawater or even other sulphates coming from the industrial activity occurring nearby.

The fact of having performed the analyses on site, might have played a key role in these findings, because they are phases prone to react with diverse environmental agents. That is the case, for instance, of portlandite, which can react with CO_2 promoting the formation of more stable compounds. The overall reactions that explain its formation and transformation can be seen in Eqs. 4.1 and 4.2:

$$CaO_{(s)} + H_2O_{(l)} \rightarrow Ca(OH)_{2(aq)} \qquad \text{(Eq. 4.1)}$$

$$Ca(OH)_{2(s)}\ \text{(portlandite)} + CO_{2(g)} \rightarrow CaCO_{3(s)} + H_2O_{(l)} \qquad \text{(Eq. 4.2)}$$

Regarding C-S-H, a recent work refers to the reaction of CO_2 with this phase[65], but in the particular atmosphere around the Arrigunaga beach, where sulphuric acid aerosols can be present due to the industrial activity, other reaction that transforms the C-S-H could also be considered, like the (Eq. 4.4) explained below[65-68].

[63] Gomez-Nubla L., Aramendia J., Fdez-Ortiz de Vallejuelo S., Castro K. and Madariaga J.M., **2013**. *From Portable to SCA Raman devices to characterize harmful compounds contained in used black slag produced in Electric Arc Furnace of steel industry*. Journal of Raman Spectroscopy 44, 1163-1171.
[64] Lenz C., Talla D., Ruschel K., Škoda R., Götze J., Nasdala L., **2013**. *Factors affecting the Nd^{3+} (REE^{3+}) luminescence of minerals.* Mineralogy and Petrolology 107, 415-428.
[65] Pan S-Y., Chang E.E., Chiang P-C., **2012**. *CO_2 Capture by accelerated carbonation of alkaline wastes: a review on its principles and applications*. Aerosol and Air Quality Research 12, 770-791.
[66] Komljenovic M., Baščarevic Z., Markanovic N., Nikolic V., **2013**. *External sulfate attack on alkali-activated slag*. Construction and Building Materials 49, 31-39.
[67] Bellmann F., Stark J., **2007**. *Prevention of thaumasite formation in concrete exposed to sulphate attack*. Cement and Concrete Research 37, 1215-1222.
[68] De Weerdt K., Justnes H., **2015**. *The effect of seawater on the phase assemblage of hydrated cement phase*. Cement and Concrete Composites 55, 215-222.

The presence of intermediate compounds like portlandite and C-S-H, that might be only detected when performing *in situ* analysis, exemplifies the kind of interactions that can occur between the trapped materials and the surrounding environment, either atmosphere and/or seawaters, denoting that the studied beachrock outcrops can be a dynamic system. Indeed, especially in this area the beachrock can be exposed to variable conditions regularly, for instance due to daily humidity changes derived from the semidiurnal tidal regime. Although further studies would be needed to infer the long-term implications of the transformations occurring in the slag, these results give some clues about the possible evolution and deterioration of the trapped materials in such a sulphate rich environment.

4.2.2 Laboratory Raman spectroscopic analysis

Many Raman spectra acquired by the laboratory instrument barely varied from the spectra obtained *in situ*. An example is shown in Figure 4.10, where an *in situ* spectrum showing the cristobalite and tephroite bands (spectrum 1 in Figure 4.9) is compared with the monocomponent spectrum of cristobalite (spectrum 2 in Figure 4.9) and tephroite (spectrum 3 in Figure 4.9) obtained in the laboratory. *In situ* spectra were clarifying enough to assign each spectrum to the identified compounds, however, in some cases better resolved spectra were obtained in the laboratory (see Table 4.6). For example, the rest of the characteristic bands were determined for the hematite at 226 and 499 cm^{-1} (spectrum 4 in Figure 4.8). Most of the laboratory quartz spectra were similar to the ones obtained *in situ*, nevertheless, not only the main band at 465 cm^{-1}, but weaker bands at 207, 356, 395, 700 and 1160 cm^{-1} were also observed off site (spectrum 3 in Figure 4.8). In the case of rhodonite, the laboratory performance allowed to decipher characteristic low region wavenumbers, like 258 cm^{-1}, as well as the higher region at 974 and 993 cm^{-1} (spectrum 4 in Figure 4.9), coinciding with more bands reported in the literature[69]. Another example to be mentioned is the identification of labradorite by the laboratory instrument (spectrum 2 in Figure 4.10), that allowed to recognise slightly more features associated with this feldspar providing a spectrum with the characteristic peaks at 280, 483, 508 and 560 cm^{-1}.

Other mineral phases were only identified in the laboratory analyses (see Table 4.7) possibly owing to the more accurate analysis facilitated by a smaller spot size and the possibility of microscopically observing the areas of interest. In the case of the ferruginous compounds, besides hematite other iron oxyhydroxides were commonly

[69] Mills S.J., Frost R.L., Kloprogge J.T., Weier M.L., **2005**. *Raman spectroscopy of the mineral rhodonite.* Spectrochimica Acta Part A *62*, 171-175.

found within the beachrock. For instance, the anhydrous form such as lepidocrocite (γ-FeOOH, with main Raman bands at 249 and 380 cm^{-1}) and hydrated forms like limonite ($FeO(OH)\cdot nH_2O$, with Raman bands at 246, 300, 394, 477 and 550 cm^{-1}) (Figure 4.12A), were among the most abundant components found composing the waste cemented materials. These mineral phases were also detected in other previous works related with adjacent beachrocks where slag coming from the same source, are also trapped into the cemented framework[70].

Table 4.7. Summary of the compounds found in the laboratory.

Compound	Formula	Laboratory Raman bands
Lepidocrocite	γ-FeOOH	249s, 380s
Limonite	FeO(OH)·nH2O	246w, 300m, 394vs, 477vw, 550w
Anatase	TiO_2	145s, 390w, 508vw, 632vw
Arsenopyrite	FeAsS	217s, 247w, 435w, 471s
Fayalite	Fe_2SiO_4	813s, 839sh
Augite	$(Ca,Na)(Mg,Fe,Al)(Si,Al)_2O_6$	664s, 1004m
Thaumasite	$3CaO\cdot SiO_2\cdot CO_2\cdot SO_3\cdot 15H_2O$	208m, 418w, 445w, 655m, 987vs,

vw: very weak, w:weak, m:medium, s:strong,vs: very strong, sh: shoulder

In addition, anatase (TiO_2) was identified in the analyses carried out in the laboratory, thanks to its characteristic intense Raman band at 145 cm^{-1} and broad weaker bands at 390, 508, 632 cm^{-1}, which are smaller than the consulted database probably because of the simultaneous detection of hematite and quartz (Figure 4.12B). It is remarkable also that arsenopyrite (FeAsS) was recognised (Figure 4.12B) by its Raman bands at 217, 247, 435, 471 cm^{-1} (it was found together with probably representing the carbonate that is acting as a cement). Its presence is not surprising, as this refractory mineral has been also found composing, for example, wastes related with other mining areas in the Basque Country[71] or in estuarine sediments contaminated with historical mining activity in Cornwall[72].

[70] Arrieta N., Goienaga N., Martínez-Arkarazo I., Murelaga X., Baceta J.I., Sarmiento A., Madariaga J.M., **2011**. *Beachrock formation in temperate coastlines: Examples in sand-gravel beaches adjacent to the Nerbioi-Ibaizabal Estuary (Bilbao, Bay of Biscay, North of Spain)*. Spectrochimica Acta Part A 80, 55-65.
[71] Marqués M.J., Martínez-Conde E., Rovira J.V., Ordoñez S., **2001**. *Heavy metals pollution of aquatic ecosystems in the vicinity of a recently closed underground lead-zinc mine (Basque Country, Spain)*. Environmental Geology 40, 1125-1137.
[72] Rollinson G.K., Pirrie D., Power M.R., Cundy A., Camm G.S., **2007**. *Geochemical and mineralogical record of historical mining, Hayle estuary, Cornwall, UK*. Proceedings of the Ussher Society 11, 326-337.

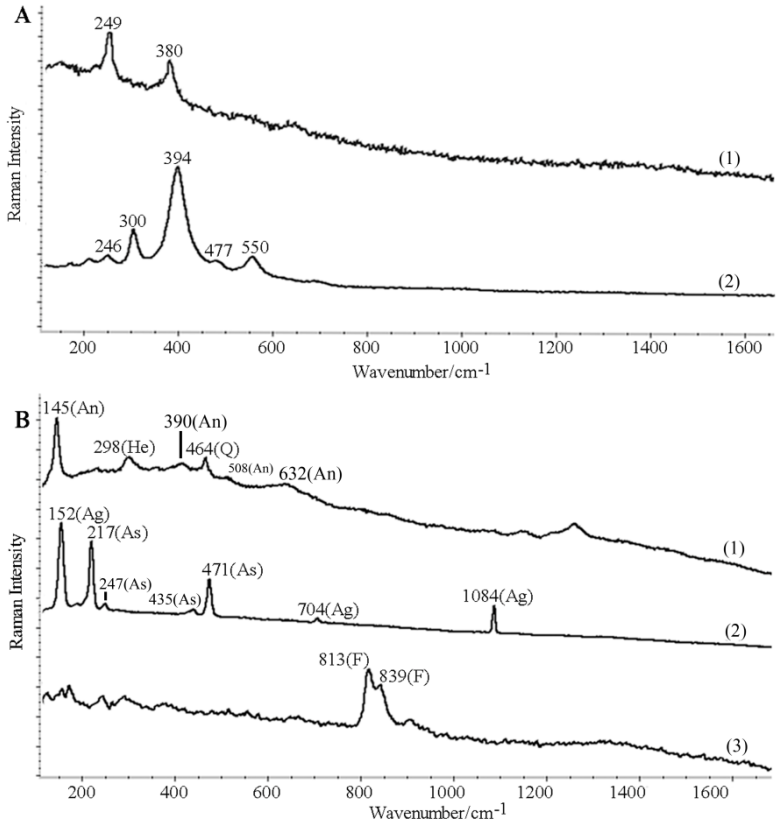

Figure 4.12. Raman spectra of the compounds recognised only in the laboratory: A) iron oxyhydroxides like 1) lepidocrocite and 2) limonite; B) spectrum 1) showing anatase (An), together with hematite (He) and quartz (Q), spectrum 2) represents arsenopyrite (As), together with aragonite (Ag), and spectrum 3) the fayalite (F).

Regarding silicates, the presence of fayalite (Fe_2SiO_4) was also evidenced through a main peak at 813 cm^{-1} and the characteristic shoulder at 839 cm^{-1} (Figure 4.12B). Fayalite is considered in the olivine group of minerals, together with the previously mentioned tephroite. Indeed, the Raman spectra of both components showed the distinctive double peak of olivines around 801-854 cm^{-1}, attributed to SiO_4 internal stretching modes. However, slight variations can be discerned in bands positions and relative intensities of fayalite and tephroite Raman spectra, possibly due to different cation substitutions, or formation conditions (i.e. pressure and temperature), as well as crystallographic orientations[73,74]. As in the case of tephroite, fayalite can be commonly found composing slag, and even in refractory linings related with copper metallurgy[75].

[73] Chopelas A., **1991**. *Single crystal Raman spectra of forsterite, fayalite and monticellite.* American Mineralogist 76, 1101-1109.
[74] Ishibashi H., Arakawa M., Ohi S., Yamamoto J., Miyake A., Kagi H., **2008**. *Relationship between Raman spectral pattern and crystallographic orientation of a rock-forming mineral: a case study of $Fo_{89}Fa_{11}$ olivine.* Journal of Raman Spectroscopy 39, 1653-1659.
[75] Malfliet A., Lotfian S., Scheunis L., Petkov V., Pandelaers L., Jones P.T., Blanpain B., **2014**. *Degradation mechanisms and use of refractory linings in copper production processes: A critical review*. Journal of the European Ceramic Society 34, 849-876.

In the micro-pores of some slag, gypsum (also identified *in situ*) was occasionally found, certainly recognised through 414, 492, 617, 670, 1006, 1134 cm^{-1} Raman bands (Figure 4.13A). In this case, more bands than in the *in situ* Raman analyses were obtained in the laboratory, because gypsum crystals were found in a pore of the collected sample, as shown in Figure 4.13A. Furthermore, in the pore walls where those crystals were found, the whitish area shown in that figure, contains calcium carbonate ($CaCO_3$, distinguished by its main Raman band at 1084 cm^{-1}) and augite $(Ca,Na)(Mg,Fe,Al)(Si,Al)_2O_6$) with Raman bands at 664 and 1004 cm^{-1}.

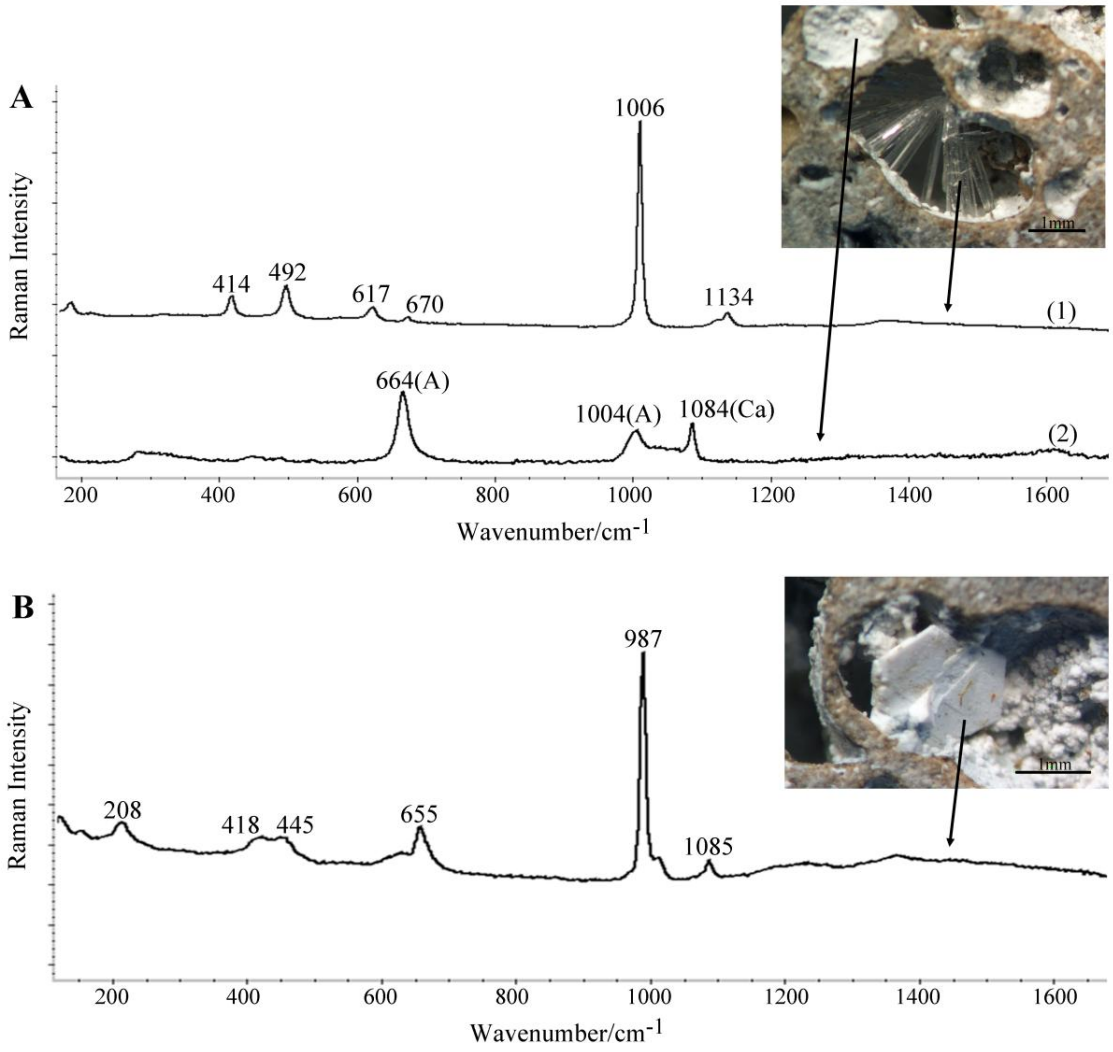

Figure 4.13. Other compounds found in the micropores of the slag through the laboratory analyses. Detailed images of the areas where the spectra were acquired are also shown: A) Raman spectrum of gypsum (Gy) in spectrum (1), as well as, augite (A) and carbonates (C) in spectrum (2); B) Raman spectrum of the thaumasite.

Additionally, thaumasite ($3CaO{\cdot}SiO_2{\cdot}CO_2{\cdot}SO_3{\cdot}15H_2O$, with its main characteristic Raman bands at 655 and 987 cm^{-1}, an weaker bands at 208, 418, 445 and 1085 cm^{-1}) was also identified in the micropores of the slag (Figure 4.13B). Thaumasite is closely related with ettringite but they can be mainly distinguished by Raman spectroscopy thanks to a distinctive peak around 655 cm^{-1} ascribed to Si-O stretching modes[76]. Although some authors evidenced that both compounds can coexist, it has been also proposed that ettringite might be a precursor of thaumasite formation, a fact supported by their similar structure[77].

Thaumasite is commonly found as a result of sulphate attack in historical building, masonry mortar and concrete located in marine environments[78]. Furthermore, it is generally assumed that the formation of thaumasite requires the presence of calcium silicates (very abundant in the slag waste materials), sulphates (that in our case could come from gypsum or the seawater), and carbonate ions, as well as a wet and cold environment[79,80]. Hence, these conditions might have been achieved within the pores of the slag giving rise to the formation of thaumasite as it is shown in Eq. 4.3, the same as reported in reference[77]:

$$3Ca^{2+} + SiO_3^{2-} + CO_3^{2-} + SO_4^{2-} + 15H_2O \rightarrow 3CaO{\cdot}SiO_2{\cdot}CO_2{\cdot}SO_3{\cdot}15H_2O \quad \text{(Eq. 4.3)}$$

But this other decaying reaction (Eq. 4.4), which is thermodynamically favoured, could also occur triggered by the attack of carbonic and sulphuric acid aerosols on the C-S-H compound:

$$Ca_3Si_2O_7{\cdot}3H_2O + H_2CO_3 + H_2SO_4 + 10H_2O \rightarrow 3CaO{\cdot}SiO_2{\cdot}CO_2{\cdot}SO_3{\cdot}15H_2O + SiO_2 \quad \text{(Eq. 4.4)}$$

That could explain the inestability of the C-S-H compounds and their possible transformation to thaumasite in the particular environment of the beachrocks in the Arrigunaga beach, supporting the hypothesis arisen from the *in situ* analyses about the formation of secondary compounds.

[76] Brough A.R., Atkinson A., **2001**. *Micro-Raman spectroscopy of thaumasite*. Cement and Concrete Research 31, 421-424.
[77] Pajares I., Martínez-Ramírez S., Blanco-Varela M.T., **2003**. *Evolution of ettringite in presence of carbonate and silicate ions*. Cement and Concrete Composites 25, 861-865.
[78] Irassar E.F., Bonavetti B.L., González M., **2003**. *Microstructural study of sulfate attack on ordinary and limestone Portland cements at ambient temperature*. Cement and Concrete Research 33, 31-41.
[79] Marchand J., Odler I., Skalny J.P., **2003**. *Sulfate attack on Concrete.* Spon Press, London, 232 pp.
[80] Rahman M.M., Bassuoni M.T., **2014**. *Thaumasite sulfate attack on concrete: Mechanisms, influential factors and mitigation*. Construction and Building Materials 73, 652-662.

4.2.3 General remarks of the in situ and laboratory Raman spectroscopic study

In the studied temperate beachrocks, special attention was paid to the high amount of slag remains found trapped within their structure. The major constituents over the slag revealed the presence of various forms of iron oxides, Ca, Mn and Fe silicates or sulphides, likely to be related with the historical disposal of wastes coming from the iron and steel making industries operating in the area from the mid 19th century till the late 20th century. Furthermore, many of the materials come in agreement with the compositional features found in an adjacent beachrocks[81]. As in that case, it can be assumed that the materials trapped in the studied beachrock have reached the shoreline after their disposal near the coast, indicating the recent formation of the outcrops.

Although the scoriaceous wastes are trapped into the cemented matrix of the beachrock deposits, *in situ* results denoted that the outcrops can be attacked or eroded by several weathering agents. Thus, considering the exposition of the sedimentary units to the atmosphere (CO_2 and SO_2 acid gases in high humidity conditions for more than half of the year) or the sulphate attack from the seawaters, numerous oxidation-reduction, hydration-dehydration cycles and chemical reactivity between alkaline compounds and acids can take place in such a dynamic system, leading to the generation of some precipitates or degradation products of the slag wastes.

The *in situ* analyses enlightened the identification of the hydration and decayed intermediate products (portlandite, C-S-H and gypsum) that depict the environmental attack that the slag and eventually, the sedimentary forms might be suffering. Those compounds might not have been found in the laboratory examinations, probably because they are prone to react with environmental factors coming from marine aerosols or sulphates coming from the industrial activity still active in the area. Thus, although further analyses would be needed regarding the implications that those transformations can have in the system, the *in situ* results provided essential information to hypothesise the interaction between beachrocks with abounding slag in sulphate rich environments and their possible deterioration.

The spectra obtained in the laboratory supported the information inferred *in situ*. In fact, later stages of hydration and sulphate attack were detected, due to the presence of

[81] Arrieta N., Goienaga N., Martínez-Arkarazo I., Murelaga X., Baceta J.I., Sarmiento A., Madariaga J.M., **2011**. *Beachrock formation in temperate coastlines: Examples in sand-gravel beaches adjacent to the Nerbioi-Ibaizabal Estuary (Bilbao, Bay of Biscay, North of Spain)*. Spectrochimica Acta Part A 80, 55-65.

crystalline gypsum, as well as the thaumasite, a product of a more advanced sulphate attack[82]. These new compounds can be considered as the ageing products of those detected *in situ*. In addition, other compounds were also identified since the smaller spot and the possibility of visualising the points of interest, allowed to delve further into the characterisation of the slag.

Therefore, both analyses provided complementary information. In any case, it should be remarked that *in situ* analyses, innovatively performed to analyse beachrock outcrops, offered the preliminary and sometimes unique clues leading to the conclusions of the study. Thus, this work allowed verifying the feasibility of the *in situ* Raman spectroscopy in the study of beachrock outcrops.

4.3 Conclusions

In view of the outcomes of the analyses explained in this chapter, it can be highlighted that thanks to the described methodologies, the presence of external anthropogenic inputs was recognised and characterised. At first, the procedure based on the grain size fractionation of the samples allowed demonstrating that the grain size distribution of the metals can be a key point in understanding what is behind the deposited structures. Furthermore, Raman spectroscopy, with special emphasis on *in situ* analyses, permitted not only to identify the main constituents of those materials, but also to exemplify the kind of reactions that could happen triggered by the interaction of the beachrocks with the seawater and/or atmosphere.

Overall, it must be remarked that an external input of materials was demonstrated prone to come from the mining and industrial activities occurring nearby. Those composites provide an inherent complexity to the beachrocks outcrops, an intricacy enhanced by the transformations that could happen derived from the interaction with the surrounding environment.

[82] Pajares I., Martínez-Ramírez S., Blanco-Varela M.T., **2003**. *Evolution of ettringite in presence of carbonate and silicate ions*. Cement and Concrete Composites 25, 861-865.

Chapter 5

Metal quantification in beachrock outcrops from Arrigunaga and La Salvaje beach

In this chapter, the metal content of beachrock outcrops from Arrigunaga and La Salvaje beach will be examined. The main interest of this approach steams from the different location of both beaches, as it gives the opportunity of contrasting a site placed inside the Nerbioi-Ibaizabal estuary, sheltered in the Abra Bay (Arrigunaga beach) and an open coast exposed beach, the more distant point where beachrock evidences have been found up to now (La Salvaje beach). The presence of anthropogenic materials has been already characterized in Arrigunaga, but to what extent can be contaminated? Is there any external input retained in outcrops of La Salvaje beach also?

In an attempt to respond to those questions, with regard to the environmental alterations around the estuary of Bilbao, it must be remarked that various studies that investigated the intertidal vegetation to determine the alterations derived from the estuary plume, stated that exists a pollution gradient along that part of the Basque coast; the northwest winds promote the transport of polluted waters eastwards, thus, the estuarine input tends to decrease as waters move away from that contamination source[1-3]. Indeed, usually in those studies Arrigunaga is considered heavily affected by the estuary plume, while areas closer to La Salvaje (such as Azkorri beach), are moderately degraded[3].

However, in front of the open sea beaches, 4 miles away from the coast, exists the slag disposal where hundreds of tons of wastes were dumped during approximately 50 years. Those materials are believed to be mainly composed of Fe, Mn, Pb and Zn and they are considered to be inert, but in any case, what we believe that it can be of utmost importance is that those materials apparently are being dispersed reaching the coastline. In fact, there is a recent concern regarding the blackening of La Salvaje beach due to the iron based particles transported to the beach[4,5].

Regarding the characteristics of beachrock, some other studies have also focused on the contamination retained in this kind of cemented structures, as witnesses of the alteration caused in the system due to diverse human pressures, such as industrial and sewage effluents occurring in southeastern India[6] or the west coast of Algeria[7]. Furthermore, previous studies carried out in beachrocks from Azkorri beach, also demonstrated that this kind of structures can store contaminants coming from the vicinity, derived from the disturbances occurring nearby[8]. So as to keep trying to analyse the components of the beachrocks located along that coast, and taking into

[1] Pagola-Carte S., Saiz-Salinas J.I., **2001**.*Changes in the sublittoral faunal biomass induced by the discharge of a polluted river along the adjacent rocky coast (N. Spain)*.Marine ecology progress series 212, 13-27.
[2] Saiz-Salinas J.I., González-Oreja J.A., **2000**. *Stress in estuarine communities: lessons from the highly-impacted Bilbao estuary (Spain)*.Journal of Aquatic Ecosystem Stress and Recovery 7, 43-55.
[3] Díez I., Secilla A., Santolaria A., Gorostiaga J.M., **1999**. *Phytobenthic intertidal community structure along an environmental pollution gradient*. Marine Pollution Bulletin 38, 463-472.
[4] Borja A., Tueros I., Belzunce M.J., Galparsoro I., Garmendia J.M., Revilla M., Solaun O., Valencia V., **2008**. *Investigative monitoring within the European Water Framework Directive: a coastal blast furnace slag disposal, as an example*. Journal of Environmental Monitoring 10, 453-462.
[5] Tueros I., **2010**. *Bizkaiko Labe Garaien lorratzak Sopelako hondartzetan*. Elhuyar Zientzia eta Teknologia 264, 12-15.
[6] Sahayam J.D., Chandrasekar N., Kumar S.K., Rajamanickam G.V., **2010**. *Distribution of arsenic and mercury in subtropical coastal beachrock, Gulf of Mannar, India*. Journal of Earth System Science 119, 129-135.
[7] Bouchentouf S., Aïnad Tabet D., Ramdani M., **2013**. *Mercury pollution in beachrocks from the Arzew gulf (West of Algeria)*. Travaux de l'Institut Scientifique, Rabat, Série Zoologie 49, 1-5.
[8] Arrieta N., **2014**. *The study of an unusual temperate latitude beachrock formation. Characterization of Azkorri beach and Tunelboka cove locations*. PhD Thesis, University of the Basque Country.

consideration this background information, the metal content of the exposed beachrock has been estimated in Arrigunaga and La Salvaje beach.

In that context, the analysis of heavy metals should be highlighted, as they are one of the main environmental concerns in this estuarine area[9]. Heavy metals are metallic elements that have a high atomic weight and a density at least five times greater than water. Generally, heaviness is interconnected with toxicity, thus, other elements considered as metalloids, such as arsenic, are usually designated as heavy metals due to their potential toxicity[10]. In addition, when analysing heavy metals, with special focus on their distribution and source, chemometric tools such as principal component analyses (PCA) can have a key role in the interpretation of the results. In fact, this multivariate statistical analysis has been widely used in environmental sciences to facilitate an overview of the relevant trends that might be behind the variables of the data set, allowing pattern recognition of the results[11-13].

Hence, the aim of this work consists on the metal quantification of beachrock samples from Arrigunaga and La Salvaje beach, where a sampling strategy based on two distinctive orientations (see transverse and longitudinal sampling in Chapter 3) was performed. That way, the general distribution of the elements along both beaches will be determined, as well as the contamination that the cemented deposits might retain. For that purpose, a microwave assisted acid digestion followed by ICP-MS analyses was performed, complemented with correlation analysis and PCA. It should be mentioned that the Ø<2mm fraction was analysed; because as concluded in Chapter 4, regardless of the accommodation of various elements in certain fractions, metals were found in all the fractions. On the whole, in this case, with the joint analysis of coarser and finer particles, a more comprehensive insight of the metal content of exposed beachrock is sought.

[9] Belzunce M.J., Solaun O., Valencia V., Pérez V., **2004**. *Contaminants in estuarine and coastal waters*. In In: Borja, A., Collins, M. (Eds.), Oceanography and Marine Environment of the Basque Country. Elsevier Oceanography Series, 70. Elsevier, Amsterdam, pp. 233–251.

[10] Tchounwou P.B., Yedjou C.G., Patlolla A.K., Sutton D.J., **2012**. *Heavy Metal Toxicity and the Environment*.In: Luch A. (Ed.) Molecular, environmental and clinical toxicology.Experientia Supplementum 101, Vol. I. Springer, Basel, pp. 133-165.

[11] Idris A. M., **2008**. *Combining multivariate analysis and geochemical approaches for assessing heavy metal level in sediments from Sudanese harbors along the Red Sea coast*. Microchemical Journal 90. 159-163.

[12] Carrero J.A., Goienaga N., Barrutia O., Artetxe U., Arana G., Hernandez A., Becerril J.M., Madariaga J.M., **2010**.*Diagnosing the Impact of Traffic on Roadside Soils Through Chemometric Analysis on the Concentrations of More Than 60 Metals Measured by ICP/MS*. In: Rauch S, Morrison GM, Monzon A (Eds.) Highway and Urban Environment. Springer, Dordrecht, pp 329-336.

[13] Landajo A., Arana G., de Diego A., Etxebarria N., Zuloaga O., Amouroux D., **2004**. *Analysis of heavy metal distribution in superficial estuarine sediments (estuary of Bilbao, Basque Country) by open-focused microwave-assisted extraction and ICP-OES*. Chemosphere 56, 1033–1041.

5.1 Metal quantification in Arrigunaga beach

5.1.1 Determination of the elemental content

In this section, numerical data of the concentration values found in the transverse and the longitudinal sampling will be exposed. The results of the elemental quantification for the transverse transect are summarised in Table 5.1. These samples are located in the northernmost part of the beach (see Figure 3.3 in Chapter 3). That zone seems to be specially supplied by materials from the adjacent erodible cliff. Furthermore, the obliquity of the waves that reach the area of the beach might have triggered a greater sediment accumulation there previously to its regeneration.

Table 5.1a. Mean concentration (g/kg) and RSD (%) values of the major elements measured in the samples belonging to the transverse transect of Arrigunaga beach.

	ART1		ART2		ART3		ART4		ART5	
	Mean	**RSD**	**Mean**	**RSD**	**Mean**	**RSD**	**Mean**	**RSD**	**Mean**	**RSD**
Ca	171	8	188	14	116	9	130	7	154	7
Al	30	9	21.45	0.1	17	5	18	7	26	28
Mg	13	3	14	25	11	5	12	7	13	17
Fe	10	12	11	23	11	17	15	7	11	20
Mn	5	3	5	20	3.6	4	4.4	7	7	16
K	3	10	2.6	9	3	24	2.7	6	3	13
Na	3	9	3	20	2.5	7	2.6	8	3	13

Table 5.1b. Mean concentration (mg/kg) and RSD (%) values of the minor elements measured in the samples belonging to the transverse transect of Arrigunaga beach.

	ART1		ART2		ART3		ART4		ART5	
	Mean	**RSD**	**Mean**	**RSD**	**Mean**	**RSD**	**Mean**	**RSD**	**Mean**	**RSD**
Sr	1 804	15	2 236	5	1 791	12	1 805	4	2 639	1
Ti	598	20	436	11	322	3	349	0.4	668	2
Ba	456	13	375	6	368	25	405	9	477	1
Zn	128	33	81	25	103	18	102	21	64	3
Pb	15	16	20	7	17	21	18.9	2	19.7	4
Cu	14	13	22	9	20	14	14.2	1	15.5	3
V	14	19	12.8	7	11	10	11.8	4	23.9	1
Cr	9	19	9	15	8	13	7.1	4	18.3	1
As	6.0	16	5.1	3	11	12	10.2	5	4.5	2
Ni	4.3	18	4.5	7	11.3	7.9	9.6	4	4.8	5
Se	4.0	23	2.8	12	3.53	1	3.6	6	3.9	15
Co	1.1	27	1.3	13	1.4	14	1.4	13	1.36	3
Sn	0.9	13	3.9	6	2.82	31	2.9	26	4.0	3
Mo	0.67	11	0.70	6	0.7	19	0.65	13	0.69	3
Sb	0.08	34	0.23	13	0.7	39	0.3	51	0.89	5
Hg	0.05	15	0.11	13	0.32	15	0.24	6	0.060	11
Tl	0.055	27	0.185	0.7	0.30	16	0.168	2	0.051	14
Cd	<LOD	-	<LOD	-	0.20	11	0.181	2	<LOD	-
Ag	<LOD	-	<LOD	-	<LOD	-	<LOD	-	<LOD	-

The samples belonging to the longitudinal transect represent a more general perspective from the northernmost point (adjacent to the cliff) up to the southern area where the beachrocks outcrops were found (see Figure 3.4 in Chapter 3).The data set is shown in Table 5.2.

Table 5.2a. Mean concentration (g/kg) and RSD (%) values of the major elements measured in the samples belonging to the longitudinal transect of Arrigunaga beach.

	ARL1		ARL2		ARL3	
	Mean	**RSD**	**Mean**	**RSD**	**Mean**	**RSD**
Ca	143	4	145	10	102	20
Al	31	10	17	19	11	13
Fe	24	15	6	18	6	14
Mg	17	7	11	15	7.0	4
Mn	4.8	5	2.1	14	1.6	6
Na	4.4	5	4.0	1	2.5	11
K	2.5	7	2	35	1.0	6

Table 5.2b. Mean concentration (mg/kg) and RSD (%) values of the minor elements measured in the samples belonging to the longitudinal transect of Arrigunaga beach.

	ARL1		ARL2		ARL3	
	Mean	**RSD**	**Mean**	**RSD**	**Mean**	**RSD**
Sr	1 916	8	2 057	3	2 630	15
Ba	357	8	376	27	433	8
Ti	340	23	415	10	530	20
Zn	137	5	180	13	265	19
Pb	33	11	37	4	55	18
Cu	21	20	24	31	23	23
V	15	19	11.5	7	18	17
Cr	13	23	6.1	16	13	29
As	9.3	5	11	32	12	11
Ni	7	14	5.4	8	8	14
Sn	5	25	14	37	2.9	20
Co	3.1	16	2.0	9	3.2	17
Se	2.6	19	2.9	23	4	28
Mo	1.1	17	0.799	0.6	1.5	17
Sb	0.6	63	0.06	28	0.49	14
Tl	0.30	11	0.5	30.1	0.43	18
Hg	0.15	11	0.13	19	0.12	15
Cd	<LOD	-	0.17	43	0.3	49
Ag	<LOD	-	<LOD	-	<LOD	-

Figure 5.1 summarises the kind of samples that represent each of the areas included in the transverse (Figure 5.1A) and longitudinal transect (Figure 5.1B). Like it was described in section 3.1.2 of Chapter 3, there are physical differences in the characteristics of the grains that compose the samples, a fact that might be needed to take into account herein.

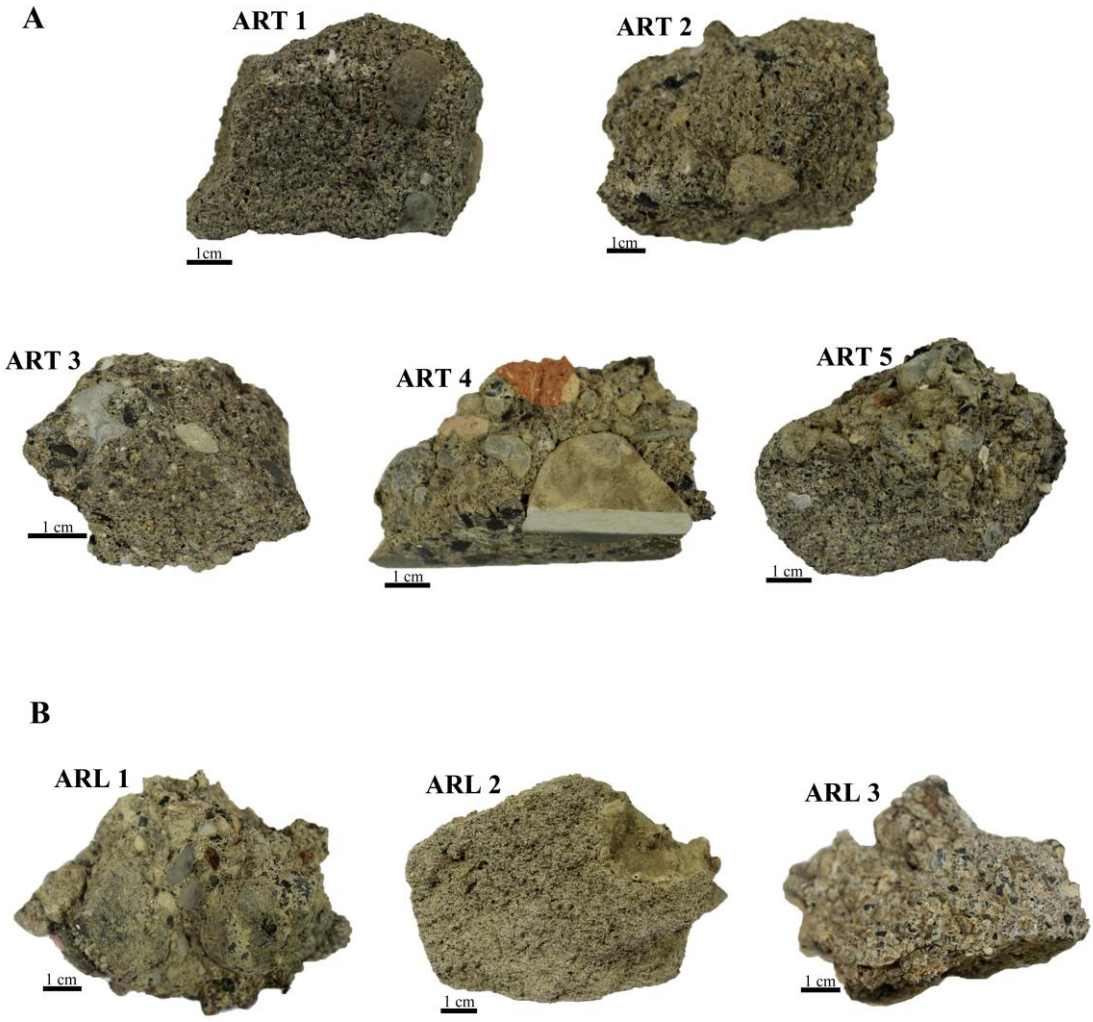

Figure 5.1. Representative samples gathered along the transverse transect and the longitudinal transect of Arrigunaga beach.

5.1.2 Description of general trends

The obtained data are also represented in Figure 5.2, according to the tendency found for each element in both transects. Many of the major elements (Ca, Al, Mg, Fe, Mn, K, Na) showed concentration values with a similar order of magnitude either in the

transverse or the longitudinal transect (Figure 5.2A). Moreover, they show diverse tendencies in the transverse transect, but it can be appreciated that in the longitudinal transect the concentration of the elements generally decreases from ARL1 to ARL3, that is, from the cliff to the middle part of the beach.

Regarding the minor elements, it is remarkable the analogous tendency found in both transects for Ti and Ba, as well as V and Cr, with a special emphasis on the high concentrations found in the sample ART5 (Figure 5.2B). Other elements, like Ni and As in contrast, are more accumulated in samples ART3 and ART4. On the whole, this group of elements, together with Se, seems to be more accommodated in the transverse transect. Nevertheless, there are other elements noticeably more abundant in the longitudinal transect. That is the case of Zn, Pb, Cu, Sn and even Co, as they show higher concentrations in the samples collected along this transect (Figure 5.2C).

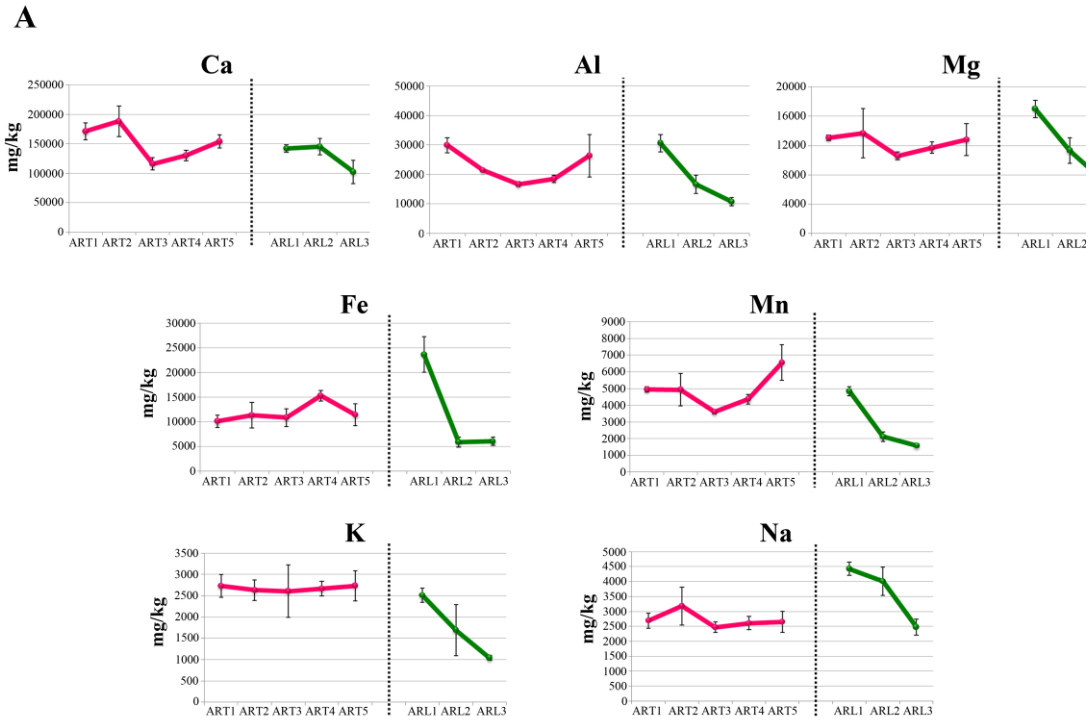

Figure 5.2. Mean concentration and standard deviation values (mg/kg) of the major elements analysed in Arrigunaga beach, comparing the transverse transect (pink line) and the longitudinal transect (green line). Continuation in the next page.

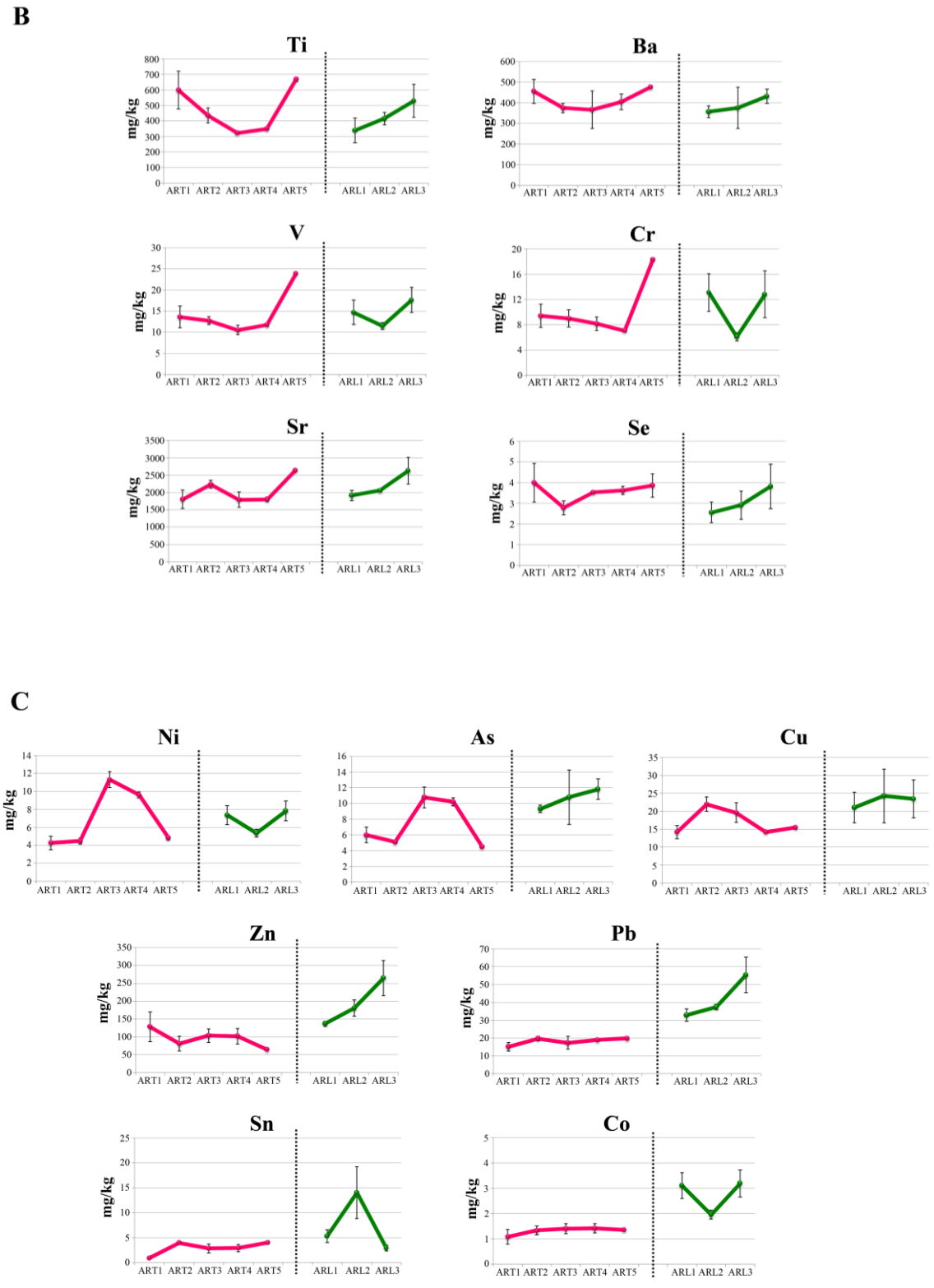

Figure 5.2. Continuation. Mean concentration and standard deviation values (mg/kg) of minor elements analysed in Arrigunaga beach, comparing the transverse transect (pink line) and the longitudinal transect (green line).

5.1.3 Chemometric analyses

5.1.3.1 Correlation analysis

Correlation analysis of all the data was carried out to find possible connections between element concentrations, as those connections could be indicative of similar origins or interactions for certain elements.

At first, an inter-sample correlation analysis was performed, showing that they were not significant statistical differences among them. Thus, as all the samples can be considered statistically similar, some elements were selected for the inter-elemental correlation analysis. In this sense, many of the major elements (more exactly, Ca, Al, Fe, Mg, Mn and K) were discarded, because they could be part either of the local lithology or part of the slag materials (as viewed in Chapter 4, section 4.2). In an attempt to avoid possible interferences, those major elements were not considered in this statistical analysis. Regarding the minor elements, those below 1 ppm (Mo, Sb, Tl, Hg) or below the detection limit (Ag, Cd) were not included either.

Thus, in this correlation analysis (Table 5.3) Na and Sr would be considered as tracers of marine environments and Ti, Ba, Zn, Pb, Cu, V, Cr, As, Ni, Se, Co and Sn, as elements prone to have an anthropogenic origin.

Table 5.3. Pearson´s correlation matrix including the samples and corresponding replicates from the transverse and the longitudinal transect of Arrigunaga beach. Correlations significantly different from zero (99% confidence level; p<0.01, r<0.52) are green coloured.

	Na	Sr	Ti	Ba	Zn	Pb	Cu	V	Cr	As	Ni	Se	Co	Sn
Na	1.00													
Sr	0.08	1.00												
Ti	-0.24	0.69	1.00											
Ba	-0.22	0.57	0.76	1.00										
Zn	0.16	0.53	0.27	0.18	1.00									
Pb	0.26	0.62	0.19	0.11	0.89	1.00								
Cu	0.37	0.51	0.00	-0.09	0.59	0.58	1.00							
V	-0.11	0.75	0.81	0.67	0.18	0.28	0.06	1.00						
Cr	-0.06	0.53	0.62	0.53	0.03	0.11	0.00	0.92	1.00					
As	0.23	0.20	-0.23	-0.02	0.73	0.69	0.44	-0.16	-0.22	1.00				
Ni	0.06	-0.10	-0.43	-0.08	0.22	0.25	0.13	-0.25	-0.19	0.80	1.00			
Se	-0.26	0.54	0.68	0.67	0.41	0.34	0.00	0.45	0.24	0.31	0.20	1.00		
Co	0.45	0.53	0.11	0.07	0.80	0.85	0.63	0.32	0.30	0.67	0.29	0.18	1.00	
Sn	0.02	0.11	-0.09	0.14	0.13	0.11	0.07	-0.03	-0.14	0.31	0.25	0.08	0.14	1.00

On this basis, Pearson´s correlation coefficients were calculated at a confidence level of 99% ($p<0.01$, $r<0.52$). This way, as shown in Table 5.3, strong positive correlations were found between Sr and Ti, Ba, Zn, Pb, V, Cr, Se and Co, probably indicating that these elements are somehow related with seawater; Sr would naturally occur in the marine environment, while seawater could be the carrier of the other elements derived from a man-made source.

Indeed, Ti, Ba, V and Cr show significant positive correlations among them, a group of elements generally showing the highest concentrations in the sample ART5. In other studies, these elements have been ascribed to pollutants derived from mining activities[14]. However, V and Cr, which showed an especially high correlation coefficient (0.92), could also come from tanneries and electrolysis factories[15] or even from metal coating activities[16]. Other elements like Zn, Pb, Cu and Co, also show a remarkable association among them. These elements were specially found in the samples from the longitudinal transect and they are usually considered as pollutants derived from mining activities[14] or from electroplating industries[17]. In addition, other diverse industrial sources could be mentioned, as Zn and Pb are among the main constituent of the steel mill powder historically dumped into the estuary from steel making industries[18], although Pb might have come also from paint industries[19].

Finally, it should be remarked the high correlation (0.82) between Ni and As, which were primarily accumulated in ART3 and ART4. These elements can be potential industrial pollutants, however, studies about the sediments of the Nerbioi-Ibaizabal River estuary demonstrated that Ni and As can belong to a rather natural background[20]. Furthermore, similar results were found in the study of adjacent beachrock formations[21].

[14] Davis R.A. Jr., Welty A.T., Borrego J., Morales J.A., Pendon J.G., Ryan R.G., **2000**. *Rio Tinto estuary (Spain): 5000 years of pollution*. Environmental Geology 39, 1107-1116.
[15] Grousset F.E., Jouanneau J.M., Castaing P., Lavaux G., Latouche C., **1999**. *A 70 year record of Contamination from Industrial Activity Along the Garonne River and its Tributaries (SW France)*. Estuarine, Coastal and Shelf Science 48, 401-414.
[16] Fdez-Ortiz de Vallejuelo S., Arana G., de Diego A., Madariaga J.M., **2010**. *Risk assessment of trace elements in sediments: the case of the estuary of the Nerbioi-Ibaizabal River (Basque Country)*. Journal of Hazardous Materials 181, 565-573.
[17] Al-Masri M.S., Al-Kharfan K., Al-Shamali K., **2006**. *Speciation of Pb, Cu and Zn determined by sequential extraction for identification of air pollution sources in Syria*. Atmospheric Environment 40, 753-761.
[18] Borja A., Tueros I., Belzunce M.J., Galparsoro I., Garmendia J.M., Revilla M., Solaun O., Valencia V., **2008**. *Investigative monitoring within the European Water Framework Directive: a coastal blast furnace slag disposal, as an example*. Journal of Environmental Monitoring 10, 453-462.
[19] Pekey H., **2006**. *Heavy metal pollution assessment in sediments of the Izmit Bay, Turkey*. Environmental Monitoring and Assessment 123, 210-231.
[20] Gredilla A., Fdez-Ortiz de Vallejuelo S., Arana G., de Diego A., Madariaga J.M., **2013**. *Long-term monitoring of metal pollution in sediments from the estuary of the Nerbioi-Ibaizabal River (2005–2010)*. Estuarine, Coastal and Shelf Science 131, 129-139.
[21] Arrieta N., **2014**. *The study of an unusual temperate latitude beachrock formation. Characterization of Azkorri beach and Tunelboka cove locations*. PhD Thesis, University of the Basque Country.

Thus, correlation analyses demonstrated diverse associations between the elements. Many of them, especially Ti, Ba, Zn, Pb, V, Cr, Se and Co, seem to have an anthropogenic origin for instance from mining and diverse industrial activities, such as metal working industry, textile or paint industry. Their positive correlation with Sr would indicate that these elements might have reached the shore driven by marine currents. Therefore, the positive correlations found among the elements, might denote a co-contamination of the analysed cemented structures with elements prone to have a man-made source.

Some of the groupings come in agreement with the similar tendencies previously described in section 5.1.1. Therefore in order to discern inherent variabilities of the considered samples, either triggered by their origin or their distribution in the analysed outcrops, a principal component analysis might be helpful.

5.1.3.2 Principal component analysis (PCA)

For this purpose, all the samples, including the corresponding replicates (R1, R2 and R3) were considered. Once the data were centered and autoscaled in the Unscramble software, the first four principal components of the model were considered, which accounted for the 88% of the variance. Figure 5.3A shows the scores over the two main components explaining the 62% of the variance (PC1: 34%; PC2: 28%). There, it can be observed that the samples belonging to the longitudinal transect (ARL, in green) are situated in the positive side of the x axis, whereas the samples of the transverse transect are displayed in the negative side. Therefore, PC1 seems to establish that, certainly, there is a difference between the two sampling orientations.

To better understand the grouping of the samples, the elements were also included in the PCA, as shown in the loadings plot of Figure 5.3B. As with correlation analyses, Na, Sr, Ti, Ba, Zn, Pb, Cu, V, Cr, As, Ni, Co, Sn, Se were considered, discarding the rest of the analysed elements to avoid misconceptions.

Some elements like V, Cr, Ti, Ba, as well as Se, coincide in the negative side of the y axis with many of the transverse samples, especially with ART5. Note that the samples ART3 and ART4 are more associated to Na, Sr as well as Ni and As and it can be observed in the PCA representation that these samples and elements tend to approach the longitudinal samples. In view of this distribution, ART3 and ART4 seem to be somehow intermediaries between the transverse and the longitudinal samples. Indeed, tt

should be mentioned as a reminder that these two samples are the most seaward samples of the transverse transect, so it makes sense that they tend to go towards the longitudinal samples, which were collected in the lower intertidal zone comprising the samples collected closer to the seawater. In this sense, the longitudinal samples are mainly grouped with elements like Co, Pb, Zn, Cu and Sn.

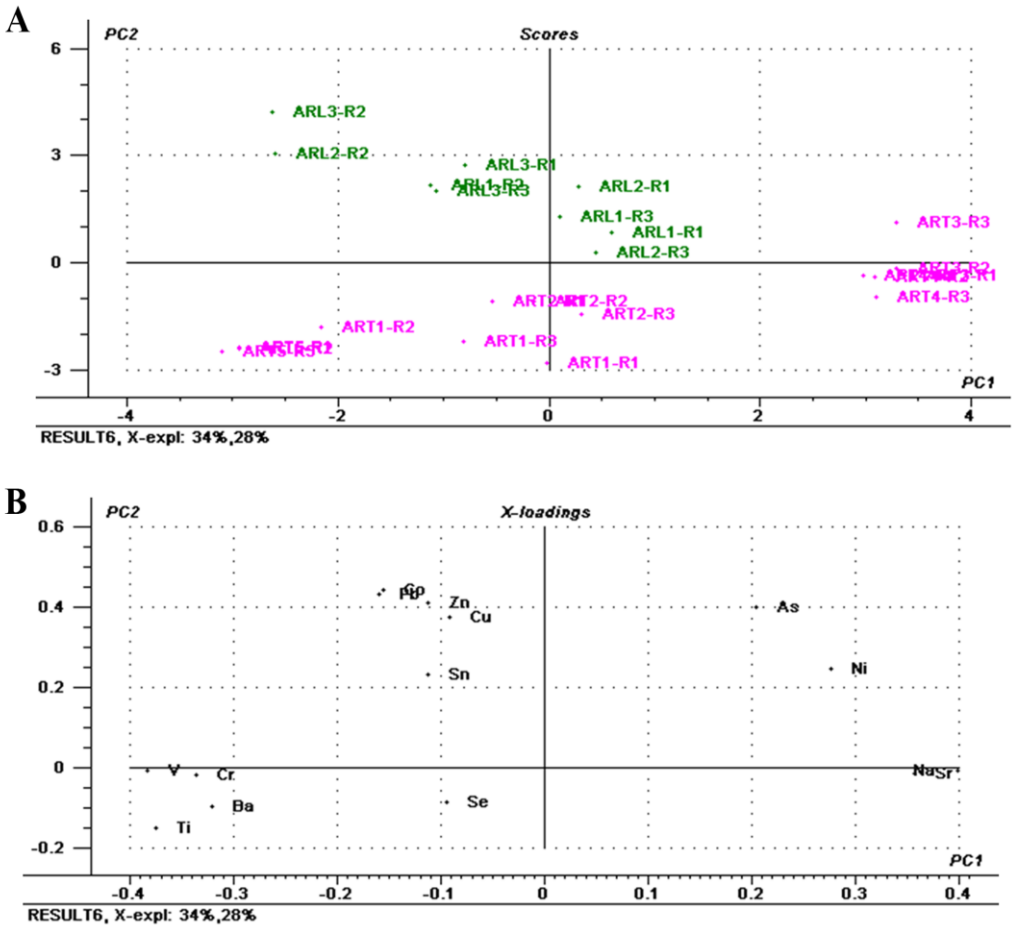

Figure 5.3. PCA model defined by two principal components (PC1, PC2) explaining the 62% of the variance (based on a model where four PCs explain the 88% of the variance). All the data set from Arrigunaga beach is considered, including samples from the transverse (ART1-ART5) and the longitudinal transect (ARL1-ARL3). A) Scores (three replicates per sample) and B) loadings (elements) plot representations.

The removal of cemented material performed during the regeneration of Arrigunaga beach, complicates the estimation of the characteristics of the original cemented outcrops. However, the study carried out by Losada et al. (1993)[22] about Arrigunaga prior to its regeneration, provided with information about the dynamics and morphodynamic features of the beach existent before the regeneration of the beach.

[22] Losada M.A., Medina R., Baquerizo A., Silva R., Tomillo C., Foyo A., Sagaseta C., Polanco J.A., Canteras J.C., **1993**. *Estudio de la playa de Arrigunaga. Situación actual y alternativas de regeneración*. Fundación Torres Quevedo. Diputación Foral de Bizkaia. Universidad de Cantabria (Inédito).

Apparently, there was an imbalance between the water flow reaching the beach from the estuary, and the flow directed back to the river. As a consequence, the possible contaminants coming down with the floods and tides were directed towards the beach and the capacity of those materials to return back to the river was reduced. Thus, there was a net flow balance toward Arrigunaga that might enhance the accumulation of external materials in the beach. In addition, the obliquity of the waves in the northern part of the beach triggered a greater sediment supply in that area. Also, the presence of gravels was derived from the erosion of Punta Galea cliff[23].

In view of the results of the metal quantification it can be suggested that the analysed beachrock samples preserve a high metal content and that the distribution of the analysed elements is different in the transverse and the longitudinal transect: the transverse transect is more related with elements like Ca, Al, Mg, Fe and Mn, whereas the samples from the longitudinal transect are more related with higher concentration values of various heavy metals (such as Pb, Zn, Cu, Co).

It is not clear if that distribution is related with the removal of the cemented sand performed during the regeneration process of the beach, or because of the particular dynamic and morphodynamic features of the beach. In fact, Al, Mg, Fe and Mn are the major elements of estuarine sediments[24] and also part of many composites found in historical industrial slag[25]. Thus, the distinctive composition of those samples could be due to the greater sediment supply and material arrival specially occurring in the northern area of the beach. However, it is believed that the massive arrival of material provoked their accumulation along the beach[23]; that fact would explain the presence of the high metal content in the longitudinal transect.

[23] Losada M.A., Medina R., Baquerizo A., Silva R., Tomillo C., Foyo A., Sagaseta C., Polanco J.A., Canteras J.C., **1993**. *Estudio de la playa de Arrigunaga. Situación actual y alternativas de regeneración*. Fundación Torres Quevedo. Diputación Foral de Bizkaia. Universidad de Cantabria (Inédito).

[24] Fdez-Ortiz de Vallejuelo S., Arana G., de Diego A., Madariaga J.M., **2010**. *Risk assessment of trace elements in sediments: the case of the estuary of the Nerbioi-Ibaizabal River (Basque Country)*. Journal of Hazardous Materials 181, 565-573.

[25] Iturregui A., Arrieta N., Aramendia J, Arrizabalaga I., Murelaga X, Baceta J.I., Olazabal M.A., Martínez-Arkarazo I., Madariaga J.M., **2015**. *In-situ and laboratory Raman spectroscopic analysis on beachrock deposits: characterisation of the trapped materials*. Journal of Raman Spectroscopy, DOI 10.1002/jrs.4815.

5.2 Metal quantification in La Salvaje beach

5.2.1 Determination of the elemental content

These samples were collected from the outcrops found in the area right adjacent to the cliff, landward to seaward, completing a transverse sampling (see Figure 3.5 in Chapter 3). The results from the elemental quantification are summarised in Table 5.4.

Table 5.4a. Mean concentration (g/kg) and RSD (%) values of the major elements measured in the samples belonging to the transverse transect of La Salvaje beach.

	LST1		LST2		LST3		LST4	
	Mean	**RSD**	**Mean**	**RSD**	**Mean**	**RSD**	**Mean**	**RSD**
Ca	134.66	6	159	23	157	11	119	14
Fe	15.54	7	19	19	27	15%	21	13
Mg	11.13	9	15	19	14.867	0.03	15	8
Al	5.50	10	15	16	11	9	17	5
Na	2.70	11	3.3	11	2.72	1	2	9
Mn	1.58	8	4	22	3	19	4.2	6
K	1.57	13	1.70	25	1.9	6	1.4	8

Table 5.4b Mean concentration (mg/kg) and RSD (%) values of the minor elements measured in the samples belonging to the longitudinal transect of La Salvaje beach.

	LST1		LST2		LST3		LST4	
	Mean	**RSD**	**Mean**	**RSD**	**Mean**	**RSD**	**Mean**	**RSD**
Sr	1569	1	1702	2	1877	4	1376	11
Zn	277	4	206	1	235	5	209	13
Ba	202	10	381	5	326	4	503	17
Ti	112	2	457	8	352	6	563	9
Pb	35.4	2	28	9	40	11	27	26
As	23.7	2	18.9	1	22	6	14	10
V	14.2	2	20.9	4	22	18	23	13
Cu	13	8	15.7	5	28	28	14.3	6
Cr	5.50	1	13	8	18	33	14	9
Ni	4.9	5	6.8	5	7.3	12	6.3	12
Co	3.2	10	3.4	7	4.2	19	3.7	8
Sn	2.3	25	1.47	1	6	45	5	34
Se	2.3	10	3.8	6	3.1	17	4.5	5
Mo	0.72	3	0.75	9	0.9	10	0.93	6
Hg	0.29	15	0.4	31	0.23	18	0.169	3
Sb	0.19	50	0.32	27	0.8	23	0.12	38
Tl	0.188	3	0.279	3	0.23	7	0.22	12
Ag	0.05	36	0.34	9	0.243	4	0.30	7
Cd	<LOD	-	0.035	19	0.016	11	<LOD	-

In this case, similarly to Arrigunaga beach, various samples were gathered along the beach from the area adjacent to the cliff (southwest part of the beach), till the furthest point (towards the northeast part of the beach) where the beachrock outcrops were visualized (see Figure 3.6 in Chapter 3).

Table 5.5a. Mean concentration (g/kg) and RSD (%) values of the major elements measured in the samples belonging to the longitudinal transect of La Salvaje beach.

	LSL1		LSL2		LSL3		LSL4		LSL5	
	Mean	**RSD**	**Mean**	**RSD**	**Mean**	**RSD**	**Mean**	**RSD**	**Mean**	**RSD**
Ca	114	7	153	13	146	9	147	4	169	27
Al	21	30	36	11	22	27	22	3	22	30
Mg	16	18	20	8	18	20	19	11	15	20
Fe	14	16	21	19	29	4	42	16	10	14
Na	3.7	10	4.1	9	5	17	6	13	6	18
Mn	3	24	5	15	3.3	12	3.3	9	2.6	16
K	2	33	3.4	14	1.2	27	1.1	10	1.3	32

Table 5.5b Mean concentration (mg/kg) and RSD (%) values of the minor elements measured in the samples belonging to the longitudinal transect of La Salvaje beach.

	LSL1		LSL2		LSL3		LSL4		LSL5	
	Mean	**RSD**	**Mean**	**RSD**	**Mean**	**RSD**	**Mean**	**RSD**	**Mean**	**RSD**
Sr	1 208	8	1 877	13	1 233	3	1 331	5	1 561	17
Ti	401	8	469	6	228	4	151	9	261	27
Ba	394	10	511	5	281	18	229	2	305	25
Zn	250	4	160	4	206	10	196	17	141	13
Pb	30	6	24	10	27	5	32	15	20	11
V	19	8	14	24	13	13	12	17	12	24
As	16.4	4	8	14	15.0	4	19	12	10.9	8
Cu	16	9	20	9	13	13	16	27	8.7	9
Cr	12	17	11	23	7	16	5.4	14	5	23
Ni	5.6	4	3.7	16	6	32	5	23	3.4	16
Co	3.7	5	1.7	20	2.9	12	3.0	23	2.1	20
Se	2.7	15	2.9	11	1.8	18	1.3	35	2.4	22
Sn	1.69	2	5.0	10	1.3	13	1.6	14	1.1	25
Hg	1.6	52	0.35	22	0.16	20	0.094	6	0.080	8
Mo	0.9	12	0.8	14	0.75	8	0.92	5	0.8	20
Tl	0.42	8	0.22	7	0.24	8	0.198	4	0.32	29
Sb	0.3	51	0.51	8	0.4	26	0.40	21	0.23	28
Cd	<LOD	-	<LOD	-	<LOD	-	<LOD	-	<LOD	-
Ag	<LOD	-	<LOD	-	<LOD	-	<LOD	-	<LOD	-

Figure 5.4 shows the physical appearance of samples representative of the diverse areas considered for the sampling in La Salvaje beach, to bear in mind if the first view of the sample can give some clues of the differences between samples.

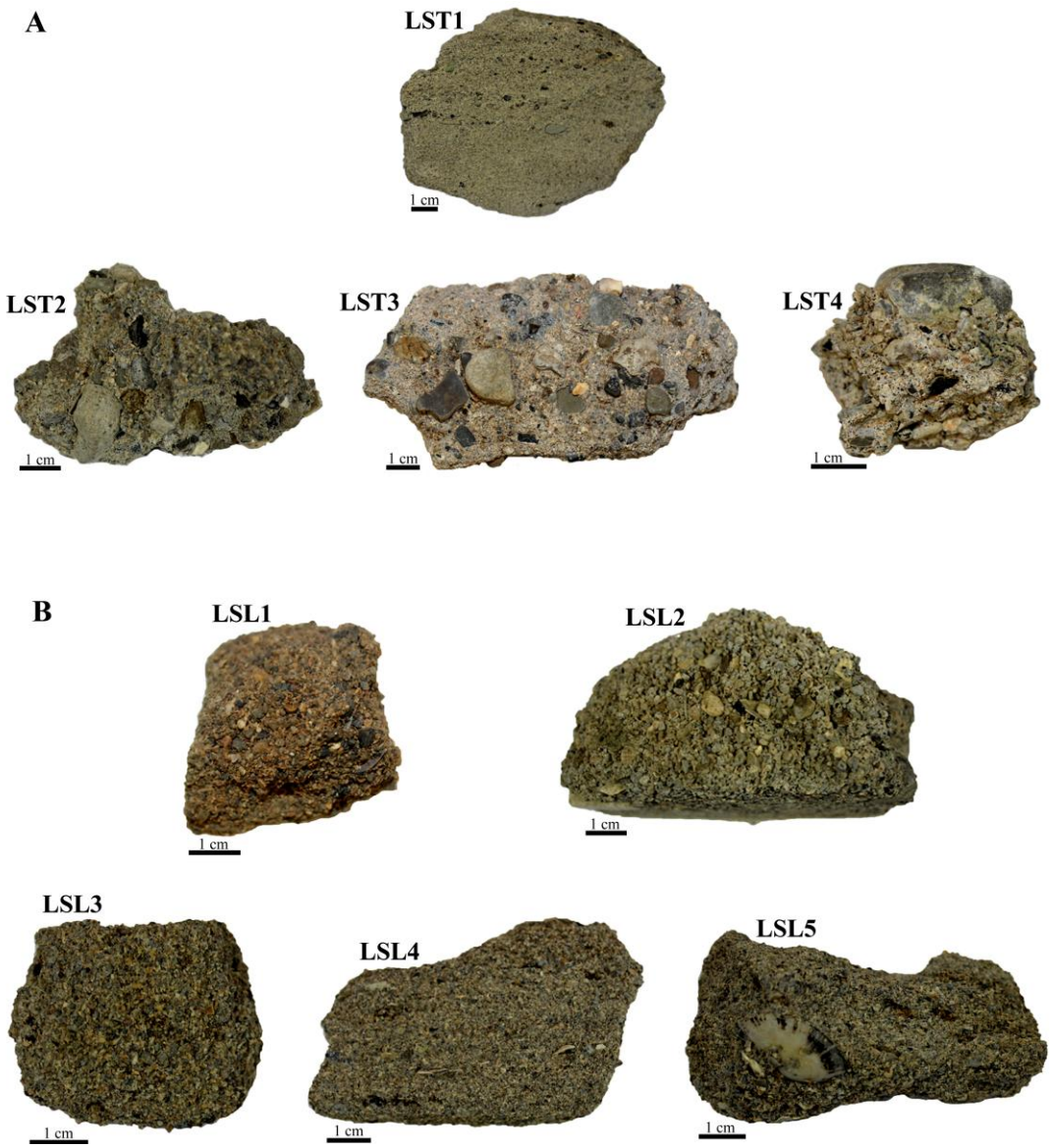

Figure 5.4. Beachrock samples collected in La Salvaje beach, along the A) transverse transect and B) the longitudinal transect.

5.2.2 Description of general trends

The quantitative data acquired from the samples of La Salvaje beach are represented in Figure 5.5, in order to discern the tendencies of each element. With regard to the major elements, many of them show similar concentration ranges in both

transects (Figure 5.5A). However, some exceptions could be worth mentioning, for instance, Na shows higher concentrations in any of the samples from the longitudinal transect. Furthermore, Fe presents a significantly higher concentration value in the samples LSL4 (Figure 5.5A), that is, in the middle part of the beach, especially affected by the blackening of the loose sand probably due to the accumulation of iron rich industrial wastes. Al is also among the elements predominant in the longitudinal transect.

In reference to minor elements, Ti, Ba as well as Se, Sn, or V, Cr and even Cu, show analogous trends in both transects; in the transverse transect tend to increase from LST1 to LST4, that is, from the most inland to the most seaward sample. In the longitudinal transect, regardless of their punctual decrease in LSL2, the concentration of those elements significantly decreases from LSL1 to LSL5; in other words, from the cliff to the mid part of the beach. Thus, this group of elements seems to be especially accommodated in the area were the transverse transect was performed. Not only those, but Zn, Pb, As, Ni and Co also show prevailing higher concentrations in the transverse transect. Moreover, they also show a decreasing tendency towards the mid part of the beach. However, unlike the previous group of the minor elements, they present a remarkable punctual decrease in the sample LSL2.

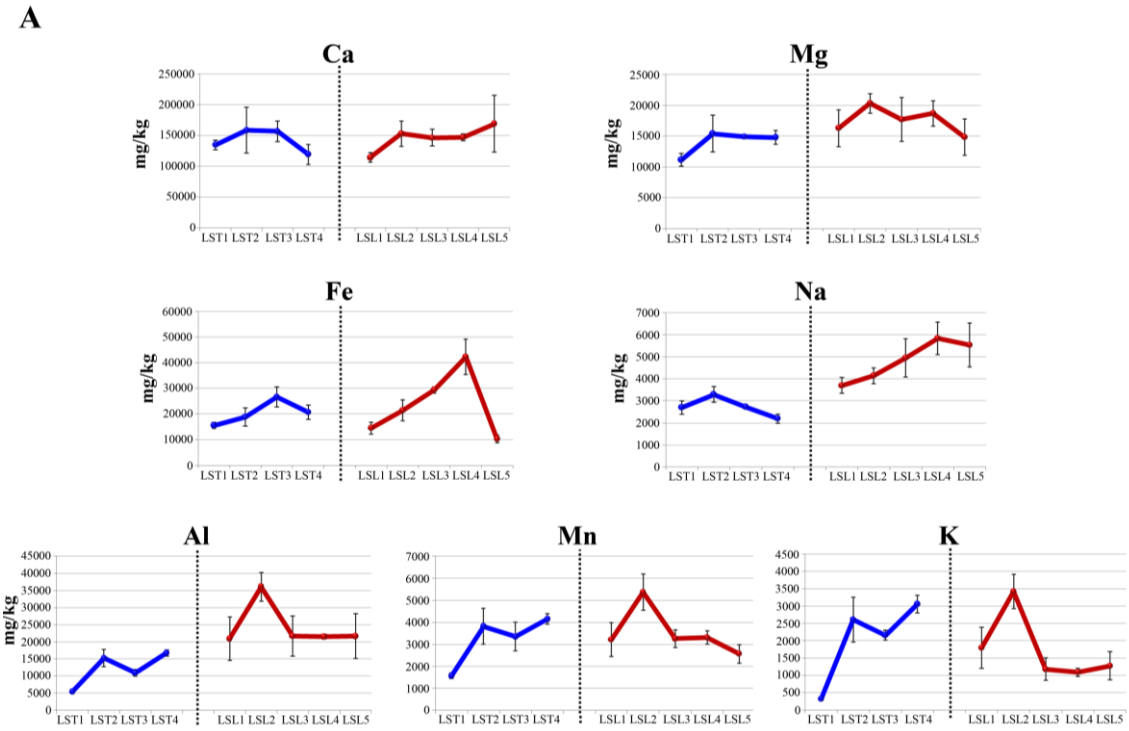

Figure 5.5. Mean concentration and standard deviation values (mg/kg) of the major elements analysed in La Salvaje beach, comparing the transverse transect (blue line) and the longitudinal transect (red line). Continuation in the next page.

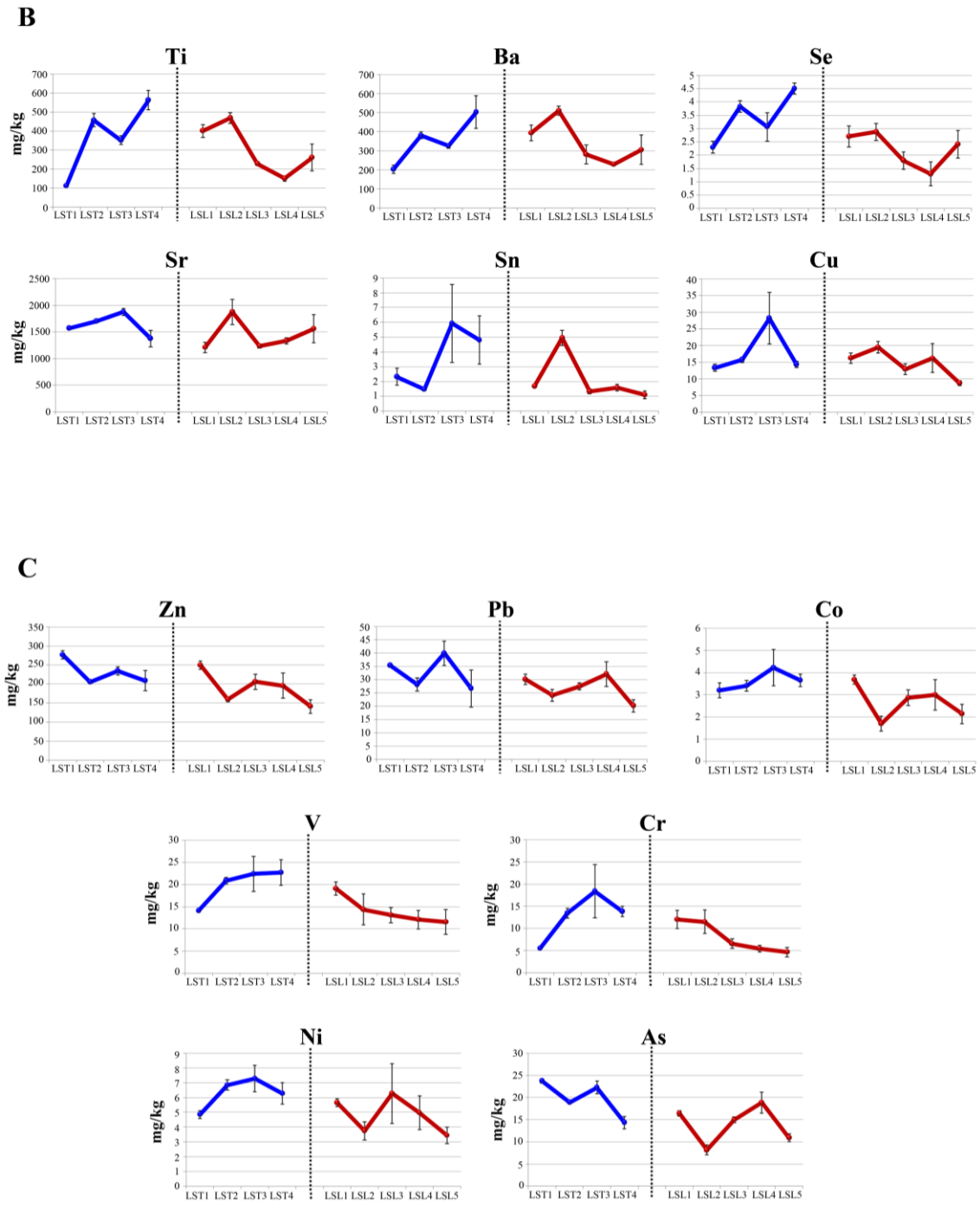

Figure 5.5. Continuation. Mean concentration and standard deviation values (mg/kg) of minor elements analysed in La Salvaje beach, comparing the transverse transect (blue line) and the longitudinal transect (red line).

5.2.3 Chemometric analyses

5.2.3.1 Correlation analysis

In an attempt to recognize connections probably indicative of similar origins or interactions for certain elements, a correlation analysis of all the data was performed.

Once again, first of all an inter-sample correlation analysis was carried out, and as a result, all the samples could be considered statistically similar. Afterwards some elements were selected for the inter-elemental correlation analysis. In this sense, to be consistent with the elements taken into account in the correlation analysis of Arrigunaga beach and avoid misconceptions Ca, Al, Fe, Mg, Mn and K were discarded among the major elements, as well as the minor elements below 1 ppm (Mo, Sb, Tl, Hg) or below the detection limit (Ag, Cd).

Table 5.6. Pearson´s correlation matrix including the samples and corresponding replicates from the transverse and the longitudinal transect of La Salvaje beach. Correlations significantly different from zero (99% confidence level; p<0.01, r<0.50) are green (positive correlation) and red (negative correlation) coloured.

	Na	Sr	Zn	Ba	Ti	Pb	As	V	Cu	Cr	Ni	Co	Se	Sn
Na	1.00													
Sr	-0.01	1.00												
Zn	-0.34	-0.69	1.00											
Ba	-0.25	-0.49	0.25	1.00										
Ti	-0.40	-0.36	0.19	0.93	1.00									
Pb	-0.31	-0.46	0.68	0.13	0.10	1.00								
As	-0.35	-0.43	0.71	-0.03	-0.03	0.94	1.00							
V	-0.64	-0.48	0.61	0.68	0.77	0.56	0.50	1.00						
Cu	-0.26	-0.43	0.39	0.33	0.32	0.52	0.43	0.48	1.00					
Cr	-0.66	-0.31	0.40	0.62	0.72	0.56	0.46	0.91	0.54	1.00				
Ni	-0.35	-0.60	0.72	0.41	0.48	0.67	0.64	0.79	0.46	0.67	1.00			
Co	-0.45	-0.65	0.81	0.38	0.39	0.79	0.80	0.82	0.52	0.69	0.83	1.00		
Se	-0.55	-0.48	0.43	0.80	0.88	0.22	0.18	0.83	0.36	0.69	0.59	0.55	1.00	
Sn	-0.38	-0.17	0.26	0.32	0.39	0.24	0.14	0.44	0.42	0.47	0.28	0.35	0.30	1.00

Pearson´s correlation coefficients were estimated at a confidence level of 99% (p<0.01, r<0.50). In view of the correlation matrix (Table 5.6), the negative correlation between Na and Sr with various heavy metals (Zn, V, Cr, Ni, Co, Se) suggests that they might have different origins; Na and Sr can have a mainly natural provenance, while the presence of diverse heavy metals might be related with man-made sources.

Indeed, regarding Zn, Pb, As, V, Ni and Co, they are highly correlated. More exactly, it is remarkable the high correlation between Ti and Ba (0.93), as well as V and Cr (0.91), as mentioned also for Arrigunaga beach. But, in contrast, here in La Salvaje beach a significantly high correlation was found between Pb and As. These two elements resulted to be remarkably associated also in the study of the sediments related with the slag disposal area located 4 miles to the north of the coast, where metal-containing-slag and diverse industrial wastes were abundantly dumped. Indeed, it is already known that elements like Zn or Pb are among the main constituents of the steel powder wastes[26]. In addition, as previously mentioned, heavy metals in general, can have diverse man-made origins, even more in such an industrialized area.

Thus, many major and minor elements have an opposite association, probably as a result of their diverse origin. Moreover, the elements believed to have an anthropogenic origin showed greater concentrations in the transverse transect, especially in the most seaward samples (LST2, LST3, LST4). Thus, to represent the general inherent variabilities that lie behind the samples analysed in La Salvaje beach, principal component analysis might be required.

5.2.3.2 Principal component analysis

Along these lines the results of the principal component analysis (PCA) will be described, where samples from the transverse and the longitudinal sampling were taken into account. For that purpose, the replicates of each sample were considered and the main four principal components of the model accounted for the 75% of the variance.

This PCA model allowed also perceiving the dispersion of the replicates, named as R1, R2 and R3 at the end of the corresponding sample. The set of three replicates is generally very close to one another, evidencing the homogeneity and representativity of the samples. However, some exceptions can be found in LSL1, as the third replicate (LSL1-R3) is further from the first two. As shown in Table 5.5, that sample showed high RSD values for Mn, K, and specially Hg and Sb (24%, 33%, 51.8% and 51.5%, respectively). Attending to the loadings (Figure 5.6B) we can see that those elements are located around LSL1, therefore, the scattering of the replicates might represent the variability of those few elements in that sample. A similar case is found with the first replicate of LSL2.

[26] Borja A., Tueros I., Belzunce M.J., Galparsoro I., Garmendia J.M., Revilla M., Solaun O., Valencia V., **2008**. *Investigative monitoring within the European Water Framework Directive: a coastal blast furnace slag disposal, as an example*. Journal of Environmental Monitoring 10, 453-462.

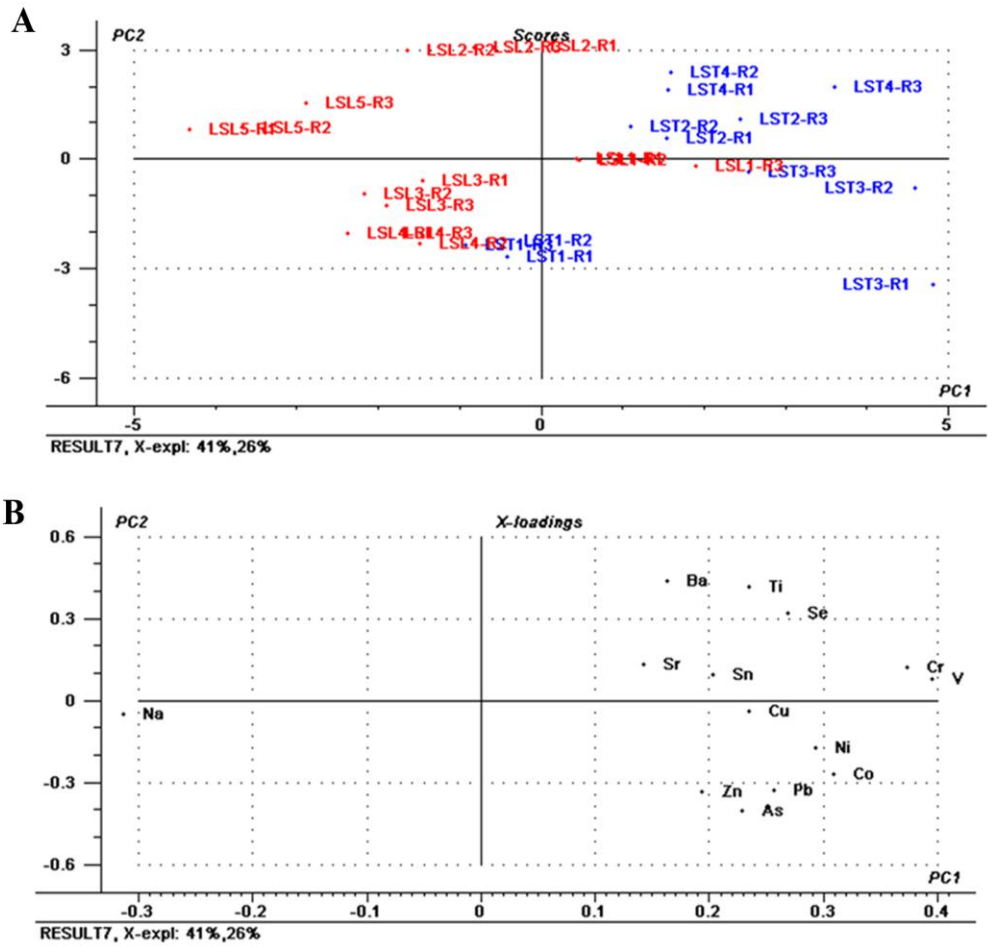

Figure 5.6. PCA model defined by two principal components (PC1, PC2) explaining the 67% of the variance (based on a model where four PCs explain the 84% of the variance). Samples from the transverse (LST1-LST4) and the longitudinal transect (LSL1-LSL5) are included. A) Scores (three replicates per sample) and B) loadings (elements) plot representations.

Figure 5.8.A shows the scores over PC1-PC2 and different clusters can be discerned (confirmed also in PC3 and PC4), specially according to transverse (LST, in red) and longitudinal (LSL, in blue) samples. In fact, generally the samples of the transverse transect are positioned in the right side of PC2 (y axis), while the longitudinal samples are grouped in the left side.

There is an exception with the longitudinal sample LSL1, which is in the right side, probably because it is a sample collected near the cliff, the area where the transverse transect was performed. Regarding the transverse samples, there is a peculiarity with sample LST1, as it is separated from the rest of the samples of the transverse transect, probably because as it was described in Figure 5.5, that landward sample is characterized by a lesser content of metals. In fact, it is grouped close to those samples from the longitudinal sampling considered to have a lower concentration of the majority

of the elements (LSL3, LSL4 and LSL5). That might explain the closeness of LST1 as well as LSL3, LSL4 and LSL5, with very few elements like Na, Ca, Al and Mg, whereas the other samples and elements are clustered in the opposite side.

In Figure 5.4 where the representative appearance of the samples collected in La Salvaje beach was shown, it could be clearly recognized that LST1, the most inland sample, significantly differs from the rest of the samples of the transverse transect, as it showed a smaller grain size, in contrast to the variety of sizes amalgamated in the other samples. Indeed, that physical appearance of LST1 resembles more to the longitudinal samples LSL3, LSL4, and LSL5. Additionally, note that LSL2 is clearly more cemented than the rest.

In order to understand the elemental distribution found in the transverse and longitudinal transects of La Salvaje beach, the characteristics of the tides and currents might be taken into account. Certainly, littoral sediment migration and deposition is mainly controlled by waves and currents[27].

Beaches in general can and do change spatially and temporally. Those changes are usually related with modifications in the local and temporal contribution of waves, tides, sediment supply or slope and even storm events. Usually, open sea sandy beaches are dominated by waves and influenced by tides[28,29]. La Salvaje beach is completely open to the sea and strong waves reach the shore especially at high energy events. Thus, diverse tidal currents can be formed in the beach. It is generally believed, and confirmed by the users of the beach, that the main current occurs in the mid part of the beach[30,31], an area that, particularly under storm wave conditions, acts as the main drain point of the system because wave energy can be balanced by seaward return flows.

In addition, other tidal currents can exist also in the two extremes of the beach. The southwestern area, where the transverse transect was performed, should be remarked because although they are not as strong as in the mid part, powerful waves can be formed accompanied by backward weaker tidal currents. Moreover, in that area, at

[27] Stanica A., Ungurenau V. G., **2010**.*Understanding coastal morphology and sedimentology*. NEAR Curriculum in Natural Environmental Science. Terre et Environnnement 88, pp 105–111.
[28] Schwartz M., **2006**. *Encyclopedia of Coastal Science*.Springer Science & Business media, 1213 pp.
[29] Scott T., Masselink G., Russell P., **2011**. *Morphodynamic characteristics and classification of beaches in England and Wales*. Marine Geology 286, 1-20.
[30] Pérez F.P., 2004. *Playas del País Vasco*. ADEVE (Cristina Ruiz Urionabarrenetxea). Editor Petronor, 293 pp.
[31] Getxo Surf Taldea, *La Salvaje*. Retrieved from: www.getxosurf.es (2015, October 26).

favourable conditions, a mix of currents can be formed. They tend to be weaker than in the middle part of the beach, probably inducing a major sediment deposition as demonstrated by an increase in the metal content. Furthermore, the supply of cliff derived materials might not be underestimated in that area.

On account of this information, it could be hypothesised that the middle area, subjected to strong currents, can be counterbalanced by landward and seaward water fluxes. That might explain the lower metal content found in the outcrops sampled in that area. The iron might be an exception, because the massive arrival of iron particles might have altered the sediment supply equilibrium, triggering a higher iron content to be entrapped in the cemented bodies of that apart of the beach.

5.3 Comparison between the two field sites

The explanations that will be given in the following lines intend to remark the main compositional characteristics encountered through the transverse and longitudinal transects selected in Arrigunaga beach and La Salvaje beach for the comparison of both sites, basing once again on principal components analysis. In previous sections, various sample combinations have been subjected to principal component analysis in an attempt to unravel the peculiarities of the transects followed in the two field sites. To culminate the description, this final PCA models will summarise the hypotheses arisen from the metal quantification. It should be mentioned that the replicates were also considered for this statistical analysis. However, as the equivalence between PCA models based on replicates and those based on the average models has been already demonstrated, these last PCAs will only show the average-based models for simplicity.

In order to better illustrate the dispersion and clustering of the samples, in this PCA model the average concentration values of all the analysed samples were considered. In this model the four principal components accounted for the 73% of the variance. To understand the main facts exposed in this representation, the key point might be PC2 (y axis). Comparing scores (Figure 5.7A) and loadings (Figure 5.7B), it can be observed that, in the positive of upper side of the axis they are positioned those samples that seem to be more related to minor elements (most of them heavy metals): the most seaward samples from the transverse transect of La Salvaje beach (LST2-LST4), the longitudinal samples of Arrigunaga beach collected more distant to the cliff (ARL2 and ARL3) and in a lesser extent, the most seaward samples from the transverse transect of Arrigunaga

beach (ART3-ART5). On the contrary, below the y axis, we found the most inland samples from Arrigunaga beach (ART1 and ART2), the most inland sample from La Salvaje beach (LST1) as well as the samples more distant to the cliff in La Salvaje beach (LSL3-LSL5).

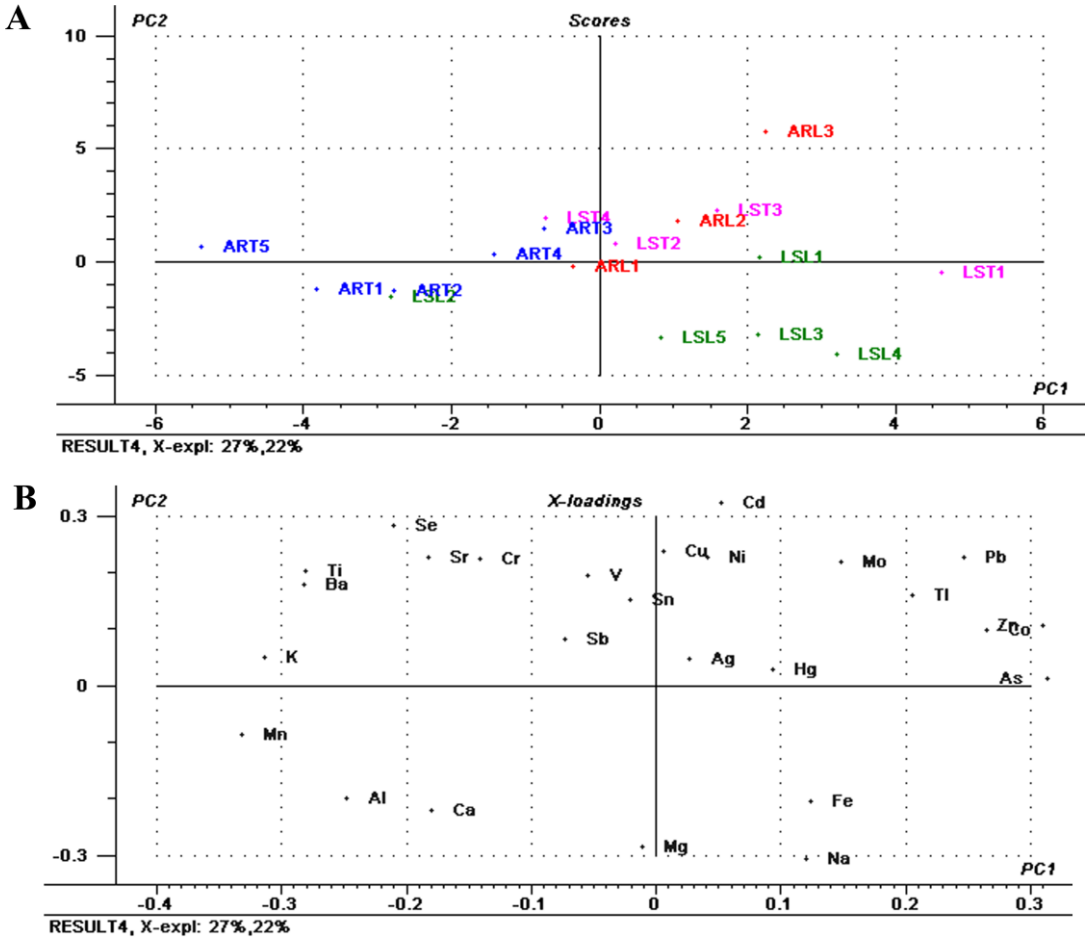

Figure 5.7. PCA model defined by two principal components (PC1, PC2) explaining the 49% of the variance (based on a model where four PCs explain the 73% of the variance). The model includes all the data set from the two site studies. A) Scores (average of three replicates) and B) loadings (analyzed elements) plot representations.

In summary, according to the analysed samples and the obtained results, there is not a common pattern between Arrigunaga and La Salvaje beach, in terms of elemental distribution. For instance, the former, contains the majority of the heavy metals along the samples gathered from side to side of the beach (longitudinal transect), whereas in La Salvaje an overwhelming amount of elements seems to be accumulated in the area next to the cliff. Thus, the metal content harboured in the beachrock might depend on the specific characteristics of the beach, such as marine dynamics or even regeneration processes performed in the area. However, beachrocks of both sites apparently retain sufficient contents of metals leading to believe that they provide certain levels of contamination to these sedimentary structures.

5.4 Assessment of the contamination

The strong human alterations occurred around the estuary of Bilbao and the adjacent coast, affected the area with miscellaneous contamination (industrial and urban wastewaters, mining, metallurgy, port and chemical industry, etc.). Thus, it is characterised by its high contamination due to diverse inputs coming from rivers as well as other direct and diffuse sources. The most quantitative information about the contamination of surface waters in the specific case of the estuaries and coastal region of the Basque Country is provided by heavy metals contamination. Moreover, primary and secondary metallurgy are considered as the most relevant and direct source of metals, especially particulate metals[7], coming for instance from sea disposal of slag materials. Another significant input of metals comes from the Nerbioi-Ibaizabal estuary plume, were sediments are generally enriched in many metals. Sediment transport near the shore is determined by wave, wind and tidal induced currents but in this estuary, as mentioned before, easterly water circulation is prevailed[32-33].

Hence, although other alterations such as dredging activities and wastewater disposals should not be underestimated, Table 2 intends to show the characteristics of the main impacts in the vicinity of the studied beaches, which could be the estuary plume and the slag disposal.

Data about the contamination of the Nerbioi estuary belong to a work about a long term monitoring carried out in eight representative locations of the estuary from 2005 to 2008[34-35]. In addition, information about the outer point is specifically included, because it is located in the mouth of the estuary, thus, it is the closest point to Arrigunaga beach (Figure 5.11) and could have distinctive values, among other reasons, because it is near the outlet of Gobelas river, a water body with a dense population and industrial activity nearby[36]. Metal concentrations referred as “Slag disposal” are also given basing on an investigation of the geophysical, chemical and ecotoxicological characteristics of metal-

[32] Belzunce M.J., Solaun O., Valencia V., Pérez V., **2004**. *Contaminants in estuarine and coastal waters*.In In: Borja, A., Collins, M. (Eds.), Oceanography and Marine Environment of the Basque Country. In: Elsevier Oceanography Series, 70. Elsevier, Amsterdam, pp. 233–251.
[33] Legorburu I., Galparsoro I., Larreta J., Germán Rodríguez, Borja A., **2013**.*Spatial distribution of metal accumulation areas on the continental shelf of the Basque Country (Bay of Biscay): A GIS-based approach*. Estuarine, Coastal and Shelf Science 134, 162-173.
[34] Fdez-Ortiz de Vallejuelo S., Arana G., de Diego A., Madariaga J.M., **2010**. *Risk assessment of trace elements in sediments: the case of the estuary of the Nerbioi-Ibaizabal River (Basque Country)*. Journal of Hazardous Materials 181, 565-573.
[35] Fdez-Ortiz de Vallejuelo S., **2008**. *Diagnóstico, evolución y predicción de la concentración metálica en el estuario del río Nerbioi-Ibaizabal*. Tesis Doctoral. Universidad del País Vasco.
[36] Seebold I., Labarta C., Amigo J.M., **1983**. *Heavy metals in the sediments of the Bilbao estuary*. Analytical Techniques in Environmental Chemistry. Pergamon Press. pp. 459-464.

containing slag disposed into the sea, mainly coming from the most important steel company of the area, Altos Hornos de Vizcaya (AHV). In addition, that study includes not only the official submarine disposal site located around 4 miles away from La Salvaje beach (43º25.5´N - 3º30´W and 43º26.5´N - 3º1.7´W), but also diverse sampling points in the water area in between that official point and the coast, where small dumping areas were detected including slag materials that might have been dispersed and mixed with the original sea bed materials (Figure 5.8)[37]. Regarding the background values, they were obtained in a previous work of the research group[38] where, through the analyses performed on preindustrial non-cemented sand acquired through core drilling in Azkorri beach, the elemental reference values were established.

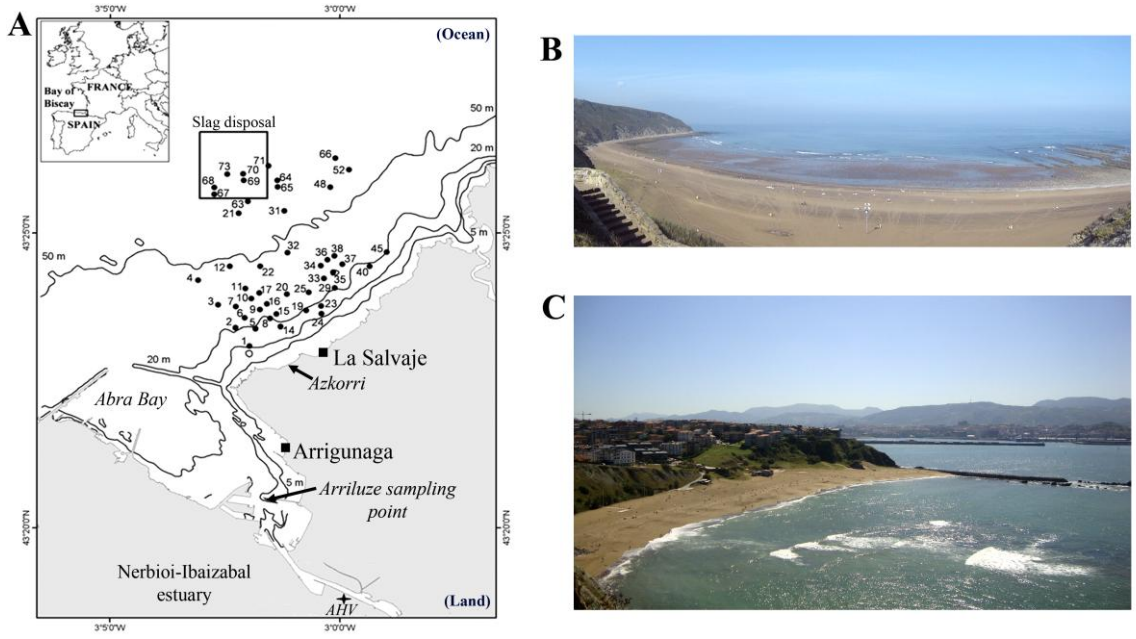

Figure 5.8. Location of the areas compared with data from Arrigunaga and La Salvaje beach. As possible contamination sources: the slag disposal and the sediment sampling points performed by Borja *et al.* (2008)[23] (bathymetric contours are shown in metres); the estuary plume represented by Arriluze as the point closest to Arrigunaga beach, and the Nerbioi-Ibaizabal estuary on the whole. The location of Azkorri beach is also specified, where background values of preindustrial non-cemented sand were obtained by Arrieta (2014)[38]. Modified from Borja *et al.* (2008)[37].Views of B) La Salvaje beach and C) Arrigunaga beach.

[37] Borja A., Tueros I., Belzunce M.J., Galparsoro I., Garmendia J.M., Revilla M., Solaun O., Valencia V., **2008**. *Investigative monitoring within the European Water Framework Directive: a coastal blast furnace slag disposal, as an example*. Journal of Environmental Monitoring 10, 453-462.

[38] Arrieta N., **2014**. *The study of an unusual temperate latitude beachrock formation. Characterization of Azkorri beach and Tunelboka cove locations*. PhD Thesis, University of the Basque Country.

Table 5.7. Comparison among the concentration ranges (mg/kg) of various elements found in the possible contamination sources (to the left of the dashed line) and the beachrock sites under study, together with background values (to the right of the dashed line).

	Nerbioi Estuary[39,40]	Nerbioi estuary mouth (Arriluze)[39,40]	Slag disposal[41]	Beachrock in Arrigunaga	Beachrock in La Salvaje	Background[42]
Fe	5230-36715	12507-16907	33000-574000	5865-23627	10294-42236	10208-12786
Mn	66-935	354-994	508-3505	1568-6556	1 577-5378	249-786
Zn	41-1260	453-1292	111-716	64-265	140-277	20-29
Pb	21-445	104-189	71-342	15-55	20-40	5-6
Cu	15-571	69-148	22-149	14-24	9-28	3-5
Ni	3.4-120	13-82	27-77	4-11	3-7	12-16
As	0.6-220	29-50	6-63	4-12	8-29	14-17
Cr	5-134	32-74	1.1-67	6-18	5-18	<LOD
Cd	0.01-17	<LOD-5	0.07-4.2	<LOD-0.205	<LOD-0.035	<LOD
Hg	N.A.	N.A.	0.16-4.3	0.05-0.32	0.08-2	0.02-0.04

*N.A.: not available

Manifold factors (chemical and geochemical processes, tidal oscillation, capability of dilution of the estuary, residence time, etc.)[43] can be involved in the transport and environmental fate of the materials coming from those sources. However, in view of the data represented in Table 5.7, the high concentrations found for many elements in Arrigunaga and La Salvaje beach, indicates that those two sites have received some kind of contamination. Note for example the high values of Mn, Zn or Pb found in both beaches, in comparison with background values. The maximum value of Fe is also higher in both beaches, although La Salvaje shows higher concentration values, probably due to the influence of the slag disposal, where the Fe is more abundant than in the estuary.

The following lines will delve further into the evaluation of the contaminants possibly retained in the analysed beachrock outcrops. It should be highlighted that the information bellow will only be referred in terms of contamination, but not pollution; as defined by Chapman (2007)[44], contamination is *the presence of a substance where it*

[39] Fdez-Ortiz de Vallejuelo S., Arana G., de Diego A., Madariaga J.M., **2010**. *Risk assessment of trace elements in sediments: the case of the estuary of the Nerbioi-Ibaizabal River (Basque Country)*. Journal of Hazardous Materials 181, 565-573.

[40] Fdez-Ortiz de Vallejuelo S., **2008**. *Diagnóstico, evolución y predicción de la concentración metálica en el estuario del río Nerbioi-Ibaizabal*. Tesis Doctoral. Universidad del País Vasco.

[41] Borja A., Tueros I., Belzunce M.J., Galparsoro I., Garmendia J.M., Revilla M., Solaun O., Valencia V., **2008**. *Investigative monitoring within the European Water Framework Directive: a coastal blast furnace slag disposal, as an example.* Journal of Environmental Monitoring 10, 453-462.

[42] Arrieta N., **2014**. *The study of an unusual temperate latitude beachrock formation. Characterization of Azkorri beach and Tunelboka cove locations*. PhD Thesis, University of the Basque Country.

[43] Belzunce M.J., Solaun O., Valencia V., Pérez V., **2004**. *Contaminants in estuarine and coastal waters*.In In: Borja, A., Collins, M. (Eds.), Oceanography and Marine Environment of the Basque Country. In: Elsevier Oceanography Series, 70. Elsevier, Amsterdam, pp. 233–251.

[44] Chapman P.M., **2007**. *Determining when contamination is pollution-Weight of evidence determinations for sediments and effluents*. Environment International 33, 492-501.

should not be or at concentrations above background; and pollution *is contamination that results in or can result in adverse biological effects to resident communities*.

5.4.1 Theoretical background of the contamination assessment

The mineralogical features of the Atlantic basin are defined by a metal rich geology, naturally loaded with iron oxides in the west of the Basque Country. Thus, natural concentration values can be locally magnified for various elements[45]. However, the above mentioned information leads to believe that some external inputs occurred in Arrigunaga and La Salvaje beach. In order to estimate the possible contribution of anthropogenic sources into the analysed beachrock samples, the **contamination factor (C_f)** of each element will be calculated. That concept was originally suggested by Hakanson (1980)[46] and it refers to the ratio between a single element concentration in a contaminated area and the background level used as a general reference, as shown in Eq. 5.1[46-48].

$$C_f^i = \frac{\overline{C}_{0-1}^i}{C_n^i} \qquad \text{(Eq. 5.1)}$$

where C_f is the contamination factor of a certain element (i) ; $\overline{C}_{0-1}^i$ the mean content ($\overline{C}$) of the element in question in superficial or uppermost sediment (0-1cm) of accumulation areas (a minimum of 5 sampling points) and C_n^i the background concentration of the element.

This index was originally applied for assessing the contamination on lakes[11], but it has been successfully used for evaluating also the contamination of diverse coastal environments such as coastal dredging areas[48], surface marine sediments[49-51], estuarine

[45] Belzunce M.J., Solaun O., Valencia V., Pérez V., **2004**. *Contaminants in estuarine and coastal waters*.In In: Borja, A., Collins, M. (Eds.), Oceanography and Marine Environment of the Basque Country. In: Elsevier Oceanography Series, 70. Elsevier, Amsterdam, pp. 233–251.
[46] Hakanson L., **1980**. *Ecological risk index for aquatic pollution control. A sedimentological approach.* Water Research 14, 975-1001.
[47] Kwon Y.T., Lee C.W., **1998**. *Application of multiple ecological risk indices for the evaluation of heavy metal in a coastal dredging area*.The Science of the Total Environment 214, 203-210.
[48] Loska K., Wiechula D., Korus I., **2004**. *Metal contamination of farming soils affected by industry*. Environmental International 30, 159-165.
[49] Pekey H., Karakas D., Ayberk S., Tolun L., Bako-glu M., **2004**. *Ecological risk assessment using trace elements from surface sediments of Izmit Bay (Northeastern Marmara Sea) Turkey.* Marine Pollution Bulletin, 48, 946-953.
[50] Muthu-Raj S., Jayaprakash M., **2007**. *Distribution and enrichment of trace metals in marine sediments of Bay of Bengal, off Ennore, south east coast of India*. Environmental Geology 56, 207-217.
[51] Esen E., Kucuksezgin F., Uluturhan E., **2010**. *Assessment of trace metal pollution in surface sediments of Nemrut Bay, Aegean Sea*. Environmental Monitoring and Assessment 160, 257-266.

samples[52], as well as other systems of environmental concern like polluted rivers[53], soils[13] and groundwaters[54]. In addition, the contamination factor resulted also a valuable tool for estimating the impact recorded in beachrock outcrops in Azkorri beach[55], leading the current assessment.

Table 5.8 shows the different classes that have been established to describe the level of contamination of specific elements based on this factor[56,57].

Table 5.8. Contamination factor (C_f) categories.

C_f	**Description**
C_f <1	no metal enrichment by natural or anthropogenic inputs
$1 \leq C_f < 3$	moderate contamination
$3 \leq C_f < 6$	considerable contamination
$C_f \geq 6$	high contamination

The C_f is a single-element index, and in relation to that, Hakanson (1980) also proposed the sum of contamination factors for all elements examined, giving as a result the contamination degree (C_d) of the environment (Eq. 5.2):

$$C_d = \sum_{i=1}^{n} C_f^i \qquad \text{(Eq. 5.2)}$$

However, some authors assert that the C_d formula showed in Equation 2 is restricted to As, Cd, Cu, Cr, Hg, Pb, Zn and polychlorinated byphenil (PCB). Those seven elements and that organic substance would need to be analysed in order to determine the correct C_d that would meet the classification of the contamination levels specified by Hakanson (1980)[56,58,59].

[52] Abrahim G. M. S., Parker R. J., **2008**.*Assessment of heavy metal enrichment factors and the degree of contamination in marine sediments from Tamaki Estuary, Auckland, New Zealand*.Environmental Monitoring and Assessment 136, 227-238.
[53] Martínez-Santos M., Probst A., García-García J., Ruiz-Romera E, **2015**.*Influence of anthropogenic inputs and high-magnitude flood event on metal contamination pattern in surface bottom sediments from the Deba River urban catchment*. Science of the Total Environment 514, 10-25.
[54] Kerndoff H., Schleyer R., Milde G., **1992**. *Geochemistry of Groundwater Pollutants at German Waste Disposal Sites*, In: Lesage S., Jacskon R.E. (Eds.), Groundwater Contamination and Analysis at Hazardous Waste Sites. Marcel Dekker Inc., New York.
[55] Arrieta N., **2014**. *The study of an unusual temperate latitude beachrock formation. Characterization of Azkorri beach and Tunelboka cove locations*. PhD Thesis, University of the Basque Country.
[56] Hakanson L., **1980**. *Ecological risk index for aquatic pollution control. A sedimentological approach.* Water Research 14, 975-1001.
[57] Esen E., Kucuksezgin F., Uluturhan E., **2010**. *Assessment of trace metal pollution in surface sediments of Nemrut Bay, Aegean Sea*. Environmental Monitoring and Assessment 160, 257-266.
[58] Caeiro S., Costa M.H., Ramos T.B., Fernandes F., Silveira N., Coimbra A., Medeiros G., Painho M., **2005**. *Assesing heavy metal contamination in Sado Estuary sediment: An index analysis approach*. Ecological Indicators 5, 151-169.

To overcome that limitation, Abrahim and Parker (2008)[60] proposed a modified **degree of contamination (mC_d)** that would allow including as many metals as the study may consider with no upper limit. In other words, the modified formula widens the application of the degree of contamination by defining the C_d as the sum of all the contamination factors (C_f) for a given set of contaminants divided by the number of analysed elements and substances (Eq. 5.3).

$$mC_d = \frac{\sum_{i=1}^{n} C_f^i}{n} \qquad \text{(Eq. 5.3)}$$

where n is the number of analysed elements, C_f the contamination factor and i the contaminant in question. Thus, mC_d provides the overall degree of contamination at a given sampling site or basin. Table 5.9 summarises the terminologies or classes used to interpret the degree of contamination[60].

Table 5.9. Degree of contamination (mC_d) categories.

mC_d	**Description**
mC_d < 1.5	Nil to very low degree of contamination
1.5 ≤ mC_d < 2	Low degree of contamination
2 ≤ mC_d < 4	Moderate degree of contamination
4 ≤ mC_d < 8	High degree of contamination
8 ≤ mC_d < 16	Very high degree of contamination
16 ≤ mC_d < 32	Extremely high degree of contamination
mC_d ≥ 32	Ultra high degree of contamination

This modified degree of contamination, complementarily to the contamination factor, has been widely used to tackle the investigation of the contamination in a wide array of environs, such as estuarine sediments[60-61], sea and lake sediments[62] as well as soils[63-64].

[59] Likuku A. S., Mmolawa K.B., G. Kabelo, **2013**.*Assessment of heavy metal enrichment and degree of contamination around copper-nickel mine in the Selebi Phikwe Region, Eastern Botswana*. Environment and Ecology Research 1, 32-40.
[60] Abrahim G. M. S., Parker R. J., **2008**.*Assessment of heavy metal enrichment factors and the degree of contamination in marine sediments from Tamaki Estuary, Auckland, New Zealand*.Environmental Monitoring and Assessment 136, 227-238.
[61] Harikumar P.S., Nasir U.P., **2010**. Ecotoxicological impact assessment of heavy metals in core sediments of a tropical estuary. Ecotoxicology and Environmental Safety 73, 1742-1747.
[62] Hahladakis J., Smaragdaki E., Vasilaki G., Gidarakos E., **2013**. *Use of Sediment Quality Guidelines and pollution indicators for the assessment of heavy metal and PAH contamination in Greek surficial sea and lake sediments*. Environmental Monitoring and Assessment 185, 2843-2853.
[63] Candeias C., Ferreira Da Silva E., Salgueiro A.R., Pereira H.G., Reis A.P., Patinha C., Matos J.X. Ávila P.H., **2010**. *Assessment of soil contamination by potentially toxic elements in the Aljustrel mining area in order to implement soil reclamation strategies*. Land degradation and development 22, 565-585.
[64] Nikolaidis C., Zafiriadis I., Mathioudakis V., Constanidis T., **2010**. *Heavy metal pollution associated with an abandone lead-zinc mine in the Kirki Region, NE Greece*. Bulletin of Environmental Contamination and Toxicology 85, 307-312.

Taking into account that information, at first, the contamination of the beachrock samples analysed in Arrigunaga beach was assessed. With that objective, samples from the transverse (ART1-ART5) and the longitudinal transect (ARL1-ARL3) were considered to get the mean concentration value of each element in that site of study. The same procedure was followed for the evaluation of the samples from La Salvaje beach, where the mean concentration value was obtained from all the data set, including the transverse (LST1-LST4) as well as the longitudinal (LSL1-LSL5) samples.

For the estimation of the contamination factor of each element in both sites, the previously mentioned background values from Azkorri beach were used as reference concentrations, because, even though it is not the exact same site, lower cores or similar uncontaminated sediments can be used for that purpose[65]; even more considering the closeness of Azkorri beach, which is located just between the analysed beaches. Finally, it should be noted that, in view of the variability in the concentration of various elements along the analysed samples, apart from the estimation of the average contamination factor, the range was also obtained (based on the minimum and maximum concentration values), in an attempt to get a more comprehensive perspective of the situation of each element.

5.4.2 Estimation of the contamination factor and degree of contamination in Arrigunaga beach

The minimum, maximum and average contamination factor values obtained from the samples analysed in Arrigunaga beach are summarised in Table 5.10.

According to the average contamination factor, it can be said that several elements show a high contamination, being in descending order, Sn > Tl > Ti > Mo > Zn > Pb > Ba > Al > Mn. Apart from the average C_f, some of them show also a minimum and maximum above the high contamination limit, that is the case of Ti, Mo and Ba. Nevertheless, in some cases, the minimum value is in the range of considerable contamination, such as for Sn, Pb, Al and Mn. Moreover, Tl and Zn show a minimum moderate contamination ($1 \leq C_f < 3$).

Other elements present a mean C_f that can be included in the considerable contamination range: Cu > Hg > Sb > K. The only element showing this level of

[65] Abrahim G. M. S., Parker R. J., **2008**.*Assessment of heavy metal enrichment factors and the degree of contamination in marine sediments from Tamaki Estuary, Auckland, New Zealand*.Environmental monitoring and Assessment 136, 227-238.

contamination in the whole range is Cu, because considering the maximum and minimum values of Hg, Sb and K their contamination factor is more variable from low to high. Various elements evidence a moderate contamination on the analysed samples, like Mg > Na > Sr > V > Co > Fe, although, the last three show minimums that indicate no natural of anthropogenic inputs. Furthermore, As, Ni and Ca are the only elements that do not show any contamination in the whole range. The overall contamination of the analysed samples, based on the modified degree of contamination, can be considered as moderate to very high (2.53 to 9.97), giving on average, a high degree of contamination (5.67).

Table 5.10. Minimum maximum and mean contamination factor values (C_f) found in the elements analysed in the beachrock samples from Arrigunaga beach, and the modified degree of contamination (mC_d).

C_f	AR min.	AR max.	AR mean	Description
Sn	4.26	25.18	**15.48**	**High contamination**
Tl	1.91	18.31	**15.11**	
Ti	8.71	18.04	**11.57**	
Mo	6.50	14.77	**11.18**	
Zn	2.78	11.51	**8.44**	
Pb	3.01	11.07	**8.37**	
Ba	7.59	10.15	**8.27**	
Al	4.06	11.63	**7.33**	
Mn	3.37	14.10	**6.11**	
Cu	3.55	6.07	**5.73**	**Considerable contamination**
Hg	1.82	10.55	**4.49**	
Sb	0.49	7.43	**3.18**	
K	1.80	4.73	**3.02**	
Mg	1.12	2.70	**1.87**	**Moderate contamination**
Na	1.20	2.16	**1.77**	
Sr	1.11	1.64	**1.37**	
V	0.96	2.17	**1.33**	
Co	0.03	1.39	**1.20**	
Fe	0.52	2.11	**1.06**	
As	0.30	0.79	**0.71**	**No metal enrichment**
Ni	0.33	0.87	**0.53**	
Ca	0.24	0.44	**0.30**	
mC_d	2.53	9.97	**5.67**	**High degree of contamination**

5.4.3 Estimation of the contamination factor and degree of contamination in La Salvaje beach

As shown in Table 5.11, the elements that show an average contamination factor considered to be high, are Sn > Hg > Tl > Zn > Ti > Mo > Ba > Mn > Al. The only

elements showing a complete range in that contamination level are Tl, Zn and Mo. Sn, Ti, Ba and Mn show a contamination level that ranges from considerable to high, while for Hg and Al, are moderate to high. Another group of elements, consisting on Pb > Cu > K > Sb, show a mean C_f that evidences a considerable contamination of those elements. Specially Pb, because Cu ranges from moderate to considerable and, K and Sb expose minimums that indicate no enrichment. In addition, Mg, Fe, Na, V, Co and As evidence a moderate contamination of those elements. However, except from Na and Mg, the rest contain the lowest C_f on the no enrichment level, a group where Sr, Ni and Ca are completely integrated. The overall contamination of the analysed samples, based on the modified contaminated degree, can be considered as moderate to very high (2.55 to 9.69), giving on average, a high contamination degree (5.07).

Table 5.11. Minimum, maximum and mean contamination factor values (C_f) found in the elements analysed in the beachrock samples from La Salvaje beach, and the modified degree of contamination (mC_d).

C_f	LS min.	LS max.	LS mean	Description
Sn	5.23	28.24	**13.32**	**High contamination**
Hg	2.66	51.70	**12.11**	
Tl	6.96	15.52	**9.52**	
Zn	6.13	12.04	**9.08**	
Ti	3.04	15.21	**8.99**	
Mo	7.24	9.34	**8.23**	
Ba	4.30	10.87	**7.40**	
Mn	3.39	11.56	**7.32**	
Al	2.09	13.70	**7.19**	
Pb	4.03	7.98	**5.87**	**Considerable contamination**
Cu	2.17	7.06	**4.03**	
K	0.54	5.91	**3.24**	
Sb	0.98	6.35	**3.06**	
Mg	1.77	3.22	**2.54**	**Moderate contamination**
Fe	0.92	3.76	**1.97**	
Na	1.07	2.85	**1.90**	
V	1.05	2.06	**1.52**	
Co	0.74	1.84	**1.35**	
As	0.54	1.92	**1.15**	
Sr	0.75	1.17	**0.95**	**No metal enrichment**
Ni	0.26	0.56	**0.42**	
Ca	0.27	0.40	**0.34**	
mC_d	2.55	9.69	**5.07**	**High degree of contamination**

5.5 Conclusions

In this work beachrocks from a sheltered beach (Arrigunaga) and an open coast exposed beach (La Salvaje) have been analysed. Moreover, Arrigunaga is located in the mouth of the Nerbioi-Ibaizal estuary, and La Salvaje is further placed to the north east, but near a submarine slag disposal. The different locations of the beaches, their characteristics, as well as the diverse impact factors that they are exposed to, might be fundamental to understand the disparities found in the results. In this sense, the strategy based on the sampling of beachrock units at different points of the beach as part of a transverse or longitudinal transect, allowed inferring various conclusions.

The main difference along the outcrops sampled in both beaches could be the distinct distribution of the elements. In Arrigunaga beach, the transverse transect is located in an area that before the regeneration of the beach, apparently was prone to accumulate contaminants from the estuary due to the obliquity of the waves in that zone. The beach, and possibly that area particularly, was also supplied by cliff derived gravels. Those facts might explain the accumulation of Ca, Al, Mg, Fe, Mn and K mostly in the cemented deposits found in the transverse transect, although the removal of cemented sand might not be disregarded. In any case, the estimation of the contamination factor showed the high contamination level of some of those elements (Al, Mn) while other ones were moderately (K, Mg, Na, Fe) or not enriched (Ca), suggesting a combination of natural and anthropogenic source for the main elements trapped in that area. With reference to the longitudinal transect, it is generally characterised by minor elements (Pb, Zn, Co, Cu, Tl or Sn) that might be derived from the contaminant materials reaching the shore, as evidenced by the high contamination level of many of them.

In La Salvaje beach in contrast, the beachrock from the transverse transect, placed in the area next to the cliff, is more characterised by the great majority of the elements. Also, many of them (such as, Sn, Hg, Tl, Zn, Ti, Mo, Ba, Mn) showed a high contamination factor. As viewed through the longitudinal transect, the further from the cliff, going towards the mid part of the beach, the less metal content seems to be trapped in the analysed beachrock outcrops. However, there is an exception with Fe, as it is more concentrated in the deposits sampled in the mid part, a fact which comes in agreement with the blackening of the beach specially affecting the mid area due to the presence of iron particles coming from the slag and other industrial wastes. The different distribution along the transverse and longitudinal transect might be triggered by the influence of various waves and tides that can be formed in the beach.

Additionally, despite the mentioned disparities, some common results were also found in the metal quantification in beachrocks from Arrigunaga and La Salvaje beach; both of them showed high contamination factors for elements like Sn, Tl, Ti, Zn, Mn and Al, as well as moderate contamination for Cu, Sb and K. Furthermore, Ca, Ni and even As did not show barely any contamination suggesting that they come from the local lithology, as concluded in the investigation of adjacent beachrocks[66] and in the study of sediments from the Nerbioi-Ibaizabal estuary[67]. Furthermore, the results referring to Fe should be highlighted because, although its contamination factor resulted slightly higher in La Salvaje than in Arrigunaga, the two beaches show an average low contamination factor for this element. This fact denotes that in spite of the massive arrival of iron containing materials, the natural background, specially rich in iron in this part of the Atlantic basin, on average might not be very enhanced by anthropogenic sources in the studied beachrocks.

Besides, there is one primary similarity between both beaches. In view of the sampled outcrops and the analysed elements, the estimation of the overall contamination degree suggested, on average, a moderate to high degree of contamination in both places. Thus, regardless of the pollution gradient existing from the estuary to the open coast, the results suggest that the wide array of contaminant sources occurring in the vicinity of the estuary, with special attention probably in the sea disposal of slag, might have triggered also the entrapment of external inputs in La Salvaje beach.

The elemental distributions discerned throughout this work were helpfully completed thanks to chemometric analyses. The correlation analyses supported that information giving an idea of the natural or anthropogenic sources of the elements, as well as suggesting a co-contamination of various elements. In addition, the PCA allowed establishing and illustrating the general distinctive trends in all the transects considered in each beach.

Therefore, this work provided the recognition of anthropogenic effects recorded in coastal sedimentary deposits, as beachrocks. The sampling strategy and methodology applied allowed characterising compositional features of unusual beachrocks and raise awareness about the collateral effects derived from a highly altered estuarine area.

[66] Arrieta N., **2014**. *The study of an unusual temperate latitude beachrock formation. Characterization of Azkorri beach and Tunelboka cove locations*. PhD Thesis, University of the Basque Country.
[67] Gredilla A., Fdez-Ortiz de Vallejuelo S., Arana G., de Diego A., Madariaga J.M., **2013**. *Long-term monitoring of metal pollution in sediments from the estuary of the Nerbioi-Ibaizabal River (2005–2010)*. Estuarine, Coastal and Shelf Science 131, 129-139.

Chapter 6

Features and implications of beachrock cements in Arrigunaga and La Salvaje beach

In view of the results collected in the previous chapters, a wide variety of grains are trapped in the analysed cemented structures. But how are those materials cemented in the beachrock? Which are the features of the cements responsible of the cohesion of the grains? These are some of the questions that lay the foundation for the analyses and results gathered in this chapter. Some clues were already inferred in Chapter 3, where evidences of high magnesium calcite (HMC) and aragonite as being part of the cements were found during the analysis of the different particle size fractions. Thus, herein a more comprehensive investigation was pursued to get detailed information about the mineral phases that compose the cements.

Cement is a precipitate that grows in pores and that requires a supersaturation of the pore fluids with respect to the cement phase, giving rise to a diagenetic process known as cementation[1]. Therefore, diagenetic minerals, such as beachrock cements, can reflect the characteristics of the fluid medium from which they were originated. In other words, the study of the beachrock cements is of great importance as it can provide information about the environment formation and pore-water chemistry, giving an idea of the context in which the cementation occurred[2].

In any case, beachrock cementation demands a massive input of dissolved calcium and carbonate (or bicarbonate) ions[2] to reach the required supersaturation conditions of $CaCO_3$, thus, the debate on the origin of beachrock regularly lies in the circumstances that prompted those conditions. Although the certain origin of the phenomenon is not fully understood yet, it is generally believed that a series of factors and processes are involved, including diverse physicochemical and biological processes[3]. The latter deserve special attention because their key role in the precipitation of carbonates either in marine or terrestrial environments in general[4], and in beachrock formation in particular[5], is recently being highlighted.

Indeed, most petrographic studies of beachrocks demonstrated the presence of organic rich micritic layers over cemented grains. The influence of organomineralization processes might not be surprising given that bacterial populations are especially abundant and productive in the intertidal zone, an area where the cementation usually occurs[6]. In this context, it is generally believed that organomineralization processes help reaching the alkalinity conditions required for carbonate precipitations, enabling the further development of crystalline phases through physicochemical processes[7,8].

[1] Flügel E., **2014**. *Microfacies of Carbonate Rocks*. Springer Science & Business Media, New York, 976 pp.
[2] Tucker M.E., Bathurst G. C., **1990**. *Carbonate diagenesis*. Blackwell Scientific Publications, Oxford, UK, 320 pp.
[3] Vousdoukas M.I., Velegrakis A.F., Plomaritis T.A., **2007**. *Beachrock occurrence, characteristics, formation mechanisms and impacts*. Earth-Science Reviews 85, 23-46.
[4] Buczynski C., Chafetz H.S., **1993**. *Habit of bacterially induced precipitates of calciumvcarbonate: examples from laboratory experiments and Recent sediments*. In: Rezak, R.,vand Lavoie, D.L., (eds.), Carbonate Microfabrics. New York: Springer-Verlag, pp. 105-116.
[5] Webb G.E., Jell J.S., Baker J.C., **1998**. *Cryptic intertidal microbialites in beachrock, Heron Island, Great Barrier Reef: implications for the microcrystalline beachrock cement*. Sedimentary Geology 126, 317-334.
[6] Turner R.J., **2005**. *Beachrock*. In: Schwartz M.L. (Ed.), Encyclopaedia of Coastal Science. Kluwer Academic Publishers, The Netherlands, pp. 183-186.
[7] Dupraz C., Reid R.P., Braissant O., Decho A.W., Norman R.S., Visscher P.T., **2008**. *Processes of carbonate precipitation in modern microbial mats*. Earth-Science Reviews 96, 141-162.
[8] Neumeier U., **1999**. *Experimental modelling of beachrock cementation under microbial influence*. Sedimentary Geology 126, 35-46.

Usually, the composition, morphology and disposition of the cements help estimating the processes and diagenetic context involved in the cementation. For instance, in modern shallow marine environments, the most commonly precipitated cements are aragonite and high magnesium calcite (HMC), whereas low magnesium calcite (LMC) is usually derived from meteoric waters[9]. Moreover, the formation of micritic HMC is considered among the evidences related to organomineralization processes. Sometimes, not only calcium carbonates, but iron rich cements could also be present, derived from chemical and/or biological processes.

Therefore, adequate tools are required to recognize and distinguish the presence of diverse calcium carbonates and iron compounds. For that purpose, the joint use of various analytical techniques was considered. Among them, Raman spectroscopy will be specifically employed because based on its capacity to distinguish between polymorph compounds it would help in the possible differentiation of HMC, calcite and/or aragonite, as well as in the possible identification of iron rich compounds. The obtained molecular composition will be complemented with X-ray powder diffraction (XRD) analyses to estimate the relative proportions of the carbonate cements as well to quantify the mole $\%MgCO_3$ content of the magnesian calcites. Recently we have demonstrated the suitability of the X-ray based techniques for the analysis of beachrock cements[10].

The other selected techniques to analyse the cements are the different imaging (optical and spectroscopic on thin sections and raw beachrock samples) techniques, being probably one of the major breakthroughs recorded in this chapter the results obtained from the different imaging tools. First, light microscopy will be used to provide a detailed visualization of the thin sections, where framework grains and cements would be observed. These observations will be aided by the staining process of part of the thin sections. This light microscopy includes polarizing microscopy (including plane polarized light (PPL) and crossed polarized light (XPL) and fluorescence microscopy. As mentioned in Chapter 3, the results derived from fluorescence microscopy, are not well understood yet in the scientific community; nonetheless, we believe that the images obtained with this technique give clues about the different characteristics of the diverse cement layers found in beachrocks from Arrigunaga and La Salvaje beach. In addition, that information will be complemented with Scanning Electron Microscopy coupled to

[9] Gischler E., Lomando A.J., **2007**. *Beachrock and Intertidal Precipitates*. In: Nash D.J., McLaren S.J. (Eds.), Geochemical Sediments and Landscapes. Wiley-Blackwell, UK, pp. 365-390.
[10] Arrieta N., Iturregui A., Martínez-Arkarazo I., Olazabal M.A., Murelaga X., Baceta J.I., Madariaga J.M., **2015**. *Multianalytical X-ray based micro-spectroscopic approach for the analysis of carbonates in beachrock cements.* Analytical Methods 7, 8865-8876.

Energy Dispersive X-ray Spectroscopy analyses (SEM-EDS), to get more detailed information and to better understand what is behind the fluorescence observed in the microscopic analyses. The SEM-EDS technique can also be used to visualize the morphology and disposition of the cements as well as to determine the elemental distribution.

In the case of the carbonate cements, the hypotheses figured out by the already mentioned techniques were supported through stable carbon and oxygen isotope measurements. Apart from beachrocks, this kind of analysis is commonly performed in carbonate precipitates found in diverse settings like reefs[11] and speleothems[12], as it can provide valuable information to help in the reconstruction of the conditions in which the precipitates were formed[13].

On the whole, the described combination of techniques aims the characterization of two main groups of cements (carbonate cements and ferruginous cements) to estimate the processes and factors behind the formation of the beachrocks. More details of the experimental procedures followed for that purpose were explained in Chapter 3. However, the molecular and structural identification of the different compounds in the cements cannot be done without the aid of the well suited Raman spectroscopy technique. In this chapter, the two previously described Renishaw equipments will be mainly used either over bulk sample fragments or over thin sections. The samples considered for this part of the research were described in section 3.1.3 of Chapter 3.

[11] González L.A., Lohmann K.C., **1985**. *Carbon and oxygen isotopic composition of Holocene reefal carbonates*. Geology 13, 811-814.
[12] Sachez-Moral S., Portillo M.C., Janices I., Cuezva S., Fernández-Cortés A., Cañaveras J.C., Gonzalez J.M., **2012**. *The role of microorganisms in the formation of calcitic moonmilk deposits and speleothems in Altamira Cave*. Geomorpholgy 139-140, 285-329.
[13] Moore C.H., **1997**. *Carbonate diagenesis and porosity*. Elsevier, Amsterdam, 338 pp.

6.1 Carbonate cements and related features

This part of the chapter will deal with the examination of the calcium carbonate cements found in the beachrocks under study, addressing also the possible similarities and differences present in Arrigunaga and La Salvaje beach.

6.1.1 Petrographic analysis

6.1.1.1 Staining of the thin sections

As mentioned in Chapter 3 (section 3.3.1), a third of each thin section was stained using a mixture of alizarin red and potassium ferricyanide, which turns calcium carbonate to red. This way, the calcium carbonate mineral phases present in the matrix, which could include, natural grains, bioclast and the cements of the beachrock itself could be better differentiated from the rest of the matrix.

Generally, the thin sections showed features common for a marine depositional environment[14], among others, well rounded clasts, occasionally bored clasts, as well as marine fossils (see Figure 6.1). With regard to the latter, the staining of calcium carbonates enabled the easy identification of the presence of several bioclasts. This way, based on visual inspections, in samples from Arrigunaga beach, bioclasts were sporadically observed together with diverse terrigenous grains, while in samples from La Salvaje beach numerous bioclasts were observed at a time, suggesting that this kind of grains might be more abundant in the studied beachrock of La Salvaje than in Arrigunaga (compare the Figures 6.1 A-B with C-D).

On the whole, the bioclasts included mollusc fragments such as, shell fragments (Figure 6.1A-C), foraminifera (Figure 6.1D), bryozoans with encrusting organisms (Figure 6.1E), echinoid fragments like sea urchins spines (Figure 6.1F), bivalves or gastropods along with various phosphatic skeletal grains (Figure 6.1G-H), as well as fragments of marine plants like rhodophyta, also known as red algae (Figure 6.1D).

[14] Van der Straaten H.C., **2009**. *Stacked Gilbert-type deltas in the marine pull-apart basin of Abaran, late Serravallian- early Tortonian, southeastern Spain*. In: Colella A., Prior D.B. (Eds.), Coarse-Grained Deltas. John Wiley & Sons, Oxford, pp. 199-222.

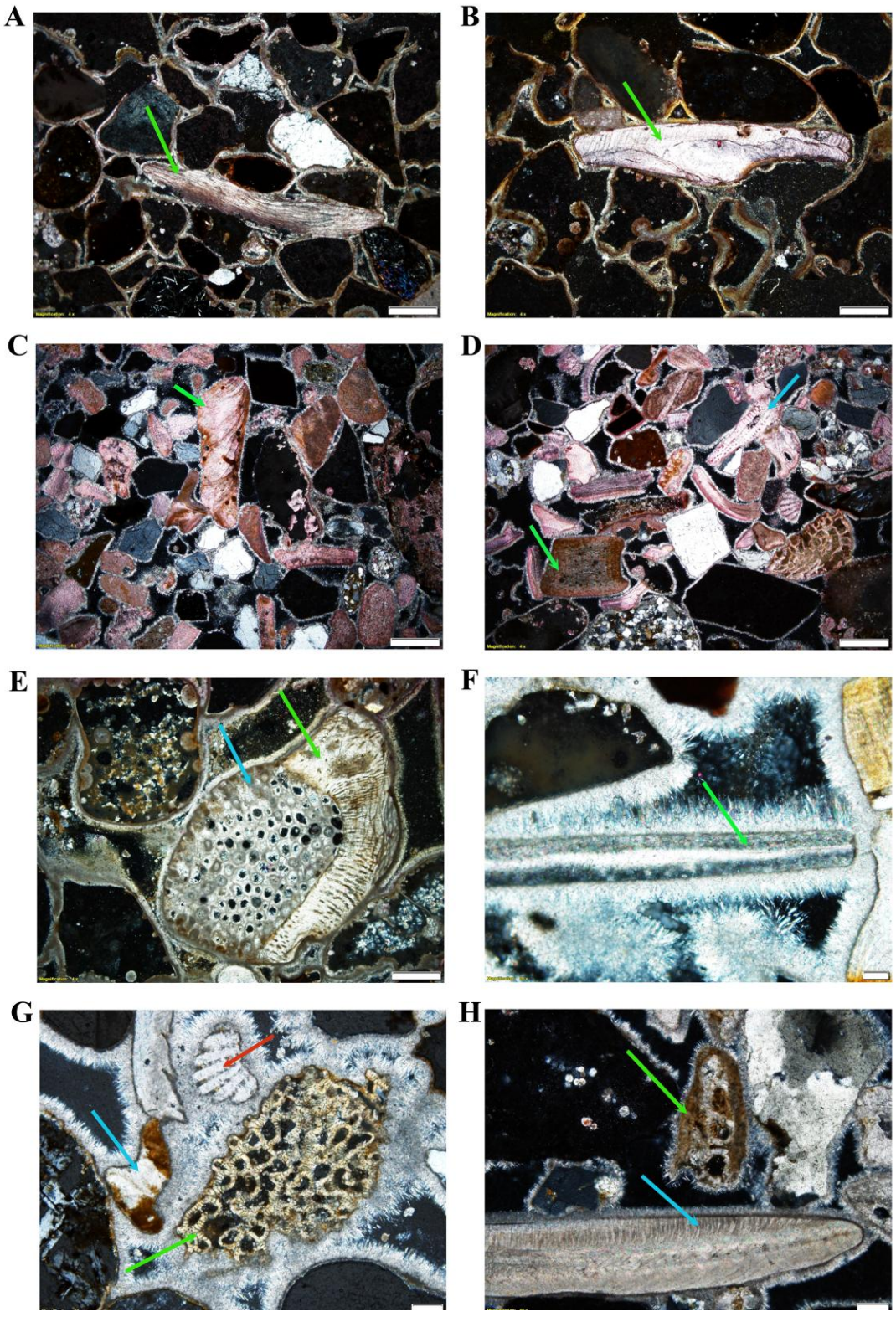

Figure 6.1. Thin section images of diverse bioclasts found within the beachrock formations: A-B) Samples from Arrigunaga beach showing shell fragments stained in red as indicated with the arrows (Scale: 200µm); C-D) Samples from La Salvaje beach with abundant bioclasts stained in red. The green arrow in C indicates a mollusc shell. In D, a red algae (green arrow) and a foraminifera (blue arrow) can be observed (Scale: 200µm); E) A shell (green arrow) encrusted in a bryoozoan (blue arrow) (Scale: 200µm); F) A sea urchin spine (Scale: 20µm); G) Close view of a gastropod (green arrow), a phosphatic fragment (blue arrow) and a shell (red arrow) (Scale: 5µm).; H) Detail of a phosphatic fragment (green arrow) and a bivalve (blue arrow) (Scale: 50µm).

Regarding the cements, in view of the areas stained in the thin sections from both sites of study, the cement more in contact with the grain in question has a more reddish coloration than the outermost cement (see Figure 6.2A-D). That different coloration denoted that micritic cements might be present in contact with the grains, which form a more compacted coating and thus might absorb more of the stain, followed by fibrous cements, which constitute a more porous layer (or less compacted) and therefore, are less stained (Figure 6.2B and Figure 6.2D). Indeed, when the thin sections were not stained, the micritic cements showed a characteristic dark-brownish colour under polarized light, as in other studies[15,16], while the transparent acicular crystals were prominently recognizable (see Figure 6.2E and Figure 6.2F).

Generally, the micritic cement is composed of HMC and acicular or needle shaped crystals are commonly made of aragonite, being both carbonates characteristic of marine conditions[17]. That concatenation of cements has been also documented in beachrocks from the Azkorri beach and Tunelboka cove[18], as well as in other cold-temperate areas like in Scotland[19], but also in lower latitudes such as the Canary Islands[20], southern Caribbean[21], or South Africa[22]. Therefore, frequently beachrock cementation starts with the precipitation of a micritic cement overlaid by a prismatic cement generation[17,23].The micritic inner coating might come from high carbonate concentrations occurring in the initial stages of the cementation[24], often aided by biological processes[23], and would control the beginning of the diagenesis. After the precipitation of the micritic cements, an abatement of the carbonates concentration can occur, moderating the precipitation of carbonates and inducing the formation of prismatic cements[17].

[15] Schölle P.A., Ulmer-Schölle D.S., **2003**. *A Color Guide to the Petrography of Carbonate Rocks: Grains, Textures, Porosity, Diagenesis*. AAPG, Memoir 77.
[16] Arrieta N., Iturregui A., Martínez-Arkarazo I., Olazabal M.A., Murelaga X., Baceta J.I., Madariaga J.M., **2015**. *Multianalytical X-ray based micro-spectroscopic approach for the analysis of carbonates in beachrock cements.* Analytical Methods 7, 8865-8876.
[17] Vousdoukas M.I., Velegrakis A.F., Plomaritis T.A., **2007**. *Beachrock occurrence, characteristics, formation mechanisms and impacts*. Earth-Science Reviews 85, 23-46.
[18] Arrieta N., Goienaga N., Martínez-Arkarazo I., Murelaga X., Baceta J.I., Sarmiento A., Madariaga J.M., **2011**. *Beachrock formation in temperate coastlines: Examples in sand-gravel beaches adjacent to the Nerbioi-Ibaizabal Estuary (Bilbao, Bay of Biscay, North of Spain)*. Spectrochimica Acta Part A 80, 55-65.
[19] Kneale D., Viles H.A., **2000**. *Beach cement: incipient CaCO3-cemented beachrock development in the upper intertidal zone, North Uist, Scotland*. Sedimentary Geology 132, 165-170.
[20] Calvet F., Cabrera M.C., Carracedo J.C., Mangas J., Pérez-Torrado F.J., Recio C., Travé A., **2003**. *Beachrocks from the island of La Palma (Canary Islands, Spain)*. Marine Geology 197, 75-93.
[21] Friedman G.M., **2004**. *Holocene chronostratigraphic beachrocks and their geological climatic significance*. In: Hill R.J., Leventhat J., Aizenshtat Z., Baedecker M.J., Claypool G., Eganhouse R., Goldhaber M., Peters K. (Eds.), Geochemical Investigations in Earth and Space Sciences: A Tribute to Isaas R. Kaplan. Elsevier, The Netherlands. pp. 125-142.
[22] Cawthra H., Uken R., **2012**. Modern beachrock formation in Durban, KwaZulu-Natal. South African Journal of Science 108, 1-5.
[23] Neumeier U., **1999**. *Experimental modelling of beachrock cementation under microbial influence*. Sedimentary Geology 126, 35-46.
[24] Scoffin, T.P., **1987**. *An Introduction to Carbonate Sediments and Rocks*. Blackie, Glasgow and Hall, New York. 274 pp.

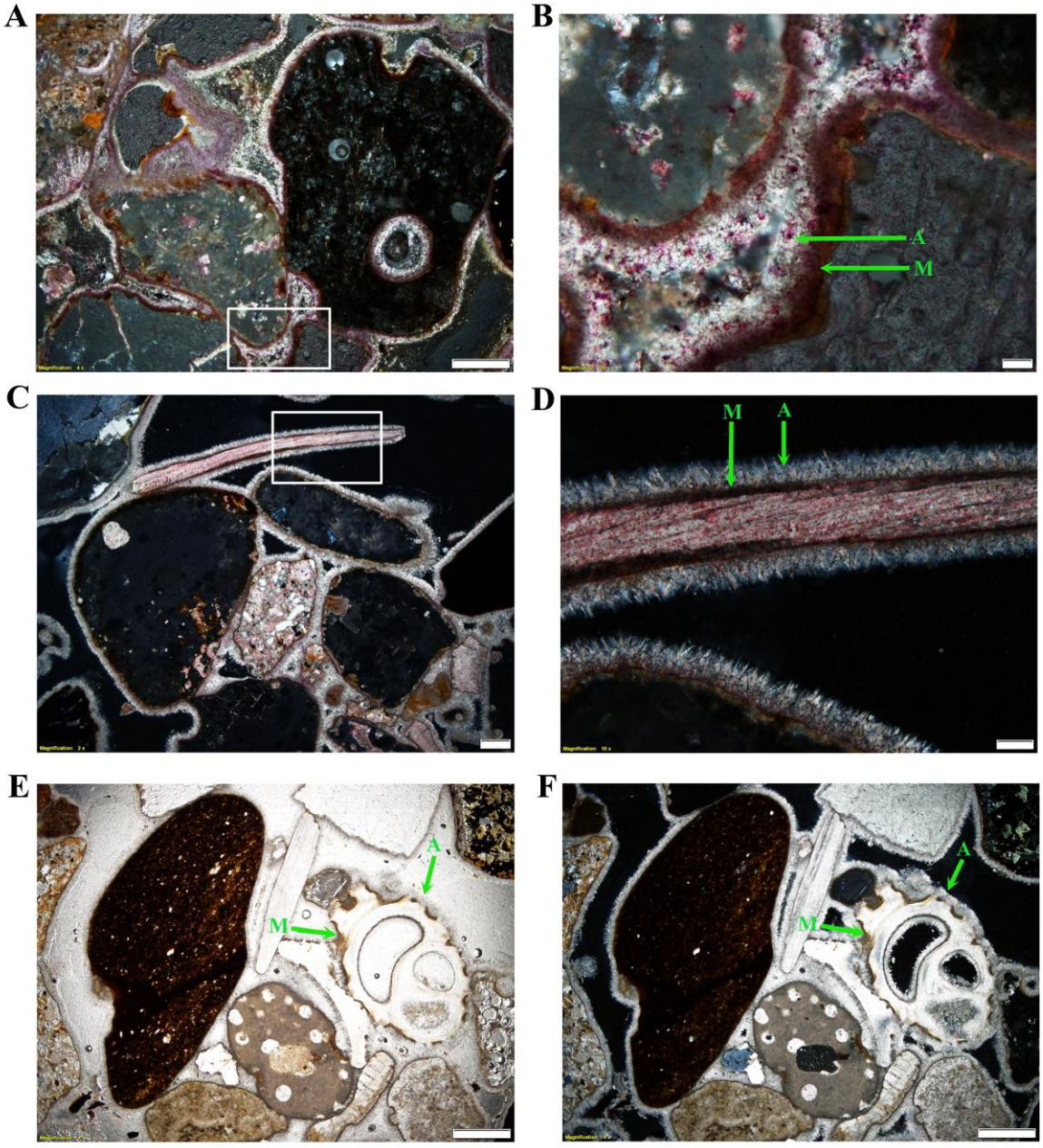

Figure 6.2. Microscopic images of stained thin sections where the reddish coloration of the calcium carbonate cements can be appreciated: A) Cross polarized light image of a sample from Arrigunaga beach, where the area shown in the image B is indicated (Scale: 200 µm); B) Close view of the area shown in the image A, where different red intensities can be observed depending on the morphology of the cement (Scale: 20 µm). C) Cross polarized light image of a sample from La Salvaje beach, showing the area zoomed in the image D (Scale: 200 µm); D) Close view of the urchin spine shown in the image C (Scale: 50 µm). Not stained thin section microscopic images: E) Plane polarized light image; F) Cross polarized light image (Scale: 200 µm), where the micritic cements show a brownish colour and the acicular are rather transparent. M: micritic. A: Acicular.

As explained before, the micritic and the acicular cements were present either in Arrigunaga or La Salvaje beach. However, some peculiarities were observed in Arrigunaga that are worth explaining. Indeed, the samples collected in the area next to the cliff, in the northernmost part of the beach, showed an envelope coating the acicular crystals that exhibited a uniform thickness and a darker colour than the needles (Figure 6.3A). This envelope resembles diagenetic features registered in other beachrocks by Viera and De Ros[25], who described a dark micritic envelope occurring over previously precipitated calcium carbonate cements and it was attributed to the presence of organic matter infiltrated in the cement under stagnant conditions.

Furthermore, frequently the intergranular pore space is filled with hetereogeneous micritic particles, generally forming a mass that fills the pore-spaces completely as shown in Figure 6.3C. However, these particles can also form irregular patches or meniscus bridges between the grains. Those conformations and the fact of not being as stained as the calcium carbonate cements, led to believe that this particles could be sediments derived from the water infiltrated through the sand in the vadose zone, as described elsewhere[25]. Moreover, similar intergranular fillings have been also found in other beachrocks[25,26].

As the micritic particles found overlapping the acicular crystals and the ones found filling the intergranular space seem to co-occur, from now on, they will be considered jointly under the category of infiltrated micritic particles in order to confirm their origin.

In summary, according to the petrographic examination, the different diagenetic features observed were: (1) micritic coating; (2) isopachous acicular rim; (3) infiltrated micritic particles. A cement sequence composed of these three main features was only observed in beachrock formations sampled in the northern area of Arrigunaga beach (Figure 6.3A-B and Figure 6.3C-D). But the samples collected in the southern point of Arrigunaga beach (Figure 6.3E-F) as well as all the samples studied from La Salvaje beach (Figure 6.4), only showed features (1) and (2).

[25] Vieira M.M., De Ros L.F., **2006**. *Cementation patterns and genetic implications of Holocene beachrocks from northeastern Brazil*. Sedimentary Geology 192, 207-230.
[26] Calvet F., Cabrera M.C., Carracedo J.C., Mangas J., Pérez-Torrado F.J., Recio C., Travé A., **2003**. *Beachrocks from the island of La Palma (Canary Islands, Spain)*. Marine Geology 197, 75-93.

6.1.1.2 Polarized light microscopy and fluorescence microscopy

In order to obtain further information about the characteristics of the cements, fluorescence microscopy was also used to examine the thin sections, as this technique can highlight the presence of relic structures or even to distinguish zoning in the cements[27].

One of the main applications of fluorescence microscopy is the detection of organic matter trapped within crystals or as remnants in pore spaces[28]. As an example, Figure 6.3A shows a microscopic image of an area (taken from a sample of Arrigunaga beach) with acicular cement covered by micritic fillings that might have an organic nature. When observed under the ultraviolet light (Figure 6.3B), those fillings were part of the most fluorescent area (brighter); the same effect was observed in the case of the pore-filling micritic particles which also resulted to be fluorescent (Figure 6.3C-D), therefore, it could confirm that during the percolation of interstitial waters, organic materials could have been deposited or formed in the pore space. In contrast, in La Salvaje beach, the beachrock formations do not show organic and fluorescent compounds neither over the acicules nor within the intergranular space (Figure 6.4A-B and Figure 6.4E-F).

The presence of organic matter is not surprising in the area where Arrigunaga beach is located, because since the end of the 19th century, the estuary of Bilbao has received loads of wastes from mining, industrial and urban effluents, which among other consequences, caused the presence of high contents of organic matter in the estuary in the middle of the 20th century[29,30]. The Nerbioi and Ibaizabal Rivers (both contributing to the formation of the estuary) are part of a nutrient rich estuarine system that gets loads of dissolved and particulate organic matter coming from the catchment basin. In addition, the estuary was characterized for decades (1890 till 1980) by eutrophic waters containing high amounts of bacteria and organics[31].

[27] James N.P., Jones B., **2015**. *Origin of Carbonate Sedimentary Rocks*. John Wiley and Son, United Kingdom.
[28] Schölle P.A., Ulmer-Schölle D.S., **2003**. *A Color Guide to the Petrography of Carbonate Rocks: Grains, Textures, Porosity, Diagenesis*. AAPG, Memoir 77.
[29] Saiz-Salinas J.I., González-Oreja J.A., **2000**. *Stress in estuarine communities: lessons from the highly impacted Bilbao estuary (Spain)*. Journal of Aquatic Ecosystem Stress and Recovery 7, 43-55.
[30] Borja A., Muxika I., Franco J., **2006**. *Long-term recovery of soft-bottom benthos following urban and industrial sewage treatment in the Nervión estuary (southern Bay of Biscay)*. Marine Ecology Progress Series 313, 43-55.
[31] Urrutxurtu I., Orive E., de la Sota A., **2003**. *Seasonal dynamics of ciliated protozoa and their potential food in an eutrophic estuary (Bay of Biscay)*. Estuarine, Coastal and Shelf Science 57, 1169-1182.

In this context, according to historical documents belonging to the *Basque Studies Society*[32], coastal currents transported impurities thrown into the ocean and they were displaced along the coast, without moving too far; indeed, urban waste waters tend to deposit in the proximities of the estuary mouth, reaching the beaches located nearby where the suspended solid materials are discharged, forming deposits of fermentable materials that produced unpleasing emanations (not nowadays with the treatment facilities that were implemented more than 20 years ago), especially in the summer time.

Therefore, the presence of an organic layer over the acicular cements and organic compounds within the pore space of the beachrock formations located in Arrigunaga, could be triggered by the influence of the estuary or even the emissions coming from Tunelboka cove, where the waters from the first sewage treatment plant of Bilbao (started in 1900 and closing in 1950) were discharged. In contrast, in La Salvaje beach, the beachrock formations do not show such organic and fluorescent compounds probably because it is an open sea beach, located away from the mouth of the estuary and from the discharge of effluents from Tunelboka cove.

However, it might be highlighted that in those cases in which the only main cements were the micritic coating and the acicular rim, the micritic cement shows the strongest fluorescence, either in Arrigunaga (Figure 6.3E-F) or in La Salvaje (Figure 6.4). Among the theories about the formation of carbonate cements commonly found in the literature, it is generally assumed that the precipitation of micritic calcium carbonate is derived from microbiological activity[33], so those crystals might contain some characteristics, such as organic traces, that provide possible evidences of the origin of the cement.

[32] Beraza R., **1919**. *El mar recipiente de todas las aguas*. Programa de Saneamiento de Poblaciones. Los Ayuntamientos y La Salud Pública. Asamblea Municipal Vasca, Sociedad de Estudios Vascos, Bilbao, pp. 369-370.
[33] Turner R.J., **2005**. *Beachrock*. In: Schwartz M.L (Ed.), Encyclopaedia of Coastal Science. Kluwer Academic Publishers, The Netherlands, pp. 183-186.

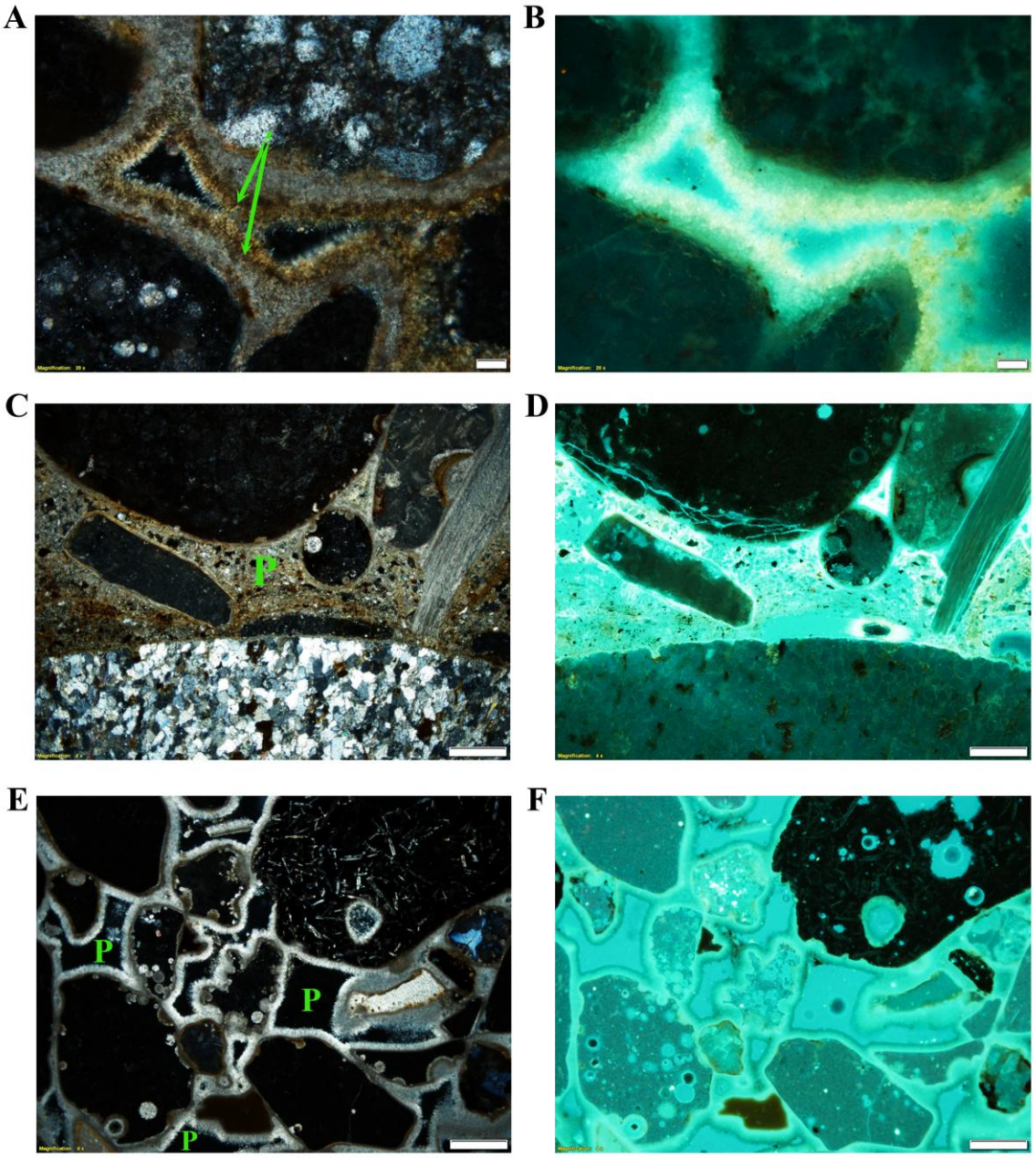

Figure 6.3. Microscopic images of thin sections belonging to beachrock formations located in Arrigunaga beach; A) Crossed polarized image of an area showing the particles infiltrated over the acicular crystals, as indicated with the arrow (Scale: 20µm); B) Same area as A, under UV light, possibly denoting the organic nature of the dark envelope indicated in the image A; C) Crossed polarized image image showing the infiltrated particles completely filling the intergranular pore space (P) (Scale: 200µm); D) Same area as C, under UV light; E) Crossed polarized image detailing a sample containing only the micritic coating and the acicular cement. Note the empty intergranular space (Scale: 200µm); F) Same area as C, under UV light.

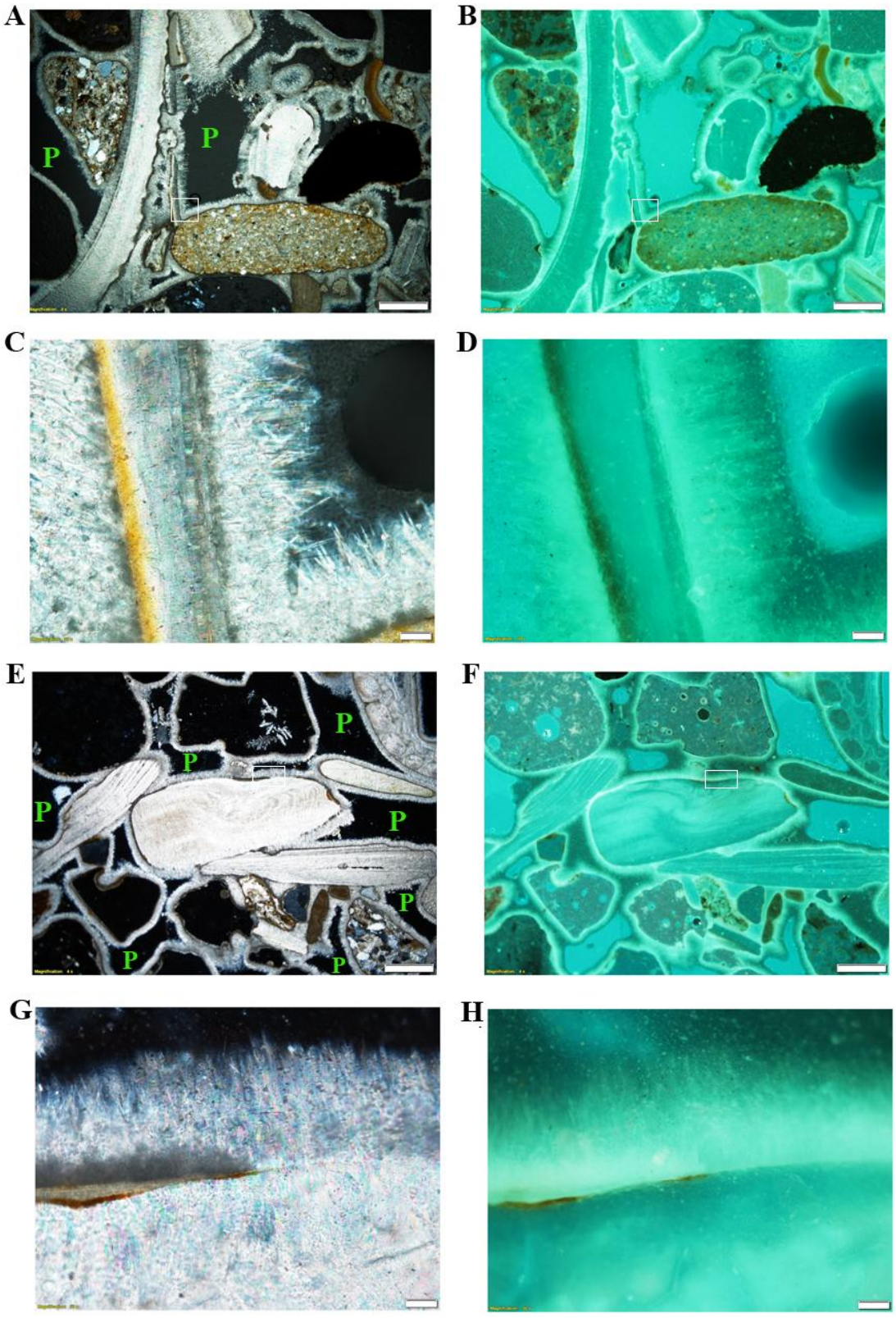

Figure 6.4. Microscopic images of thin sections belonging to beachrock formations located in La Salvaje beach. A) Crossed polarized image detailing a sample containing the micritic coating and the acicular cement (Scale: 200µm).The area analysed in C is squared; B) Same area as A, under UV light; C) Close view of image A (Scale: 10µm); D) Area shown in C, under UV light; E) Another crossed polarized image showing the typical features found in this beach (Scale: 200µm); F) Same area as E, under UV light; G) Maximised area of the E image (Scale: 10µm); H) Fluorescence microscopic image of G. P: Pore space.

6.1.2 Raman spectroscopy analyses

The straightforward molecular data provided by Raman spectroscopy, added to its ability to distinguish among polymorph compounds, make this technique a fruitful tool in the identification of not only a great variety of beachrock grains, but also in the distinction of diverse calcium carbonate cements as previously seen in Chapter 4.

In this context, calcite ($CaCO_3$) was sporadically detected among the cements with the characteristic 154, 281, 710, 1085 cm^{-1} Raman bands. In many cases, the Raman bands of the calcite were shifted few wavenumbers (for example showing bands at 155, 284, 714 and 1087 cm^{-1}), indicating the presence of high magnesium calcite ($Ca(Mg)CO_3$) and it was mainly found within the first cement layer that coats the grains. This is a common marine carbonate, containing more than 4 mole % of $MgCO_3$, randomly replacing the Ca^{2+} by Mg^{2+} in the calcite lattice[34,35] and the greater magnesium percentage yields a displacement of the bands to higher wavenumbers with respect to the calcite Raman spectrum[36-38]. In addition, differences in the halfwidth of the Raman bands (Full Width at Half Maximum of the band height, also named as FWHM), can also be relevant. The FWHM is a parameter that depends on the temperature, measurement conditions, cristallinity or replacement of trace elements. Considering the later, it is believed that the FWHM of the Raman bands belonging to calcites can be increased with a greater magnesium percentage under uniform conditions[36,37].

These facts are mainly based on a study performed by Bischoff et al. (1985)[36], where synthetic magnesium calcites with known $MgCO_3$ content were analysed by means of Raman spectroscopy. The results of that study are summarised in Table 6.1a, where the data about synthetic calcite (0 mole % of $MgCO_3$) and diverse magnesium calcites (containing 1.9, 3.9, 5.7, 8, 9.9 or 12.5 mole % of $MgCO_3$) can be observed, showing that the wavenumber and FWHM values of the bands seems to be a function of the $MgCO_3$ content.

[34] Vousdoukas M.I., Velegrakis A.F., Plomaritis T.A., **2007**. *Beachrock occurrence, characteristics, formation mechanisms and impacts*. Earth-Science Reviews 85, 23-46.
[35] Andersson A.J., Mackenzie F.T., Bates N.R., **2008**. *Life on the margin: implications of ocean acidification on Mg-calcite, high latitude and cold-water marine calcifiers*. Marine Ecology Progress Series 373, 265-273.
[36] Bischoff W.D., Sharma S.K., Mackenzie F.T., **1985**. *Carbonate ion disorder in synthetic and biogenic magnesian calcites: a Raman spectral study*. American Mineralogist, 70, 581-589.
[37] Urmos J., Sharma S.K., Mackenzie F.T., **1991**. *Characterization of some biogenic carbonates with Raman Spectroscopy*. American Mineralogist 76, 641-646.
[38] Gomez-Nubla L., Aramendia J., Fdez-Ortiz de Vallejuelo S., Castro K. and Madariaga J.M., **2013**. *From Portable to SCA Raman devices to characterize harmful compounds contained in used black slag produced in Electric Arc Furnace of steel industry*. Journal of Raman Spectroscopy 44, 1163-1171.

Therefore, to confirm the presence of HMC, Table 6.1b shows the Raman bands as well as the FWHM of various Raman spectra belonging to our calcite beachrock cements obtained with the Renishaw InVia confocal micro Raman spectrometer (described in Chapter 3) under the same measurement conditions (5 seconds, 20 accumulations and 40% of laser power), to appreciate differences just due to the compound itself. The corresponding spectra can be observed in Figure 6.5.

In the data provided in Table 6.1b, *Calcite 1* refers to an example of a set of Raman bands assigned to calcite, and there are other four compounds referred as *Mg calcite*, as examples of Raman bands attributed to probable high magnesium calcites. Comparing the calcites and the high magnesium calcites identified in the beachrock cements of this study, it can be seen that the position of the bands is generally shifted to higher wavenumbers possibly due to a greater mole percentage of $MgCO_3$. In addition, differences in the FWHM can also be perceived, which might be worth mentioning.

For instance, it can be seen that the position of the lattice mode (~279 cm^{-1}) of *Calcite 1* is similar to *Mg calcite 1*, but the halfwidht varies from one to another, being larger in the magnesium calcite (Table 6.1b). The same trend can be observed in the synthetic magnesium calcites provided by Bischoff et al. (1985)[39] (Table 6.1a), between the Calcite and the phases with 1.9 and 3.9 mole % of $MgCO_3$, or even between magnesium calcite containing 8 and 9 mole % of $MgCO_3$.

Regarding the in-plane bending mode (~710 cm^{-1}) *Mg calcite 3* and *Mg calcite 4* show a similar position at 714 cm^{-1} but the FWHM differs between them, as it consists in 11.7 and 15.0 cm^{-1}, respectively (Table 6.1b). Again, that tendency of having a similar band position, but a dissimilar FWHM, is observed in the synthetic phases containing 8, 9 and 12.5 mole % of $MgCO_3$ (Table 6.1a). Furthermore, *Mg calcite 3* and *Mg calcite 4* also show that peculiarity in the symmetric stretching mode (~1087 cm^{-1}), as well as the just mentioned synthetic phases.

[39] Bischoff W.D., Sharma S.K., Mackenzie F.T., **1985**. *Carbonate ion disorder in synthetic and biogenic magnesian calcites: a Raman spectral study*. American Mineralogist, 70, 581-589.

Table 6.1a Summary of the Raman bands position (and FWHM) cm^{-1} belonging to synthetic magnesian calcite phases documented by Bischoff et al. (1985)[40]. Laser used: 488nm.

	Magnesian calcite synthetic phases (mole % $MgCO_3$)						
Vibration mode	**Calcite**	**1.9**	**3.9**	**5.7**	**8**	**9.9**	**12.5**
L	281 (10.1)	281 (12.0)	281 (13.8)	282 (15.6)	284 (15.1)	284 (18.3)	283 (20.0)
ν_4	711 (3.6)	711 (4.8)	712 (5.9)	712 (7.4)	714 (8.7)	714 (9.7)	714 (12.2)
ν_1	1085 (2.5)	1085 (4.2)	1086 (5.6)	1086 (6.5)	1087 (7.1)	1087 (7.6)	1087 (9.2)

Table 6.1b Summary of the Raman bands position (and FWHM) cm^{-1} belonging to calcites and magnesian calcites found in beachrock cements of this study. Laser used: 785 nm.

	Beachrock cements of this study				
Vibration mode	**Calcite 1**	**Mg calcite 1**	**Mg calcite 2**	**Mg calcite 3**	**Mg calcite 4***
L	281 (12.0)	280 (18.2)	280 (20.0)	281 (21.7)	283 (25.0)
ν_4	710 (8.0)	712 (9.9)	713 (10.0)	714 (11.7)	714 (14.0)
ν_1	1085 (7.0)	1086 (9.9)	1086 (9.9)	1087 (10.1)	1087 (12.0)
Estimated mole % $MgCO_3$	0.0%	3.9-5.7%	5.7-8%	8-9.9%	9.9-12.5%

L: librational higher wavenumber lattice mode; ν_4: in-plane bending internal mode; ν_1: symmetric stretching internal mode.

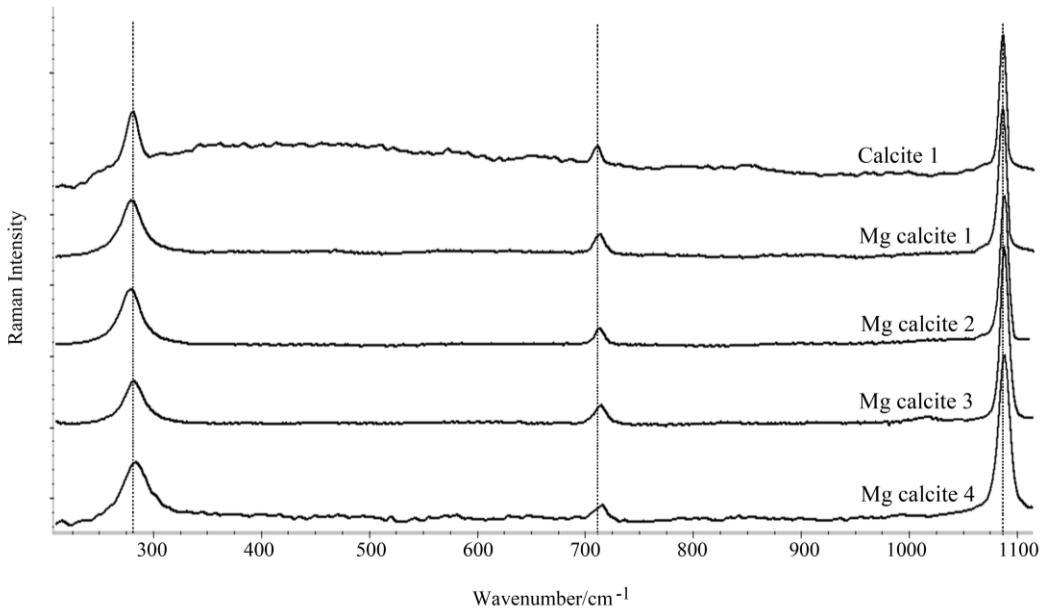

Figure 6.5. Raman spectra obtained in the analysis of the first cement layer that covers the grains. *Calcite 1* represents the spectrum of a calcite with 0 mole % of $MgCO_3$, while *Mg calcite 1*, *Mg calcite 2*, *Mg calcite 3* and *Mg calcite 4* represent magnesian calcites that, according to the band shift to higher wavenumbers and the greater FWHM, presumably contain certain mole % of $MgCO_3$. The dashed lines help in observing those differences in the position of the bands and the FWHM.

[40] Bischoff W.D., Sharma S.K., Mackenzie F.T., **1985**. *Carbonate ion disorder in synthetic and biogenic magnesian calcites: a Raman spectral study*. American Mineralogist, 70, 581-589.

It should be clarified that when comparing the results of the synthetic phases and the beachrock cements, it has to be taken into account that Bischoff et al. (1985)[41] used a 488 nm laser, while our beachrock cements were measured with a 785 nm laser. The use of different laser wavelengths does not necessarily influence in the band position specially when dealing with carbonates, but it could certainly change the FWHM of the bands. Moreover, compounds synthesized in the laboratory and naturally occurring minerals have inherent differences that may not produce the same Raman response. Therefore, the point here is not the comparison between the values themselves, but the tendencies and the proportion incremented. For example, Table 6.1a shows a synthetic Calcite with a Raman band at 281 cm^{-1} and a FWHM value of 10.1 cm^{-1}, while the Magnesium calcite containing 12.5 mole % of $MgCO_3$, shows a Raman band at 283 cm^{-1} and a FWHM value of 20.0 cm^{-1}. In other words, according to the data of Bischoff et al. (1985)[41] the difference between the pure calcite and the magnesium calcie (12.5%) is two units (in cm^{-1}) in the Raman band position and around 10 units (in cm^{-1}) in the FWHM. Focusing now on the compounds identified in the beachrock cements (Table 6.1b), *Calcite 1* exhibited a Raman band also at 281 cm^{-1} and *Mg calcite 4* at 283 cm^{-1}, and although the values of FWHM do not exactly coincide with the Table 6.1a, they show again an increment of around 10 units (in cm^{-1}).

Making that comparison with all the bands of the compounds summarised in Table 6.1b, it can be suggested that apart from the presence of pure calcite, cements composed of magnesium calcite containing between 3.9 and 12.5 mole % of $MgCO_3$ might have been unravelled with Raman spectroscopy (Table 6.1b). Thus, the presence of HMC would confirm that the micritic coating observed during the petrographic analyses could be composed of this carbonate phase. This result can be rather relevant because magnesium calcite in contact with seawater is believed to have mainly a biogenic provenance[42], so the presence of HMC micritic cement could give some clues about the first stages of the cementation provably related to organomineralization processes.

[41] Bischoff W.D., Sharma S.K., Mackenzie F.T., **1985**. *Carbonate ion disorder in synthetic and biogenic magnesian calcites: a Raman spectral study*. American Mineralogist, 70, 581-589.
[42] Bischoff W.D., Bishop F.C., Mackenzie F.T., **1983**. *Biogenically produced magnesian calcite: inhomogeneities in chemical and physical properties; comparison with synthetic phases*. American Mineralogist, 68, 1183-1188.

In order to progress in the understanding of the formation of the cements, in a next step, the acicules found over the micritic HMC were analysed. Within those acicules, aragonite was ascertained showing Raman bands at 152, 205, 704, 1084 cm^{-1}. In spite of the presence of micritic HMC, aragonite has been occasionally found as the unique mineral that binds beachrock grains. The aragonite might be detected in solitude, or, as shown in Figure 6.6, accompanied by other bands between 1160 and 1939 cm^{-1}, probably attributed to a result of the luminescence emission phenomenon triggered by the presence of siliceous materials containing rare earth elements[43,44], as it was already mentioned in Chapter 4 (section 4.2.1). Figure 6.6 also shows that aragonite can be found even together with other carbonate minerals like hydromagnesite ($Mg_5(CO_3)_4(OH)_2 \cdot 4H_2O$), recognised through its main Raman band at 1118 cm^{-1}. Other secondary bands were also detected at 181 cm^{-1} and 1490 $cm^{-1,}$ which can be characteristic either of aragonite or hydromagnesite, thus, they probably, belong to overlappings of CO_3^{2-} vibration modes.

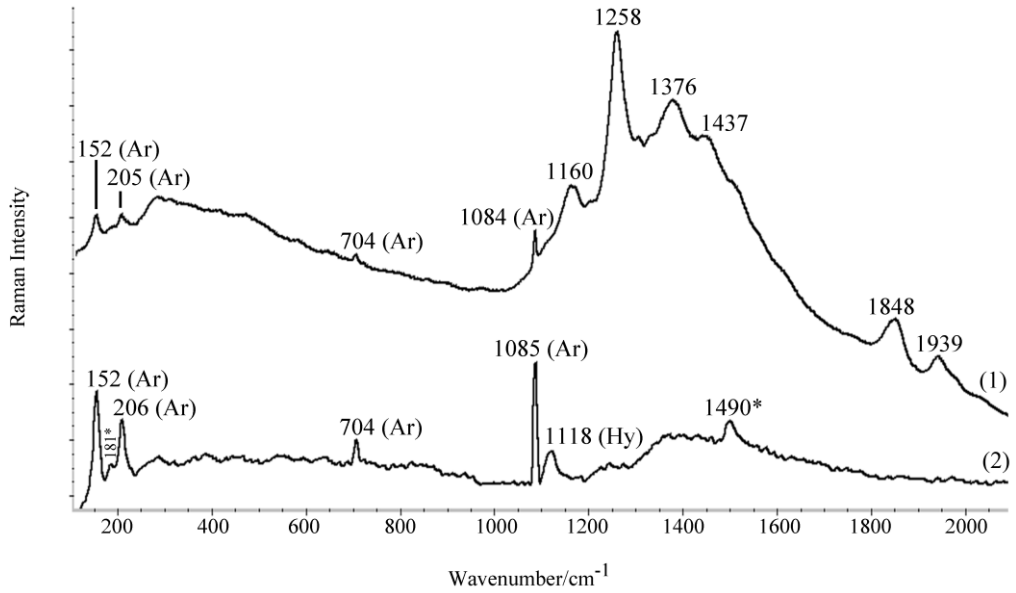

Figure 6.6. 1) Raman spectrum of aragonite (Ar), the main phase composing the acicular cement. Sometimes, various signals can be detected in the 1160-1939 cm^{-1} region probably derived from siliceous materials containing rare earth elements; 2) Occasionally, the Raman spectrum of the aragonite (Ar) detected within the acicular cement also shows bands belonging to hydromagnesite (Hy). *Raman signals attributable to a mixture of aragonite and hydromagnesite.

[43] Gomez-Nubla L., Aramendia J., Fdez-Ortiz de Vallejuelo S., Castro K. and Madariaga J.M., **2013**. *From Portable to SCA Raman devices to characterize harmful compounds contained in used black slag produced in Electric Arc Furnace of steel industry*. Journal of Raman Spectroscopy 44, 1163-1171.
[44] Lenz C., Talla D., Ruschel K., Škoda R., Götze J., Nasdala L., **2013**. *Factors affecting the Nd^{3+} (REE^{3+}) luminescence of minerals.* Mineralogy and Petrolology 107, 415-428.

Hydromagnesite can be a naturally occurring mineral in evaporites, but it also appears in weathered synthetic bricks, mortars or even meteorites[45]. Hydromagnesite usually comes from the alteration of magnesium rich minerals[46] and it has been also found in highly alkaline lacustrine water bodies, associated to extensive biofilms formed over stromatolite deposits[47], and even in karstic cave deposits[48] together with aragonite needles formed under microbial influence[49]. Therefore, the presence of hydromagnesite within the beachrock cements gives us some clues about the factors involved in the precipitation of aragonite. Thinking on possible biological factors, it should be mentioned that aragonite appears here together with a repeated silhouette with distinctive Raman peaks at around 1109-1853 cm^{-1}, as well as at 3136, 3229, 3278 cm^{-1} (Figure 6.7).

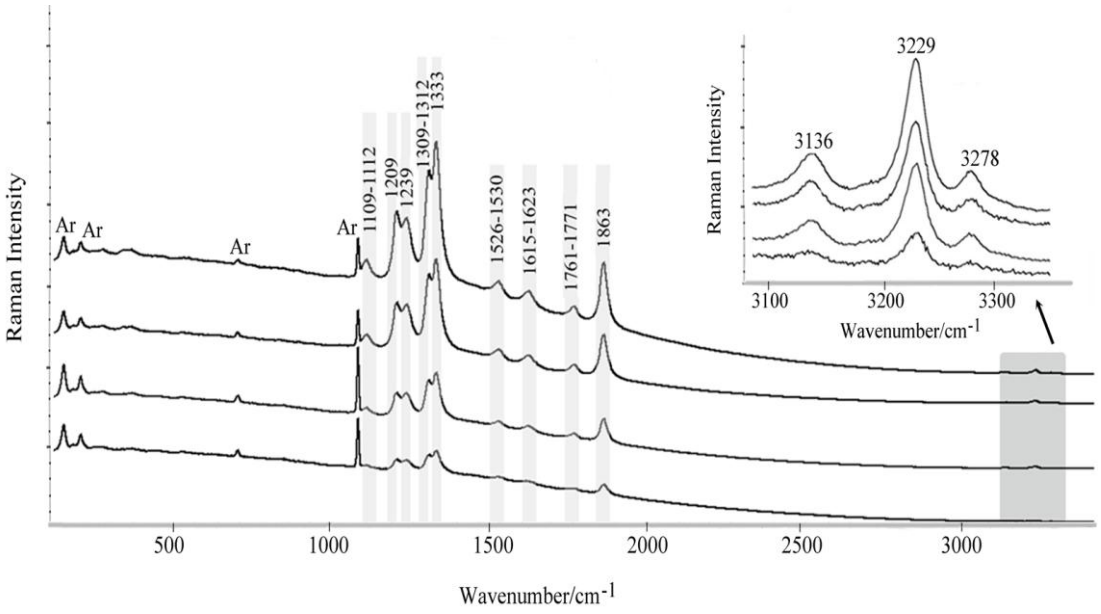

Figure 6.7. Raman spectra of the aragonite acicular cement, with other Raman bands in the 1109-1863 cm^{-1} region, as well as around 3100-3300 cm^{-1}, denoting the possible presence of an organic compound (see the text for band assignment).

In the literature, the processes whereby biologically mediated activities of organisms promote calcium carbonate nucleation and growth have been widely researched. It is believed that microbially derived organics might enhance the cohesion

[45] Frost R.L., **2011**. *Raman spectroscopic study of the magnesium carbonate mineral-hydromagnesite*. Journal of Raman Spectroscopy 42, 1690-1694.
[46] Edwards H.G.M., Jorge Villar S.E., Jehlicka J., Munshi T., **2005**. *FT-Raman spectroscopic study of calcium-rich and magnesium-rich carbonate minerals*. Spectrochimica Acta Part A 68, 1058-1064.
[47] Braithwaite C.J.R., Zedef V., **2008**. *Hydromagnesite stromatolites and sediments in an alkaline lake, Salda Golu, Turkey*. Journal of Sedimentary Research 66, 991-1002.
[48] Martínez-Arkarazo I., Angulo M., Zuloaga O., Usobiaga A., Madariaga J.M., **2007**. *Spectroscopic characterisation of moonmilk deposits in Pozalagua tourist Cave (Karrantza, Basque Country, North of Spain)*. Spectrochimica Acta Part A 68, 1058-1064.
[49] Cañavera J.C., Hoyos M., Sanchez-Moral S., Sanz-Rubio E., Bedoya J., **1999**. *Microbial communities associated with hydromagnesite and needle-fiber aragonite deposits in a karstic cave (Altamira, Northern Spain)*. Geomicrobiology Journal 16, 9-25.

of the grains, leading to the formation of micritic coatings (commonly composed of HMC) and the succeeding epitaxial development of acicular cements[50-53], as in this case.

The macromolecules composing the organic matrix involved in the organomineralization processes provide an acidic character to the biofilm mainly due to the presence of amino acids like aspartic acid and glutamic acid. Those negatively charged carboxyl groups (-COOH) tend to bind dissolved Ca^{2+} increasing the alkaline level of the pore water and thus, enabling the precipitation of calcium carbonate[54-56]. The aforementioned group of bands resembles those documented for organic and biological systems. Indeed, between 1000 and 1200 cm^{-1} C-C single bond stretching vibrations and contributions from C-N and C-O vibrations can be found. Furthermore, the range of 1239-1333 cm^{-1} could be related with amide III, including overlapping of C-H bending modes and CH_2 twisting vibrations[57]; more specifically, the intense Raman band at 1335 cm^{-1} resembles the main Raman band of the aspartic acid[58,59]. In addition, the 3000-3500 cm^{-1} region is commonly attributed to water or hydroxyl (-OH) group. In proteins N-H stretching vibrations arise near that region but its measurement might be an arduous labour because of their width and the presence of various strongly overlapping OH and NH bands from water and other amino acid residues[60]. However, in general, amino acids, peptides, and proteins usually display C-H stretching vibration bands in the 2800-3200 cm^{-1} region of the Raman spectrum[61].

[50] Bernier P., Guidi J.B., Bottcher M.E., **1997**. *Coastal progradation and very early diagenesis of ultramafic sands as a result of rubble discharge from asbestos excavations (northern Corsica, western Mediterranean)*. Marine Geology 144, 163-175.
[51] Teng H.H., Dove P.M. **1997**. *Surface site-specific interactions of aspartate with calcite during dissolution: Implications for biomineralization*. American Mineralogist 82, 878-887.
[52] Webb G.E., Jell J.S., Baker J.C., **1998**. *Cryptic intertidal microbialites in beachrock, Heron Island, Great Barrier Reef: implications for the microcrystalline beachrock cement*. Sedimentary Geology 126, 317-334.
[53] Dupraz C., Pamela Reid R., Braissant O., Decho A.W., Sean Norman R., Visscher P.T., **2008**. *Processes of carbonate precipitation in modern microbial mats*. Earth-Science Reviews 96, 141-162.
[54] Braissant O., Callileau G., Dupraz C., Verecchia E.P., **2003**. *Bacterially induced mineralization of calcium carbonate in terrestrial environments: the role of exopolysaccharides and amino acids*. Journal of Sedimentary Research 73, 485-490.
[55] Vousdoukas M.I., Velegrakis A.F., Plomaritis T.A., **2007**. *Beachrock occurrence, characteristics, formation mechanisms and impacts*. Earth-Science Reviews 85, 23-46.
[56] Dupraz C., Visscher P.T., Baumgartner L.K., Reid R.P., **2004**. *Microbe-mineral interactions: early carbonate precipitation in a hypersaline lake (Eleuthera Island, Bahamas)*. Sedimentology 51, 745-765.
[57] Sánchez-Román M., Fernández-Remolar D., Amils R., Sánchez-Navas, Schmid T., San Martin-Uriz P., Rodríguez N., McKenzie J.A., Vasconcelos C., **2014**. *Microbial mediated formation of Fe-carbonate minerals under extreme acidic conditions*. Scientific Reports 4, 1-7.
[58] Culka A., Jehlička J., Edwards H.G.M., **2010**. *Acquisition of Raman spectra of amino acids using portable instruments:Outdoor measurements and comparison*. Spectrochimica Acta Part A 77 (5), 978-983.
[59] Maruyama K., Yoshino T., Kagi H., **2011**. *Synthesizing a composite material of amorphous calcium carbonate andaspartic acid*. Materials Letters 65, 179-181.
[60] Braiman M.S., Briercheck D.M., Kriger K.M., **1999**. *Modelling Vibrational Spectra of Amino Acid Side Chains in Proteins: Effects of Protonation State, Counterion, and Solvent on Arginine C-N Stretch Frequencies*. The Journal of Physical Chemistry 103, 4744-4750.
[61] Howell N.K., Arteaga G., Nakai S., Li-Chan E.C.Y., **1999**. *Raman Spectral Analysis in the C-H Stretching Region of Proteins and Amino Acids for Investigation of Hydrophobic Interactions*. Journal of Agricultural and Food Chemistry 47, 924-933.

The presence of some kind of organic compound in association with aragonite cements was already suspected on account of the results described in Chapter 4 (section 4.1.2). Moreover, this finding was not only based on beachrock cements from Arrigunaga and La Salvaje beach, but also in results obtained from the study of the adjacent cemented deposits in Azkorri beach[62].

6.1.3 X-Ray Diffraction analysis (XRD)

In an attempt to support the information acquired so far about the molecular composition of the cements, XRD analyses were commissioned to the G*eneral X-ray Service* of the University of the Basque Country (SGiker-UPV/EHU). Three objectives were pursued through this analysis: the identification of minerals, estimation of the carbonate mineral percentages and the determination of mole % of $MgCO_3$ in HMC.

Regarding the minerals detected probably not directly related to the beachrock cements, mineral phases like gypsum ($CaSO_4 \cdot 2H_2O$) and halite (NaCl) were found. Both of them are considered as evaporate minerals possibly formed due to daily alternation of the tides; it could happen that there is seawater movement, which in most arid periods is evaporated, increasing the salts contents in the interstitial waters and gypsum and halite salts precipitate[63]. In addition, trigonal quartz (SiO_2) and silicates belonging to the akermanite-gehlenite ($Ca_2Mg(SiO_7)$-$Ca_2Al(AlSiO_7)$) series were identified, which could be part of the matrix of framework grains. For instance, akermanite and gehlenite are believed to be typical slag minerals[64], indeed these mineral phases have been also found in beachrock formations from Azkorri and Tunelboka as part of slag materials[65], and some studies suggest that they can be a result of slag recrystallization[66]. Moreover, an amorphous phase that could be attributed either to natural organic matter or to vitreous phases present in slag was also recognised.

Focusing more in detail on the cements, three calcium carbonate phases were discerned: trigonal calcite ($CaCO_3$), trigonal high magnesium calcite ($Ca(Mg)CO_3$) and orthorhombic aragonite ($CaCO_3$). Figure 6.8 and Figure 6.9 show some representative

[62] Arrieta N., **2014**. *The study of an unusual temperate latitude beachrock formation. Characterization of Azkorri beach and Tunelboka cove locations*. PhD Thesis, University of the Basque Country.
[63] Warren J.K., **2006**. *Evaporites: Sediments, Resources and Hydrocarbons*. Springer, Berlin, 1036pp.
[64] Engström F., Adolfsson D., Samuelsson C., Sandström Å., Björkman B., **2013**. *A study of the solubility of pure slag minerals*. Minerals Engineering 41, 46-52.
[65] Arrieta N., Iturregui A., Martínez-Arkarazo I., Olazabal M.A., Murelaga X., Baceta J.I., Madariaga J.M., **2015**. *Multianalytical X-ray based micro-spectroscopic approach for the analysis of carbonates in beachrock cements.* Analytical Methods 7, 8865-8876.
[66] Puertas F., Gil-Maroto A., Palacios M., Amat T., **2006**. *Morteros de escoria activada alcalinamente reforzados con fibra de vidrio AR. Comportamiento y propiedades.* Materiales de construcción 56, 79-90.

examples of the diffractograms from which the information about the cements was extracted.

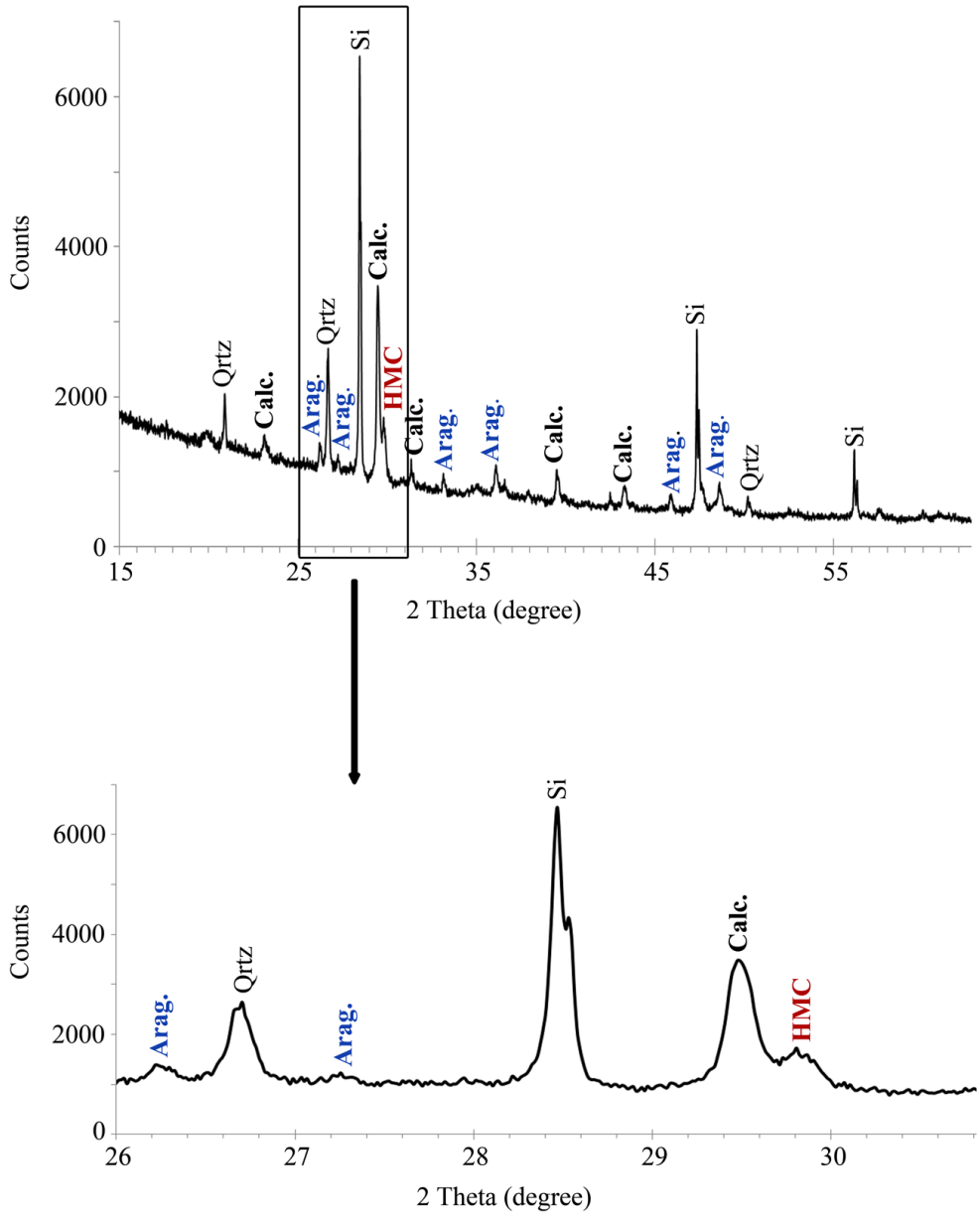

Figure 6.8. XRD diffractogram obtained from powdered cements of a sample from Arrigunaga beach and magnification of the 26-31 2Theta (degree) region, to remark the signals derived from calcium carbonates. Arag.: aragonite; Qrtz.: quartz; Si; silicon; Calc.: calcite; HMC: high magnesium calcite with 13.1 mol % of $MgCO_3$.

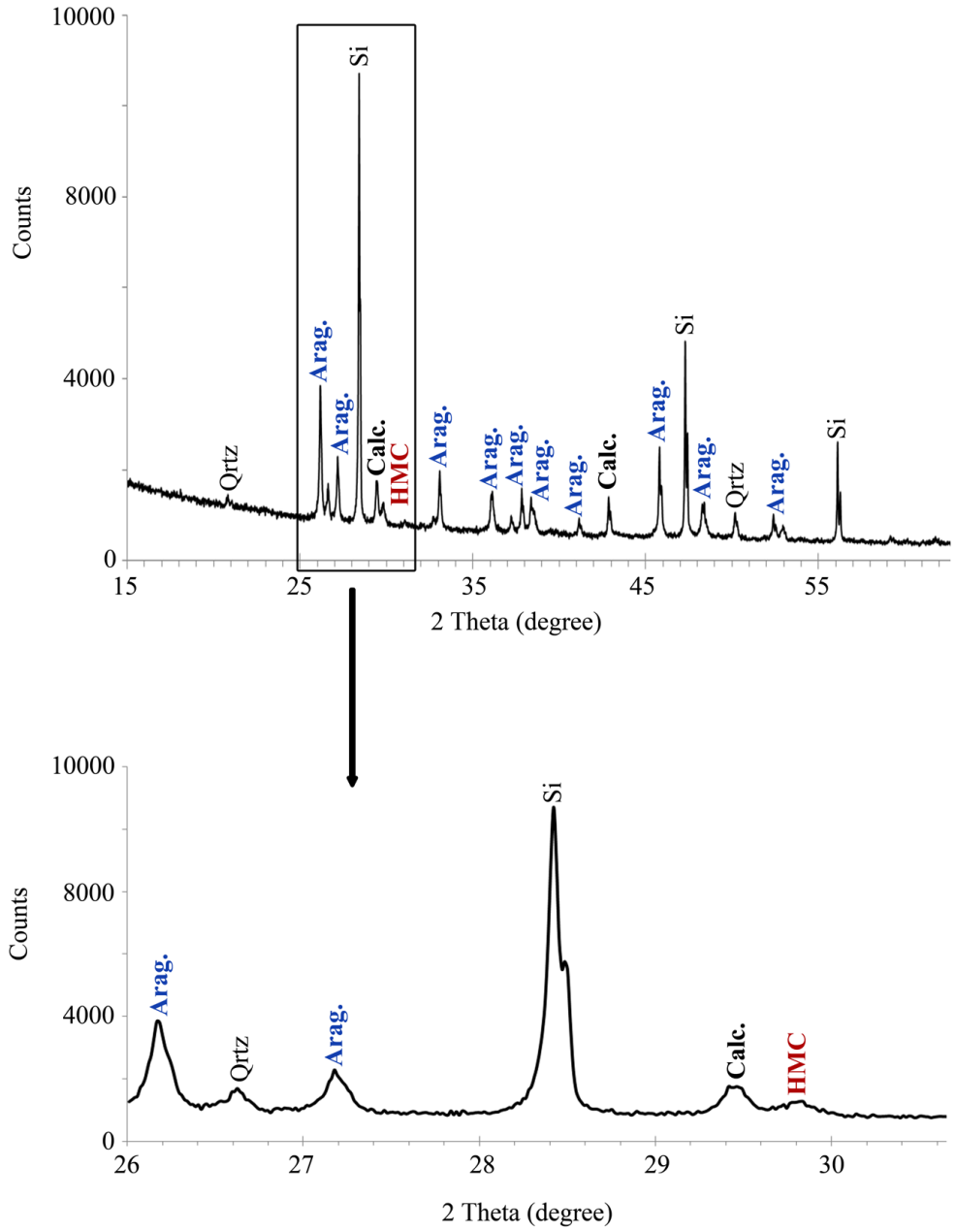

Figure 6.9. XRD diffractogram obtained from powdered cements of a sample from La Salvaje beach, maximising the 26-31 2 Theta (degree) region, to remark the signal derived from calcium carbonates. Arag.: aragonite; Qrtz.: quartz; Si; silicon; Calc.: calcite; HMC: high magnesium calcite with 13.8 mol % of $MgCO_3$.

Considering that the calcium carbonate phases are the main components of the cements, a semiquantitative estimation of their relative proportions was carried out basing on the RIR (*Reference Intensity Ratio*) values. To recognise the relative proportions of the carbonate phases, in all the cases cubic silicon was added to the samples. The three carbonate cements would account for the 100%, as the other mineral and amorphous phases were not considered. The results confirmed that aragonite is the main carbonate composing the cements, as this mineral phase represented around the 67-68% of the carbonates in the samples from Arrigunaga and La Salvaje beach. On the contrary, calcite accounted for the 26-29% of the carbonates in both sites of study, and HMC around the 6-9%.

Regarding the mol % of $MgCO_3$ content of the calcites, it must be explained that when HMC is detected, the diffractogram shows a shoulder in the main calcite peak because of the changes occasioned by Mg in the cell size (see Figure 6.7 and Figure 6.8). Indeed, increasing amounts of Mg in the calcite lattice reduce the cell size, which causes a displacement of the peak to a higher 2Theta; the greater the Mg content in the HMC, the greater is the displacement of the peak. Thus, the $MgCO_3$ content can be estimated following the Lumsden (1979)[67] equation, which relates the mol % $MgCO_3$ content of the calcite with the displacement of the peak[68]. The silicon added to each sample was used as an internal standard to correct the position of the displacement previously to the application of the equation. On this basis, the lowest values of mol % $MgCO_3$ in the calcites ranged between 1 and 4.4%, but the higher ones between 10.7 and 14.3%. Thus, similarly to the results obtained through Raman Spectroscopy, a wide range of magnesium calcites was found, from low to high magnesium calcite. The presence of low magnesium calcite suggests that the studied beachrock formations might have been exposed to meteoric conditions, an ambience where this kind of calcite is typical[69]. Furthermore, these results confirm the presence of HMC, which might be composing the first cement layer (the micritic coating) precipitated in shallow marine conditions and commonly considered as a biologically mediated carbonate mineral[70,71].

[67] Lumsden D.N., **1979**. *Discrepancy between thin section and X-ray estimates of dolomite in limestone*. Journal of Sedimentary Petrology 49, 429-436.
[68] James N.P., Jones B., **2015**. *Origin of Carbonate Sedimentary Rocks*. John Wiley and Son, United Kingdom.
[69] Gischler E., Lomando A.J., **2007**. *Beachrock and Intertidal Precipitates*. In: Nash D.J., McLaren S.J. (Eds.), Geochemical Sediments and Landscapes. Wiley-Blackwell, UK, pp. 365-390.
[70] Bontognali T.R.R., McKenzie J.A., Warthmann R.J., Vasconcelos C., **2014**. *Microbially influenced formation of Mg-calcite and Ca-dolomite in the presence of exopolymeric substances produced by sulphate-reducing bacteria*. Terra Nova 2014, 72-77.
[71] McCutcheon J., Wilson S.A., Southam G., **2016**. *Microbially accelerated carbonate mineral precipitation as a strategy for in situ carbon sequestration and rehabilitation of asbestos mine sites*. Environmental Science and Technology 50, 1419-1427.

6.1.4 SEM-EDS analyses

Once the cementation pattern and mineralogy was identified through light microscopy, Raman spectroscopy and XRD, the electron microscopy coupled to X-ray microanalysis was used to define more in detail the morphologic and compositional characteristics of the previously described cements (see Figure 6.10 and Figure 6.11).

6.1.4.1 Micritic coating

This kind of cement is characterised by irregular undulations, as in the case of beachrock cements from Arrigunaga beach for example, where it presents a thickness varying from 10 µm to 50 µm, the maximum width being found in the lower intertidal zone (compare Figure 6.10C-D vs Figure 6.10E-F). This coating is also present in La Salvaje beach, discontinuously found bellow the aragonite needles, as shown in Figure 6.10D or 6.10F. In both cases, the Mg is among the main differential compositional characteristic with the aragonite needles, supporting that micritic cement can be composed by HMC. Micritization of the grains is a common feature in beachrocks and in many cases micritic cements have been related with organic matter and microbial activity[72-74]. Bathurst described in 1975[75] the generally believed role of the micritic coating in diagenesis, citing that it contains high amounts of organic matter, and that it is posed over pre-existing organic matter, sometimes referred also as “organic mucus”, which acts as a mould for this cement to precipitate and stabilize. This is the first diagenetic process that takes place in the water-sediment interface and it is stimulated by recurrent wetting and drying alternated periods[76,77]. Furthermore, the micritic coating is considered to be formed as a result of high carbonate concentrations during the initial phase of cement precipitation and apparently, it controls the first stage of beachrock diagenesis[75,78].

[72] Webb G.E., Jell J.S., Baker J.C., **1998**. *Cryptic intertidal microbialites in beachrock, Heron Island, Great Barrier Reef: implications for the microcrystalline beachrock cement*. Sedimentary Geology 126, 317-334.
[73] Guerra N.C., Kiang C.H., Sial A.N., **2005**. *Carbonate cements in contemporaneous beachrocks, Juaribe beach, Itamaracá island, northeastern Brazil: petrographic, geochemical and isotopic aspects*. Anais da Academia Brasileira de Ciências 77, 343-352.
[74] Vousdoukas M.I., Velegrakis A.F., Plomaritis T.A., **2007**. *Beachrock occurrence, characteristics, formation mechanisms and impacts*. Earth-Science Reviews 85, 23-46.
[75] Bathurst, R.G.C., **1975**. *Carbonate sediments and their diagenesis*. Elsevier, Amsterdam.
[76] Foos A.M., Bain R.J., **1995**. *Mineralogy, chemistry and petrography of soils, surface crusts, and soil stones, San Salvador and Eleuthera, Bahamas*. In: Curran H.A., Whian B. (Eds.) Terrestrial and shallow marine geology of the Bahamas and Bermuda. Geological Society of America, Colorado, pp. 223-232.
[77] Adams A.E., McKenzie A., **1998**. *A Colour Atlas of Carbonate Sediments and Rocks under the Microscope*. Manson Publishing Ltd, London.
[78] Scoffin, T.P., **1987**. *An Introduction to Carbonate Sediments and Rocks*. Blackie, Glasgow and Hall, New York. 274 pp.

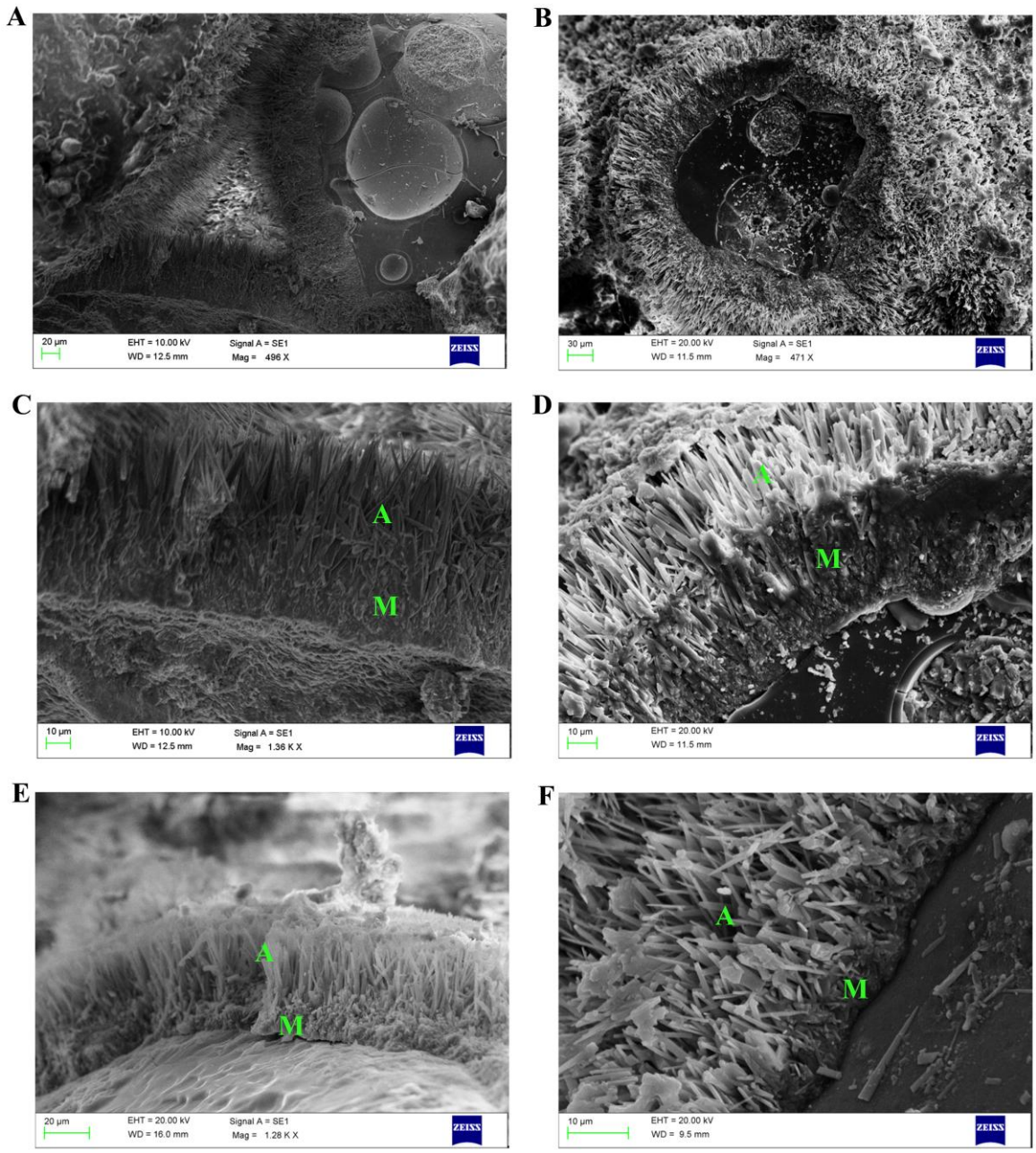

Figure 6.10. A-B) Diverse grains cemented by a micritic coating and an aragonite acicular rim that displays an isopachous diposition tangentially to the grain surfaces. C-D) Details of micritic cements and aragonite fibers found in the low intertidal zone. E-F) View of the micritic and acicular cement from samples located in the higher intertidal zone. A: Aragonitic acicules; M: micritic.

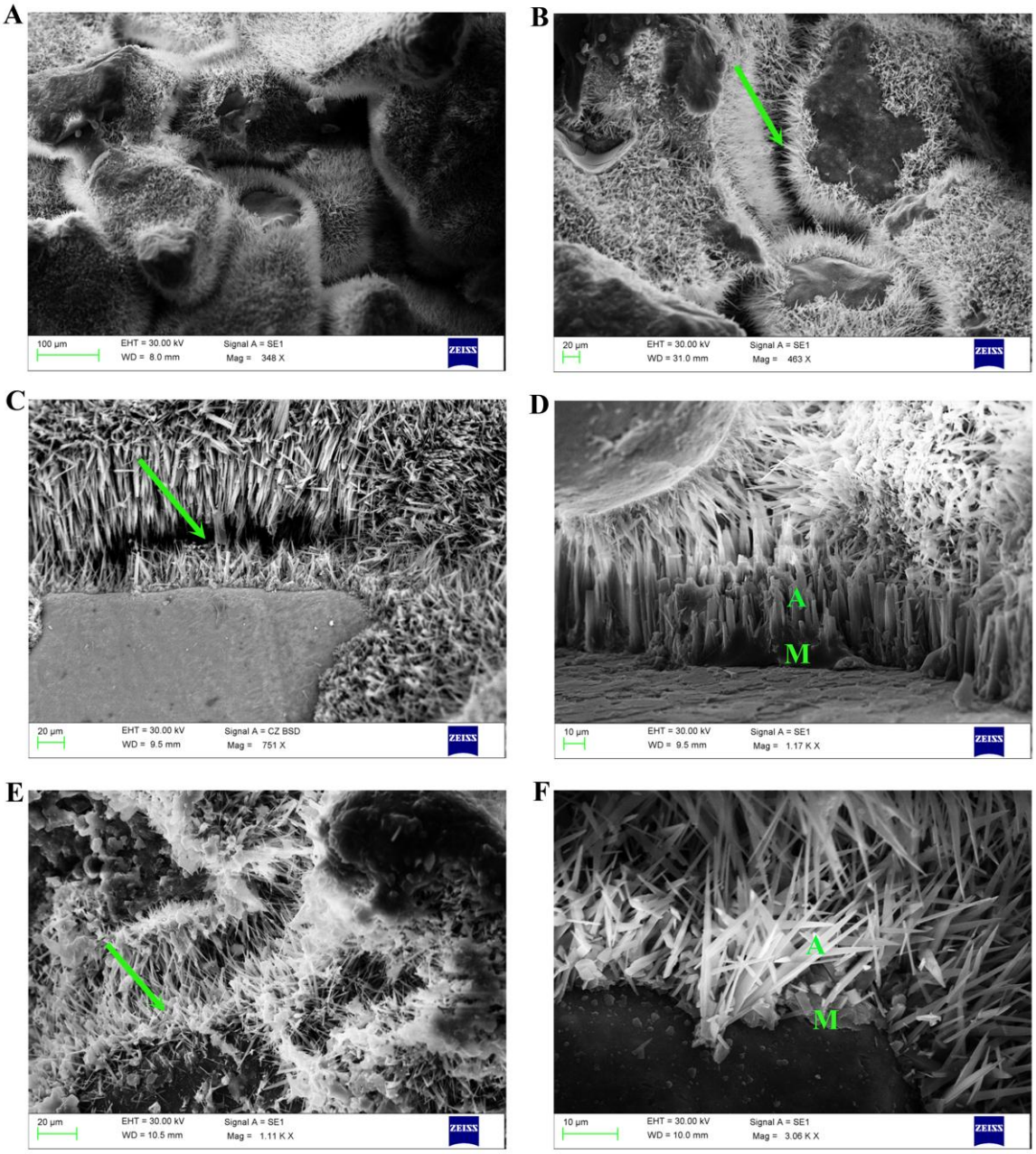

Figure 6.11. A) General view of the cements from La Salvaje beach where diverse grains covered with aragonite cement can be distinguished. B) Grains cemented with aragonite needles, where interlocking polygonal boundaries can be appreciated (marked with an arrow). C) Close view of the isopachous acicular rim, where interlocking polygonal boundaries can be observed again (marked with an arrow). D) Detail of a discontinuous micritic coating followed by an isopachous acicular rim. E) Mesh of aragonite needles (indicated with the arrow). F) Close view of a micritic coating followed by a mesh of aragonitic needles or acicules. M: micritic, A: Aragonitic acicules or needles.

Micritic coatings are found enveloping either carbonate or siliclastic grains, thus both of them will be separately illustrated. In the case of bioclasts, it is assumed that carbonate grains are micritized as a result of the repeated activity of bacteria, algae and fungi over the substrate; microbes attack the outside part of the grain, which is then infilled by a micritic cement[79,80]. Therefore, despite the typical constituents like HMC, this coating could also contain some impurities and high contents of organic matter[81].

As an example, Figure 6.12 shows a bioclast with a micritic coating (Figure 6.12A-B) that results to be fluorescent (Figure 6.12C). The micritic layer can be observed in the SEM image (Figure 6.12D), and the EDS mappings (Figure 6.12E) revealed that is mainly composed of C, O, Mg as well as Al and Si. The presence of Ca is not so obvious in the micritic layer possibly because the high content of this element in the bioclast, or even in the acicules, makes neglictible its presence in the micritic layer.

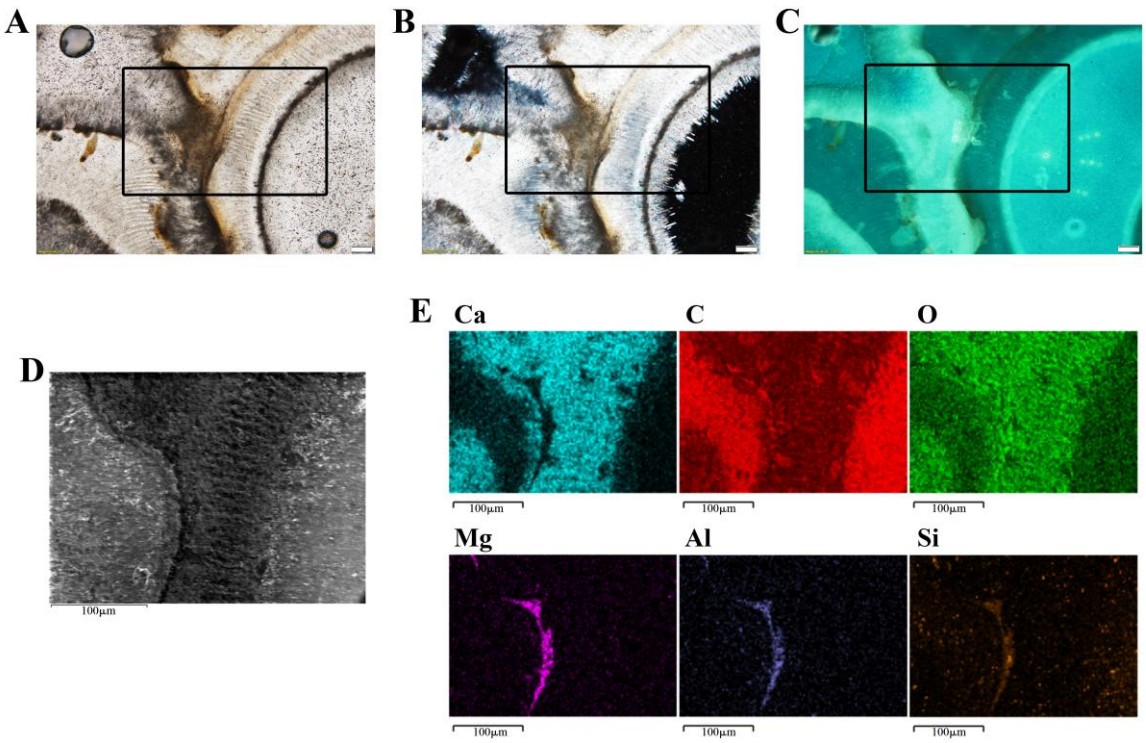

Figure 6.12. A) Plane polarized light image, B) Crossed polarized light image and C) UV light (fluorescence microscopy) images acquired in a thin section, presenting a bioclast surrounded by micritic cement (Scale: 20µm); D) SEM image of the area indicated in A-C and E) relevant EDS distribution maps of the elements found in the area.

[79] Vousdoukas M.I., Velegrakis A.F., Plomaritis T.A., **2007**. *Beachrock occurrence, characteristics, formation mechanisms and impacts*. Earth-Science Reviews 85, 23-46.
[80] Morse J.W., Mackenzie F.T., **1990**. *Geochemistry of sedimentary carbonates*. Developments in Sedimentology 48.
[81] Bathurst, R.G.C., **1975**. *Carbonate sediments and their diagenesis*. Elsevier, Amsterdam.

Thus, the micritic layer contains a remarkably different composition than the grain and even than the above acicular cement, probably due to the biological influence involved in its formation, which might be witnessed by the presence of diverse trace elements within the micritic coating. For instance, in micritic envelopes found in adjacent beachrock, apart from calcium carbonates, other elements such as Mg and Si were also detected, attributed to remains of the organomineralization activities[82].

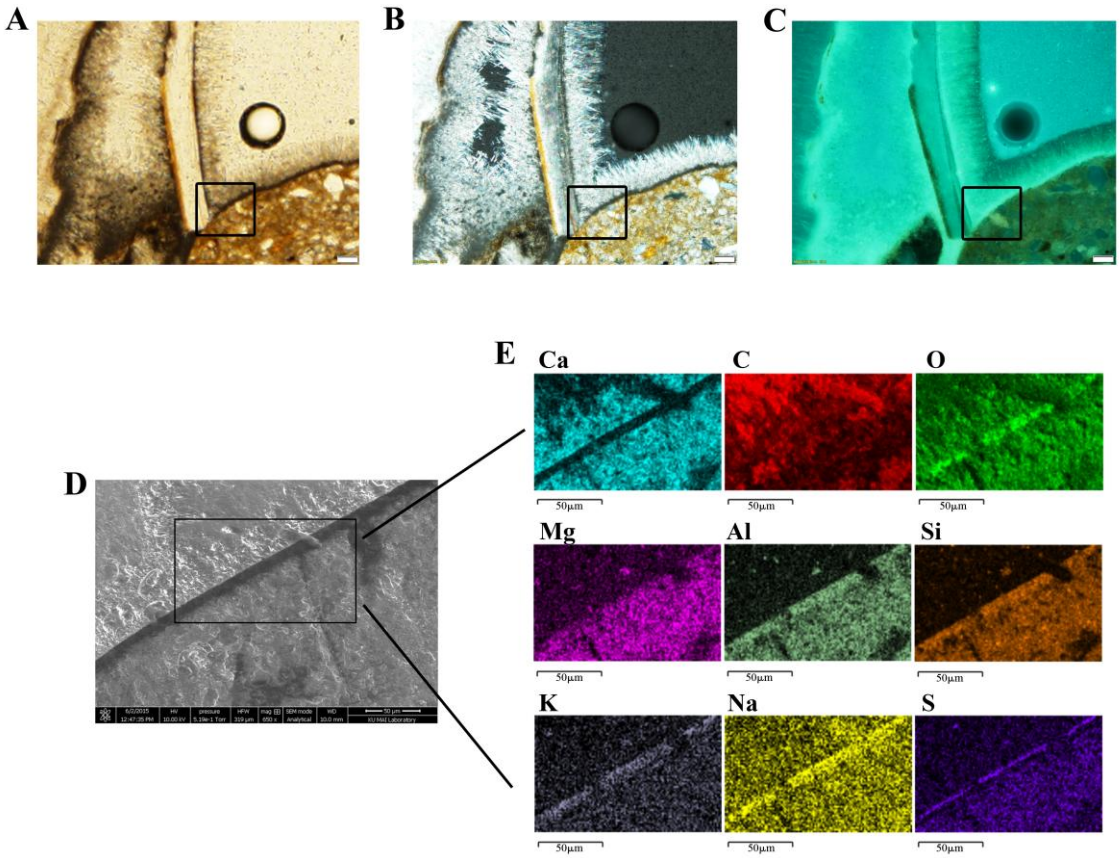

Figure 6.13. A) Plane polarized light image, B) Crossed polarized light imageand C) UV light (fluorescence microscopy) images obtained over a thin section, focusing on a siliclastic grain that is covered by micritc cement (Scale: 20µm); D) SEM image of the area indicated in A-C (Scale: 50µm) and E) its EDS element distribution maps.

But what can be the nature of the micritic layer if the host grain is a siliclastic grain? In this case, according to the literature, it is suggested that the micritization is derived from a rapid supersaturation occurring in the interstitial waters[83,84].

[82] Arrieta N., Iturregui A., Martínez-Arkarazo I., Olazabal M.A., Murelaga X., Baceta J.I., Madariaga J.M., **2015**. *Multianalytical X-ray based micro-spectroscopic approach for the analysis of carbonates in beachrock cements.* Analytical Methods 7, 8865-8876.
[83] Vousdoukas M.I., Velegrakis A.F., Plomaritis T.A., **2007**. *Beachrock occurrence, characteristics, formation mechanisms and impacts*. Earth-Science Reviews 85, 23-46.
[84] Vieira M.M., De Ros L.F., **2006**. *Cementation patterns and genetic implications of Holocene beachrocks from northeastern Brazil*. Sedimentary Geology 192, 207-230.

For instance, observing Figure 6.13, it can be distinguished a rock fragment, mainly composed of Ca, O, Mg, Al, Si, K, Na, and S. In the micritic layer Ca seems to be insignificant, but a distinctive layer can be recognised composed of O, Mg, Al, Mg, Si, K, Na and K. Thus, the micritic layer again contains low contents of Ca and seems to be enriched with those elements present in the grain, forming a clearly distinguishable layer that corresponds to the disposition of the micritic envelope.

The similar presence of the elements suggests that the composition of the micritic layer might be derived from the host grain. Certainly, the alteration of silicates, especially through microbial activity, and the associated formation of carbonates have been cited in several scientific investigations. For instance, Ferri et al. (1994)[85] stated that the weathering of silicates is associated to the deposition of carbonate minerals by microorganisms. Furthermore, field and laboratory analyses carried out by Roberts et al. (2004)[86] demonstrated the formation of dolomite ($CaMg(CO_3)_2$) as a result of the basalt weathering induced by microorganisms and subsequent release of Ca, Mg and Fe.

Likewise, Benzerara et al. (2005)[87] described that when pyroxenes are weathered Fe, Mg, Ca, Al and Si can be released, being trace elements required for microbial development that could induce the necessary alkaline conditions for carbonate precipitation. Moreover, Vorhies and Robert (2009)[88] found that microbial activity could stimulate the dissolution of clay minerals liberating dissolved ions into pore waters, and through microbial oxidation of organic matter and reduction of sulphate, generated alkalinity conditions to encourage calcium carbonate precipitation.

In this context, it might be worth mentioning the carbonation reactions naturally occurring through the interaction between carbon dioxide and silicate minerals described by Daval et al. (2009)[89]. When atmospheric CO_2 dissolves in water, carbonic acid is formed and dissociates in free proton (H^+) and bicarbonate (HCO_3^-) ions (Eq. 6.1) at the current pH of the natural system. The dissolved H^+ can interact with a silicate phase promoting its dissolution (weathering) and leaving the equivalent amount of soluble

[85] Ferris F.G., Wiese R.G., Fyfe W.S., **1994**. *Precipitation of carbonate minerals by microorganism: implications for silicate weathering and the global carbon dioxide budget*. Geomicrobiology 12, 1-13.
[86] Roberts J.A., Bennet P.C., González L.A., Macpherson G.L., Milliken K.L., **2004**. *Microbial precipitation of dolomite in methanogenic groundwater*. Geology 32, 277-280.
[87] Benzerara K., Menguy N., Guyot F., Vanni C., Gillet P., **2005**. *TEM study of a silicate-carbonate-microbe interface prepared by focused ion beam milling*. Geochimica et Cosmochimica Acta 69, 1413-1422.
[88] Vorhies J.S., Gaines R.R., **2009**. *Microbial dissolution of clay minerals as a source of iron and silica in marine sediments*. Nature Geoscience 2, 221-225.
[89] Daval D., Martinez I., Corvisier J., Findling N., Goffé B., Guyot F., **2009**. *Carbonation of Ca-bearing silicates, the case of wollastonite: Experimental investigations and kinetic modeling*. Chemical Geology 265, 63-78.

HCO_3^- (see Eq. 6.2). These two reactions can be explained by the global weathering reaction expressed as Eq. 6.3. Thus, the solubilisation of the silicate phase consumes protons and liberates cations and HCO_3^- enhancing the alkalinity of the surrounding microenvironment, The basification of this microenvironment can promote the saturation condition of metal carbonates giving raise to its precipitation through (Eq. 6.4 or Eq. 6.5).

$$H_2O + CO_2 \leftrightarrow H_2CO_3 \leftrightarrow H^+ + HCO_3^- \quad \text{(Eq. 6.1)}$$

$$M_xSi_yO_{x+2y-t}(OH)_{2t} + 2xH^+ \leftrightarrow xM^{2+} + 2xHCO_3^- + ySiO_2 + (x+t)H_2O \quad \text{(Eq. 6.2)}$$

$$M_xSi_yO_{x+2y-t}(OH)_{2t} + 2xCO_2 \leftrightarrow xM^{2+} + 2xHCO_3^- + ySiO_2 + (t-x)H_2O \quad \text{(Eq. 6.3)}$$

$$xM^{2+} + xCO_3^{2-} \leftrightarrow xMCO_3 \quad \text{(Eq. 6.4)}$$

$$xM^{2+} + 2xHCO_3^{2-} \leftrightarrow xMCO_3 + xH_2O + xCO_2 \quad \text{(Eq. 6.5)}$$

Apart from carbonic acid, other acids could also supply the protons (H^+) required for the dissolution of silicates, as shown in Eq. 6.2. In that sense, the possible influence of the biological activity could be addressed again, focusing on the possible bioturbation (chemical stress at the microenvironment scale) of the sediments.

Rock surfaces can be colonized by immensely diverse microbial communities that can form biofilms, creating a microenvironment that allows them to live in the surrounding conditions. Biofilms induce changes over time, either physical or chemical, in the rock substrate leading to bioweathering mechanisms[90]. Those weathering processes can involve oxidation-reduction reactions and the production of weathering agents, like chelating molecules and organic acids[91,92]. The interaction between those compounds and the grain could alterate the grain surfaces contributing to the formation of secondary minerals, such as oxalates or carbonates[93].

[90] Gorbushina A. **2007**. *Life on the rocks*. Environmental Microbiology 9, 1613-1631.
[91] Uroz S., Calvaruso C., Turpault M.P., Pascale F.K., **2009**. *Mineral weathering by bacteria: ecology, actors and mechanisms*. Trends in Microbiology 17, 378-387.
[92] Benzerara K., Menguy N., Guyot F., Vanni C., Gillet P., **2005**. *TEM study of a silicate-carbonate-microbe interface prepared by focused ion beam milling*. Geochimica et cosmochimica Acta 69, 1413-1422.
[93] Gadd G.M., **2010**. *Metals, minerals and microbes: geomicrobiology and bioremediation*. Microbiology 156, 609-643.

Therefore, similarly to what is reported in the scientific community, Figure 6.13 could probably show an example of the weathering of silicates, either by biotic or abiotic mechanisms, which could induce an increase in the pH of the pore water favouring the precipitation of calcium carbonates.

6.1.4.2 Isopachous acicular rim

Over the micritic cement, aragonite is the prevailing main cement which is extensively distributed in the intergranular pore-space as a felted mass of acicular and fibrous crystals either in beachrock outcrops found in Arrigunaga beach (Fig. 6.10A–B) and in La Salvaje beach (Fig. 6.11A–B). Usually, aragonite acicules display an isopachous disposition tangentially to the grain surface (as shown for example in Figure 6.10 A-B), indicating the existence of active pore water circulation in the marine phreatic environment[94]. The rims of acicular crystals found in different grains can interlock showing polygonal boundaries between them (Figure 6.11B-C), which is also a common characteristic of marine cements[95], like in other beachrock formations[96-98].

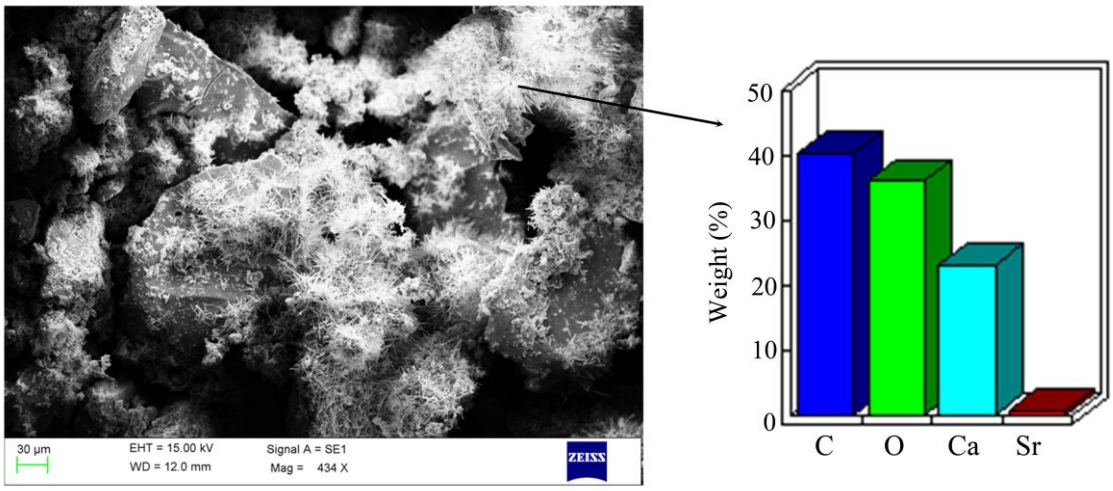

Figure 6.14. SEM image and EDS semiquantitative analyses obtained from a bulk beachrock fragment, displaying a mesh of aragonite needles composed of C (40%), O (36%), Ca (23%) and Sr (0.6%).

[94] Parker A., Sellwood B.W., **1994**. *Quantitative Diagenesis: Recent Developments and Applications to Reservoir Geology*. Kluwer Academic Publishers, NATO ASI Series.
[95] Moore C.H., **1997**. *Carbonate diagenesis and porosity*. Elsevier, Amsterdam, 338 pp.
[96] Howie F.M.P., **2009**. *Beachrock development along the North coast of Cornwall*. Geoscience in South-West England 12, 85-94.
[97] Arrieta N., **2014**. *The study of an unusual temperate latitude beachrock formation. Characterization of Azkorri beach and Tunelboka cove locations*. PhD Thesis, University of the Basque Country.
[98] Vieira M.M., De Ros L.F., **2006**. *Cementation patterns and genetic implications of Holocene beachrocks from northeastern Brazil*. Sedimentary Geology 192, 207-230.

In Arrigunaga beach, for instance, in the samples of the beachrock outcrops present in the low intertidal zone the fibrous crystals have a size range around 50-90 μm in length, while those of the higher intertidal zone range from 10 to 30 μm. Hence, the closer to the seawater, the higher the development of both cement coatings, suggesting the favourable influence of the marine environment over the beachrock formation (compare Figure 6.10C-D with Figure 6.10E-F).

However, in some cases the aragonite cement can also form a mesh of needles, where the crystals are chaotically displayed over the surface of the grain (Figure 6.11E-F). This cement forms, as well as the isopachous fringes, are indicative of an active pore-water circulation in the phreatic zone[99]. Based on the EDS analyses (Figure 6.14) the needles are made of Ca, C, and O but also contain Sr (~6000 ppm), resembling the inherent composition of modern marine aragonite cements[100,101]. In the studied samples, usually the isopachous rim displays over the micritic coating (see Figure 6.10C-F or Figure 6.11F), which is in agreement with the general consensus found in the literature; aragonite precipitates over nucleation sites like organic matter or organic micrite[102,103].

Indeed, there are two main sources generally attributed to the origin of aragonite needles: calcareous algae and abiotic processes[104]. Regarding the former, Guerra et al (2005)[103] suggested that the rapid growth rate of aragonite crystals in beach grains could be a consequence of seawater supersaturation and intensification of favouring conditions for precipitation, through evaporation as well as by pH and partial pressure of CO_2 fluctuations, due to photosynthesis by algae living in and on the beach sand.

For example, in samples from the most intertidal zone, micritic crystals of calcium carbonate were found. This could resemble to globular masses found by Neumeier[105] during the study of beachrock cements formed under microbial influence (compare

[99] Parker A., Sellwood B.W., **1994**. *Quantitative Diagenesis: Recent Developments and Applications to Reservoir Geology*. Kluwer Academic Publishers, NATO ASI Series.
[100] Tucker M., **1990**. *Diagenetic processes, products and environments.* In: Tucker M.E., Wright V.P. (Eds.), Carbonate Sedimentology. Wiley-Blackwell, UK, pp. 314-362.
[101] Morse J.W., Mackenzie F.T., **1990**. *Geochemistry of sedimentary carbonates*. Developments in Sedimentology 48.
[102] Guerra N.C., Kiang C.H., Sial A.N., **2005**. *Carbonate cements in contemporaneous beachrocks, Juaribe beach, Itamaracá island, northeastern Brazil: petrographic, geochemical and isotopic aspects*. Anais da Academia Brasileira de Ciências 77, 343-352.
[103] Vousdoukas M.I., Velegrakis A.F., Plomaritis T.A., **2007**. *Beachrock occurrence, characteristics, formation mechanisms and impacts*. Earth-Science Reviews 85, 23-46.
[104] Morse J.W. *Formation and diagenesis of carbonate sediments*, **2003**. In: Mackenzie F.T. (Ed.). Sediments, Diagenesis and Sedimentary Rocks, Vol.7, Treatise on Geochemistry (Holland H.D., Turekian K.K., Eds.), Elsevier-Pergamon, Oxford, pp. 67-86.
[105] Neumeier U., **1999**. *Experimental modelling of beachrock cementation under microbial influence*. Sedimentary Geology 126, 35-46.

Figure 6.15A and Figure 6.15B). In that work, the author suggested that poorly crystallized minerals derived from microbial activity, can serve as nucleation sites for physic-chemically formed acicular aragonite. Basing on that hypothesis Figure 6.15A shows a poorly crystallized mass, mainly composed of Ca, C, O, Mg, Si and Al (Figure 6.15C), that might have served as nuclei for needle-shaped cements further developed through abiotic processes.

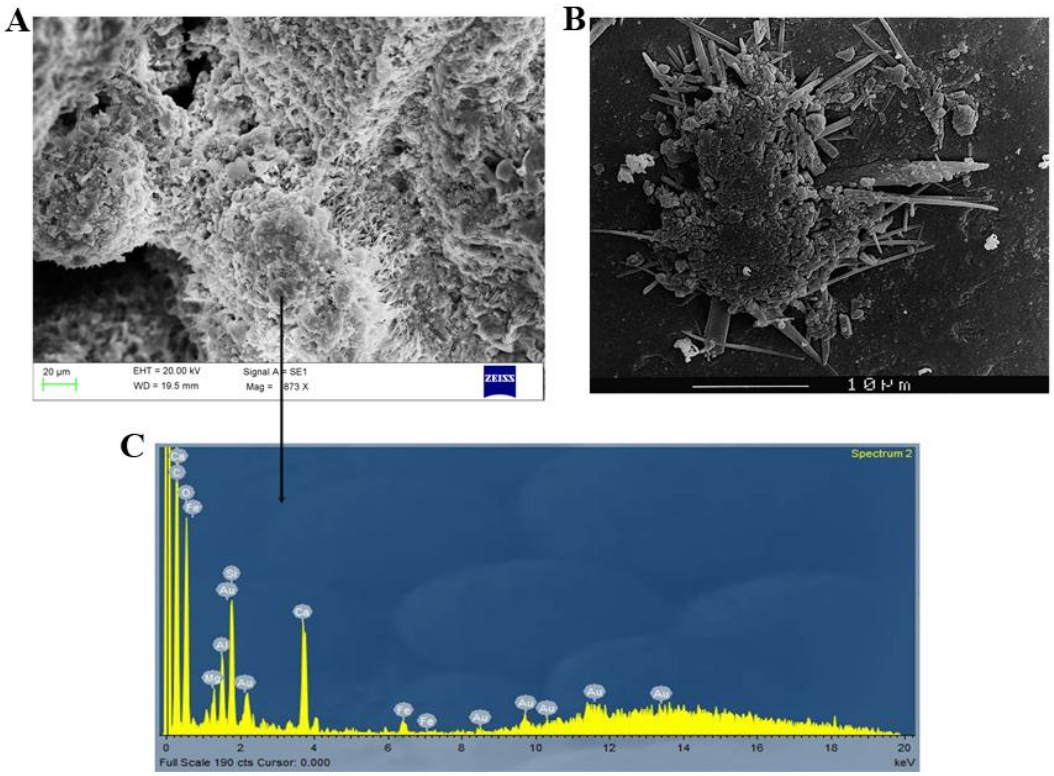

Figure 6.15. A) SEM image of poorly crystallized mineral mass found in the beachrock formations under study., that as viewed in the EDS spectrum. This globular mass might have served as nucleation points from where needle-shaped cements emerge, similarly to the morphologies showed by Neumeier (1999)[106] in image B. C) EDS spectrum showing that the poorly crystallized mineral mass is mainly composed of Ca, C, O, Mg, Si and Al (Au represents the gold coating used for SEM imaging).

Some spherical microstructures (Figure 6.16), observable also in samples of the low intertidal zone, could be relevant in the understanding of the early stages of the cementation. Spherule-shaped features are frequent in superficial sediments or soils and, although their origin remains unclear, commonly they are associated with a possible organic mediation and the presence of microorganisms. This kind of structures can also be common in calcium carbonate minerals[107], indeed, when exploring the mechanisms

[106] Neumeier U., **1999**. *Experimental modelling of beachrock cementation under microbial influence*. Sedimentary Geology 126, 35-46.
[107] Durand N., Curtis Monger H., Canti M.G., **2010**. *Calcium carbonate features*. In: Interpretation of micromorphological features of soils and regoliths. Elsevier, Oxford, pp.149-194.

involved in the precipitation of carbonates, one of the generally documented biological evidence lies in the presence of spherical particles. For instance, the initial stages of carbonate precipitation occurring in microbial mats are related with nanospheres of amorphous carbonates[108-110].

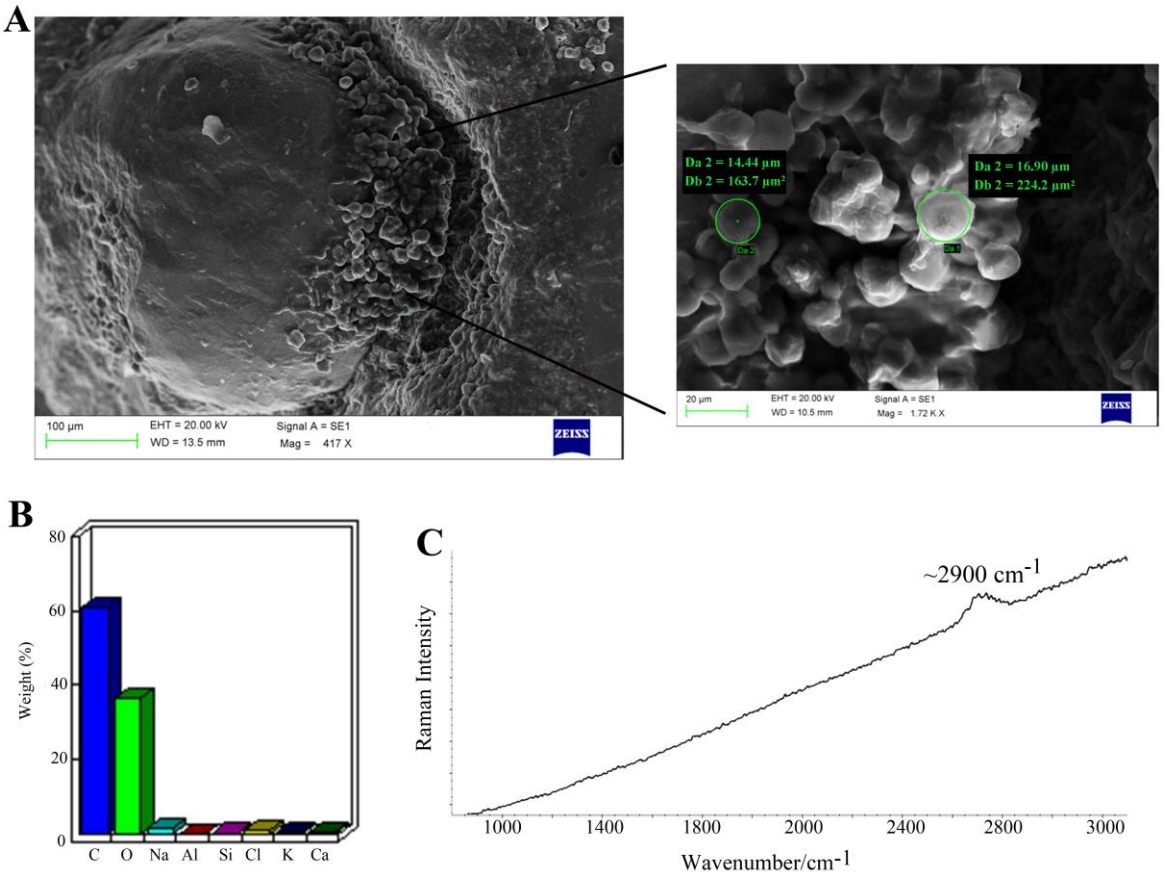

Figure 6.16. A) SEM image obtained from a bulk beachrock fragment, showing an area with spherule-shaped structures; B) Maximised view of those structures; B) EDS semiquantitative graph showing the composition of the spherules and C) the corresponding Raman spectrum obtained by the SCA (Structural and Chemical Analyzer) device showing a band possibly related with C-H stretching vibrations.

The spherules found in the studied beachrocks, have a diameter around 7-17µm and their composition consists mainly of C (59%), O (29%), Na (3,5%) and minor amounts of other elements like Al, Si, Cl, K or Ca (1-2%), with sporadic presence of Fe, Mg or Ti. To get more detailed information about the composition of these structures, an Structural and Chemical Analyzer (SCA) analysis was performed (Figure 6.15C),

[108] Chafetz H.S., **1990**. *Bacterially induced precipitation of $CaCO_3$: an example from studies of cyanobacterial mats*. In: Krumbein W.E., Paterson D.M., Stal L.J., (Eds.). Biostabilization of Sediments. BIS-Verlag, Oldenburg, Germany, pp. 149–163.
[109] Peckmann J., Paul J., Thiel V., **1999**. *Bacterially mediated formation of diagenetic aragonite and native sulphur in Zechstein carbonates*. Sedimentary Geology 126, 205-222.
[110] Dupraz C., Reid R.P., Braissant O., Decho A.W., Norman R.S., Visscher P.T., **2009**. *Processes of carbonate precipitation in modern microbial mats*. Earth-Science Reviews 96, 141-162.

appearing a clear and broad Raman band at around 2900 cm^{-1}. That region is characteristic of CH_2 and CH_3 stretching vibrations, including for example C-H stretching bands derived from amino acids like lysine and even aspartic acid or glutamic acid[111].

Taking into account that information, the existence of the spheres shown in Figure 6.16A could be associated with the simultaneous presence of the amorphous calcium carbonate (ACC) phase, which is commonly considered as a precursor in the precipitation of calcium carbonate at relatively high supersaturation conditions[112,113], because similar structures have been described in other studies focused on micritic carbonate cements, where a microbial origin was ascribed to the cement type[114], and especially in the adjacent beachrocks of Azkorri beach and Tunelboka cove[115].

There are various works where it is described that this kind of structures are part of the commencement of biomineralization processes[116,117]. It has been suggested that microorganism can produce similar structures as a storage phase prior to the formation of calcium carbonates[118]. Although the mechanisms are not fully understood yet[119], it is believed that ACC can be stabilized aided by the presence of macromolecules such as aspartic-rich proteins[120], to be gradually transformed into a crystal mass that would finally evolve toward most crystalline phases[121]. These results come in agreement with the presence of organic compounds found by means of Raman spectroscopy in association with aragonite cements (see Figure 6.7).

---

[111] Howell N.K., Arteaga G., Nakai S., Li-Chan E.C.Y., **1999**. *Raman Spectral Analysis in the C-H Stretching Region of Proteins and Amino Acids for Investigation of Hydrophobic Interactions*. Journal of Agricultural and Food Chemistry 47, 924-933.

[112] Brecevic L. and Kralj D., **2007**. *On Calcium Carbonates: from Fundamental Research to Application.* Croatica Chemica Acta 80, 467-484.

[113] Ihli J., Ching Wong W., Noel E.H., Kim Y., Kulak A.N, Christenson H.K., Duer M.J., Meldrum F.C., **2014**. *Dehydration and crystallization of amorphous calcium carbonate in solution and in air*. Nature Communications 5, 1-10 pp.

[114] Mutti M., **2000**. *Microbial origin of microcrystalline carbonate sediment and cements filling fractures in basalts recovered at site 1001, Caribbean Sea*. In: Leckie R.M., Sigurdsson H., Acton G.D., Draper G. (Eds.), Proceedings of the Ocean Drilling Program, Scientific Results, v.165, 227-232 pp.

[115] Arrieta N., **2014**. *The study of an unusual temperate latitude beachrock formation. Characterization of Azkorri beach and Tunelboka cove locations*. PhD Thesis, University of the Basque Country.

[116] Morse J.W., Arvidson R.S., Lüttege A., **2007**. *Calcium Carbonate Formation and Dissolution*. Chemical Reviews 107, 342-381.

[117] Long X., Ma Y., Qi L., **2011**. *In Vitro Synthesis of High Mg Calcite under Ambient Conditions and Its Implication for Biomineralization Process*. Crystal Growth Design 11, 2866-2873.

[118] Stolarski, J., Mazur M., **2005**. *Nanostructure of biogenic versus abiogenic calcium carbonate crystals*. Acta Palaeontologica Polonica 50 (4): 847-865.

[119] Ihli J., Ching Wong W., Noel E.H., Kim Y., Kulak A.N, Christenson H.K., Duer M.J., Meldrum F.C., **2014**. *Dehydration and crystallization of amorphous calcium carbonate in solution and in air*. Nature Communications 5, 1-10 pp.

[120] Tao J., Zhou D., Zhang Z., Xu X., Tang R., **2009**. *Magnesium-aspartate-based crystallization switch inspired from shell molt of crustacean*. Proceedings of the National Academy of Sciences 106, 22096-22101.

[121] Silva-Castro G.A., Uad I., Gonzalez-Martinez A., Rivadeneyra A., Gonzalez-Lopez J., Rivadeneyra M. A., **2015**. *Bioprecipitation of Calcium Carbonate Crystals by Bacteria Isolated from Saline Environments Grown in Culture Media Amended with Seawater and Real Brine.* BioMed Research International, doi:10.1155/2015/816102.

6.1.4.3 Infiltrated micritic particles

Following with the diagenetic features found in the beachrocks under study, the next analyses will focused on the characteristics of the infiltrated particles found in two arrangements: over the aragonite acicules and in the intergranular pore space. These characteristics were only encountered in the beachrock units sampled in the northern area of the Arrigunaga beach, as described in section 6.1.1. In that section it was explained also that the ultraviolet light used for fluorescence microscopy, allowed detecting fluorescent areas especially in association with this type of cement.

Figure 6.17A-B visualizes an area of a thin section containing in the upper side a grain that, in view of its porous nature, can be slag and also a bioclast down in the image. Both of them, apart from the transparent acicular rim, contain the dark outer film over the cement and in the intergranular space diverse particles can be observed. The dark layer that covers the cement, and some part of the intergranular space, results to be fluorescent under UV light (Figure 6.17C). Indeed, Figure 6.17E demonstrates that the transparent acicular rim cement is mainly composed of Ca and covered by C. Note that the more fluorescent areas (Figure 6.17C) show a dark colouring in the BSE image (Figure 6.17D), denoting the presence of a light elements, being especially rich in C (Figure 6.17E). These results support the idea that the dark layer over the transparent acicular cement might be composed of organic matter infiltrated and deposited on top of the cement. The organic nature of the dark layer as well as its uniform thickness, indicate that it might have been deposited under stagnant conditions.

With reference to the particles found within the intergranular space, Figure 6.17E shows clearly discernible particles made of Ca, O, Mg, as well as Si, K, Al, Fe, and even smaller amounts of Na and Ti. Once again, the material filling the pore spaces can be irregularly fluorescent (Figure 6.17C), denoting possibly the presence of organic components. Furthermore, according to the disposition of the particles in the intergranular space and their composition, this feature can be comparable to infiltrated silt-sized carbonate and siliciclastic sediments registered in other beachrocks[122,123]. These sediments are believed to come from the passage of muddy waters through sandy particles that might have percolated for instance after storm events[123].

[122] Ghandour I.M., Al-Washmi H.A., Bantan R.A., Gadallah M.M., **2014**. *Petrographical and petrophysical characteristics of asynchronous beachrocks along Al-Shoaiba Coast, Red Sea, Saudi Arabia.* Arabian Journal of Geosciences 7, 355-365.
[123] Vieira M.M., De Ros L.F., **2006**. *Cementation patterns and genetic implications of Holocene beachrocks from northeastern Brazil*. Sedimentary Geology 192, 207-230.

It should be reminded that this is a characteristic just visualized in the samples located in the northern area of Arrigunaga beach, where the marine dynamics (main seawater currents and flows) prompted the accumulation of sediments and materials that came from the estuary, thus loaded in metallic particles and organic matter. Therefore, the fact of having found micritic sediments in the intergranular space apparently rich in organic matter is consistent with the kind of materials deposited in that area during the pollution periods occurred in the estuary. In addition, micritic pore filing cements are usually indicative of well cemented beachrocks[124].

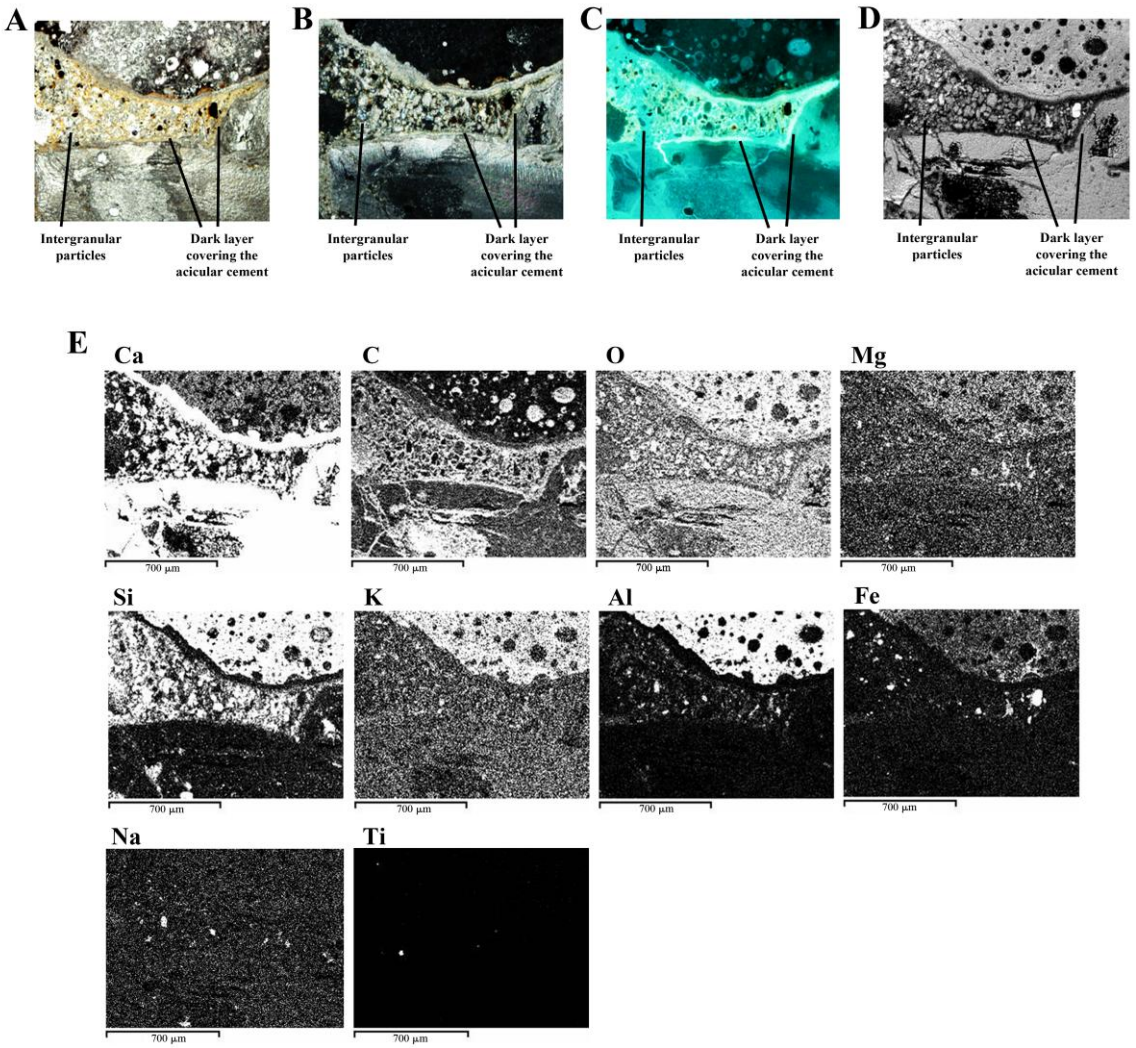

Figure 6.17. Images of infiltrated micritic particles forming a dark layer that covers the acicular cement or filling the intergranular space. A) Plane polarized light image, B) Crossed polarized light image, C) UV light (fluorescence microscopy) image, D) Backscattered electron image, E) EDS element distribution maps.

[124] Vousdoukas M.I., Velegrakis A.F., Plomaritis T.A., **2007**. *Beachrock occurrence, characteristics, formation mechanisms and impacts*. Earth-Science Reviews 85, 23-46.

6.1.4.4 Other diagenetic features

Exceptionally, another peculiarity was found in the beachrock formations from Arrigunaga beach that might be worth describing. Figure 6.18A-B shows two grains with diverse intergranular particles between them. Anyway, the point here would be the grain down in the left, which is covered by various layers, that are fluorescent, not only the coatings but the intergranular material (Figure 6.18C). EDS mappings (Figure 6.18E) revealed that the grain was a silicate rich in Al, Si, Mg, K and Mn. Coating the grain calcium carbonate cements are found, but surprisingly, Fe and P were also detected within the cements.

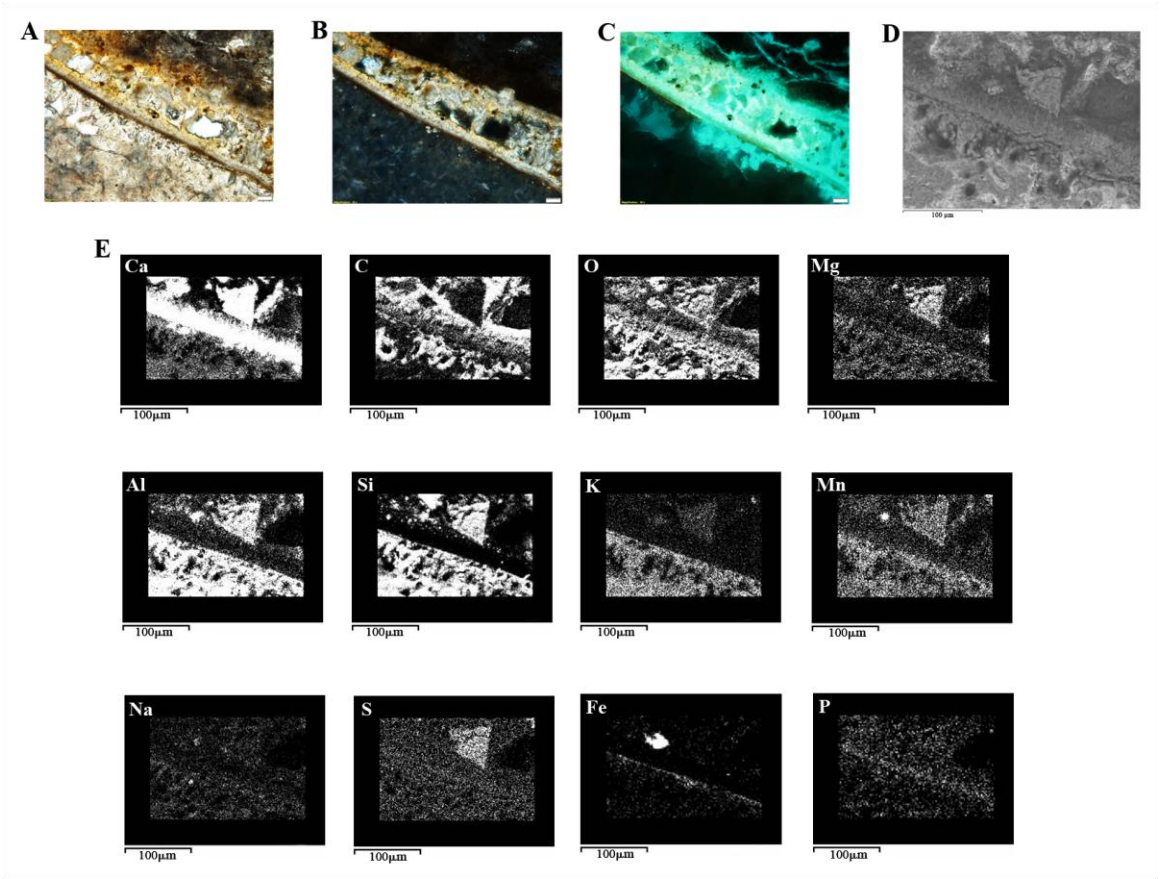

Figure 6.18. A) Plane polarized light image, B) Crossed polarized light image, C) UV light (fluorescence microscopy) image representing the diverse cement layers as well as the intergranular micritic particles found in beachrock outcrops from Arrigunaga (Scale: 20µm); D) Secondary electron image; E) EDS element maps of that area.

According to the literature, isopachous rims of aragonite needles can cover a dark layer rich in iron or sulphur[125]. It is known that high iron concentrations favour the

[125] Gischler E., Lomando A.J., **2007**. *Beachrock and Intertidal Precipitates*. In: Nash D.J., McLaren S.J. (Eds.), Geochemical Sediments and Landscapes. Wiley-Blackwell, UK, pp. 365-390.

formation of biofilms[126], but it is not fully understood the formation of iron (or Mn) biofilms, According to Reitner, they could be formed as a consequence of environmental crises because eutrophic episodes might cause a rapid growth of this kind of biofilms[127].

Regarding the phosphorus, inorganic sorption and precipitation of phosphate can occur with clays. Nevertheless, this element is an essential nutrient in primary production of the oceans and it is believed that 90% of the flux of phosphorus to sediments, is derived from organic debris and related subproducts[128]. Moreover, organisms that have a siliceous skeleton (for example, radiolarian or diatoms) dissolve in acidified seawaters, sometimes together with carbonates (calcite and primarily aragonite), producing a notable phosphate enrichment[129].

When dealing with marine carbonate sedimentary deposits, phosphorus is widely cited in relation with the oxidation of organic matter. Indeed, the biological uptake and incorporation into particulate organic matter, is considered as the major mode of transport of P from the upper water column to sediments[130]. It was described, in the case of marine plankton, that the derived organic matter oxidation occurs through sulfate reduction, being phosphate and ammonia formed as a result[131].

In an attempt to understand the simultaneous presence of Fe and P, it should be mentioned that the relation of Fe and P can be found in several investigations that discuss the presence and formation of phosphorus containing minerals in the marine realm. As an example, Sherwood et al. (1987)[130] suggested that phosphorus is related with (Fe, Mn)-oxide coatings in several carbonate sediments. Sanchéz-Román et al. (2014)[132] found that phosphate groups placed in the outer wall of bacterial membranes promoted the precipitation of amorphous ferrous phosphate phases that lead to the formation of further carbonates in extreme acidic conditions. Moreover, Benítez-Nelson

[126] Oglesby-Sherrouse A., Djapgne L., Nguyen A.T., Vasil A.I., Vasil M.L., **2014**. *The complex interplay of iron, biofilm formation, and mucoidy affecting antimicrobial resistance of Pseudomonas aeruginosa*. Pathogens and Disease 70, 307-320.
[127] Reitner J., **1993**. *Modern cryptic microbialite/metazoan facies from Lizard Island (Great Barrier Reef, Australia): formation and concepts*. Facies 29, 3-40.
[128] Froelich P.N., Bender M.L., Luedtke N.A., **1982**. *The marine phosphorus cycle*. American Journal of Science, pp. 474-511.
[129] Bjorlykke K., **2015**. *Petroleum Geoscience: from sedimentary environments to rock physics*. Springer-Verlag, Germany.
[130] Sherwood B.A., Sager S.L., Holland H.D., **1987**. *Phosphorus in foraminiferal sediments from North Atlantic Ridge cores and in pure limestones*. Geochimica et Cosmochimica Acta 1987, 1861-1866.
[131] Morse J.W. Formation and diagenesis of carbonate sediments, **2003**. In: Mackenzie F.T. (Ed.). Sediments, Diagenesis and Sedimentary Rocks, Vol.7, Treatise on Geochemistry (Holland H.D., Turekian K.K., Eds.), Elsevier-Pergamon, Oxford, pp. 67-86.
[132] Sánchez-Román M., Fernández-Remolar D., Amils R., Sánchez-Navas, Schmid T., San Martin-Uriz P., Rodríguez N., McKenzie J.A., Vasconcelos C., **2014**. *Microbial mediated formation of Fe-carbonate minerals under extreme acidic conditions*. Scientific Reports 4, 1-7.

(2000)[133] described that phosphorus can be adsorbed onto the surface of shells via iron oxyhydroxide coatings. In this sense, Delaney (1998)[134] stated that iron oxyhidroxides are efficient scavengers of P, and in fact, P burial is favoured by the burial of organic carbon and the formation of iron oxyhydroxide coatings in sedimentary particles.

It is a fact that in Figure 6.18, P and Fe appear closely related with carbonate cements, producing a fluorescent layer. So it could be a result of diverse chemical changes, microbial activity, as well as burial and exposure alternations that can take place in the cemented bodies located in the intertidal area, resulting in sediments reworking and accumulation of iron probably forming a biofilm and phosphorus within calcium carbonate cements.

6.1.5 Stable isotope analysis

With the objective of supporting the previously explained results and decipher the characteristics of the diagenetic environment in which beachrock carbonate cements were formed, $\delta^{18}O$ and $\delta^{13}C$ stable isotope analyses were measured.

The $\delta^{18}O$ and $\delta^{13}C$ values of the PDB standard are defined as 0‰, but deviation from those values could be related with diagenesis and further alteration processes. Marine waters can show a wide range of values depending on factors like temperature or evaporation, but they usually show high $\delta^{18}O$ and $\delta^{13}C$ values[135-137]. In contrast, meteoric waters can show relatively lower $\delta^{18}O$ values, although it varies as a function of the altitude and latitude[137].

In any case, the isotopic values of the carbonate cements would reflect the isotopic characteristics of the fluid from where they precipitated, therefore, these analyses could bring us closer to the origin of the carbonate cements.

Given that diverse carbonate cement layers exist covering the grains, special efforts were made to try to separate the different possible cements that could be distinguished at first sight. As an example, in Figure 6.19A, it can be observed two grains

[133] Benítez-Nelson C.R., **2000**. *The biogeochemical cycling of phosphorus in marine systems*. Earth-science Reviews 51, 109-135.
[134] Delaney M.L., **1998**. *Phosphorus accumulation in marine sediments and the oceanic phosphorus cycle*. Global Biogeochemical Cycles 12, 563-572.
[135] Sharp Z., **2007**. *Principles of Stable Isotope Geochemistry*. Pearson Prentice Hall, Upper Saddle River NJ, USA, 344 pp.
[136] Hoefs J., **2009**. *Stable Isotope Geochemistry*. Springer-Verlag, Germany, 285 pp.
[137] Moore C.H., **1997**. *Carbonate diagenesis and porosity*. Elsevier, Amsterdam, 338 pp.

belonging to beachrock samples of Arrigunaga beach, with cements that show a different coloration; some can be greysh (that would be named as "1st cement layer") and over it, it can be found a brownish cement (named as "2nd cement layer"). Those two layers were carefully separated using a scalpel and collected for isotope analyses (Figure 6.19B). In case sufficient powder was obtained, samples were divided for coordinated stable isotopic and XRD analyses. Those two analyses were only possible in the cements samples obtained from *Grain 2* (Figure 6.19).

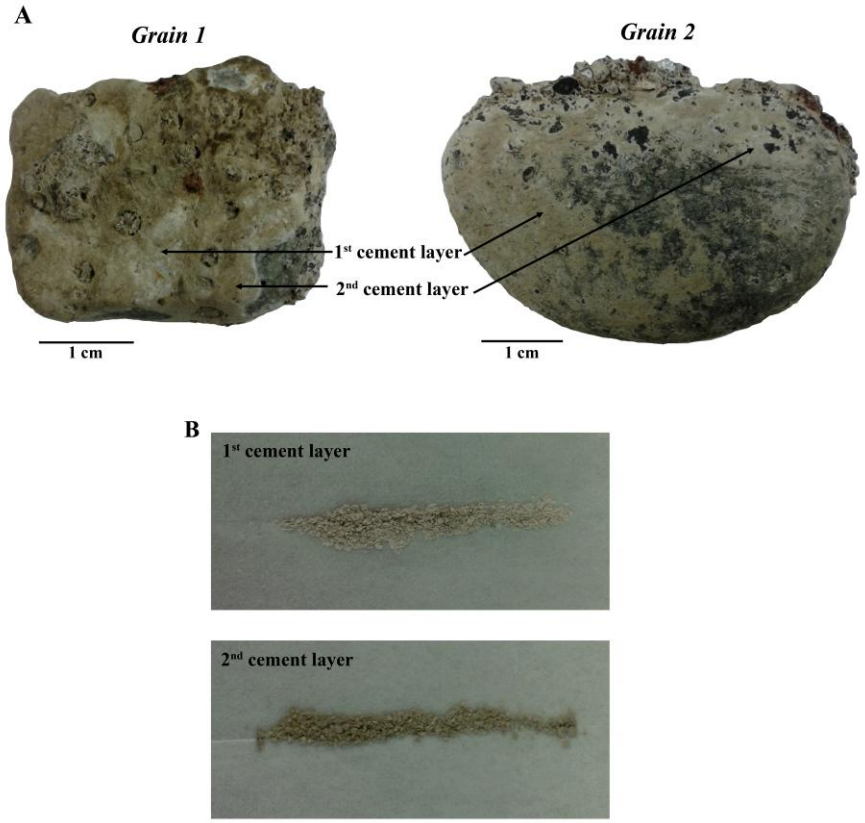

Figure 6.19. A) Examples of grains cemented within the beachrock, where apparently different cement layers can be discerned. B) Powdered cement extracted from the *Grain 2*.

Figure 6.20 shows the cross-plot of $\delta^{18}O$ and $\delta^{13}C$ stable isotopes in the two layers of those two grains used as an example. For *Grain 1*, the greyish layer shows a $\delta^{13}C$ value of 0.26‰ and a $\delta^{18}O$ value of -0.13‰, while the darker layer shows 0.40‰ $\delta^{13}C$ and -1.45‰ $\delta^{18}O$. Thus, the main difference between the two layers seems to be represented through the $\delta^{18}O$ isotope. Focusing now on the other example, *Grain 2*, those differences can be more marked: the greyish layer shows a $\delta^{13}C$ value of -0.85‰ and $\delta^{18}O$ of 0.45‰, while the darker layer shows more positive $\delta^{13}C$ values (0.20‰) depleted in $\delta^{18}O$ (-1.04‰). In addition, in that *Grain 2*, XRD analyses revealed that the

greyish layer is composed in 59% of aragonite, 24% LMC and 17% of HMC (with 12.2% mol $MgCO_3$). In contrast, the brownish layer contained 14% of aragonite, 69% LMC and 17% of HMC (with 13.1% mol $MgCO_3$).

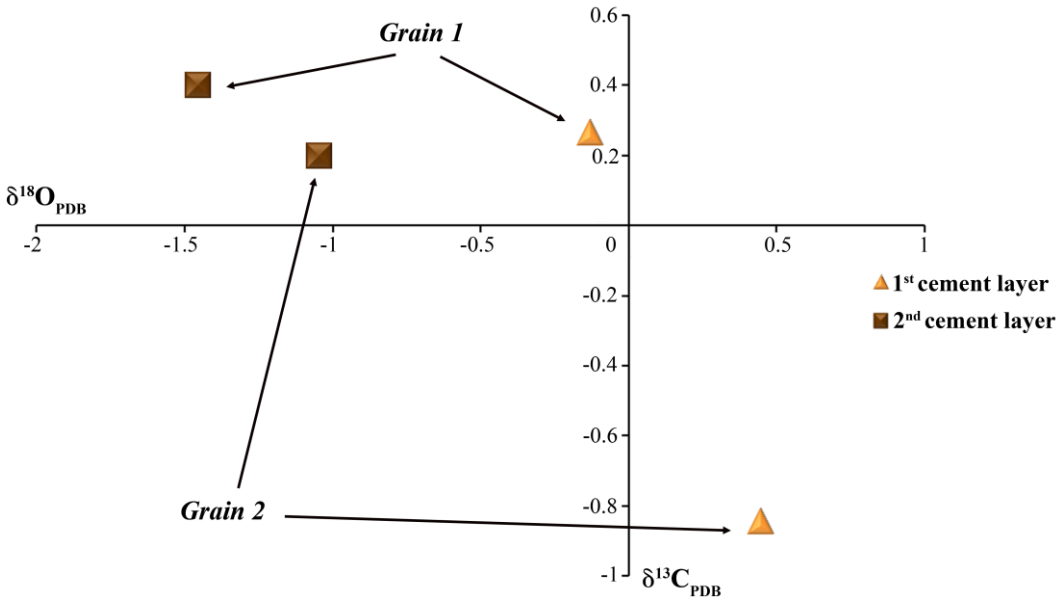

Figure 6.20. Cross-plot representing the $\delta^{13}C$ and $\delta^{18}O$ values (‰ PDB) in cement layers assumed to be different in composition and origin.

A $\delta^{13}C$ value in the range of around 0-3‰ is generally related with a marine composition[138]. Besides a $\delta^{13}C$ depletion has been sometimes attributed to an increased organic activity[139]. Furthermore, in marine and early diagenetic environments, as aragonite and HMC tend to evolve to stable LMC, a depletion of $\delta^{18}O$ can occur because of the influence of isotopically lighter waters like those coming from rainwater or groundwater[140-142]. Thus, specially *Grain 2*, can show the evolution of distinct cements, where there is at first mainly marine type cement (*1st cement layer*) that, in view of the relatively lower $\delta^{13}C$ value, could be possibly related with organic activity (which comes in agreement with the presence of HMC). The brownish cement (*2st cement layer*) is

[138] Hoefs J., **2009**. *Stable Isotope Geochemistry*. Springer-Verlag, Germany, 285 pp.
[139] Guerra N.C., Kiang C.H., Sial A.N., **2005**. *Carbonate cements in contemporaneous beachrocks, Juaribe beach, Itamaracá island, northeastern Brazil: petrographic, geochemical and isotopic aspects*. Anais da Academia Brasileira de Ciências 77, 343-352.
[140] Immenhauser A., Kenter J.A.M., Ganssen G., Bahamonde J.R., Van Vliet A., Saher M.H., **2002**. *Origin and significance of isotope shifts in Pennsylvanian carbonates (Asturias, NW Spain)*. Journal of Sedimentary Research 72, 82-94.
[141] Sharp Z., **2007**. *Principles of Stable Isotope Geochemistry*. Pearson Prentice Hall, Upper Saddle River NJ, USA, 344 pp.
[142] Sacks L.A., Tihansky A.B., **1996**. *Geochemical and isotopic composition of ground water, with emphasis on sources of sulfate, in the upper Floridan Aquifer and Intermediate Aquifer System in Southwest Florida*. U.S. Geological Survey, Water-Resources Investigations Report 96-4146.

mainly composed of LMC, typically formed under meteoric conditions (lower values of $\delta^{18}O$), as evidenced by Gonzalez and Lohmann (1985)[143].

It must be mentioned that both layers showed the same amount of HMC, which could denote two facts: (1) the two layers were not probably completely separated during the sampling of the cement; (2) it is known that HMC tends to evolve to LMC in meteoric conditions, as freshwaters can remove the Mg from the HMC[144]. Therefore, the amount of HMC in the greyish layer could be originally higher but it was diminished upon the formation of LMC. Although more analyses should be made on this regard, these first premises exemplify the characteristics that could be found within the carbonate cements and would hopefully contribute to a better understanding of further results.

During the mechanical removal of the cement grains, it was not always possible to separate the different layers of cements; in those cases, the cements were removed as a whole both in samples from Arrigunaga (where 16 samples could be used for cement extraction) and La Salvaje beach (where 10 samples could be used for cement extraction), which were described in section 3.1 of Chapter 3. Whatever the case, the cements were always carefully removed to avoid contamination and mistaken results.

Based on the analysed samples, stable isotope ratios of the cements from Arrigunaga beach showed quite variable $\delta^{13}C$ values ranging from -6.66 to 1.34‰. A similar fluctuation can be also found for $\delta^{18}O$ values, showing values between -5.81 and 1.14‰. In contrast, the results obtained in the samples from La Salvaje beach exhibit a lesser variability either for $\delta^{13}C$ values (which go from -1.51 to 1.49‰) or $\delta^{18}O$ values (that range between -2.42 and 0.73‰). These results are plotted in Figure 6.21a, to simultaneously shown the relation of the oxygen and carbon isotopes in both settings.

Considering the positive $\delta^{13}C$ and $\delta^{18}O$ values, both Arrigunaga and La Salvaje beach contain cements formed in a shallow marine context. Furthermore, the data denote that the bulk precipitation seems to occur at temperatures characteristic of the area of study (15ºC on average)[145]. Some cement samples show positive $\delta^{18}O$ values but are more depleted in $\delta^{13}C$ (Figure 6.21a), indicating that the cements might have precipitated from marine fluids modified by the contribution of organically derived CO_2, as

[143] González L.A., Lohmann K.C.,**1985**. *Carbon and oxygen isotopic composition of Holocene reefal carbonates*. Geology 13, 811-814.
[144] Folk R.L., **1974**. *The natural history of crystalline calcium carbonate; effect of magnesium content and salinity*. Journal of Sedimentary Petrology 44, 40-53.
[145] Moore C.H., **1997**. *Carbonate diagenesis and porosity*. Elsevier, Amsterdam, 338 pp.

already suggested in Figure 6.20. The $\delta^{13}C$ could be modified for instance by aerobic oxidation of organic matter[146]. Nevertheless, the origin of the marine modification has not been identified.

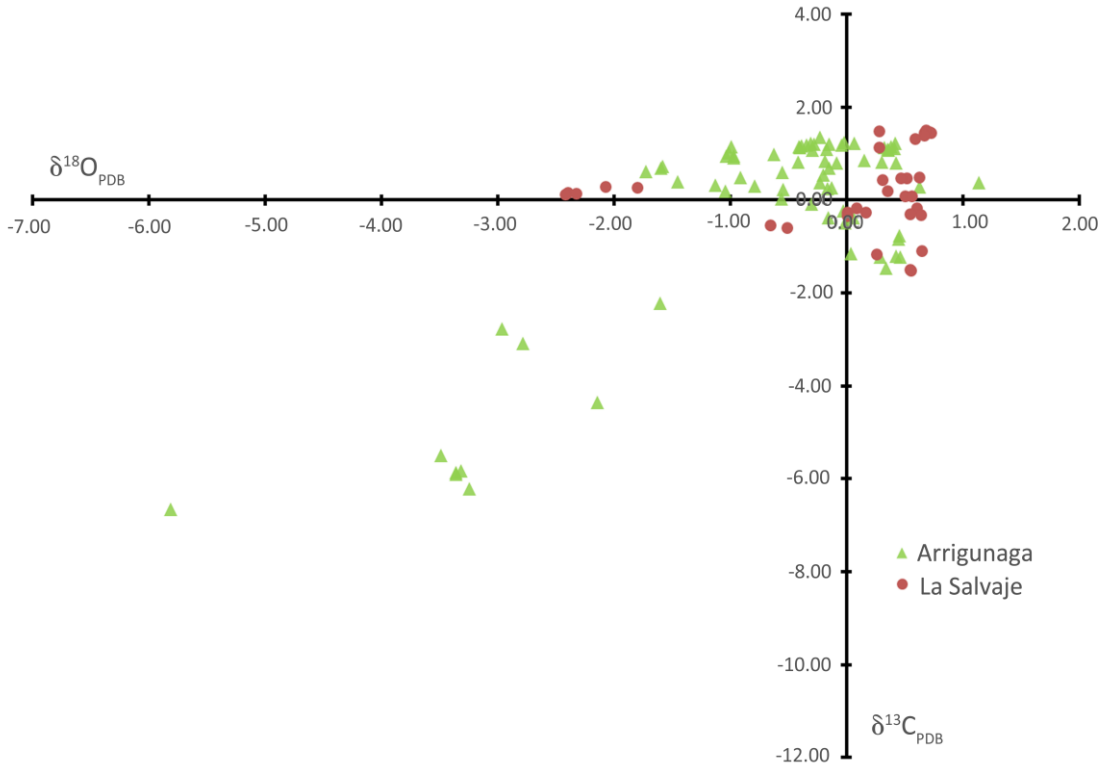

Figure 6.21a. Cross-plot representing the $\delta^{13}C$ and $\delta^{18}O$ values (‰ PDB) of carbonate cements belonging to beachrock outcrops from Arrigunaga and La Salvaje beach.

Additionally, the positive $\delta^{13}C$ values and the $\delta^{18}O$ depletion found especially in Arrigunaga beach suggest that the marine fluids from which the cement was precipitated, might have been influenced by the mixing with isotopically lighter freshwater fluids. The majority of the samples related with such data belong to beachrock outcrops located in the north of the Arrigunaga beach (areas ART1-ART5 and ARL1, see section 3.1.2 in Chapter 3), where the cements can suffer the influence of percolating freshwaters (some likely to occur after storm events) and/or groundwaters from a nearby (less than 10 meters) spring that flows directly in the beach. Exceptionally, isotopic evidences of mixing waters were also found in samples from La Salvaje beach, in the area LSL4 (see section 3.1.2 in Chapter 3); it could be caused by the presence of meteoric cements like LMC, or also considering that LSL4 is located in the mid part of the beach, in less

[146] Hoefs J., **2009**. *Stable Isotope Geochemistry*. Springer-Verlag, Germany, 285 pp.

consolidated outcrops where groundwaters from the spring of La Salvaje beach arrive, having lower $\delta^{18}O$ values due to calcites precipitated on the subsurface in shallow burial conditions[147].

With respect to Arrigunaga beach there is also another set of beachrock samples, collected in the central part of the beach, with depleted $\delta^{13}C$ and $\delta^{18}O$ values that should be explained. The oxygen depletion indicates again a mixture between freshwater and seawater during the cementation process. As it has been previously mentioned, groundwaters can be a possible source of that isotopically lighter freshwater[148,149], and this central part of the beach has a second spring that is continuously flowing to the area of such beachrocks.

In any case, the geochemical characteristics of the groundwater can vary depending on climate, catchment lithology, chemical weathering rates, nutrient amount or even anthropogenic impacts (domestic, industrial and agricultural pollutants)[150]. The influence of those factors can be reflected in the $\delta^{13}C$ values and for example, regarding the anthropogenic impact, depleted values of $\delta^{13}C$ could be attributed to the influence of sewage waters. In fact, stable isotopes have been used to examine sewage impacts[151,152], and carbonates derived from sedimentary organic matter or sewage can have $\delta^{13}C$ values varying from -16 ‰ to +2 ‰[153]. A previous study carried out by our research group in the Tunelboka cove, revealed that $\delta^{13}C$ values between -5 and -7.5‰ can be reached in points of the cove especially affected by the sewage outfalls disposed there[154]. Similar values have been also found in the presence of active microbial communities with a high accumulation of nutrients in clays of Altamira Cove[155].

[147] Moore C.H., **1997**. *Carbonate diagenesis and porosity*. Elsevier, Amsterdam, 338 pp.
[148] Sacks L.A., Tihansky A.B., **1996**. *Geochemical and isotopic composition of ground wáter, eith emphasis on sourcces of dulfate, in the upper Floridan Aquifer and Intermediate Aquifer System in Southwest Florida*. U.S. Geological Survey, Water-Resources Investigations Report 96-4146.
[149] Van Geldern R. And Barth J.A.C., **2014**. *Oxygen and Hydrogen Stable Isotopes in Earth's Hydrologic Cycle*. In Grupe G. and McGlynn (Eds.), Isotopic landscapes and bioarchaeology. Springer, Germany, pp. 173-188.
[150] Schulte P., Van Geldern R., Freitag H., Karim A., Négrel P., Petelet-Giraud E., Probst A., and Probst, J.-L., Telmer K., Veizer J., Barth J.A.C., **2011**. *Applications of stable water and carbon isotopes in watershed research: Weathering, carbon cycling, and water balances*. Earth-Science Reviews 109, 20-31.
[151] Lepoint G., Dauby P., Gobert S., **2014**. *Applications of C and N stable isotopes to ecological and environmental studies in seagrass ecosystems.* Marine pollution bulletin 49, 887-891.
[152] Rogers K.M., **2003**. *Stable carbon and nitrogen isotope signatures indicate recovery of marine biota from sewage pollution at Moa Point,New Zealand*. Marine Pollution Bulletin 46, 821-827.
[153] 2016 May 8 Personal Communication from L. Gonzalez.
[154] Arrieta N., **2014**. *The study of an unusual temperate latitude beachrock formation. Characterization of Azkorri beach and Tunelboka cove locations*. PhD Thesis, University of the Basque Country.
[155] Sanchez-Moral S., Portillo M.C., Janices I., Cuezva S., Fernández-Cortés A., Cañaveras J.C., Gonzalez J.M., **2012**. *The role of microorganisms in the formation of calcitic moonmilk deposits and speleothems in Altamira Cave*. Geomorphology 139-140, 285-329.

The samples with the strongest $\delta^{13}C$ depletion (-6.6‰) were found in Arrigunaga beach, in the stratigraphic column described in section 3.1.1 of Chapter 3, which is located in the highest intertidal zone, i.e. further away from the sea, where the influence of groundwaters coming from the nearby spring is more evident.

To understand the influence of mixing seawaters with isotopically lighter waters (groundwaters) in the cementation process, the $\delta^{18}O$ vs $\delta^{13}C$ data have been plotted in Figure 6.21b with a model developed by Gonzalez L.[156] to simulate the behaviour of negative $\delta^{18}O$ vs. $\delta^{13}C$ values as a function of mixing seawater and groundwater with different levels of CO_2 concentration. As seen our experimental isotopic data match within the boundaries of the referred model, suggesting that some areas of the beachrocks have been affected by the influence of freshwaters (groundwaters) arriving at the intertidal areas of the beach.

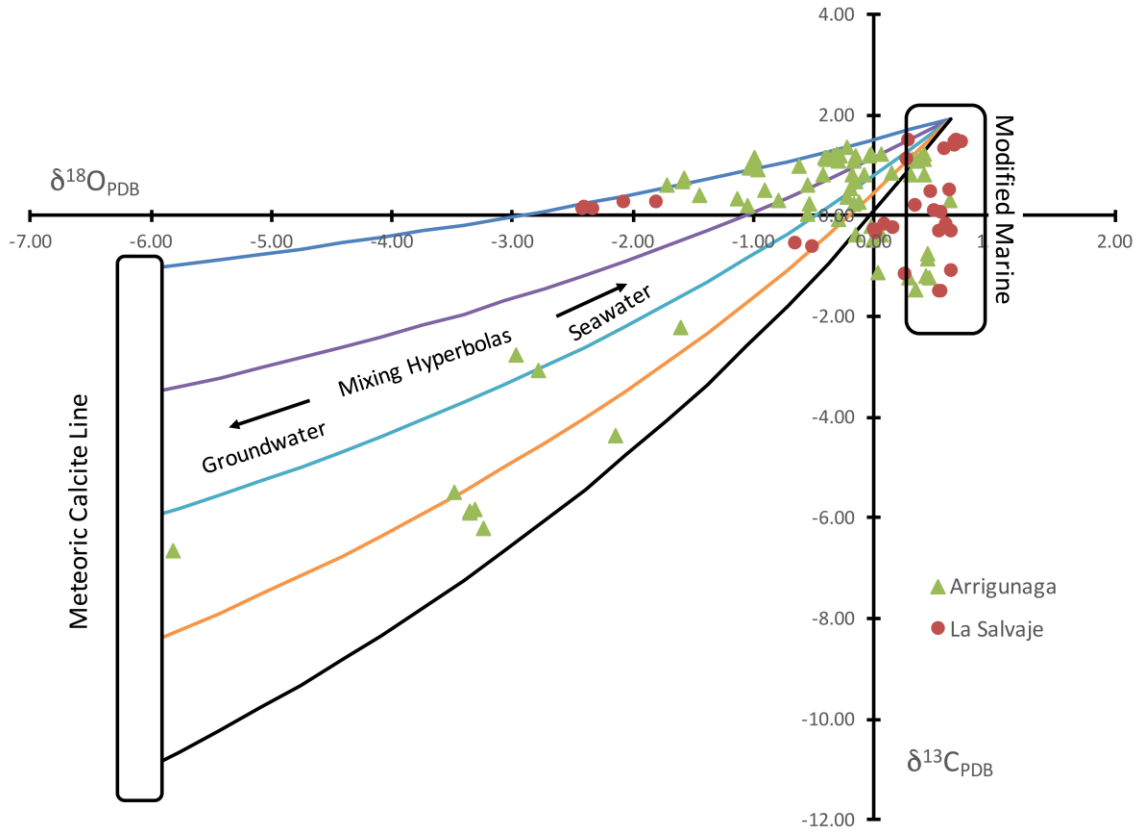

Figure 6.21b. Cross-plot representing the $\delta^{13}C$ and $\delta^{18}O$ values (‰ PDB) of carbonate cements belonging to beachrock outcrops from Arrigunaga and La Salvaje beach. The arrows indicate the mixing influence in calcite precipitation between seawater and freshwater (groundwater). The hyperbolic lines of the model are calculated from low to medium $\delta^{13}C$ values when mixing seawater (with 2.5 mmol/L CO_2 and $\delta^{13}C$=1) and groundwaters (with 4 mmol/L CO_2 at four levels of $\delta^{13}C$=-2.0,-4.5,-7.0, -9.5 and -12.0)[156].

[156] 2016 May 8 Personal Communication from L. Gonzalez.

Additionally we should consider that the Arrigunaga beach was in a rather anthropized area, affected by the estuary plume and diverse urban effluents coming from the estuary itself (e.g. Gobelas river), through the Kantarepe cove or from sewage outfalls disposed in Tunelboka cove (see section 1.2.4 in Chapter 1). Thus, it seems that the carbonate cements precipitated from mixing waters can be influenced not only by natural freshwaters but also from modified natural waters impacted by anthropogenic sources. This cannot be differentiated in this PhD work and it remains to be determined the possible contribution of those anthropogenic impacts, like the disposal of sewage waters, on that mixing to further research works.

6.1.6 General remarks of the study of carbonate cements

The results obtained in relation with the carbonate cements allowed hypothesising about the factors and possible mechanisms involved in their formation. Frequently, a micritic coating was found in direct contact with the grains, either in bioclasts or siliclastic grains. Regarding the composition, the position and broadening of the Raman bands, as well as XRD results, indicated the presence of HMC, composed on average with 10.7-14.3% mol $MgCO_3$. The fluorescent nature of this layer and the diverse elements found within it (mainly C, O, Mg, Al and Si) denotes the influence of the microbiological activity, for example through possible bioturbation mechanisms that promote alkaline conditions in the interstitial fluids, favouring the precipitation of calcium carbonates.

Furthermore, some spherule-shaped structures likely to be related with ACC, could act as precursors of further carbonaceous phases like HMC. Indeed, successive to HMC, aragonite acicules were identified, which is the main calcium carbonate composing the cements (according to XRD analyses, around 70%). The detection of Raman bands characteristic of certain organic compounds, as well as the presence of hydromagnesite, would support the biological influence on the formation of carbonates. In addition, globular morphologies (Figure 6.15) found in SEM analyses, would indicate that microbially induced or mediated micritic crystals would enable the subsequent development of more prismatic crystals (composed of aragonite) by physicochemical processes, similarly to a sequence reported elsewhere[157].

Both, the micritic coating and the aragonitic rim, show a greater size in those samples located in the lowest intertidal zone, which could show the favouring of the

[157] Neumeier U., **1999**. *Experimental modelling of beachrock cementation under microbial influence*. Sedimentary Geology 126, 35-46.

marine environment over beachrock formation. Indeed, HMC and aragonite are usually the main marine carbonate cements in this kind of sedimentary structures[158]. Also, the isopachous disposition of the aragonite crystals, as well as the presence of the mesh of needles, are indicative of an active pore water circulation. On the whole, a marine phreatic environment was involved in the diagenetic processes. However, the sporadic presence of other carbonate phases like LMC (composed of 1-4.4% mol of $MgCO_3$) indicates that the cements have been influenced also by meteoric waters. The marine context was confirmed trough the stable isotope analyses, which showed that the meteoric influence is more remarkable in Arrigunaga than in La Salvaje.

With regard to the differences detected between beachrock formations of Arrigunaga (Figure 6.22A) and La Salvaje beach (Figure 6.22B), some relevant diagenetic features should be remarked. In fact, in the northern area of Arrigunaga beach (Figure 6.22A), infiltrated micritic sediments were found disposed in two types of arrangements: over the aragonite rim and within the intergranular pore space. According to the literature[159], the fluorescence that these cements display under the ultraviolet light and their heterogeneous composition (where the explicit presence of C should be highlighted) indicates that the components of the cement covering the acicular rim might have been infiltrated in stagnant conditions through percolation of muddy waters loaded in organic materials. Additionally, the intergranular micritic particles might come from the infiltration of heterogeneous silt-sized particles percolated specially in storm events. Those provenances would explain the presence of these diagenetic features only in the northern area of Arrigunaga beach, where apparently materials coming from the estuary plume, as well as cliff-derived clasts, were accumulated along the years. The presence of intergranular infiltrated particles is indicative of well-cemented structures. Therefore, the fact of having found these characteristics in some beachrock formations from Arrigunaga and not in La Salvaje, suggests that beachrock formations from La Salvaje beach are less consolidated or that they are less exposed to the vadose conditions that induce the percolation of particles. These differences between both beaches were also visualized through the stable isotope analyses.

[158] Vousdoukas M.I., Velegrakis A.F., Plomaritis T.A., **2007**. *Beachrock occurrence, characteristics, formation mechanisms and impacts*. Earth-Science Reviews 85, 23-46.
[159] Vieira M.M., De Ros L.F., **2006**. *Cementation patterns and genetic implications of Holocene beachrocks from northeastern Brazil*. Sedimentary Geology 192, 207-230.

Figure 6.22. A) View of the beachrock outcrops found in the northernmost part of Arrigunaga beach. B) Image of some beachrock outcrops located in La Salvaje beach.

6.2 Ferruginous cements and related features

Apart from the cements based in different forms of calcium carbonate (ACC, HMC, aragonite and calcite), it is noteworthy the presence of iron rich cements in the beachrocks from both beaches. Herein, some representative areas cemented with iron rich compounds will be described, as examples of this kind of iron containing cements.

Iron is common in detritic materials and it could come from the weathering of silicates and phyllosilicates present in the matrix[160]. However, in this particular case where many framework grains consist on iron rich slag, ferruginous cements could also be formed from the leaching of those anthropogenic materials trapped in the beachroks. In this context, it is worth recalling that, as described in Chapter 4, diverse slag were found within the beachrock formations of Arrigunaga, which were mainly composed of iron oxides, Ca, Mn and Fe silicates as well as sulphides, that could be altered by diverse weathering agents.

In the beachrock formations analysed in La Salvaje beach, similar compounds were also found. As an example, Figure 6.23 represents some mineral phases found by means of Raman spectroscopy in some trapped slag, where tephroite (Fe_2SiO_4) (with Raman bands at 809 and 839 cm^{-1}) and ilmenite ($FeTiO_3$) (with Raman peaks at 230 and 683 cm^{-1}) were identified, being both of them common in this kind of wastes[161,162]. Furthermore, other compounds were also detected, as shown in Figure 6.24 that includes the three titanium oxide (TiO_2) polymorphs: anatase, brookite and rutile. Apparently, anatase tends to transform to rutile influenced by atmospheric conditions, reduction or oxidation reactions, and the presence of impurities[163]. During that transformation, brookite could act as an intermediate phase[164]. Thus, the presence of the three TiO_2 forms in a slag could suggest that framework grains of La Salvaje beach are being subjected to alterations through weathering processes, resembling the affections found in the beachrock of Arrigunaga beach (see Chapter 4, section 4.2.1).

[160] Bojanowski M.J., Jaroszewicz E., Kosir A., Lozinski M., Maynowski L., Wysocka A., Derkowski A., **2015**. *Root-related rhodochrosite and concretionary siderite formation in oxygen-deficient conditions induced by a ground-water table rise*. Sedimentology, DOI 10.1111/sed.122227.
[161] Gomez-Nubla L., Aramendia J., Fdez-Ortiz de Vallejuelo S., Castro K. and Madariaga J.M., **2013**. *From Portable to SCA Raman devices to characterize harmful compounds contained in used black slag produced in Electric Arc Furnace of steel industry*. Journal of Raman Spectroscopy 44, 1163-1171.
[162] Guéguin M., Cardarelli F., **2007**. *Chemistry and mineralogy of titania-rich slags. Part 1-Hemo-ilmenite, sulphate and upgraded titania slags*. Mineral processing & Extractive Metallurgy Review 28, 1-58.
[163] Hanaor D.A.H., Sorrell C.C., **2011**. *Review of the anatase to rutile phase transformation*. Journal of Materials Science 46, 855-874.
[164] Rezaee M., Mousavi K., Seyyed M., Liu K.H., **2011**. *The role of brookite in mechanical activation of anatase-to-rutile transformation of nanocrystalline TiO_2: An XRD and Raman spectroscopy investigation*. Crystal Engineering Communications 13, 5055-5061.

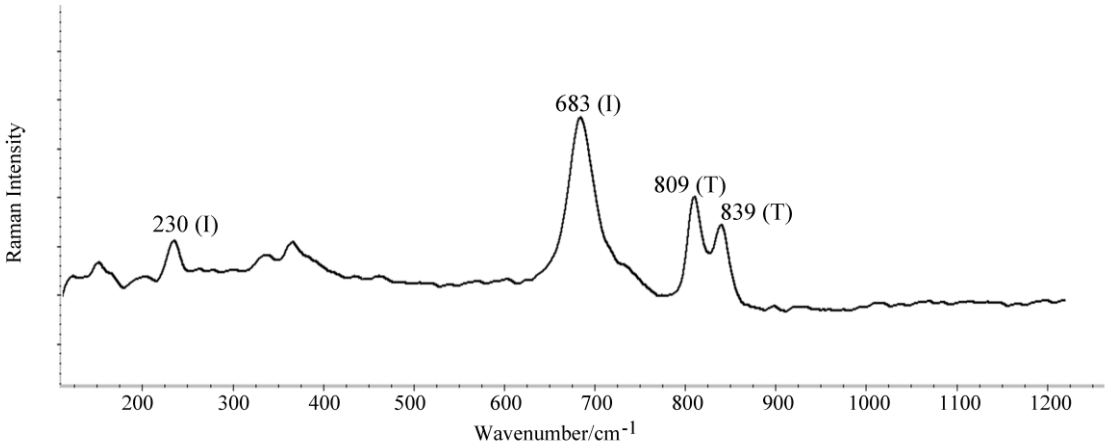

Figure 6.23. Raman spectrum of a slag where ilmenite (I) and tephroite (T) were observed.

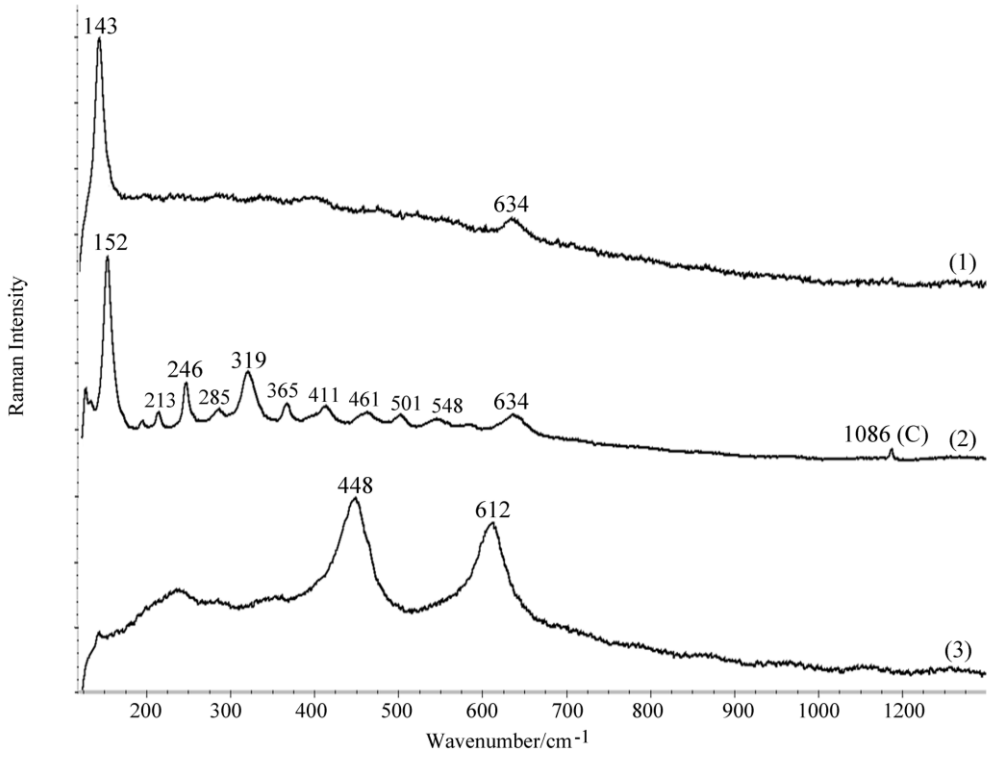

Figure 6.24. Raman spectrum of (1) anatase, (2) brookite together with carbonate (C) and (3) rutile found in a slag trapped in a beachrock sample of La Salvaje beach.

6.2.1 Microscopic and compositional analysis

Taking into consideration that framework grains, as the ones mentioned in the previous section, are being weathered, the characteristics of ferruginous cements will be described herein trying to understand their formation and estimate if the weathering has any implications in the cementation.

For that purpose, the joint use of polarizing microscopy, fluorescence microscopy, electron microscopy (especially based on BSE imaging) was selected, which will be aided by the determination of the main composition of the areas of interest through EDS and Raman spectroscopy, to identify compounds and features.

For example, Figure 6.25A-B, shows diverse grains bound by reddish cement broadly extended in the intergranular space. Moreover, fluorescent spots were recognized specially within some grains (Figure 6.25C) and general compositional differences can be immediately perceived in the BSE image (Figure 6.25D). The semiquantitative mappings shown in Figure 6.25E, allowed recognising that the grains are mainly composed of Ca, Si as well as Fe, surrounded by the iron rich cements. The fluorescence might be triggered by the presence of particles made of Ca, Si, Al, O and C (see the detailed view in Figure 6.25F).

As this example also provides a great chance to appreciate the convenience of BSE imaging in this kind of studies, that part will be described more in detail. Indeed, Figure 6.25D shows the BSE image, with a detailed view in Figure 6.25F of a grain surrounded by a grey layer and covered by an extensive white area. The diverse colorations found with the BSE detector already suggest that the composition might be different due to the presence of elements with distinctive atomic number (Z); the elements with higher atomic number backscatter more electrons than light elements, so they produce brighter spots in the image and certainly, the EDS mappings (Figure 6.25F) indicated that the grey cement is composed of Ca, Mg and smaller amounts of Si (Z=20, Z=12, and Z=14 respectively), while the brighter extensive white area is composed of Fe (Z=26). Therefore, thanks to this technique alternations of carbonate and ferruginous cements can be straightforwardly detected.

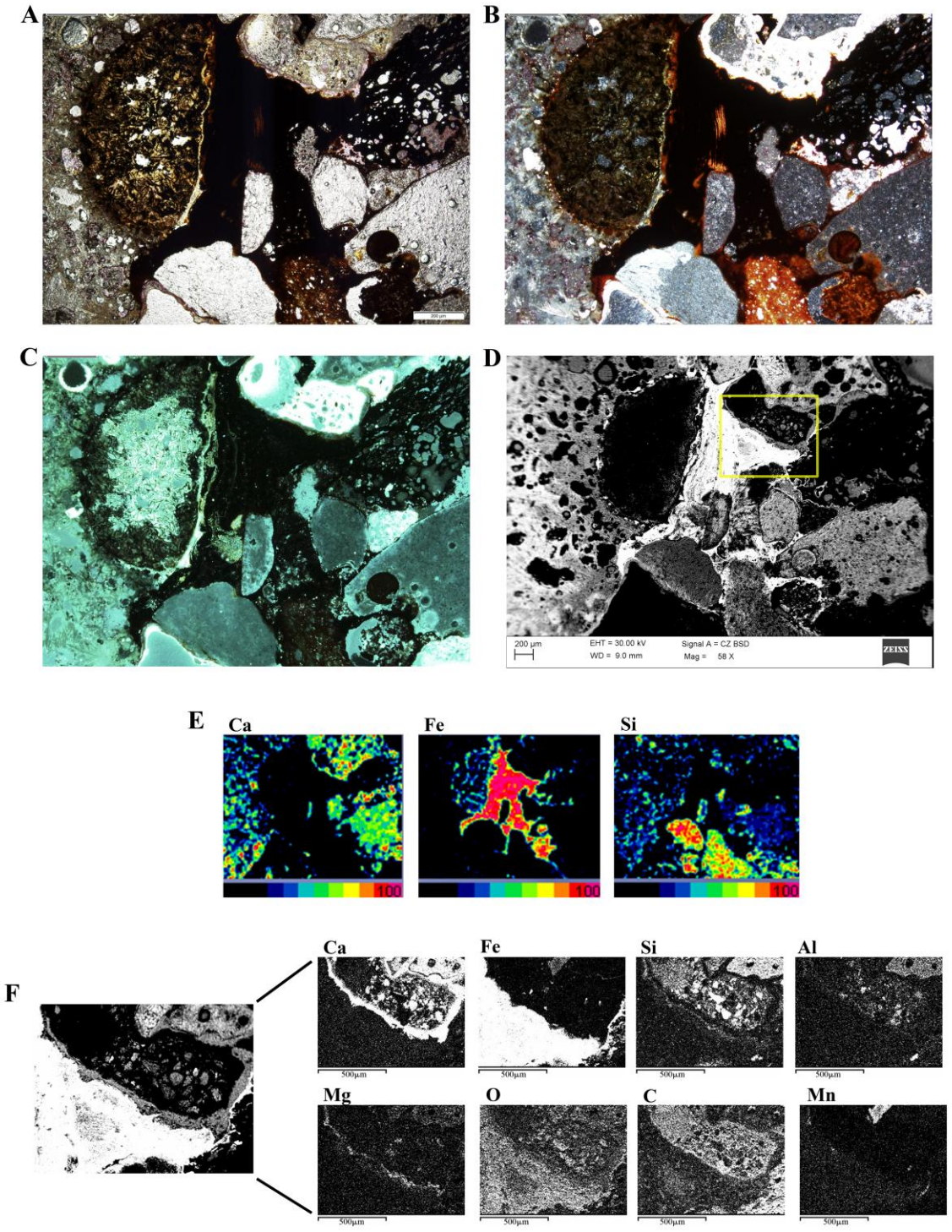

Figure 6.25. A) Plane polarized light, B) Crossed polarized light and C) UV light (fluorescence microscopy) image obtained over a thin section that shows diverse grains amalgamated with ferruginous cement (Scale: 2mm); D) Backscattered electron image indicating with a square the area measured in F; E) False colour semiquantitative EDS element mappings of A-D; F) Detailed backscattered electron image of the square area marked in D, and the corresponding EDS element map distributions.

To our surprise, we have detected in some cases (a) the nearly absence of carbonate cements or (b) the carbonate cement completely covered by ferruginous cements. For example, Figure 6.26 shows an area of a sample from Arrigunaga beach where reddish cement can be observed coming out from a main grain and spread across smaller framework grains present in the matrix. The reddish colour observed at light microscopy (Figure 6.26A-B) and the brightness in the BSE image (Figure 6.26D), suggested the presence of an element with a higher atomic number like Fe, which was confirmed through the EDS mapping (Figure 6.26E-F). Indeed, the reddish cement is mainly constituted of Fe, which spreads out from a grain composed of Ca, Si, Al, Mg, C and O. Although fluorescence may be altered or attenuated by the presence of iron[165], observing the same area under ultraviolet light, some fluorescent composites can be discerned (Figure 6.26C) specially in Fe rich spots (Figure 6.26E-F).

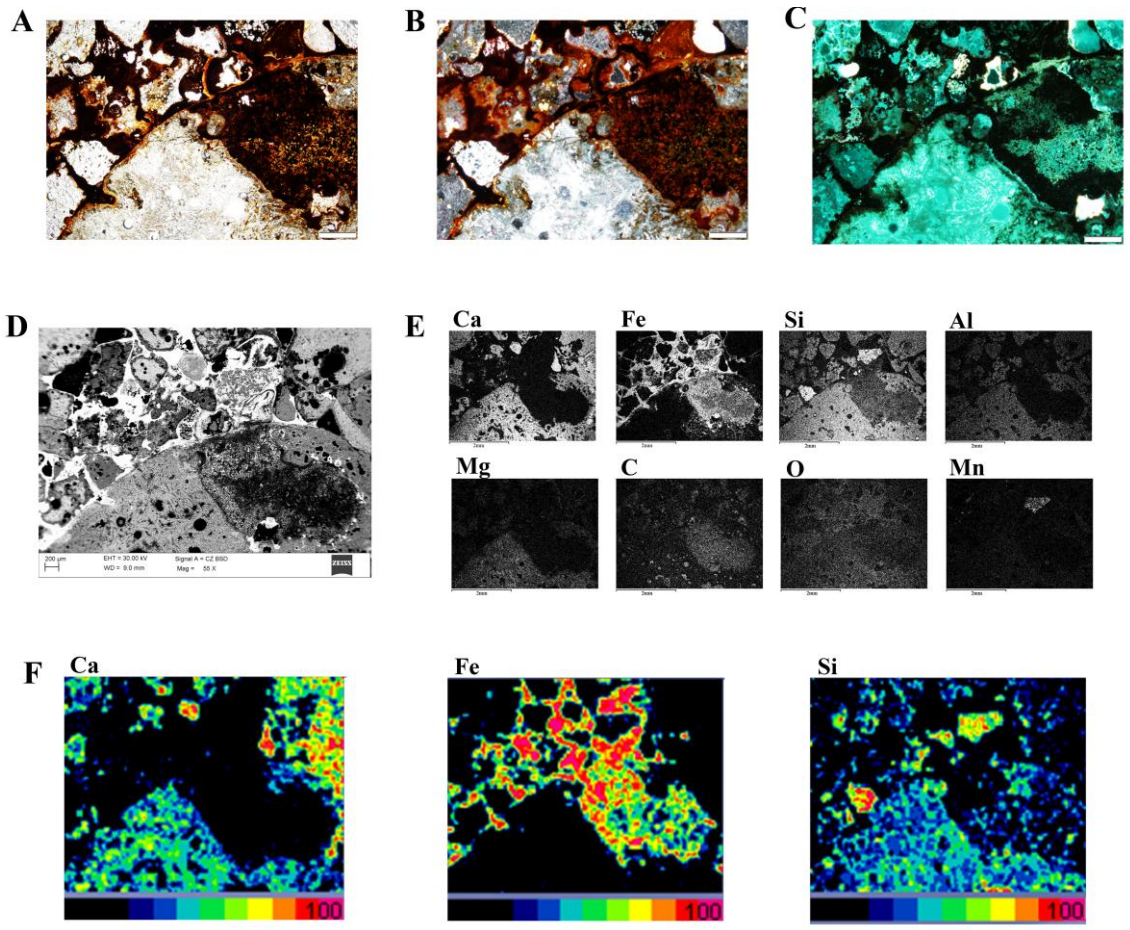

Figure 6.26. A) Plane polarized light image, B) Crossed polarized light image and C) UV light (fluorescence microscopy) image of a thin section showing a grain covered by ferruginous cement (Scale: 200µm); D) Backscattered electron image of the area of interest; E) the corresponding EDS element map distributions; F) False-colour semiquantitative EDS element mappings for Ca, Fe and Si .

[165] Rost F.W.D., **1995**. *Fluorescence Microscopy, Volumen 2*. Cambridge University Press, 473 pp.

Focusing more in detail on the characteristics of the iron-rich cements, Raman spectroscopy allowed unravelling the mineralogical composition. This way, the iron oxide hematite (α-Fe_2O_3) was found with characteristic Raman bands at 224, 244, 292, 409, 498 and 612 cm^{-1} (Figure 6.27). In addition, one of the major phases was the hydrated iron oxyhydroxide limonite ($FeO(OH)\cdot nH_2O$, with characteristic Raman bands at 299, 396 and 552 cm^{-1}, see Figure 6.28), which could be detected individually or together with carbonates.

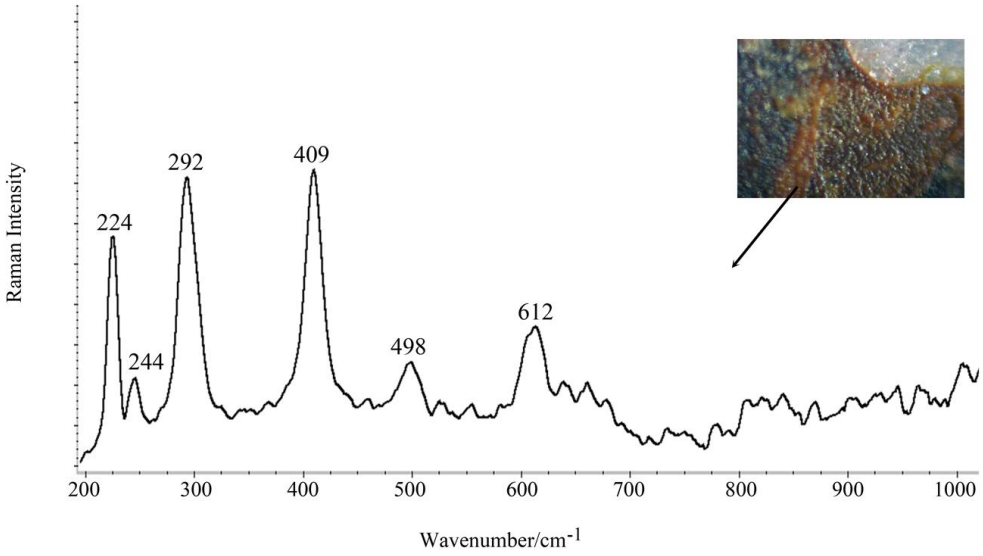

Figure 6.27. Raman spectrum of hematite found within the ferruginous cement.

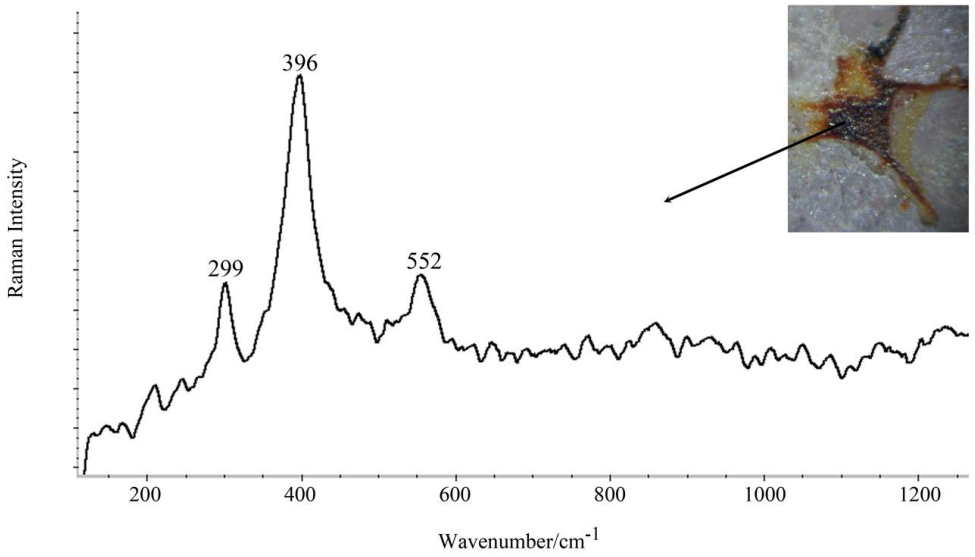

Figure 6.28. Raman spectrum of limonite found within the ferruginous cements.

In addition, often diverse mixtures of iron compounds were detected within the cements. As shown in Figure 6.29, some mixtures include the iron oxyhydroxide goethite (α-FeO(OH), with the characteristic Raman bands at 248, 299, 387, 477, 549 cm^{-1}) and the mixed iron oxide magnetite (Fe_3O_4, recognised thanks to its Raman bands at 320, 549 and 681 cm^{-1}). Other ones (Figure 6.30) could contain the oxyhydroxides limonite ($FeO(OH)\cdot nH_2O$) and lepidocrocite (γ-FeO(OH), with characteristic Raman bands at 148, 217, 251, 302, 348, 380, 527 and 643 cm^{-1}).

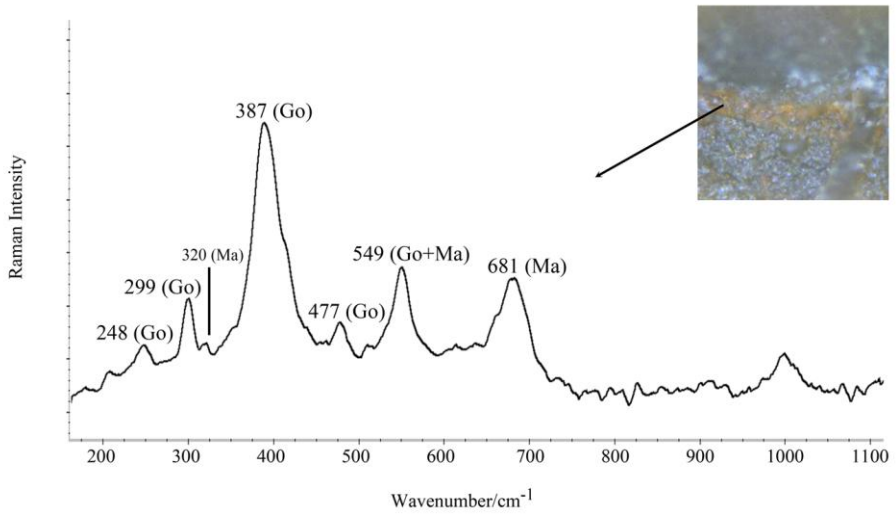

Figure 6.29. Raman spectrum showing a mixture of goethite (Go) and magnetite (Ma) found in the iron-rich cement.

.

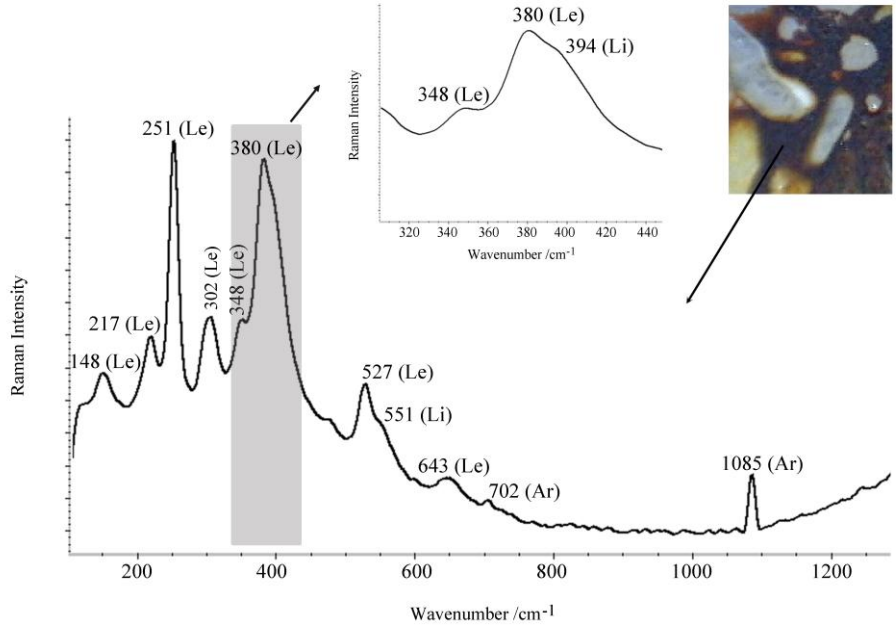

Figure 6.30. Raman spectrum with a mixture of lepidocrocite (Le), limonite (Li) and aragonite (Ar) found in the iron-rich cement.

Furthermore, as it has been previously mentioned, the described iron compounds could be found together with carbonates within the ferruginous cements. The carbonate compounds usually were aragonite (as shown in Figure 6.30) and sporadically, calcite. Nonetheless, other carbonate phases were also recognized, as it is illustrated in Figure 6.31, belonging to a beachrock sample from La Salvaje. There, it can be observed a clast, mainly composed of Ca, O, Si, Al and Mg, enclosing reddish cements, which in turn, are placed among other smaller grains (Figure 6.31A-C).

The diverse white and black colour range shown in the BSE image (Figure 6.31D) already suggests that various elements with significantly different atomic weights (numbers) are distributed in the area of interest. Indeed, the main element found in the clast is Ca, while in the reddish areas Fe and even Mn are dispersed across the framework grains and the cement (Figure 6.31E). Certainly, Fe is especially accumulated within the cement, while Mn forms some kind of discontinuous layers in certain points; furthermore, the presence of both of them, coincides to some extent with C and O.

Thus, all that information provided the clues to infer the presence of other compounds, and certainly, Raman spectroscopy allowed identifying in that area not only iron rich compounds like limonite and lepidocrocite, and carbonates like aragonite and HMC; but, as shown in Figure 6.32, rhodochrosite ($MnCO_3$) was detected in the spots rich in Mn, due to its main Raman bands at 282, 716 and 1086 cm^{-1}, and also siderite ($FeCO_3$) was detected in the surrounding a bioclast made of HMC and recognized by its main Raman bands at 281, 733 and 1088 cm^{-1}. Siderite is ascribed to early diagenetic processes[166] and it can be formed in intertidal or nearshore sediments undergoing alternating anoxic and oxic conditions[167]. As it has been already stated, the iron present in detritic (silicates and slag) materials can be released to pore waters though weathering processes. In oxic conditions, the iron form oxides and oxyhydroxides with Fe^{3+} ions. But when a depletion of the oxygen occurs, those phases are reduced and Fe^{2+} ions are liberated. In case that the reducing conditions last in time, and the alkaline conditions are promoted, the precipitation of siderite might occur. Remember that iron and manganese have a similar behaviour in shallow diagenetic environments[168].

[166] Gautier D.L., **1982**. *Siderite concretions: indicators of early diagenesis in the Gammon shale (Cretaceous)*. Journal of Sedimentary Petrology 52, 859-871.
[167] Hicks K.S., Compton J.S., McCracken S., Vecsei A., **1996**. *Origin of diagenetic carbonate minerals recovered from the New Jersey continental slope*. In: Mountain G.S., Miller K.G., Blum P., Poag C.W., Twichell D.C. (Eds.), Proceedings of the Ocean Drilling Program, Scientific Results, Vol. 150, p. 311-328.
[168] Bojanowski M.J., Jaroszewicz E., Kosir A., Lozinski M., Maynowski L., Wysocka A., Derkowski A., **2015**. *Root-related rhodochrosite and concretionary siderite formation in oxygen-deficient conditions induced by a ground-water table rise*. Sedimentology, DOI 10.1111/sed.122227.

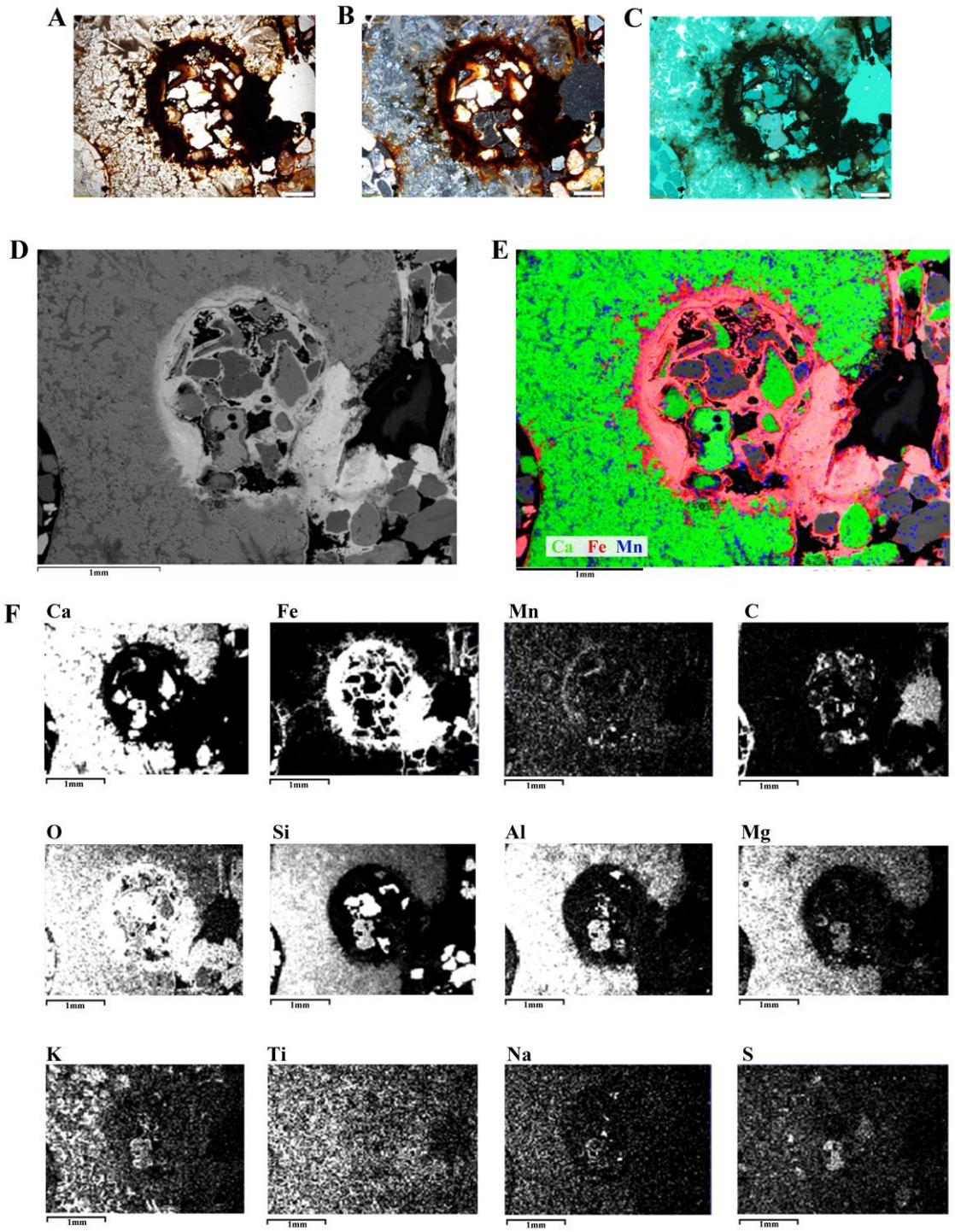

Figure 6.31. A) Plane polarized light, B) Crossed polarized light and C) UV light (fluorescence microscopy) images of a thin section corresponding to a clast that contains ferruginous cement (Scale: 200µm); D) Backscattered electron image of the same spot (Scale: 1mm); E) False colour backscattered electron image; F) EDS elemental mappings of the area of interest.

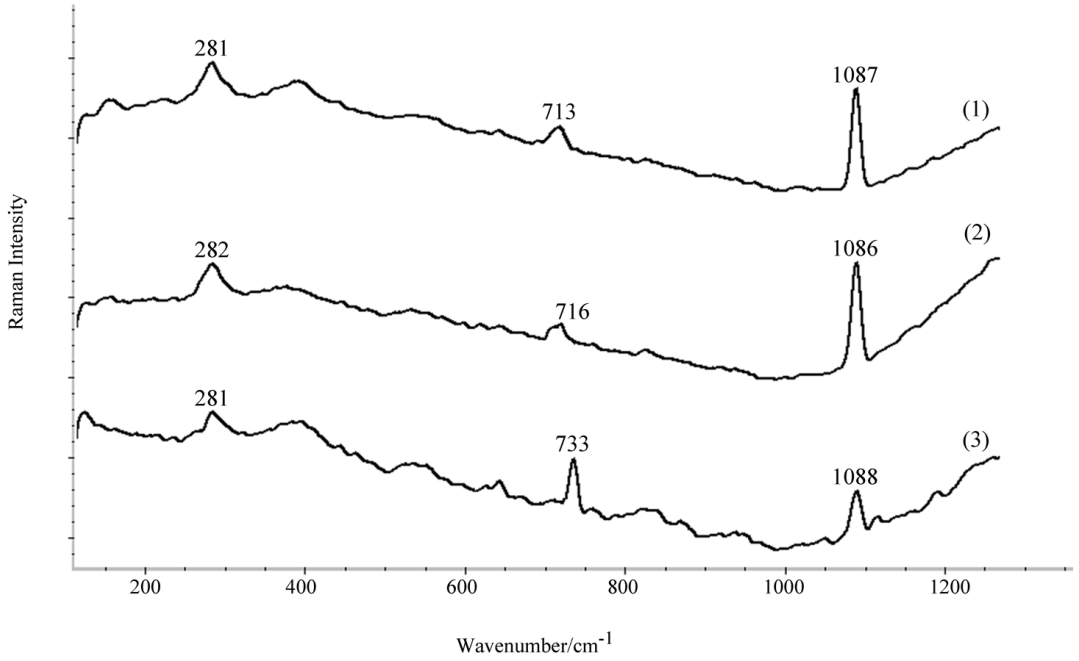

Figure 6.32. Comparison between the Raman spectra of (1) HMC, (2) rhodochrosite found in Mn-rich spots and (3) siderite detected surrounding a bioclast composed of HMC.

Therefore, during the diagenesis, diverse secondary iron and manganese minerals can be formed, like for example, authigenic siderite or rhodochrosite. Although iron and manganese can be chemically reduced[169], in natural settings this process is usually mediated by biological activity[169,170]. According to the literature, both minerals are formed in rapidly accumulating organic-rich sediments, where the bicarbonate ion HCO_3^- is generated as a consequence of organic matter oxidation[171]. As an example, the formation of siderite in sedimentary rocks or marine sediments has been related with the degradation of organic material upon methanogenic bacteria, with anoxic conditions of deep-sea sediments and even with the Fe(III) reduction through sulphate-reducing bacteria (SRB)[171] or iron-reducing bacteria[172]. Actually, most known dissimilatory Fe-reducing bacteria, reduce manganese as well[173] and especifically the presence of rhodocrhosite has been related for instance with organic-rich carbonates[174].

[169] Burdige D.J., **1993**. *The biogeochemistry of manganese and iron reduction in marine sediments*. Earth-Science Reviews 35, 249-284.
[170] Frederichs T., Von Dobeneck T., Bleil U., Dekkers M.J., **2003**. *Towards the identification of siderite, rhodochrosite and vivianite in sediments by their low-temperature magnetic properties*. Physics and Chemistry of the Earth 28, 669-679.
[171] Konhauser K.O., **1998**. *Diversity of bacterial iron mineralization*. Earth-Science Reviews 43, 91-121.
[172] Sánchez Román M., Fernández-Remolar D., Amils R., Sánchez-Navas A., Schmid T., San Martin-Uriz P., Rodríguez N., McKenzie J.A., Vasconcelos C., **2014**. *Microbial mediated formation of Fe-carbonate minerals under extreme acidic conditions*. Scientific Reports 4, 1-7.
[173] Thamdrup B., Rosselló-Mora R., Amann R., **2000**. *Microbial manganese and sulfate reduction in Black Sea Shelf Sediments*. Applied and Environmental Microbiology 66, 2888-2897.
[174] Roy S., **2006**. *Sedimentary manganese metallogenesis in response to the evolution of the Earth system*. Earth-Science Reviews 77, 273-305.

On the whole, it must be emphasized that various compounds were found composing the ferruginous cements (see Table 6.2), triggered by oxidizing and reducing conditions that could have been promoted through abiotic or/and biotic circumstances.

Table 6.2. Compounds detected within the ferruginous cement through Raman spectroscopy.

Mineral phase	Formula	Raman bands
Fe(III) minerals		
Hematite	α-Fe_2O_3	224s, 244m, 292vs, 409vs, 498m, 612m
Limonite	$FeO(OH)\cdot nH_2O$	299s, 396vs, 552m
Lepidocrocite	γ-FeO(OH)	148w, 217m, 251vs, 302m, 380s, 527m, 643br
Goethite	α-FeO(OH)	248w, 299s, 387vs, 477m, 549m
Mixed Fe(II)-Fe(III) mineral		
Magnetite	Fe_3O_4	320w, 549w, 681vs
Fe(II) mineral		
Siderite	$FeCO_3$	281w, 733s, 1088s
Mn(II) mineral		
Rhodochrosite	$MnCO_3$	282m, 716w, 1086vs

Generally, the ferruginous cements found in beachrock outcrops from Arrigunaga beach were from the outcrops located in the northern area of the beach that, according to the results described in Chapter 5, were characterized by greater amounts of various elements like for example Fe, Mn, Ca, Al or even K and Ti. A similar situation was encountered in La Salvaje beach, because the ferruginous cements were generally detected in the area with significantly higher amounts of metals (the southwestern area). These findings do not exclude the presence of ferruginous cements in other areas of the beaches, but it does suggest that the higher concentration of diverse elements might make those outcrops more prone to contain ferruginous cements.

The presence of various Fe(II)/Fe(III) phases within the cements indicates that hydration-dehydration processes as well as oxidation-reduction processes are involved in the formation of this kind of cements, as it was observed in other studies focused on adjacent beachrocks[175]. Additionally, the presence of iron and manganese carbonates has been also registered in similar sedimentary structures[176], which provides relevant information to enlighten the processes that might occur in the pore water domain.

[175] Arrieta N., Goienaga N., Martínez-Arkarazo I., Murelaga X., Baceta J.I., Sarmiento A., Madariaga J.M., **2011**. *Beachrock formation in temperate coastlines: Examples in sand-gravel beaches adjacent to the Nerbioi-Ibaizabal Estuary (Bilbao, Bay of Biscay, North of Spain)*. Spectrochimica Acta Part A 80, 55-65.
[176] Morad S., **1998**. *Carbonate cementation in sandstones: distribution patterns and geochemical evolution*. In: Morad S. (Ed.), Carbonate Cementation in Sandstones. International Association of Sedimentologists Special Publications 26, 1-26.

6.2.2 General remarks of the study of ferruginous cements

We must start highlighting that very few examples of ferruginous cements are described in the literature in regard to beachrock outcrops, especially from a temperate zone like the one we are studying. Some examples of similar systems were described by Adams and Schofield (1983)[177] that documented the presence of carbonate and hematite cements in gravels found next to a sunken ship in Scotland, concluding that the cementation was favoured by the activity of anaerobic bacteria through iron corrosion. Two years later, James (1985)[178] explored the early diagenesis in terrigenous deposits of sand and gravel, describing cements composed of limonite, calcite and gypsum, while Strasser and Bernier (1985)[179] described an early diagenetic cementation in a siliciclastic and temperate environment, containing ferruginous cements formed through physical and chemical properties of its interstitial waters, and the influence of microbial activity.

In addition, the adjacent beachrock formations from Azkorri beach and Tunelboka cove also enclose ferruginous cements, as described by Arrieta (2014)[180], innovatively using a multianalytical approach to discern the morphology, composition and general characteristics of the cements. That way, it was concluded that the formation of this kind of cements could be related with different weathering processes or even to microbiological mediated iron reduction processes, which induced dissolution episodes over the bulk iron mineral wastes encrusted between the natural bedrock.

Similarly, in beachrocks from Arrigunaga and La Salvaje beach the diverse iron-rich mineral phases, either made of Fe(III) or Fe(II), composing the ferruginous cements, lead to believe that their formation and transformations might be induced by the weathering and the wide range of pH and redox conditions that would occur in the interstitial fluids, following the biogeochemical iron cycle (see Figure 6.33).

[177] Adams A.E., Schofield K., **1983**. *Recent submarine aragonite, magnesian calcite, and hematite cements in a gravel from Islay, Scotland*. Journal of Sedimentary Petrology 53, 417-421.
[178] James W.C., **1985**. *Early diagenesis, Atherton formation (Quaternary): a guide for understanding early cement distribution and grain modifications in nonmarine deposits*. Journal of Sedimentary Petrology 55, 135-146.
[179] Strasser A., Bernier P., **1988**. *Early diagenetic ferruginous cementation in the intertidal zone: example from Nourmoutier Island, France*. Oceanologica Acta 11, 353-357.
[180] Arrieta N., **2014**. *The study of an unusual temperate latitude beachrock formation. Characterization of Azkorri beach and Tunelboka cove locations*. PhD Thesis, University of the Basque Country.

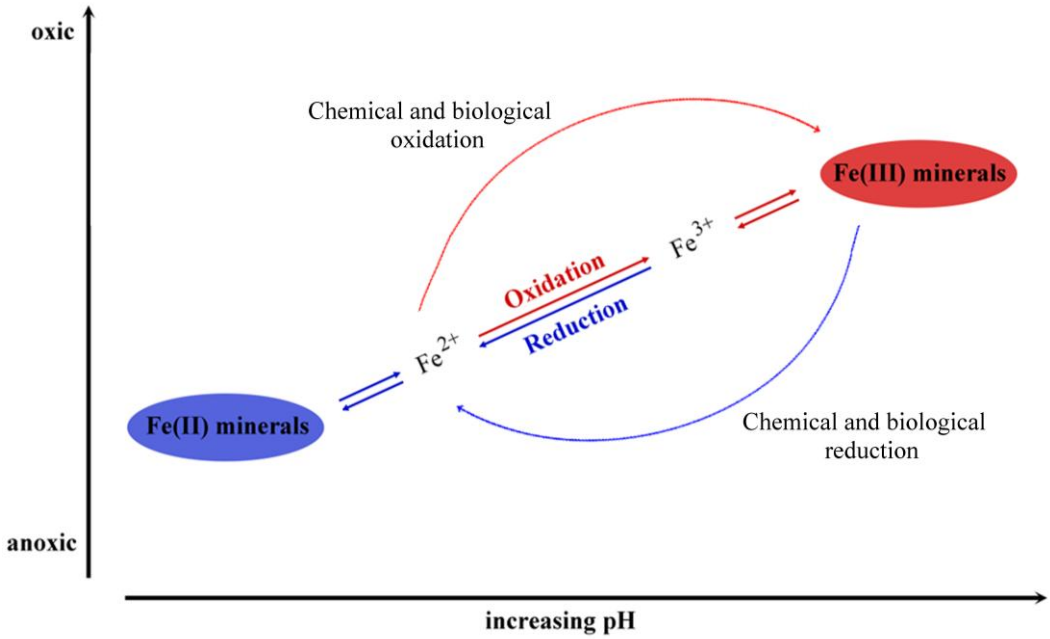

Figure 6.33. Representation of the chemical and microbial reactions predominant in the iron cycle. Modified from Kappler and Straub (2005)[181] and Oswald et al. (2009)[182].

The mixed-mineral system that is enclosed in the beachrock would be the main source of iron. Atmospheric conditions or other acidic gases could lead to the corrosion of the iron rich framework grains (like hematite, α-Fe_2O_3) releasing soluble Fe^{3+} ions to the interstitial fluid[183,184]. If that ferric iron encounters an area with a higher pH, for example due to the presence of bicarbonates, ferric oxyhidroxides like limonite ($FeO(OH)\cdot nH_2O$) could precipitate. Limonite is the most unstable and hydrated form of Fe (III) oxyhydroxides, thus, would tend to evolve through lepidocrocite (γ-FeOOH) or the most stable phase, goethite (α-FeO(OH)). Moreover, if anoxic conditions occur, iron can be (partially or totally) reduced and can form Fe(II) containing minerals like magnetite, and even siderite ($FeCO_3$). Other elements as manganese also appear in a reduced state of valence under such conditions and can form similar precipitates like rhodochrosite ($MnCO_3$). These alternating conditions could be triggered by chemical or biological factors, being the latter especially relevant possibly in the siderite and rhodochrosite formation.

[181] Kappler A. and Straub K.L., **2005**. *Geomicrobiological cycling of iron*. Reviews in Mineralogy and Geochemistry 59, 85-108.
[182] Oswald K., Melton E.D., Scmidt C., Kappler A., **2009**. *Microbial iron mineral formation and dissolution: creating a biogeochemical iron cycle in a bottle*. Master Thesis, University of Tübingen.
[183] Aramendia J., Gómez-Nubla L., Arrizabalaga I., Prieto-Taboada N., Castro K., Madariaga J.M., **2013**. *Multianalytical approach to study the dissolution process of weathering steel: The role of urban pollution.* Corrosion Science 76, 154-162.
[184] Arrieta N., **2014**. *The study of an unusual temperate latitude beachrock formation. Characterization of Azkorri beach and Tunelboka cove locations*. PhD Thesis, University of the Basque Country.

6.3 Conclusions

In view of the described set of results, the following **diagenetic features** are defined:

- A ***micritic coating*** primarily composed of HMC, containing on average 10.7-14.3% mol $MgCO_3$. Apart from Mg, it can generally contain C, O, Al, or Si, and even other elements presumably derived from the grains, for instance as a result of bioturbation processes. This layer is fluorescent when observed under ultraviolet light, therefore, it might indicate that the biological activity would encourage the alkaline conditions required for the precipitation of calcium carbonates.

- An ***isopachous acicular rim*** following the micritic coating. This is the prevailing carbonate cement (around 70%) and it is formed with aragonite crystals mainly composed of Ca, C, O and Sr. It is hypothesised that the aragonite needles were emerged from micritic crystals and developed under abiotic conditions.

- ***Infiltrated micritic particles*** with two arrangements: (1) covering the acicular aragonitic rim (containing diverse elements like Ca, Ti, O, Fe, Mg, Si, and specially C, possibly infiltrated upon the percolation of muddy waters under stagnant conditions; (2) filling the intergranular porosity with micritic materials probably infiltrated after storm events. In both cases, the micrites show fluorescence under ultraviolet light. Generally they were only found in an area prone to accumulate waters coming from the estuary plume, in the north of Arrigunaga beach. The lack of these characteristics in the beachrock formations studied in La Salvaje beach might imply that the analysed cemented outcrops are less consolidated or that they are less exposed to the meteoric conditions that induce the percolation of the particles.

- ***Ferruginous cements*** were found within the beachrock formations analysed in both settings. These cements can be composed of various iron oxides and oxyhydroxides, like hematite, limonite, lepidrocrocite, goethite and magnetite. In addition, Fe and Mn carbonates were also present, such as siderite and rhodochrosite, respectively. It is suggested that these mineral phases, can be formed upon oxidation-reduction and hydration-dehydration processes prone to occur associated to the iron (and manganese) cycle, influenced either by chemical or microbiological factors.

With regard to the **diagnetic environments** involved in the cementation:

- The concatenation of HMC and aragonite, common in marine environments, as well as, the abundance of the aragonite cemented forms and the micromorphology of the crystals (isopachous or forming a mesh or needles) evidences a ***marine phreatic*** formation context.

- The influence of a ***meteoric*** environment was evidenced through the presence of LMC, infiltrated intergranular particles (sometimes from the ***vadose*** zone) and even ferruginous cements.

The presence of carbonate cements formed either in marine and meteoric environments was also confirmed by the stable isotope analysis.

Furthermore, the probable **organic or biological influence** in the diagenesis alluded to throughout the chapter is mainly inferred on the basis of the following findings:

- Spherule-shaped structures that could act as precursors of further crystalline calcium carbonates.

- The morphology and heterogeneous composition of HMC, especially if it is compared with the pure composition of the aragonite crystals. The fluorescence of this micritic layer is probably associated with the presence of biofilms.

- The presence of hydromagnesite as well as the evidences of organic macromolecules in association with the aragonite cemented forms.

- The $\delta^{13}C$ depletion of some cements analysed in Arrigunaga and La Salvaje beach suggests that those cements are related with marine fluids influenced by an important organic activity, for instance, through the oxidation of organic matter. Also the low $\delta^{13}C$ and $\delta^{18}O$ values could be related with meteoric waters modified by sewage effluents.

- The presence of reduced mineral phases like siderite and rhodochrosite, within the ferruginous cements.

From the technical point of view, the tools used, either over bulk fragments or thin sections, resulted valuable for the identification of the wide array of characteristics that are still preserved in the beachrock outcrops. For example, the innovative use of fluorescence microscopy in combination with electron microscopy could help not only to illustrate the overlying characteristics of the cements, but also for a better understanding of the technique itself. Altogether, this study provides information that can be valuable for the record, to try to comprehend the marine cementation phenomena, above all in temperate settings taking into consideration also the influence of the surrounding conditions, like in this highly altered estuarine area.

Chapter 7

Final conclusions

The goals of this study, established through three main objectives and their corresponding operational objectives, have been successfully achieved leading to the conclusions of the thesis, as they will be summarised herein. Additionally, in view of the outcomes of this work, some possible future research directions will be proposed.

7.1 Concluding summary

Following the research on beachrock started in Azkorri beach and Tunelboka cove[1], the area of study has been widened with this PhD work, through the examination of Arrigunaga and La Salvaje beach. This way, it contributes to the understanding of this phenomenon in an uncommon temperate coastline.

Beachrock outcrops seem to be complex structures, even more in this case in which they are so influenced by the industrial past of the area. Therefore, prior to describing the main achievements of the work, some remarks will be outlined in reference to the methologies used. The first challenge was to characterize the heterogeneous composites of the cemented structures, to get some preliminary notions of their main characteristics. Through a grain size based geochemical analysis, the possible cements were recognised and above all, the presence of the external inputs prone to have an anthropogenic origin. To further characterise those anthropogenic materials, *in situ* and laboratory Raman spectroscopic analyses were performed.

The next demanding task was to evaluate the significance of trapped anthropogenic materials and particularly if they are coming from past or more recent industrial spills. For that purpose, the metal content of the beachrock outcrops was quantified though ICP-MS based on a sampling strategy made fit for purpose; various samples were collected at different directions of the beaches to estimate their distribution along the beaches. These analyses were performed both in Arrigunaga and La Salvaje beaches, to compare the metal content trapped in the beachrocks belonging to both settings. The signification of the metal content was properly assessed through standard environmental indexes and it was compared with the knowledge on the surrounding environment, concluding that the anthropic materials trapped in the analysed beachrocks were coming from recent (not more than hundred years) industrial-human activities.

Last but not least, the research work dealt with the characterisation of cements to see how those anthropogenic materials are retained, and to estimate the environment of formation as well as the factors that induced the precipitation of the cements. Here, Raman spectroscopy allowed identifying more in detail the composition of the cements, denoting the versatility of the technique. Those analyses were complemented through X-ray diffraction. When finer scales were needed, the staining method and the various

[1] Arrieta N., **2014**. *The study of an unusual temperate latitude beachrock formation. Characterization of Azkorri beach and Tunelboka cove locations*. PhD Thesis, University of the Basque Country.

microscopic techniques used successfully helped in deciphering the morphology and disposition of the cements. It is remarkable the use of fluorescence microscopy, because the specific causes that yield the fluorescence are not well known in carbonate rocks, but this study might shed some light on that regard, likely to help in the detection of organic rich areas. Finally, the conclusions were properly complemented and confirmed through stable isotope analyses.

Using that combination of tools, the objectives set to success in the research have been fulfilled as it will be concluded in the following lines.

One of the principal aims of this PhD work was to examine the main physical and compositional characteristics of the beachrock outcrops. As such, it can be said that there are various evidences that helped understanding the physical and compositional characteristics of the outcrops. Before anything, the field observation of the cemented bodies allowed estimating somehow the differences in the evolution stage of the outcrops; the epilithic colonization (green algae) that can be covering the surface of some cemented bodies denotes a exposure time longer than those structures that do not show any colonization. That way, the outcrops observed in the north of Arrigunaga beach or in the southwestern area of La Salvaje beach, seemed to be exposed longer than in the rest of the areas of each beach. Furthermore, once in the laboratory, the observation of different grain sizes resulted also valuable for the distinction of the composition that might be collected in the different grain sizes. Not only that, when the work was focused on the analysis of the anthropogenic material like slag, the observation of the outward appearance of the slag was essential for instance to recognise slag samples that might have been weathered, which was then confirmed by Raman spectroscopy, with a remarkable contribution of *in situ* analyses, performed to the best of our knowledge, for the first time in beachrock outcrops.

Regarding the second main objective, the quantitative estimation of the metal content of the cemented bodies and assessment of the possible contamination trapped in them, several conclusions can be obtained. The disparities in the distribution of the analysed elements denote that, it depends on the characteristics of the beach, including factors like the location, the tidal currents and diverse exposition to environmental alterations. Likewise, the results of Arrigunaga beach might have been influenced by the regeneration of the beach occurred in the late 90s. However, through the standard indexes used, it was possible to estimate that even though one of the settings is inside the estuary (Arrigunaga beach) and the other one exposed to the open coast (La Salvaje

beach), the diverse environmental alterations of the vicinity affected each of the beaches somehow, because both of them show a moderate to high contamination degree contained in the beachrock outcrops.

Moreover, the third main objective of the research aimed the determination of the characteristics of the cements to estimate the environment in which they were formed and/or the processes involved in the cementation. In that sense, the various observed cements can be resumed as: (1) a micritic coating primarily composed of HMC, containing on average 10.7-14.3% mol $MgCO_3$; (2) an isopachous acicular rim, which is the predominant carbonate cement and it is formed with aragonite crystals; (3) infiltrated micritic particles that can be found over the aragonite crystals or occluding the pore space, only in certain areas of Arrigunaga beach; (4) ferruginous cements composed of various iron oxides and oxyhydroxides (like hematite, limonite, lepidrocrocite, goethite and magnetite) together with composites like Fe and Mn carbonates. The diversity of the cements assumes that the beachrock outcrops were subjected to frequently changing diagenetic environments. Evidences characteristic of either the marine and meteoric realm have been found in beachrock outcrops from Arrigunaga and La Salvaje beach. Micritic HMC and isopachous aragonite, present in both settings, would be representative of a marine environment. Nevertheless, taking into consideration the stable isotope analyses, the meteoric influence is much more obvious in Arrigunaga than in La Salvaje beach. Certainly, the most remarkable meteoric influence has been found in the north of Arrigunaga beach; it is also the area that shows cements as infiltrated particles.

On the whole, the results suggested that biological and chemical factors might have been involved in the cementation. The amorphous spherule-shaped structures (probably associated to ACC) as well as the possible presence of biofilms suggest that a biological source could be among the precursors of the cement. That hypothesis is supported by the fluorescence microscopy observations, in combination with polarized light microscopy and SEM-EDS or even BSE-EDS analyses, allowing to estimate the organic nature of the first cement layers, especially in the southern area of Arrigunaga beach and in La Salvaje beach. Those features could be related with micritic crystals, which would evolve to acicular cements upon the influence of physicochemical factors. A precipitating fluid influenced by organically derived CO_2, for instance as a consequence of oxidation of organic matter, was detected by the analysis of the stable isotope in the cements. Moreover, in certain points of Arrigunaga beach, believed to greatly represent

the cemented bodies existing previously to the regeneration/adaptation actions carried out in the beach, the possible influence of sewage waters was also suggested.

Deciphering the origin of beachrock formation can be quite challenging regardless of the location. But it is believed that the cementation phenomenon leading to beachrock formation is rather exceptional in temperate coastlines, in contrast to the common occurrence in tropical and (sub)tropical areas. Thus, throughout this work it has been intended to seek for the events and factors that might have promoted the precipitation of the cements. As such, the background of the studied areas was taken into consideration because certainly, to understand the present, it is necessary to understand the past. Therefore, confirming the theories inferred in previous work of the adjacent coast[2], it is believed that the miscellaneous contamination derived from the vicinity of the estuary, that reached the adjacent high energy coastline, might have provided the ideal frame for the cementation to occur.

It is remarkable that in Arrigunaga beach silt sized particles can occlude the pore space or the cement covering the acicular rim might have been infiltrated in stagnant conditions through percolation of muddy waters loaded in organic materials; those facts would come in agreement with the environmental alterations that the beach has been exposed to. In La Salvaje beach, in contrast, significantly high amounts of iron can be retained in some cemented bodies, which come in agreement with the blackening of the loose sand, likely to be a consequence of the accumulation of iron-rich industrial wastes. That being said, it seems that beachrock cementation can reflect the environmental circumstances occurring in its area of influence. On the whole, beachrock cementation is an intriguing phenomenon that it remains to be seen if it would be developed under normal environmental circumstances around the Nerbioi-Ibaizabal estuary.

7.2 Possible future research directions

Even though the performed analyses have been clarifying enough to assume that beachrock outcrops belonging to Arrigunaga beach were formed in shallow marine and meteoric environments, while in La Salvaje beach were mainly formed in a marine environment, both of them with carbonate precipitation induced by biological and physicochemical factors, some questions still remain on this regard.

[2] Arrieta N., **2014**. *The study of an unusual temperate latitude beachrock formation. Characterization of Azkorri beach and Tunelboka cove locations*. PhD Thesis, University of the Basque Country.

It would be of great interest to examine the beachrock cementation phenomenon occurring in Alpenarri cove, a highly difficult accessible area nearby. It seems to be quite well preserved and besides, it would allow to have the whole picture of the settings presenting beachrock formations around the Nerbioi-Ibaizabal estuary. Similarly, it would also be interesting to widen the area of study to other areas of the North of Spain, as it has been started with the Portazuelos beach in Aviles (Asturias, 250 km to the west of the analysed area).

Knowing that we are raising awareness about the possibility and the facts of biological activity being somehow involved in the cementation phenomenon, it could be helpful to keep working on that to understand their role and indirectly, perhaps contributing to develop the biotechnological applications derived from them.

Also, taking into account that some beachrock structures occurring in this temperate coastline can harbour vast amounts of wastes, it could be necessary to study the degradation of the cemented deposits and the possible release of contaminants into the environment due to eroding factors but also leaching processes.

Annexes

Annexe 1 | Glossary

Mineral phases

Anatase: TiO_2

Aragonite: $CaCO_3$

Arsenopyrite: FeAsS

Augite: $(Ca,Na)(Mg,Fe,Al)(Si,Al)_2O_6$

Brookite: TiO_2

Calcite: $CaCO_3$

Cristobalite: SiO_2

Fayalite: Fe_2SiO_4

Gypsum: $CaSO_4 \cdot 2H_2O$

Goethite: α-FeO(OH)

Halite: NaCl

Hematite: $\alpha\text{-}Fe_2O_3$

HMC: $CaCO_3$

Hydromagnesite: $(Mg_5(CO_3)_4(OH)_2 \cdot 4H_2O)$

Ilmenite: $FeTiO_3$

Labradorite: $(Ca, Na)(Si, Al)_4O_8$

Lepidocrocite: γ-FeOOH

Limonite: $FeO(OH) \cdot nH_2O$

Magnetite: Fe_3O_4

Thaumasite: $3CaO \cdot SiO_2 \cdot CO_2 \cdot SO_3 \cdot 15H_2O$

Tephroite: Fe_2SiO_4

Portlandite: $Ca(OH)_2$

Siderite: $FeCO_3$

Rhodochrosite: $MnCO_3$

Rhodonite: $MnSiO_3$

Rutile: TiO_2

Quartz: SiO_2

Abbreviations

ACC: Amorphous Calcium Carbonate

ARL: Longitudinal transect of Arrigunaga beach

ART: Transverse transect of Arrigunaga beach

BSE: Backscattered Electrons

EDS: Electron Dispersive X-ray Spectroscopy

EM: Electron Microscopy

FWHM: Full Width at Half Maximum

HMC: High Magnesium Calcite

ICP-MS: Inductively Coupled Plasma Mass Spectrometry

LMC: Low Magnesium Calcite

LSL: Longitudinal transect of La Salvaje beach

LST: Transverse transect of La Salvaje beach

PPL: Plane Polarized Light

SE: Secondary Electron imaging

SEM: Secondary Electron Microscopy

XRD: X-ray Diffraction

XPL: Crossed Polarized Light

Definition of terms

Authigenic: minerals that are formed in situ within the depositional site as a result of diverse geochemical processes. On the contrary, if minerals come from elsewhere transported by water or wind, they are considered as “allogenic”.

Basalt: dark-coloured and fine-grained igneous rock mainly composed of calcium-rich plagioclase feldspar and pyroxene.

Bessemer process: an industrial process for making steel using a Bessemer converter to blast air through molten iron, allowing to burn the excess of carbon and impurities. It was the first succesful process to produce great amounts of steel at low cost and the most important technique for making steel in the nineteenth century.

Bioclast: a sedimentary rock consisting of fragments or broken remains of organisms.

Biofilm: a consortium of microorganisms which are immobilized at a substratum surface and embedded in an organic polymer matrix of microbial origin.

Biomineralization: processes by which living organisms produce minerals composed of both mineral and organic components, and known as “biominerals”.

Bioturbation: a type of organic weathering that implies the disturbance of sediment or the soil by living organisms. It can include displacing soil by plant roots, excavation by burrowing animals, taking sediment away, or eating and excreting sediment.

Blast furnace: a cylindrical reaction vessel made of heat-resistant bricks, into which “blasts” of high-pressure hot air and other gases are blown to generate metal from ore. Commonly, it is used to produce iron for steel-making, but lead, copper, tin, and other metals can also be processed there.

Cement: a precipitate formed post-depositionally that grows in pores and that requires a supersaturation of the pore fluids with respect to the cement phase, giving rise to a diagenetic process known as cementation.

Cementation: the binding of grains through the precipitation of mineral cements.

Cementitious: a material having cement properties. Generally, cementitious products refer to the paste that maintains concrete together. These products include traditional Portland cement as well as fly ash, ground granulated blastfurnace slag (GGBS) or limestone fines.

Clast: a fragment of pre-existing rocks or minerals that form a sedimentary rock.

Diagenesis: all the processes that involve physical, chemical and biological changes occurring during the conversion of sediment to sedimentary rock. It includes compaction and cementation, but not weathering and metamorphic changes. No clear limit can be diposed in the series of changes that might occur during the diagenesis; however, early diagenesis is used to diagenetic processes taking place right after deposition or burial, and late diagenesis occurs a long time after deposition when the sediment is already relatively compacted into a rock and correspond to burial processes acting in the subsurface over a long geological time.

Deposition: a geological process whereby sediments that are carried by water or wind, settle in a new location.

Detritic: related to detritus materials, which account for gravel, sand, silt, or other material produced by erosion or even for the organic matter produced by the decomposition of organisms.

Eutrophic water: referring to water bodies with overabundance of nutrients, especially phosphates and nitrates that can occur in aquatic systems promoting an excessive growth of algae. Those blooms of algae and other microscopic organisms are generally developed in the surface of the water bodies, hindering the penetration of light, and thus, the development of underwater life. Furthermore, the death and decomposition of algae cause a decrease in the available oxygen level, triggering the decease of aquatic organisms. It can be a naturally occurring process, but also speed up by human activity for example due to the presence of excessive amounts of fertilizers, detergents or sewage discharges.

Evaporite: salt deposits precipitated from saturated brackish waters due to the evaporation produced by solar radiation.

Gravel: any loose rock ranging in size from 2 millimeters to 63 millimeters.

Isopachous: characteristic of a cement forming a layer of uniform thickness.

Lithification: a process through which loose grains of sediments are transformed into a rock.

Meteoric water: it refers to water recently implicated in atmospheric circulation. That is, water derived from rain, snow, water courses, and other bodies of surface water that percolates in rocks and displaces their interstitial water.

Micrite: an abbreviation of “microcrystalline”. It generally refers to crystals with a size range between 1 to 4 μm in diameter.

Mineral: naturally occurring, inorganic, solid, crystalline substance that has a fixed structure and a chemical composition which is either fixed or which may vary within certain defined limits. This excludes synthetic substances (e.g. synthetic diamonds), organic substances (e.g. chitin), and substances without a fixed composition which are classified as “mineraloids” (e.g. volcanic glass, also named as obsidian).

Neap tide: especially weak tides that occur every 14 days, near the times of quarter moons.

Offshore: in beach terminology, the comparatively flat zone of variable width, extending from the shoreface to the edge of the continental shelf. It is continually submerged. This term can be also used to refer to the direction of currents or winds going seaward from the land.

Onshore: a term referring to the land zone of the beach, or the water body close to it. It can be also used to refer to the direction of currents or winds going landward from the sea.

Organomineral: any mineral precipitated by interaction with organopolymers, bioorganic, and/or non-biological organic compounds, without evidence of direct skeletal, intracellular or extracellular biological control. Organominerals can be considered then as indirect testimonies of life.

Organomineralization: the set of processes that lead to the precipitation mediated by non-living organic substrates in soils and sediments. These processes include microbially-induced (active process) or microbially-influenced (passive process) mineralization.

Phreatic: also known as “saturated zone”, it refers to the subsurface zone between the land surface and the groundwater (the deepest water table), where the pore space within the rock or soil is fully filled with air and water.

Plagioclase: a silicate of the feldspar group that consists on a solid solution of albite ($NaAlSi_3O_8$) and anorthite ($CaAl_2Si_2O_8$). The two compounds can be mixed and form a continuous chemical range (known as a solid-solution series) between albite and anorthite (the end-members of the series). Intermediate members are homogeneous mixtures of the pure end-members. In any case, the members of the series are usually characterised occurring as light-coloured, glassy, transparent to translucent, friable crystals.

Pyroxene: rock-forming silicate mineral common in many igneous and metamorphic rocks. Pyroxenes can be represented by the general formula $XY(Si,Al)_2O_6$, and although the composition can be variable, they are generally rich in calcium, magnesium and iron.

Sediment: a naturally occurring solid material formed as a result of weathering and erosion, and further transported by the action of wind, water, or ice, and/or by of gravity.

Sediment reworking: a process derived from diverse mechanisms of benthic infauna (such as burrowing, feeding and locomotion), intensely affecting the physical, chemical and biological features of marine sediments. As a result, sediment reworking strongly influences organic matter mineralization, the structure and porosity of the sediment matrix, the sequestration of pollutants and contaminants and the liberation of nutrients from the sediment to the water column.

Sedimentary rock: one of the major rock types (together with igneous and metamorphic rocks) that composes the Earth crust. This kind of rock is generally formed through the deposition of weathered fragments of other rocks, as a consequence of biological activity, or by precipitation from a solution.

Shore: the land alongside the edge of an ocean, sea, lake, or river; that is, the coast.

Siliciclastic rock: sedimentary rocks composed mainly of silicate minerals and transported and deposited as particles.

Slag: a solid waste by-product derived from metallurgical processes of smelting ore.

Surf zone: the relatively narrow strip of a water body that borders the land, and that contains waves breaking due to the shallow water depth. Nevertheless, the width and character of the surf zone vary continually, because of changes occurring in the tide level, incident waves, local wind speed, and direction.

Spring tide: a tide that is especially strong, either very low or very high relatively to the mean sea level. Spring tides occur twice each lunar month (during the full moon and the new moon) all year long regardless of the season. Therefore, this term is not particularly related with the season of spring. Instead, it is derived from the idea of the tide "springing forth."

Swash zone: the area of the beach between the inner surf zone and back beach that is intermittently submerged and exposed by the processes of wave uprise and backwash.

Vadose: also known as “unsaturated zone”, it refers to the subsurface zone between the land surface and the groundwater (the deepest water table), where the pore space within the rock or soil is partly filled with air and water. The water moves downward influenced by gravity, and is called vadose water or gravitational water.

Weathering: the decay of rocks, soil, minerals as well as artificial materials by the contact of the atmosphere, waters or biota. This process is different from “erosion”, as it does not imply the movement or removal of the matter in question**.**

Annexe 2 | Scientific publications

Articles

- Iturregui A., Arrieta N., Murelaga X, Baceta J.I., Olazabal M.A., Martínez-Arkarazo I., Madariaga J.M., 2014. *The relevance of the analytical methodology in the geochemical characterization of beachrock outcrops: Arrigunaga beach inside the Nerbioi-Ibaizabal estuary* (*Getxo, Basque Country)*. Analytical Methods, 6, 8247-8257.

- Iturregui A., Arrieta N., Aramendia J, Arrizabalaga I., Murelaga X, Baceta J.I., Olazabal M.A., Martínez-Arkarazo I., Madariaga J.M., 2015. *In-situ and laboratory Raman spectroscopic analysis on beachrock deposits: characterisation of the trapped materials*. Journal of Raman Spectroscopy 47, 329-336.

Congresses

Oral communications

- Iturregi A., Arrieta N., Arana G., Sarmiento A., Martínez-Arkarazo I., Madariaga J.M. *Characterization of the anthropogenic materials trapped in a beachrock of the Nerbioi-Ibaizabal estuary (Arrigunaga Beach, Bay of Biscay).* EMEC 12- 12th European Meeting on Environmental Chemistry. Clermont-Ferrand (France), 2011.

- Iturregui A., Arrieta N., Arrizabalaga I., Olazabal M., Martínez-Arkarazo I., Madariaga J.M. *Sulphate exposed beachrock cement quantification: the case of high magnesium calcite.* EMEC15-15th European Meeting on Environmental Chemistry. Brno (Czech Republic), 2014.

Poster communications

- Iturregi A., Arrieta N., Martinez-Arkarazo I., Murelaga X., Baceta J.I., Sarmiento A., and Madariaga J.M. *Molecular Characterization of a Temperate Beachrock Formation in the Nerbioi-Ibaizabal Estuary (Arrigunaga Beach, Bay of Biscay).* CORALS11- Conference on micro-Raman and luminescence studies in the Earth and planetary sciences. Madrid (Spain), 2011.

- Iturregi A., Arrieta N., Arana G., Baceta J.I., Murelaga X., Martinez-Arkarazo I., Madariaga J.M. *Granulometric and compositional analysis of a beachrock outcrop in Arrigunaga Beach (Bay of Biscay).* ISMS- International Symposium in Marine Science. Cádiz (Spain), 2012.

- Iturregi A., Arrieta N., Baceta J.I., Murelaga X., Martinez-Arkarazo I. and Madariaga J.M. *Analysis of cements from beachrock remnants in the Arrigunaga beach (Bilbao estuary, Bay of Biscay)*. Georaman Xth international Conference on Raman Spectroscopy. Nancy (France), 2012.

- Iturregui A., Arrieta N., de Diego A., Olazabal M., Martinez-Arkarazo I. and Madariaga J.M. *Distribution of metals in temperate beachrocks*. ISMEC- International Symposium on metal complexes. Wroclaw (Poland), 2015.

Beachrocks are defined as friable to well-cemented sedimentary coastal structures typically formed in the intertidal zone due to the precipitation of carbonates (principally) that act as cements, packing together the wide array of sediments that might be present in the beach. The research work described herein is focused on two settings known as Arrigunaga beach and La Salvaje beach, which are located in the vicinity of the Nerbioi-Ibaizabal estuary (Basque Country, North of Spain), an uncommon temperate coastline for beachrock formation. The inherent complexity of this cementation phenomenon and the environmental alterations occurred in the area of study during the recent past decades will go hand in hand along this work, in an attempt to recognize the underlying characteristics of the studied beachrock outcrops.

At first, after detecting the presence of possible anthropogenic external inputs, *in situ* and laboratory Raman spectroscopic analyses were carried out, which allowed to estimate the industrial origin of the wastes trapped in the cemented outcrops, simultaneously denoting the recent formation of the beachrock. In addition, quantitative analyses performed afterwards by ICP-MS, aided by chemometric analyses, allowed suggesting that those external inputs might provide a moderate to high contamination degree. Finally, a thorough study of the cements was performed based on staining methods, microscopic techniques (polarized light microscopy, fluorescence microscopy and electron microscopy, including SEM-EDS and BSE mode), together with XRD and Raman spectroscopy. Those analyses were complemented by stable isotope analyses of the carbonate cements. On the whole, the diverse characteristics of the cements suggest that they were exposed to changing diagenetic environments, where the cementation was likely to be induced by a combination of biological and chemical factors that lead to the conditions required for the precipitation of the cements.

eman ta zabal zazu

Universidad del País Vasco

Euskal Herriko Unibertsitatea